
This item was submitted to [Loughborough's Research Repository](#) by the author.
Items in Figshare are protected by copyright, with all rights reserved, unless otherwise indicated.

An analytical and experimental investigation into chain elasticity effects in power loader haulage units

PLEASE CITE THE PUBLISHED VERSION

PUBLISHER

Loughborough University of Technology

LICENCE

CC BY-NC 4.0

REPOSITORY RECORD

Webster, Brian P.. 2020. "An Analytical and Experimental Investigation into Chain Elasticity Effects in Power Loader Haulage Units". Loughborough University. <https://doi.org/10.26174/thesis.lboro.13128869.v1>.

AN ANALYTICAL AND EXPERIMENTAL INVESTIGATION INTO
CHAIN ELASTICITY EFFECTS IN POWER LOADER HAULAGE UNITS

by

BRIAN P WEBSTER, C.Eng., M.I.Mech.E.

A Master's Thesis

Submitted in partial fulfilment of the requirements for the
award of Master of Science of the Loughborough University
of Technology March 1976

Supervisor: T P Priestley, B.Sc.(Eng.), M.Sc. Nottingham

© by Brian P Webster, 1976

Loughborough University	
of Technology Library	
Date	July 1976
Class	
Acc. No.	032578/02

SYNOPSIS

ACKNOWLEDGEMENTS

NOTATION APPROPRIATE TO APPENDICES I AND III

NOTATION APPROPRIATE TO APPENDIX II AND SECTIONS 3 AND 6

1	INTRODUCTION	1
2	DESCRIPTION OF FACE EQUIPMENT ASSOCIATED WITH POWER LOADERS	4
2.1	The Longwall Mining System	4
2.2	The Power Loader	4
2.3	The Chain and Chain Tension	5
2.4	Power Loader Haulage Units	6
2.4.1	Hydrostatic Haulage Unit	6
2.4.2	The Mechanical Haulage Unit	7
2.5	The British Jeffrey-Diamond Haulage Unit	8
2.5.1	The Hydrostatic Transmission	9
2.5.2	The Auxiliary Circuits	10
3	THE EFFECTS OF CHAIN ELASTICITY, CHAIN TENSIONERS AND SPROCKET LOSSES ON THE DISPLACEMENT-TORQUE CHARACTERISTICS OF SPROCKET DRIVE SYSTEMS	12
3.1	Introduction	12
3.2	Frictional Losses in Round Link Chain Sprocket Drive Systems	12
3.3	Determination of the Torque-Displacement Characteristics of Power Loader Haulage Units Working on Round Link Chain with Spring Tensioners	15
3.4	Torque-Displacement Characteristics using Hydraulic Type Compensating Devices	18
3.5	Comparison between Chain Systems Employing Compensating Devices and Solid Anchorages	18
3.6	Tension Losses Due to Chain Drag	20
3.7	Force Extension Characteristics of Round Link Chain	21
4	EXPERIMENTAL EXAMINATION OF A POWER LOADER HAULAGE UNIT LOADED WITH A CHAIN SYSTEM	22
4.1	Introduction	22
4.2	Description	22
4.3	Instrumentation	22
4.4	Test Procedure	23
4.5	Results	24
4.6	Observations	25
4.6.1	Tension Characteristics	25
4.6.2	Sprocket Torque Characteristics	26
4.6.3	Haulage Pressure Characteristics	27
4.6.4	Strain Energy Release Speed Characteristics	27

	<u>Page No</u>
5 DETERMINATION OF HAULAGE UNIT AND ABSORBER CHARACTERISTICS	29
5.1 Introduction	29
5.2 Description	29
5.3 Instrumentation	30
5.4 Test Procedure	31
5.4.1 Absorber Torque-Pressure Characteristics	31
5.4.2 Absorber Leakage Characterististics	31
5.4.3 Haulage Leakage Characteristics	32
5.4.4 System Inertia	32
5.4.5 Pump Stroke Rate	32
5.4.6 Determination of the By-Pass Valve Pressure - Flow Characteristics	33
5.4.6.1 Experimental Method	33
5.5 Observations	33
5.5.1 Absorber Torque-Pressure Characteristics	33
5.5.2 Absorber Leakage Losses	34
5.5.3 System Inertia	35
6 THE SELECTION OF ACCUMULATOR BANK CHARGING PRESSURES TO GIVE APPROXIMATIONS TO LINEAR PRESSURE-VOLUME RELATIONSHIPS	36
6.1 Pressure-Volume Characteristics of a Single Accumulator	36
6.2 Pressure-Volume Characteristics of Accumulator Banks	37
6.3 Empirical Method for Determining the Charge Pressures of Accumulator Banks for Linear Pressure Volume Approximation	38
6.4 Computational Methods for Determining the Charge Pressures of Accumulator Banks for Pre-determined Pressure Volume Approximations	42
6.4.1 Terminal Section 1 Accumulator Pre-Charge Pressure Setting using Pressure Incrementing Technique	42
6.4.2 Terminal Section 2	43
6.4.3 Terminal Section 3	44
7 EXPERIMENTAL DETERMINATION OF HYDRO-PNEUMATIC ACCUMULATOR DISCHARGE CHARACTERISTICS	45
7.1 Introduction	45
7.2 Experimental Method	45
7.3 Experimental Procedure	46
7.3.1 Determination of Initial Gas Volume	47
7.4 Experimental Results	48
7.5 Observations	48
7.6 Conclusions	50

	<u>Page No</u>
8 EXPERIMENTAL EXAMINATION OF ACCUMULATOR AND CURVE FOLLOWER CHAIN ELASTICITY SIMULATION TECHNIQUES	52
8.1 Introduction	52
8.2 Description	52
8.3 Test Procedure	53
8.3.1 Simulation using Accumulator Banks	53
8.3.2 Simulation using Curve Follower Techniques	54
8.4 Observations	55
8.4.1 Simulation using Accumulator Banks	55
8.4.2 Simulation using Curve Follower Technique	58
9 THE CSMP SIMULATION LANGUAGE	61
10 A CSMP MODEL OF THE HAULAGE UNIT LOADED BY THE CHAIN SYSTEM AND THE HYDROSTATIC ABSORBER	63
10.1 Introduction	63
10.2 Representation of the Haulage Unit	63
10.3 Representation of the Absorber Unit	65
10.4 Model Organisation	65
10.5 Model Outputs	67
11 APPLICATION OF THE DYNAMIC MODEL TO THE HAULAGE UNIT AND ABSORBER LOADING SYSTEM	69
11.1 Introduction	69
11.2 Comparison of Accumulator Pre-Charge Pressure Setting Procedures	70
11.2.1 The Pressure Increment Method of Accumulator Pre-Charge Pressure Setting	70
11.2.2 Empirical Method of Accumulator Pre-Charge Setting	72
11.2.3 Empirical Method of Accumulator Pre-Charge Pressure Setting without the use of Dynamically Determined Pressure Volume Characteristics	72
11.3 Effects of Accumulators Charging and Discharging at Differing Polytrropic Indices	73
11.4 The Effects of Tripping Pressure Adjustment for Frictional Loss Compensation between Chain System and Absorber	74
11.5 A Comparison between Release Speeds for By-Pass Valves with Varying Restrictions	75
11.6 Some General Observations on the Model and its Operation	75
12 A CONVERSATIONAL PROGRAMME FOR SETTING THE PRE-CHARGE PRESSURES OF A BANK OF ACCUMULATORS TO ENABLE A HYDRO-STATIC POWER ABSORBER TO SIMULATE CHAIN ELASTICITY EFFECTS ON POWER LOADER HAULAGE UNITS	78

	<u>Page No</u>
13 A DYNAMIC MODEL OF A MECHANICAL HAULAGE UNIT	81
13.1 Description	81
13.2 Observations on the Outputs of the Mechanical Haulage Model	82
14 CONCLUSIONS	84
14.1 Chain System	84
14.2 Absorber Type	84
14.3 Accumulator Performance	85
14.4 Accumulator Bank Pre-Charge Pressure Setting Procedures	85
14.5 The CSMP Model	85
14.6 Curve Follower and Accumulator Simulation Technique	87
14.7 Mechanical Haulage Unit	87
14.8 Further Use of Hydrostatic Power Absorbers for Chain Elasticity Simulation	87
15 RECOMMENDATIONS	88

APPENDIX

I	A CSMP Model of a Power Loader Haulage Unit with Chain and Absorber Loading
II	A Conversational Programme for Setting the Pre-Charge Pressures of a Bank of Accumulators to enable a Hydrostatic Power Absorber to Simulate Chain Elasticity Effects on Power Loader Haulage Units
III	A CSMP Model of a Mechanical Haulage Unit
IV	References
V	Instrumentation

SYNOPSIS

An experimental and analytical examination of energy stored in the chain by power loader haulage units is described. Particular attention is paid to the use of hydrostatic absorbers and accumulators banks to simulate haulage forces including chain elasticity.

The IBM 360 CSMP modelling programme is used for an analytical examination of the hydrostatic absorber and accumulator bank simulation method to determine its accuracy. This dynamic modelling technique is seen to be ideal for the dynamic analysis of hydraulic systems.

A series of full scale surface tests on a haulage unit loaded by a chain is described. These tests provide data for the dynamic model and serve as a comparison for the absorber loading tests. An examination is made into the effects of sprocket friction losses and chain anchorage methods on the torque-displacement characteristics of haulage units under energy release conditions.

An experimental method is described to determine the pressure-volume characteristics of hydropneumatic accumulators. These are shown to operate under polytropic conditions for both charging and discharging at flow rates corresponding to those found in chain elasticity simulation. Two methods are described of predicting the pre-charge pressures of accumulators used in combinations to achieve linear pressure-volume characteristics.

A conversational computer programme is presented which sets accumulator pre-charge pressures to achieve a suitable simulation for a given haulage chain system using an hydrostatic absorber.

ACKNOWLEDGEMENTS

The author wishes to express his sincere thanks to the undermentioned for their part in making this research possible.

Professor J N Butters for placing the facilities of the Department of Mechanical Engineering of Loughborough University of Technology at the author's disposal, and to Mr T P Priestley for his help and guidance throughout the work.

The National Coal Board for their financial support of the author during the undertaking of this research.

Mr P G Tregelles, Director of the Mining Research and Development Establishment and Mr D J Skidmore the former Director for their support and for making available the facilities of the Laboratories at Bretby.

Mr G C Knight and Mr J D Kibble of the Mining Research and Development Establishment for the support and encouragement.

Members of the staff of MRDE particularly I Bexon and D D Harlington for assistance with computer programming; D Blake and J Dennis for instrumentation services and all members of the Rotary Testing Laboratory and Swadlincote Test Site for help with rig construction and operation.

Miss P Baker for the typing and assistance given in the preparation of this thesis.

NOTATION APPROPRIATE TO APPENDIX I AND III

AFAC	Absorber leakage factor
AJ	Absorber inertia
AL	An array containing accumulator bank pressures required to give an identical load to that produced by the chain
ALEAK	Function defining the absorber leakage characteristic
AP	An array containing accumulator bank pressures
APDF	Absolute value of pressure difference
AV	An array containing accumulator bank fluid volumes
AVOL	Fluid volume required by absorber obtained with $KAB = 0$
BM	Bulk modules of haulage fluid
BPA	An array containing values of PA
BT	Braking torque
EVOL	An array containing values of AVOL
BYPS	Function defining the by-pass valve pressure-flow characteristic
DA	Displacement of absorber
DM	Displacement of haulage hydrostatic motor
DTDG	Function defining the displacement-torque characteristic of the haulage with the sprocket driving
DTIN	Function defining the displacement-torque characteristic of the haulage with the sprocket driven
FBP	Flow through by-pass valve
FD1	Fluid flow into line 1
FD2	Fluid flow into line 2
FIV1	Inlet valve flow line 1
FIV2	Inlet valve flow line 2
FLIN	Haulage internal leakage
FMAX	Maximum flow from haulage pump
FMOT	Fluid flow from motor
FPUMP	Fluid flow from pump
FRAC	Proportion of maximum forward speed
FRV1	Relief valve flow line 1
FRV2	Relief valve flow line 2

FS	Maximum forward speed
FX1	External leakage line 1
FX2	External leakage line 2
HJ	Haulage inertia
HRATIO	Haulage gear ratio
ILEAK	Function defining haulage internal leakage
IN	Number of accumulators in bank
IVC	Function defining the inlet valve pressure-flow characteristic
KAB	Switch for run control, KAB = 0, haulage is chain loaded KAB = 1 absorber loaded
KP	Accumulator fluid pressure during incrementing procedure
KPA	An array of accumulator pre-charge pressures
KPMAX	Maximum absorber pressure
KPMIN	Minimum absorber pressure
KPX	Minimum absorber pressure
KR	Pressure increment
KSTOP	Flag for FINISH statement
LSWITCH	Switch for by-pass operation
P	Accumulator gas pressure
P1	Pressure in line 1
P2	Pressure in line 2
PA	Absorber pressure
PAR	Stiffness compensation factor
PATR	Maximum absorber pressure calculated from static characteristics
PCOMP	Haulage tripping pressure compensated for difference in sprocket and absorber efficiency
PDF	Pressure difference across haulage motor
POWC	Polytropic index of compression for accumulators charging
POWE	Polytropic index of expansion for accumulators discharging
PTAM	Function defining the absorber pressure-torque characteristic with the absorber driving
PTAP	Function defining the absorber pressure-torque characteristic with the absorber driven

PTHM	Function defining the haulage pressure-torque characteristic with the sprocket driving
PTHP	Function defining the haulage pressure-torque characteristic with the sprocket driven
RBV	Fluid volume required from accumulator bank to reproduce chain loading conditions, calculated from static characteristics
RPA	Absorber pressure due to accumulator bank with $KAB = 1$
RPL	Absorber pressure required to produce an identical load to that produced by the chain load
RV	Function defining haulage relief valve pressure-flow characteristic
RVM	Fluid volume displaced by absorber with $KAB = 1$
SP2	Initial condition haulage pressure line 2
SPDF	Sign of pressure difference
SPOS	Haulage pump swash prior to by-pass operation
STA	Initial absorber pressure
STB	Initial condition for absorber volume
STF	Haulage fluid stiffness
STF1	Stiffness of fluid in line 1
STF2	Stiffness of fluid in line 2
STH	Initial condition haulage sprocket angular velocity
STT	Initial condition for sprocket displacement
STX	Initial condition sprocket torque
STY	Initial condition haulage pressure line 1
STZ	Initial condition haulage leakage
SWASH	Function defining haulage pump swash reduction
TA	Absorber torque
TBP	Simulation time prior to by-pass operation
TBP1	Simulation time after by-pass operation
TCH	Torque on haulage sprocket due to either chain load or absorber load
TDDG	Function defining haulage torque-displacement characteristic sprocket driving
TDIN	Function defining haulage torque-displacement characteristic sprocket driven

TH	Sprocket angular displacement
THD	Sprocket angular velocity
TH2D	Sprocket angular acceleration
TIME	CSMP simulation time variable
TM	Torque developed by haulage motor
TPAM	Function defining the absorber torque-pressure characteristic with the absorber driven
TPAP	Function defining the absorber torque-pressure characteristic with the absorber driving
TPHM	Function defining the haulage torque-pressure characteristic with the sprocket driving
TPHP	Function defining the haulage torque-pressure characteristic with the sprocket driven
TRIP	Pressure at which the by-pass valve is switched into the haulage circuit. Haulage tripping pressure
TTRIP	Haulage tripping torque
USL	Dimensionless value of the gradient of the required pressure-volume characteristic (unity slope)
V	Accumulator gas pressure
VA	An array containing accumulator initial gas volumes
VFAC	Viscosity compensation factor
VIC	Function defining inlet valve flow-pressure characteristic
VJ	Individual accumulator gas volume
VLINE	Accumulator bank total gas volume required to reproduce chain loading conditions
VP	Volume of haulage transmission pipes
VT	An array of accumulator gas volumes at the maximum pressure
VTa	Total gas volume of accumulator bank at maximum pressure
VTF	Total gas volume of all the accumulators whose pre-charge pressures have not been set
VTR	Viscous damping torque
VTT	Total gas volume of accumulator bank
XLEAK	Function defining haulage internal leakage
XTH	Initial condition haulage displacement
YI	Accumulator increment factor

NOTATION APPROPRIATE TO APPENDIX II AND SECTIONS 3 AND 6

abeff	Absorber mechanical efficiency
abfac	Absorber leakage factor
ac	Available compression from chain tensioner
accrot	Sprocket rotation produced by release of energy from the accumulator bank
ad	Absorber displacement
at	Interlink rotation angle
at1	Total interlink rotation angle onto or off sprocket system
bp	Absorber boost pressure
chsl	The equivalent chain elasticity seen by the sprocket under release conditions
fc	Chain tensioner full compression
idt	Number of haulage idler sprocket teeth
k1	Interlink tension loss coefficient
k1t	Total interlink tension loss coefficient onto or off sprocket system
L	Length of chain under tension
La	Length of chain between the machine and point at which the chain contacts the floor
Lb	Length of chain between the anchorage point and the point at which the chain contacts the floor
mu	Interlink friction coefficient
mus	Friction coefficient for chain drag
n, n1, n2	Accumulator polytropic expansion and compression indices
nb	Number of accumulators in bank
pa	An array of accumulator pre-charge pressures
pamax	Maximum absorber pressure
pc	Chain tensioner pre-compression
pchpr	The percentage haulage pressure reduction for efficiency compensation
pcr	Haulage drive sprocket effective radius

pitch	Haulage chain pitch
prtn	Haulage chain pre-tension
P	Accumulator pressure
Pa	Accumulator pre-charge pressures
Pc	Accumulator pre-charge pressure
Pd	Pressure difference
Pf	Final accumulator pressure
Ps	Supply pressure
rot	Sprocket rotation produced by release of energy from the chain system
s	Spring rate of chain tensioners
sag	Vertical distance between chain anchorage point and floor
sc	Spring rate of haulage chain
slope	The gradient of the pressure-volume characteristic required from the accumulator bank
spt	Number of haulage drive sprocket teeth
s2, s3, s4, s5, st	Gradients of accumulator bank pressure-volume characteristics
tab	The absorber torque (expressed as a force at pcr) which is required with the absorber driven to give torque tp1 at a change of direction to driving assuming constant pressure
tmax	Maximum chain tension
tmm	Maximum forwards sprocket torque
tm1	A sprocket torque (expressed as a force at pcr) required to produce tension tmax with the sprocket driving
tp1	A sprocket torque (expressed as a force at pcr) produced by tension tmax with the sprocket driven
tp2	A sprocket torque (expressed as a force at pcr) produced on the sprocket by the chain at the point just prior to tension equilibrium
Ta	Tension in chain adjacent to the machine
Tb	Tension in chain adjacent to anchorage point
Tl	Tension loss
Tm	A sprocket torque (expressed as a force at pcr) with the sprocket driving

T_p	A sprocket torque (expressed as a force at per) with the sprocket driven
T_{rm}	Sprocket torque with haulage driving
T_{rp}	Sprocket torque with haulage driven
T_1	Haulage chain tension (tight side)
T_2	Haulage chain tension (slack side)
usl	Dimensionless value of the gradient of the required pressure-volume characteristic (unity slope)
v_a	Accumulator initial gas volumes
V	Accumulator gas volume
V_a	Accumulator initial gas volumes
V_d	Volume difference
V_s	Accumulator gas volume at supply pressure
VV	Total accumulator bank gas volume
w_d	Wire diameter of round link chain
w_l	Weight for unit length of chain
y_i	Accumulator increment factor
z	Movement of chain through the sprocket system
z_{max}	The maximum release displacement

1 INTRODUCTION

Power loader haulage chain is a well known underground safety hazard. Projects relating to improvements in its usage continue to be of importance within the NCB.

With safety in mind the Mines Inspectorate issued a directive stating that power loader haulage units should release chain tension at a controlled rate. Headquarters staff then gave the Mining Research and Development Establishment the task of ensuring that present and future haulage units working on chain systems comply.

A typical power loader haulage unit working on a 200 m face equipped with 18 mm chain can exert a force of about 150 kN (15 tons). With the machine hauling on the maximum chain length this would produce a chain extension of about 1 m. Any uncontrolled release of the energy contained in the chain at this point can cause violent movements of both the chain and machine. It is required that when the machine is stopped, either manually or by the overload protection systems, that the tensions either side of the machine equalise at a rate such that there is no dangerous movements of machine or chain. Haulage force cannot be left 'locked in' since this is also a serious danger to machine operators and maintenance workers through sudden unexpected movements of the machine as the restraining forces relax.

As an initial approach to simulating this phenomenon within the laboratory, a test rig was designed by MRDE Design Branch which employed a bank of compression springs to give a similar spring rate to that of a 200 m length of haulage chain. Whilst this work was proceeding however, several haulage units were undergoing life and performance tests within the rotary test laboratory and differing types of loading systems were being evaluated. This led to an alternative to the 'spring' rig.

To absorb power from a haulage unit a brake is required that will operate between 0 - 0.6 rad/sec (0 - 6 rev/min) at a torque rating of up to 54,000 N m (40,000 lb ft). This duty is outside the performance of

conventional dynamometers which operate at much higher speed and therefore need step up gearboxes so the speeds can be matched. Such dynamometers can be used for endurance tests but they are unsuitable for dynamics or response tests due to their high inertia when referred to the loading shaft.

Two systems of low speed dynamometry have been proved successful for this torque speed range, water cooled pneumatically operated disc brakes and slow speed hydrostatic motors operating as pumps. Both these devices have low inertia and are suitable for either endurance or dynamic response tests on power loader haulage units. Hydrostatic absorbers have the additional advantage that the stiffness of the loading system can be adjusted by incorporation of hydro-pneumatic accumulators into the circuit such as to enable chain elasticity simulation.

As this line of approach to chain elasticity simulation seemed to eliminate the need for a large expensive special purpose rig it was decided to delay the decision to build the 'spring' rig until an evaluation of the alternative approach had been made.

For the purpose of this work two test facilities were made available, a laboratory rig which utilised a hydrostatic power absorber to simulate loading conditions on a power loader haulage unit and a full scale mock face at Swadlincote Test Site employing a power loader haulage unit with appropriate chain and chain tensioners.

A mathematical model using the IBM modelling technique CSMP (Continuous System Modelling Programme) was used to check the validity of using hydrostatic absorbers to simulate chain elasticity effects. The model operates in two sections. A release of strain energy is simulated assuming a power loader haulage unit to be loaded by a chain system. A series of calculations is then performed to choose the correct charge pressures of a bank of accumulators to enable a hydrostatic power absorber to exhibit the simulated effects. The second section of the model assumes the haulage to be loaded by the hydrostatic power absorber and

the accumulator bank. Outputs from both sections can then be compared to assess the accuracy of the hydrostatic power absorber method of loading.

Results from the surface trials were used as input data to the dynamic model. Characteristics of the haulage unit and three absorbers were determined using the laboratory rig also for inclusion in the model.

Two methods of setting accumulator bank pre-charge pressures are described, a pressure incrementing computational method and an empirical method. The CSMP model is used to compare these two techniques. The need for a precise knowledge of accumulator characteristics leads to an ~~experimental examination of their performance being made.~~

Factors which effect the haulage sprocket displacement - torque relationship such as interlink friction, chain drag are considered mathematically and comparisons made with the surface trials.

This information together with data from the sections on accumulator characteristics and the CSMP model are combined in a conversational computer programme. This programme enables a selection of absorber and accumulator bank details to be made to reproduce an adequate simulation for any haulage, chain and chain tensioner details.

2 DESCRIPTION OF FACE EQUIPMENT ASSOCIATED WITH POWER LOADERS

2.1 The Longwall Mining System

Most of the coal produced from British mines is obtained using the longwall mining system. Two tunnels, approximately 200 m apart are driven along a strata of coal. Between the roadways coal is removed from a connecting tunnel known as the coalface. As coal is removed from the face by a cutting machine working along its length, the power loader, both the face and the roadways are advanced into the strata.

A scraper type conveyor, the armoured face conveyor, runs the length of the face and transports coal discharged by the power loader to one of the supply roadways, the main gate, and hence to a belt conveyor for delivery to the pit bottom. The face is supported by hydraulically operated roof supports positioned every 1 m, these advance with the face allowing the unsupported area from which the coal has been removed to collapse. Power and water for the power loader is supplied by trailing cables looped along the face. A typical coalface layout is shown in Fig. 2.1.

2.2 The Power Loader

Several types of power loader are in use with the NCB, the two basic categories being trepanners, machines with the cutting drum axis parallel to the face and shearers machines with a cutting drum axis perpendicular to the face, shearers being used on approximately 75% of all faces. Power loaders have three basic components, a water cooled induction motor, a haulage unit, and gearheads to transfer the drive from the motor to the cutting drums which they support and position.

The machine is able to slide on the pans of the armoured face conveyor and is propelled along the face by winding itself along a round link chain running the length of the face and attached to anchorage points at the face ends. Rotation of a drive sprocket and two idler sprockets on the haulage

unit, in mesh with the chain, provide the necessary force to drag the machine along the face.

2.3 The Chain and Chain Tensioner

For efficient operation of the haulage system it is essential that the tension in the slack side of the chain T_2 is at all times sufficient to strip the chain from the sprockets and stop 'bunching'. As the forces involved are high and the chain elastic, it is possible, on a typical face, for the haulage unit to extend the chain by as much as 1 m. To eliminate this slack chain and ensure that sufficient slack side tension is available, a variety of compensating devices for use at the chain anchorage points and setting procedures are available.

Solid anchorage points can be used if sufficient pre-tension, ie the tension left in the chain with the haulage producing no effort, is induced into the chain. This method is undesirable however since the maximum hauling tension is approximately twice the value developed when using compensating devices, leading to increased chain wear and breakage. High pre-tension is also an undesirable safety hazard.

The most frequently used compensating device is the Anderson Boyes spring tensioner Fig. 2.2. Here the reaction of the chain tension is taken through a group of compression springs. This system is set up by stalling the machine and applying maximum tension T_1 to the maximum chain length, pulling the slack chain produced through the T_2 compensating device and connecting the chain. As T_1 is reduced the amount of chain extension reduces and the T_2 compensating device compressed. This system ensures that T_2 is maintained at all machine positions and chain tensions.

Due to the difficulties of pulling all the slack chain through the compensating device and because of the danger of operating the haulage pressure overload devices when exerting maximum chain tension, spring type compensators have a locking device which can hold the springs in any state of compression. This allows the slack chain to be pulled through

the compensator with the springs slightly compressed, removal of the lock eliminates any remaining slack chain.

Other compensating devices in use employ similar principles with combinations of hydraulic rams and springs to achieve compensation and incorporate methods of tensioning or detensioning the chain without use of the haulage unit. Their operational characteristics are similar to the Anderson Boyes spring tensioners.

2.4 Power Loader Haulage Units

2.4.1) Hydrostatic Haulage Units

The basic requirements of a power loader haulage unit are that it provides the necessary force to propel the machine along the face, that the machine speed is controllable by the operator and bi-directional, and that internal overload protection systems are incorporated to limit the maximum machine effort and the maximum current taken by the drive motor. Until recently these requirements were found to be satisfied by use of haulage units employing hydrostatic transmission drives with some degree of final gear reduction to the chain drive sprocket. Hydrostatic transmissions give controllable, infinitely variable bi-directional drives. In most cases output torque is proportional to the system pressure which can easily be sensed and used for control purposes.

A wide range of hydrostatic haulage units are in use with the NCB employing many types of transmission elements. One early and still widely used haulage unit employs two, three piston plunger pumps, one fixed and one with variable displacement. These supply fluid to a fixed displacement motor with radial pistons operating through pivoted rollers onto an internal multi-lobed cam. The relatively large displacement of the motor compared with the pumps gives a speed reduction between the input to the pumps and the motor output reducing the required gear ratio. Direction control is achieved by means of a direction control valve in the main fluid transmission circuit. Later haulage units employ axial piston swash plate

pumps with similar low speed motors. Overload protection on haulage force is achieved using a control signal, from the main circuit pressure, to either reduce the pump output (thus reducing the haulage speed) or interrupting the drive by operating the main circuit direction control valve into a neutral position. In most haulage units an element of speed control is introduced by sensing the current to the power loader drive motor and reducing the pump output if this becomes greater than the full load value. In this way, the control mechanism can override the speed selected by the operator and the machine speed maintained at the optimum level consistent with the maximum motor current. Any large increase in motor current is used to interrupt the haulage drive by operation of the direction control valve, with subsequent reduction of the pump output.

To control the rate of release of strain energy from the chain on either manual or automatic interruption of the drive, circuits are usually designed such that in the neutral condition, a restricting orifice is connected across the motor ports. In this condition, energy from the chain rotates the motor, passing fluid through the restriction. This eliminates any rapid discharge of strain energy from the chain.

Some haulage units exploit overcentre pumps to eliminate the need to use direction control valves for bidirectional operation.

2.4.2) The Mechanical Haulage Unit

Over the last few years interest has been growing in mechanical haulage units. Hydrostatic haulage units have become increasingly complicated. Also operational reliability is of primary importance. Fluid contamination is a major cause of haulage breakdown and attempts at repair underground lead to even greater contamination. Mechanical haulage units can operate at higher levels of contamination through the elimination of high tolerance components such as pumps, motors and spool valves. A reversion to purely mechanical transmissions is seen to give fewer maintenance problems and the simpler construction is more easily understood by underground maintenance

personnel even though this is at the expense of the controllability obtained with hydrostatic haulage units.

Mechanical haulage units employ a series of linkage operated change gears to give a range of output speeds. Friction clutches, operated either by linkages or an auxiliary hydraulic control circuit, are used to engage-disengage the drive and in some cases increase the speed range. Torque overload sensing is by either strain gauges or slipping clutch mechanisms. The speed of the mechanical haulage unit is not variable, an optimum speed setting is chosen for the existing conditions and any current overload on the power loader motor is used to disengage a drive clutch. This lack of control, makes the mechanical haulage unit incapable of operating the power loader at the maximum motor current, other than by skilful selection of the optimum gear ratio.

To control the rate of release of energy from the chain, when the drive is interrupted, the mechanical haulage unit uses a parking brake. This friction brake also has the effect of maintaining a certain level of haulage effort after the drive is disconnected.

In cases where the power loader is working in seams with considerable gradient however, this is a desirable effect as it stops the machine sliding down the face under its own weight.

2.5 The British Jeffrey Diamond B14 Haulage Unit

The basic form of this haulage accounts for a large proportion of haulage units in use with the NCB. The unit consists of a hydrostatic transmission and a 215/1 ratio epicyclic reduction gearbox driving the output sprocket. Four independent circuits are included in the hydraulic system (Fig. 2.3), the main transmission and the three auxiliary control circuits.

A section through the haulage unit is shown in Fig. 2.4 and Fig. 2.5 shows the sprocket drive configuration.

2.5.1) The Hydrostatic Transmission

This comprises a variable delivery Helo-Shaw type piston pump with a capacity of $0.0 - 2.57 \text{ dm}^3/\text{s}$ ($0 - 34 \text{ gal/min}$) and fixed delivery radial piston motor of the same capacity, the rotating assemblies being identical in both. The rotor assembly contains two rows of six radial bores, the two rows being displaced to provide the unit with twelve equi-spaced pistons. It has an inner valve ring and is located on a fixed cantilevered pintle shaft, which contains the fluid flow and return connections, by two ball races. The rotor also incorporates one half of a dog coupling which provides the input or output drive to the units.

The piston follower assemblies have a wheel and axle type construction, with two follower wheels, one each side of the piston. A needle roller bearing supports the axle which is integral with one of the follower wheels. The second wheel is swaged onto the axle. A ground bore in the piston provides the outer track of the needle bearing. Rotation of the piston in its bore is controlled by bronze spring loaded cheek plates either side of the rotor assembly.

The rotor is located within a floating ring which is supported on two roller bearings in the casing. The motor casing is fixed to give a constant displacement but the end covers of the pump casing have elongated bores to allow movement relative to the rotor pintle shaft. This eccentricity, either side of the rotor centre line, provides linear movement of the pistons relative to their bores as the rotor rotates, adjustment of this eccentricity giving varying flow rate and a facility to reverse the direction of flow. The floating ring is rotated at a speed slightly less than that of the rotor by action of the piston follower assemblies in contact with it. This enables the followers to operate at low rotational speeds, reducing wear and friction.

The pump casing is moved by a thruster block consisting of a main piston with two shuttle valves controlling the flow of fluid from the auxiliary circuits to either side of the main piston.

A closed loop hydraulic circuit connects the pump and motor, fluid losses from the circuit being provided by suction through check valves, a strainer and a water cooled oil cooler from the sump. Overload protection is by means of two single stage relief valves which discharge directly to the sump.

2.5.2) The Auxiliary Circuits

A plunger type auxiliary pump, with three pistons, supplies fluid to individual control circuits, each having a pre-set single stage relief valve.

The manual circuit provides fluid to displace the thruster block assembly. This system incorporates a positional feedback device, to enable any position of the thruster block assembly to be chosen and maintained by movement of the speed control handle.

The 'Magnamatic' circuit provides the power loader motor with protection against overload and allows the machine to operate at maximum power conditions. When the motor current rises to 10% above the full load value, the Magnamatic overload valve diverts fluid to the thruster block and discharges fluid from the manual circuit to the sump. This causes the pump body to move towards the neutral position, thus reducing the haulage speed. This action continues until the motor current falls below its full load value, thus acting to operate the power loader at a speed commensurate to the optimum power level.

Under normal operating conditions the emergency stop circuit supplies fluid through the emergency stop valve, via the pilot operator shuttle valve, to the by-pass valve. This pressurised fluid holds the spool of the by-pass valve in a closed position against a spring force. When the emergency stop valve is operated, fluid is redirected to the manual speed interlock unit and the fluid maintaining the by-pass valve in a closed position is allowed to discharge to sump. This permits the spring force to move the by-pass spool, to a position where fluid in the main circuit can by-pass the hydraulic motor, at a rate which is controlled by the spool geometry.

The manual speed interlock unit comprises a fixed cylinder with two opposed pistons. These pistons operate against two adjustable stops, fitted to the mechanical linkage of the manual circuit speed control and force the linkage to return to the neutral position.

Pressure overload in the main circuit is sensed by the D-valve. Fluid is directed from the high pressure line of the main circuit, through a choke, to one end of the D-valve spool. This spool is normally kept closed by the action of a spring force at the opposite end. When pressure overload occurs, the spool is operated against the spring force and fluid is directed to the shuttle valve spool. This performs a similar function to the emergency stop valve in allowing the by-pass valve to operate. Also, on operation of the pressure overload, fluid is directed to the thruster block, causing the pump body to move to the neutral position thus reducing the haulage speed to zero. Once activated, the overload valve is held in the energised position, until reset by operation of the emergency stop valve.

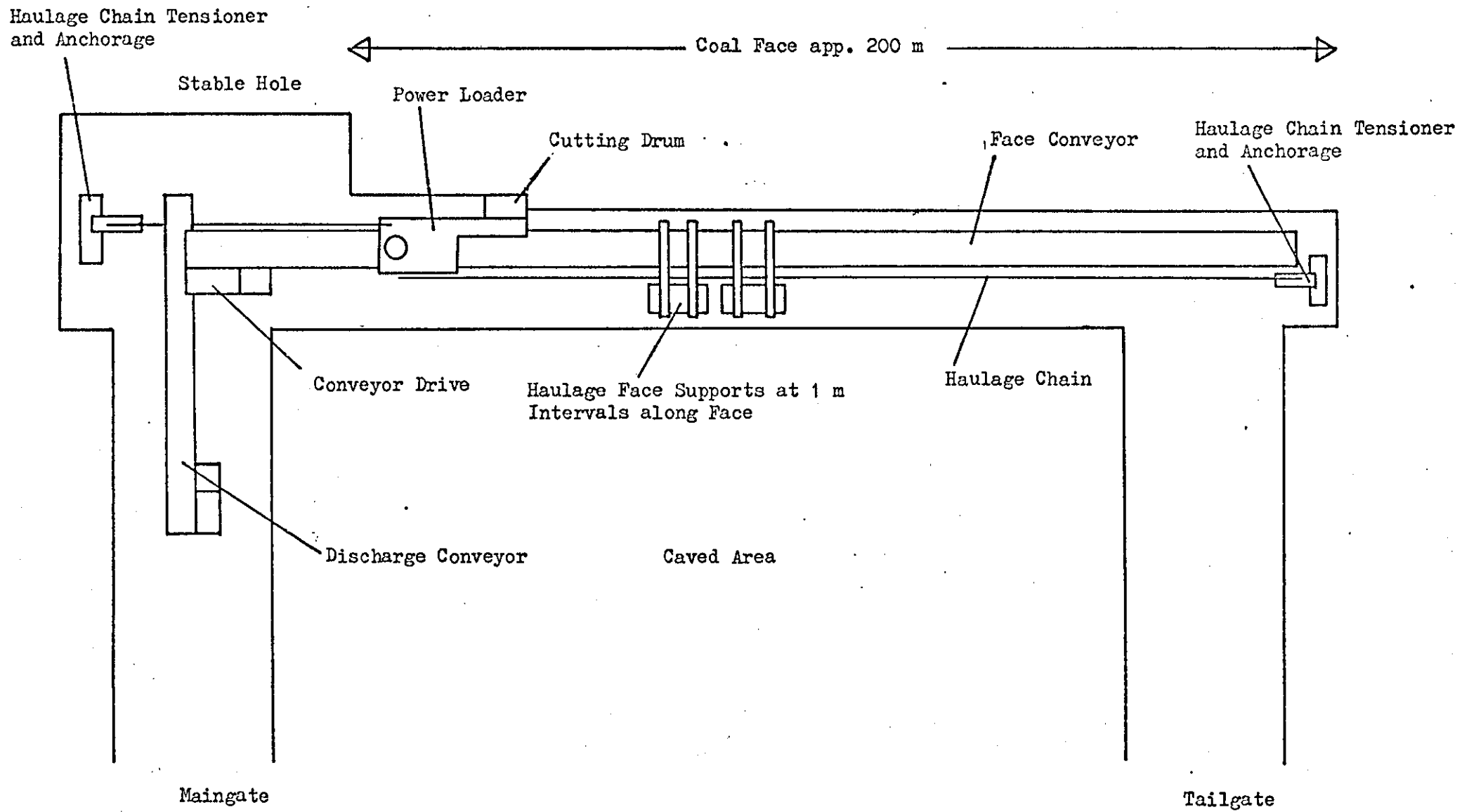


Fig. 2.1 Typical Coalface Layout

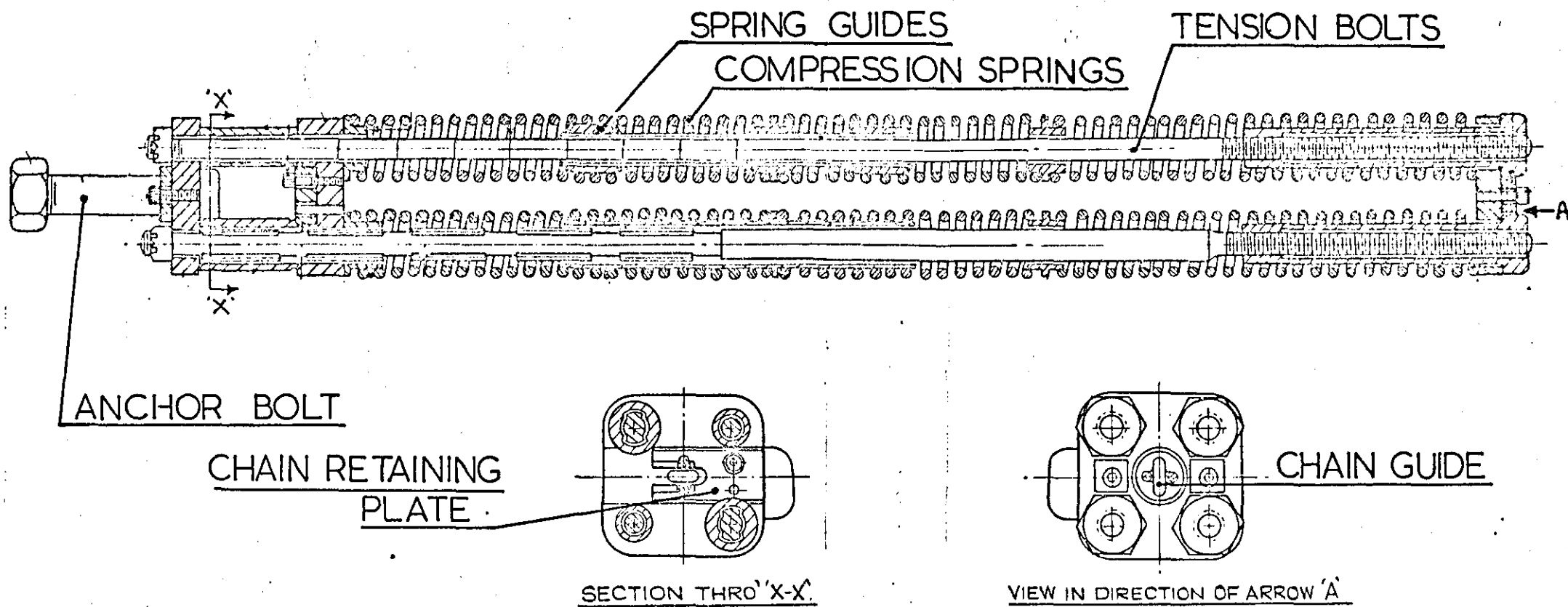


Fig. 2.2 Anderson Mavor Spring Type Chain Tensioner

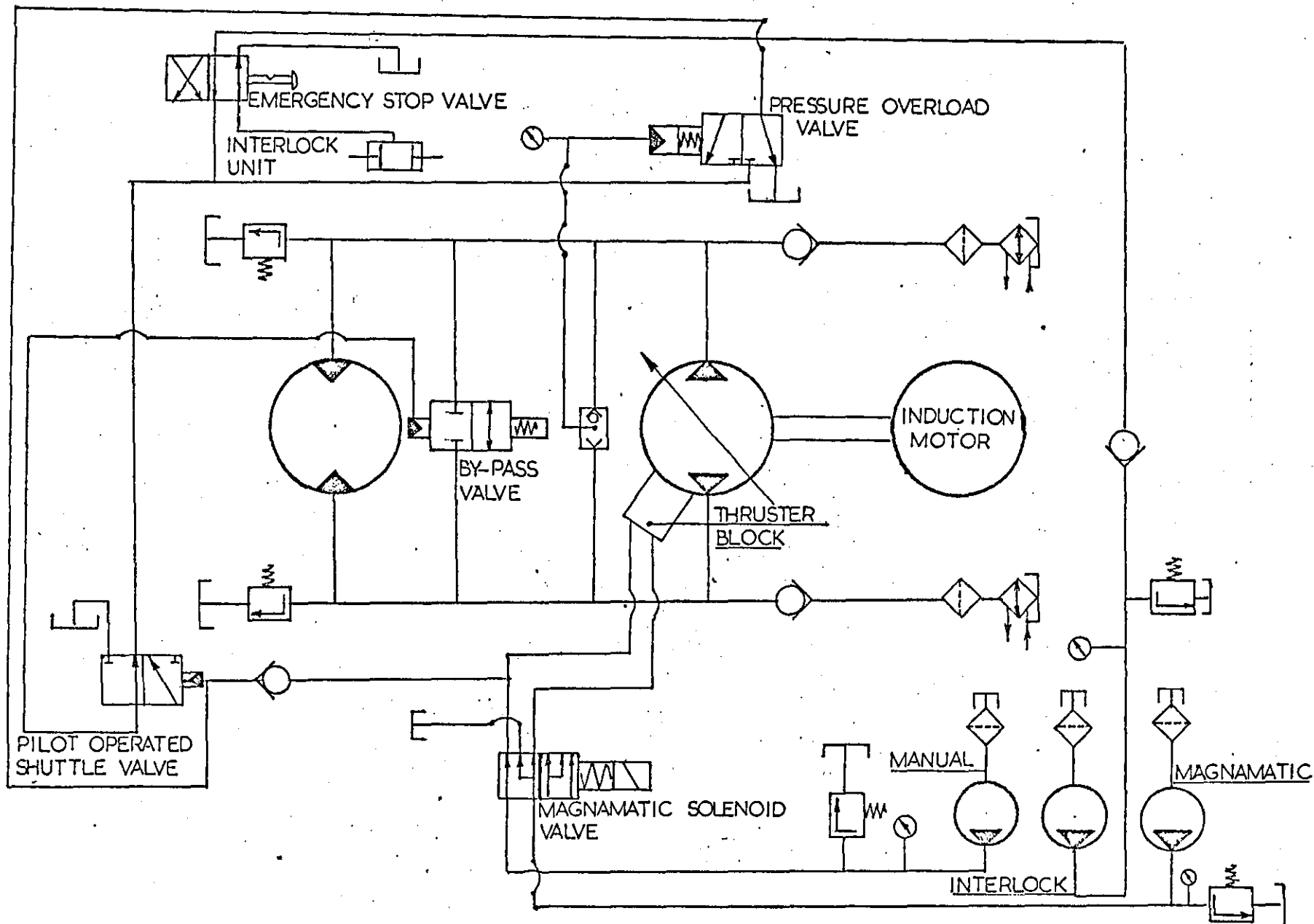
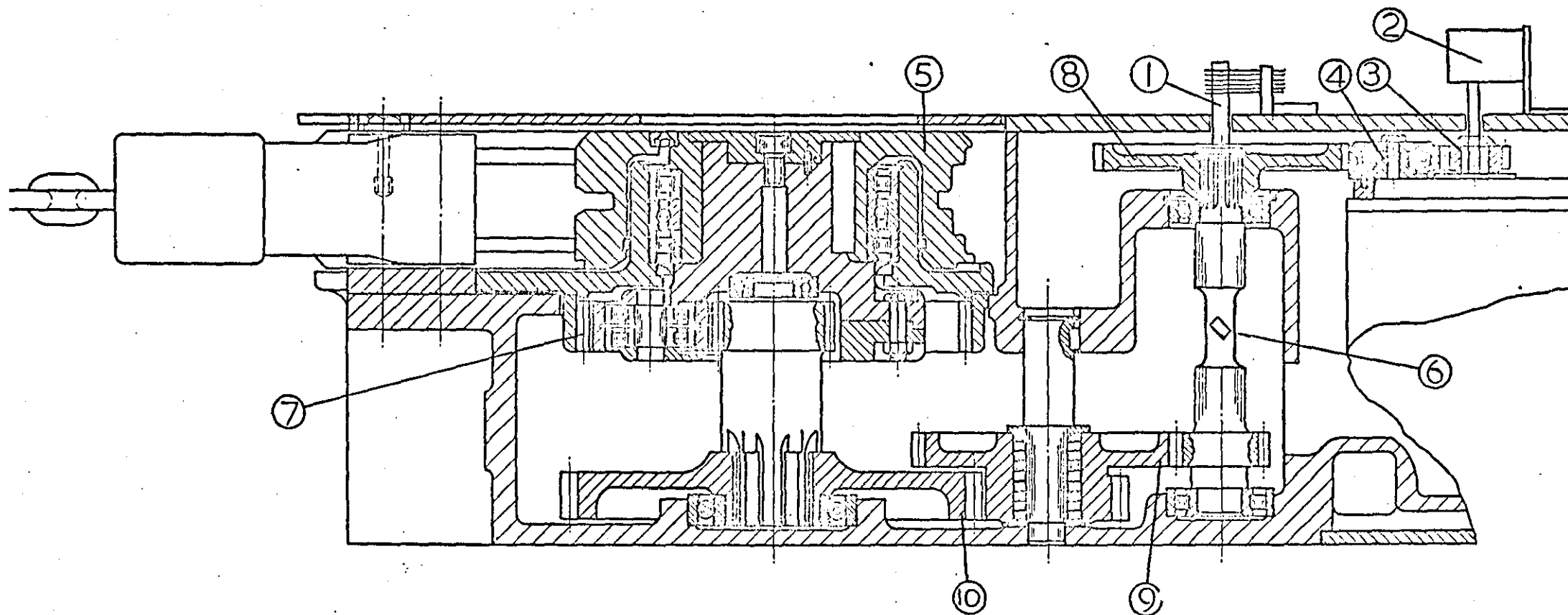
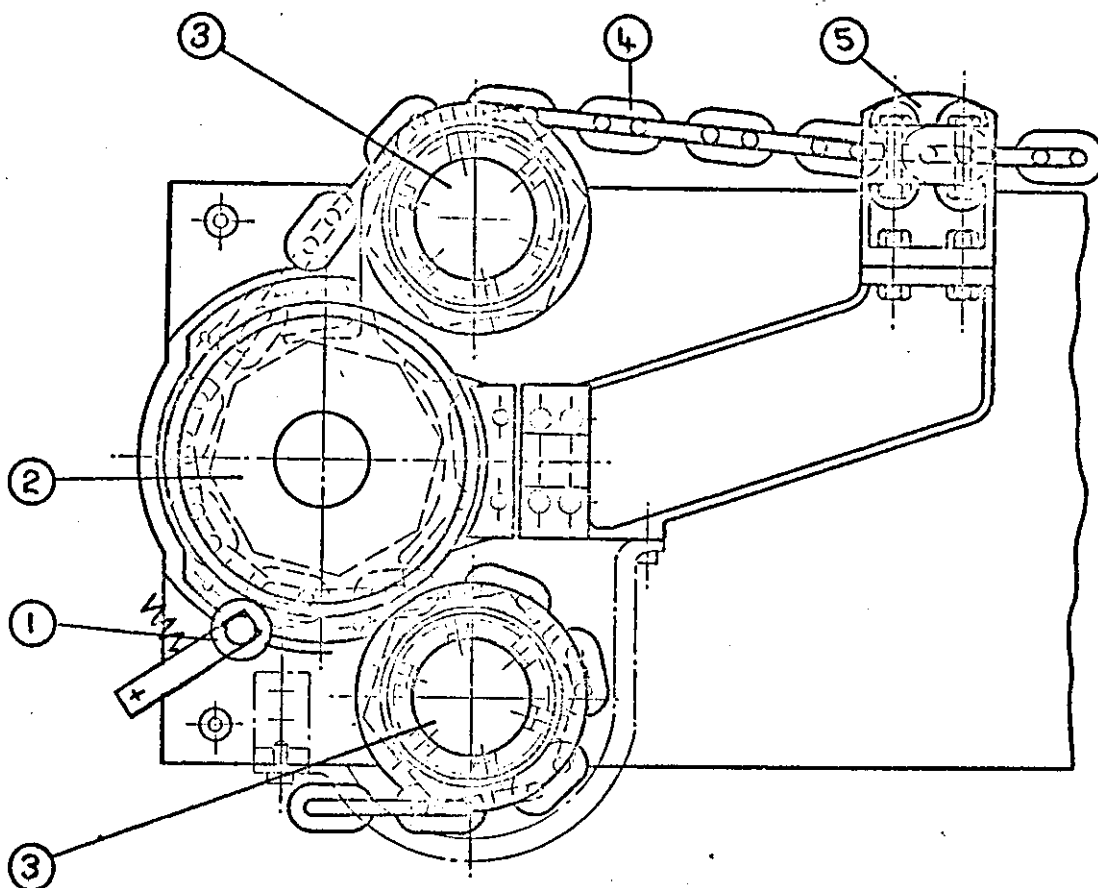


FIG. 2.3 BRITISH JEFFERY - DIAMOND B14D HAULAGE UNIT CIRCUIT DIAGRAM



- | | | | |
|---|----------------------------|----|---------------------------------|
| 1 | Slip rings | 6 | Torque measurement strain gauge |
| 2 | Tachometer | 7 | Epicyclic reduction gear |
| 3 | Hydraulic motor drive gear | 8 | 1st reduction wheel |
| 4 | Idler gear | 9 | 2nd reduction spur gears |
| 5 | Drive sprocket | 10 | 3rd reduction spur gears |

Figure 2.4 Cross section through BJ-D Ltd B14 haulage unit
showing position of instrumentation



- 1 Angular displacement transducer
- 2 Drive sprocket
- 3 Idler sprocket
- 4 Round link chain
- 5 Chain guide

Figure 2.5 Sprocket drive arrangement of a BJ-D Ltd B15 haulage unit showing the position of the angular displacement transducer

Note - Tests were carried out on a B14 haulage unit. This is similar to the above with the exception that the B14 has a 10 tooth drive sprocket and 8 tooth idler sprockets.

3 THE EFFECTS OF CHAIN ELASTICITY, CHAIN TENSIONERS AND SPROCKET LOSSES ON THE DISPLACEMENT-TORQUE CHARACTERISTICS OF SPROCKET DRIVE SYSTEMS

3.1 Introduction

To simulate the elasticity effects of haulage chain, on power loader haulage units using hydrostatic power absorbers, it is necessary to obtain torque-displacement characteristics for the haulage sprocket. This characteristic is dependent on the haulage chain and tensioner, tension-extension relationship, the frictional characteristics of the chain sprocket drive and the chain floor drag.

Many types of haulage chain installations are in use with the NCB, these together with their correct operational practice are fully described elsewhere, references 2 and 8. Brief descriptions however can be found in Section 2.3.

For the purpose of this analysis only the most common type of compensating device is considered, the Anderson Boyes spring tensioner. Other compensating devices have similar characteristics, only the undesirable solid anchorage system being different. The solid anchorage system however, gives lower elasticity effects on the haulage unit and since this analysis is concerned with safety aspects of chain elasticity, it is not considered in detail. As chain elasticity effects are greatest with the power loader at the end of the face, this analysis is also restricted to the condition where the power loader is hauling on the maximum chain length.

3.2 Frictional Losses in Round Link Chain Sprocket Drive System

As round link chain passes over a sprocket sliding movements with associated frictional losses occur, at the interlink connection and at the contacts between sprocket and chain. Interlink friction constitutes the major loss and is associated with high levels of wear. A laboratory assessment of tension loss due to round link chain passing over a 5 tooth

idler sprocket has been made, reference 3, the results of which are shown in Fig. 3.1.

To establish an elementary relationship between chain tension and interlink friction loss it is necessary to consider the connection between two links, Fig. 3.2.

Let (α) be the angle in rads. of rotation between two links as a chain moves onto a sprocket.

Angle (α) is dependent only on the number of sprocket teeth (spt). As 2 chain pitches are required per tooth.

$$\alpha = \frac{\pi}{spt} \quad \text{eqn. 3.01}$$

Each link intersection rotates through this angle twice, once passing onto a sprocket and once passing off. A condition can exist when the rotation angle is less than $\frac{\pi}{spt}$. When the angle between the chain line on and off the sprocket is less than $\frac{\pi}{spt}$, α becomes equal to this angle. This condition however does not usually occur on power loader haulage units. A detailed explanation of this rotation angle and its values for various haulage units is given in reference 8.

Work lost on one intersection under tension T_1 .

$$\text{Work lost per pitch} = \frac{T_1 \cdot \mu \cdot w \cdot \alpha}{2} \quad \text{eqn. 3.02}$$

If this chain is passing over a sprocket and the chain is moving a distance ($dist$)

$$\text{Total work lost} = \frac{dist}{pitch} \cdot \frac{T_1 \cdot \mu \cdot w \cdot \alpha}{2} \quad \text{eqn. 3.03}$$

Now let T_s be the chain tension on the sprocket after this loss has occurred

$$T_s \cdot dist = T_1 \cdot dist - \frac{dist}{pitch} \cdot \frac{T_1 \cdot \mu \cdot w \cdot \alpha}{2} \quad \text{eqn. 3.04}$$

giving a value of

$$T_s = T_1 - \frac{T_1}{pitch} \cdot \frac{\mu \cdot w \cdot \alpha}{2} \quad \text{eqn. 3.05}$$

$$T_1 \text{ tension loss due to interlink friction} = T_1 \left(\frac{\mu}{\text{pitch}} \cdot \frac{wd}{2} \cdot at \right)$$

This is only an average value over a distance, dist. sprocket geometry would considerably modify the instantaneous values of T_1 .

The tension loss T_1 can now be expressed in terms of a friction loss coefficient k_1 ie $T_1 = T_1 \cdot k_1$

$$k_1 = \frac{\mu \cdot wd \cdot at}{\text{pitch} \cdot 2} \quad \text{eqn. 3.06}$$

Values of k_1 associated with various sprocket sizes, chain sizes and friction coefficients have been calculated from this relationship and are shown in Table 3.1.

For a typical power loader haulage drive system with one drive sprocket and two idler sprockets, the total link rotation onto the drive system will be

$$at_1 = \frac{\pi}{spt} + \frac{2 \cdot \pi}{idt} \quad \text{where } idt = \text{teeth on idler} \quad \text{eqn. 3.07}$$

which will equal the link rotation angle off the drive system.

For simplification assume that the tension losses can be calculated with all chain coming onto the drive under tension T_1 and all chain going off the drive under tension T_2 . (This lumps the losses together, calculated at one tension, instead of their being treated individually, with new tensions calculated after each link rotation).

Let k_{1t} be the constant k_1 with at . equal to at_1 then

$$\frac{T_{rm}}{pcr} = T_1 - T_2 + k_{1t} (T_1 + T_2) \quad \text{eqn. 3.08}$$

$$\frac{T_{rp}}{pcr} = T_1 - T_2 - k_{1t} (T_1 + T_2) \quad \text{eqn. 3.09}$$

These equations for T_{rm} , the sprocket torque with the haulage driving and T_{rp} , the sprocket torque with the haulage unit being driven, can be used to assess the losses that occur in the sprocket drive system when changing from driving to driven. This condition occurs when the haulage drive is disengaged, and the chain drives the haulage in reverse.

Factor k_1 is assumed to include all frictional losses and an assessment of its value can be obtained from the results shown in reference 3. These results have been processed and values for k_1 and μ are shown in Fig. 3.1.

The following procedure was used for these calculations. Consider an idler sprocket with tensions T_1 and T_2 on either side

$$\text{Tension lost } T_l = k_1 (T_1 + T_2) \quad \text{eqn. 3.10}$$

$$\text{also } T_l = T_1 - T_2$$

Manipulation now gives

$$T_l = T_1 \left(\frac{2 \cdot k_1}{1 + k_1} \right) \quad \text{eqn. 3.11}$$

$$\& k_1 = \frac{T_l}{2T_1 - T_l} \quad \text{eqn. 3.12}$$

The use of the loss coefficient k_1 , to calculate tension losses around sprockets, assumes that the losses are due only to interlink friction. To assess the values of the losses associated with the sliding movements between sprocket and chain, data related to the sprocket and chain geometry and their conditions of wear is required. However, since these sliding contacts occur only every two pitches, as opposed to every pitch for interlink friction losses, and the relative movements are small in comparison with interlink rotation, they are thought to account for only 10 - 15% of the total losses. For this reason they are considered to be lumped together with interlink friction losses.

The results from reference 3 suggest a value of $\mu = .7$ within the linear range, this is considered reasonable since it contains the additional sliding losses. The non-linear portion of the curve at higher tensions gives values of μ increasing above 1.0. Here contact stresses are high and localised welding could be occurring together with a pinching action between adjacent links.

3.3 Determination of the Torque-Displacement Characteristics of Power Loader Haulage Units Working on Round Link Chain with Spring Tensioners

Consider a face system employing spring type compensating devices.

A diagrammatic representation of the face system is shown in Fig. 3.3 and a drawing of a spring tensioner in Fig. 2.2. The system is set up by increasing tension T_1 to the maximum value t_{max} and then securing the chain to the tensioner on the T_2 side. With $T_1 = t_{max}$ this will fully compress the springs in the T_1 tensioner and the T_2 tensioner springs will be fully extended.

→ Compensating devices should be selected to have approximately an equivalent available compression (a_c) to the maximum chain extension the haulage can produce. If the compression available from the tensioners is less than the maximum chain extension, when t_{max} is released, T_1 and T_2 will equalise leaving both tensioners fully compressed and T_1 and T_2 equal to the pre-tension value of $t_{max} - a_c$. Under these conditions the maximum chain movement through the sprocket drive system is equal to the available tensioner compression.

Alternatively, if tensioners are chosen with more available compression than the maximum chain extension, the pre-tension condition leaves the tensioners only partially compressed. As space is at a premium in the confines of the face ends it is more likely that the smaller tensioner would be chosen and the higher pre-tension accepted.

A third possibility, is that, on set up, some slack chain is left in the T_2 side, this can reduce the value of pre-tension if the available compression from the tensioners is much less than the maximum chain extension. Some power loaders, particularly those with vertical sprockets can operate satisfactorily with small amounts of slack chain. Under these conditions, the maximum chain movement through the sprocket drive system will be equal to the available compression from the tensioner plus the amount of slack chain.

For this analysis only the ideal case is considered where the maximum chain extension is slightly greater than the available compression from the tensioners.

The previously mentioned cases introduce discontinuities into the tension-displacement relationships and are not easily simulated. The conversational programme Appendix II assumes that the introduction of slack chain increases the available compression a_c of the tensioner.

Let (z) be the amount of chain that passes through the sprocket system from the set up condition, this is equivalent to the movement of the T2 tensioner. Therefore $z = 0$ when $T1 = t_{max}$.

The tensions $T1$ and $T2$ can now be described as

$$T1 = t_{max} - z.sc \quad \text{eqn. 3.13}$$

$$T2 = pc + z.s \quad \text{eqn. 3.14}$$

Combining eqn. 3.08, 3.09, 3.13 and 3.14 and making

$$T_p = \frac{T_{rp}}{p_{cr}} \text{ and } T_m = \frac{T_{rm}}{p_{cr}}$$

$$T_m = t_{max}(1 + k1t) - pc(1 - k1t) - z(sc(1 + k1t) + s(1 - k1t)) \quad \text{eqn. 3.15}$$

$$T_p = t_{max}(1 - k1t) - pc(1 + k1t) - z(sc(1 - k1t) + s(1 + k1t)) \quad \text{eqn. 3.16}$$

The relationship between T_{rp} and z gives the torque-displacement characteristic produced by the chain on the haulage under conditions of energy release, ie chain driving sprocket. Inspection of eqn. 3.16 shows this characteristic to depend on the elasticity of the chain, the stiffness of the chain tensioners and the friction loss coefficient.

Manipulation of eqn. 3.16 gives the gradient of this relationship to be

$$sc(1 - k1t) + s(1 + k1t) \quad \text{eqn. 3.17}$$

in terms of tension-displacement, ie an effective stiffness for the chain system where the chain elasticity is modified by the loss coefficient and the tensioner stiffness.

To fully describe the energy release characteristics using the gradient relationship determined above, one point is required on the characteristic. The most suitable point is the sprocket torque when $z = a_c$ the torque when the amount of chain displacement through the sprocket system is equivalent to the available tensioner displacement.

When using accumulator banks and hydrostatic absorbers for simulation of chain elasticity effects this point corresponds to the pre-charge pressure setting of the first accumulator.

With $z = ac$

$$T_p = t_{max}(1 - k_1t) - p_c(1 + k_1t) + s(1 + k_1t) \quad \text{eqn. 3.18}$$

A further important consideration in the simulation is the change in sprocket torque at the point of reversal, where the haulage stops driving the chain and is driven by the strain energy in the chain.

This reduction in torque is given by

$$\frac{T_m - T_p}{p_{cr}} = 2.k_1t (t_{max} + p_c + z(s - s_c)) \quad \text{eqn. 3.19}$$

Note: These equations have been developed using the maximum tension in T_1 , t_{max} . However, haulages are usually rated on maximum system pressure, if the corresponding maximum sprocket torque t_{mm} is known, t_{max} can be determined from $t_{max} = \frac{t_{mm}}{1 + k_1t}$ (p_c being zero under set up conditions).
eqn. 3.20

Typical characteristics of a face chain system are shown graphically in Fig. 3.4.

3.4 Torque-Displacement Characteristics using Hydraulic Type Compensating Devices

Hydraulic chain tensioners usually employ a ram working at a constant pressure to give constant values of T_2 .

For such systems equations 3.15, 3.16 and 3.19 can be modified to become

$$T_m = t_{max} (1 + k_1t) - T_2(1 - k_1t) - z s_c(1 + k_1t) \quad \text{eqn. 3.21}$$

$$T_p = t_{max} (1 - k_1t) - T_2(1 + k_1t) - z s_c(1 - k_1t) \quad \text{eqn. 3.22}$$

$$\frac{T_m - T_p}{p_{cr}} = 2.k_1t(t_{max} - z s_c + T_2) \quad \text{eqn. 3.23}$$

3.5 Comparison between Face Chain Systems Employing Compensating Devices and Solid Anchorages

The disadvantages of the solid anchorage system as compared with the use of compensating devices is best shown by an example. The method of set

up using solid anchorages is similar to that described for use with compensating devices. With the machine hauling on the maximum length of chain with the maximum haulage force (to achieve maximum chain tension the machine must be spragged into the coal face) the slack chain is pulled through the haulage and an attachment made to the anchorage point. This then gives the chain a pre-tension of t_{max} . Fig. 3.5(a) shows the system in the relaxed condition with no haulage force and a pre-tension of 100 kN (10 tons). With the machine hauling on the maximum chain length with maximum effort, Fig. 3.5(b), (also the set up condition), $T_1 = 100$ kN (10 tons) and $T_2 = 0$, giving 100 kN (10 tons) machine effort. Note: No chain need pass through the sprocket system to get to this condition from the relaxed state.

Figs. 3.5(c) and 3.5(d) show the machine at mid-face and at the face end hauling on a minimum chain length. In both cases the chain effort is 100 kN (10 tons) but in mid-face T_1 and T_2 are 150 kN and 50 kN (15 tons and 5 tons) and at the face end $T_1 = 200$ kN (20 tons) and $T_2 = 0$. To achieve the mid-face condition the chain movement through the sprocket system is equivalent to 50 kN (5 tons) acting on $\frac{1}{2}$ the face length of chain. To achieve the final condition no chain need pass through the sprocket system.

With a compensating device to hold T_2 constant at say 30 kN (3 tons) Figs. 3.5(e) to 3.5(r) at all face positions, machine effort is 100 kN (10 tons). Movement of chain through the sprocket system to achieve these conditions is equivalent to 100 kN (10 tons) acting on the full face length of chain for Fig. 3.5(e), 100 kN (10 tons) acting on $\frac{1}{2}$ face length for Fig. 3.5(c) and 100 kN (10 tons) acting on the minimum chain length for Fig. 3.5(d).

This clearly shows that a solid anchorage system generates chain tensions nearly twice those generated by the compensated system working with similar haulage forces, leading to higher chain wear and friction losses. Although

the tensions are higher the amount of chain moved through the system is less when using solid anchorages. The maximum movement occurs with the machine in mid-face and is only about 25% of the amount which moves through the compensated system with the machine hauling on maximum chain length.

As the effects of chain elasticity on haulage units are higher with compensated force chain systems further analysis is confined to systems employing chain tensioners. Such systems are preferred operationally but are less common in service.

3.6 Tension Losses due to Chain Drag

The weight of a tensioned haulage chain is supported partly by either the floor or any other lower restraint such as the armoured face conveyor pans. Between $\frac{1}{2}$ and $\frac{3}{4}$ of the chain length is supported for a nominally tensioned chain.

When a chain supported in this way is stretched, a portion of the work done will be absorbed in friction with the support surface. As the tension is reduced, further energy will be absorbed and some residual tension will be left in the chain.

For a catenary it can be shown that for a uniform chain, where the tension is much greater than the weight of the chain

$$L_a = k_s \sqrt{T_a} \text{ where } k_s = \sqrt{\frac{2 \cdot \text{sag}}{w l}} \text{ (see Fig. 3.6)} \quad \text{eqn. 3.24}$$

$$\text{so } T_a - T_b = (L - L_a - L_b) w l \cdot \text{mus} \quad \text{eqn. 3.25}$$

assuming $L_a = L_b$

$$T_a - T_b = (1 - 2k_s \sqrt{T_a}) w l \cdot \text{mus} \quad \text{eqn. 3.26}$$

Fig. 3.6 shows assessment of the tension loss due to chain drag for a typical haulage chain. The tension extension relationship can be seen to be displaced by 5 kN (0.5 ton) between the tension increasing and decreasing conditions.

This assessment is very idealised when compared with the conditions under which any face chain would actually operate. All faces are not

straight in either the horizontal or vertical planes so the chain could be forced on to either the floor or the face wall, leading to extra drag.

→ Conditions could exist where the chain was lying on the face conveyor^{or}, if this was running, the flight bars would increase the drag in one direction and assist the tension in the opposite direction. Devices also exist to keep the chain clear of any contact with conveyor floor which may or may not be used on any installation. It is unlikely that any chain drag could be represented by friction coefficients, operating conditions are never constant, chains can get snagged and are often completely covered in coal.

Chain drag effects will be similar and additional to chain hysteresis effects.

3.7 Force Extension Characteristics of Round Link Chain

Extensive tests to determine the force-extension characteristics of round link chain have been described in reference 1. This characteristic is affected by the shape of the chain link, the area of contact between the adjacent links and the general condition of the chain. Reference 1 quotes "no absolute force-extension characteristic exists for a particular type of chain". However, this reference recommends the use of average linear values for chain elasticity calculations.

Tension loss coefficient k ₁						
Coefficient of friction	$\mu = .5$			$\mu = .6$		
Chain size	18 mm	22 mm	26 mm	18 mm	22 mm	26 mm
Sprocket teeth						
5	.044	.040	.044	.053	.048	.053
6	.037	.036	.037	.044	.043	.044
7	.032	.029	.032	.038	.035	.038
8	.028	.025	.028	.037	.030	.037
9	.025	.022	.025	.030	.026	.030
10	.022	.020	.022	.026	.024	.026

Table 3.1 Tension loss coefficient values for typical chain and sprocket combination.

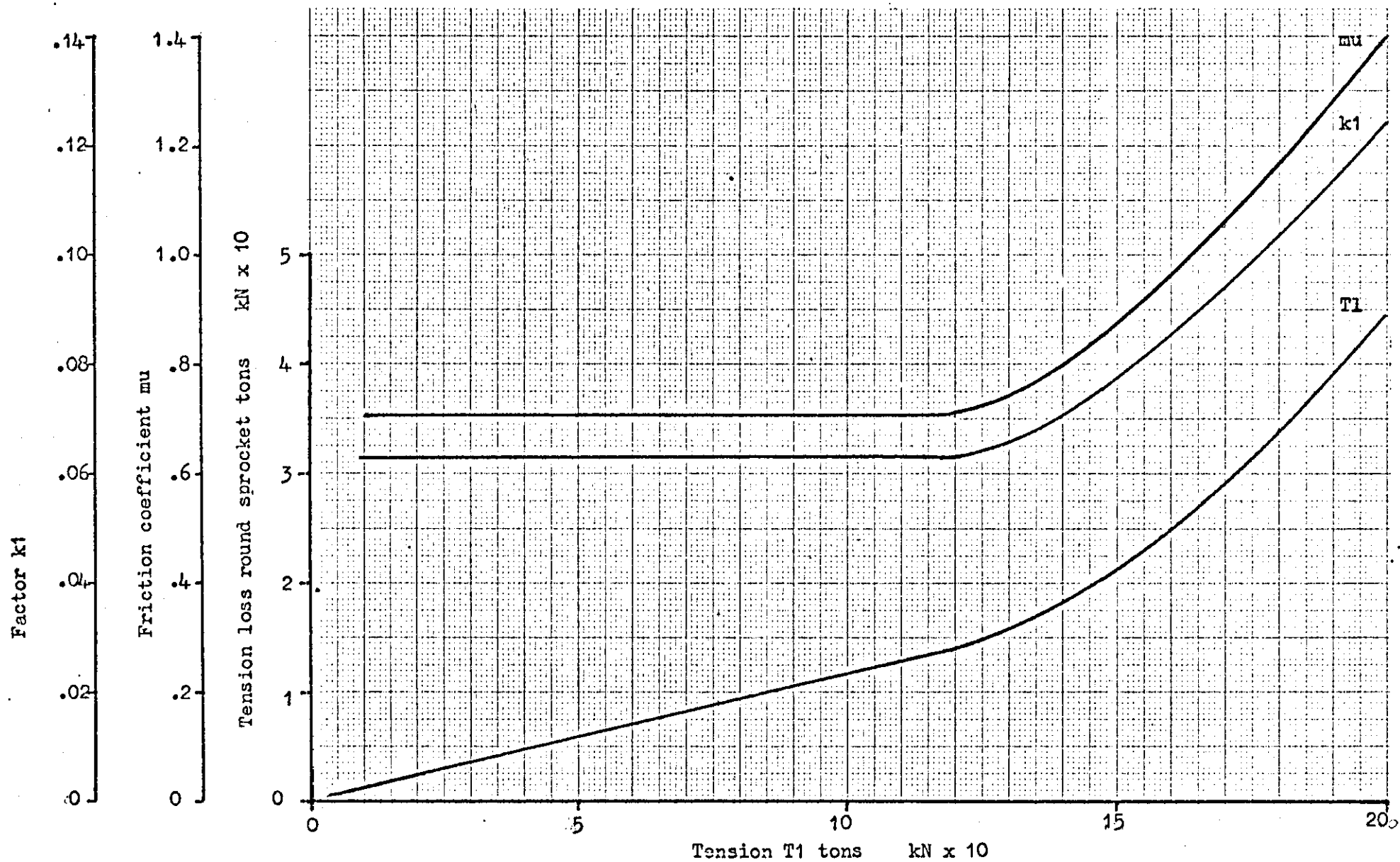
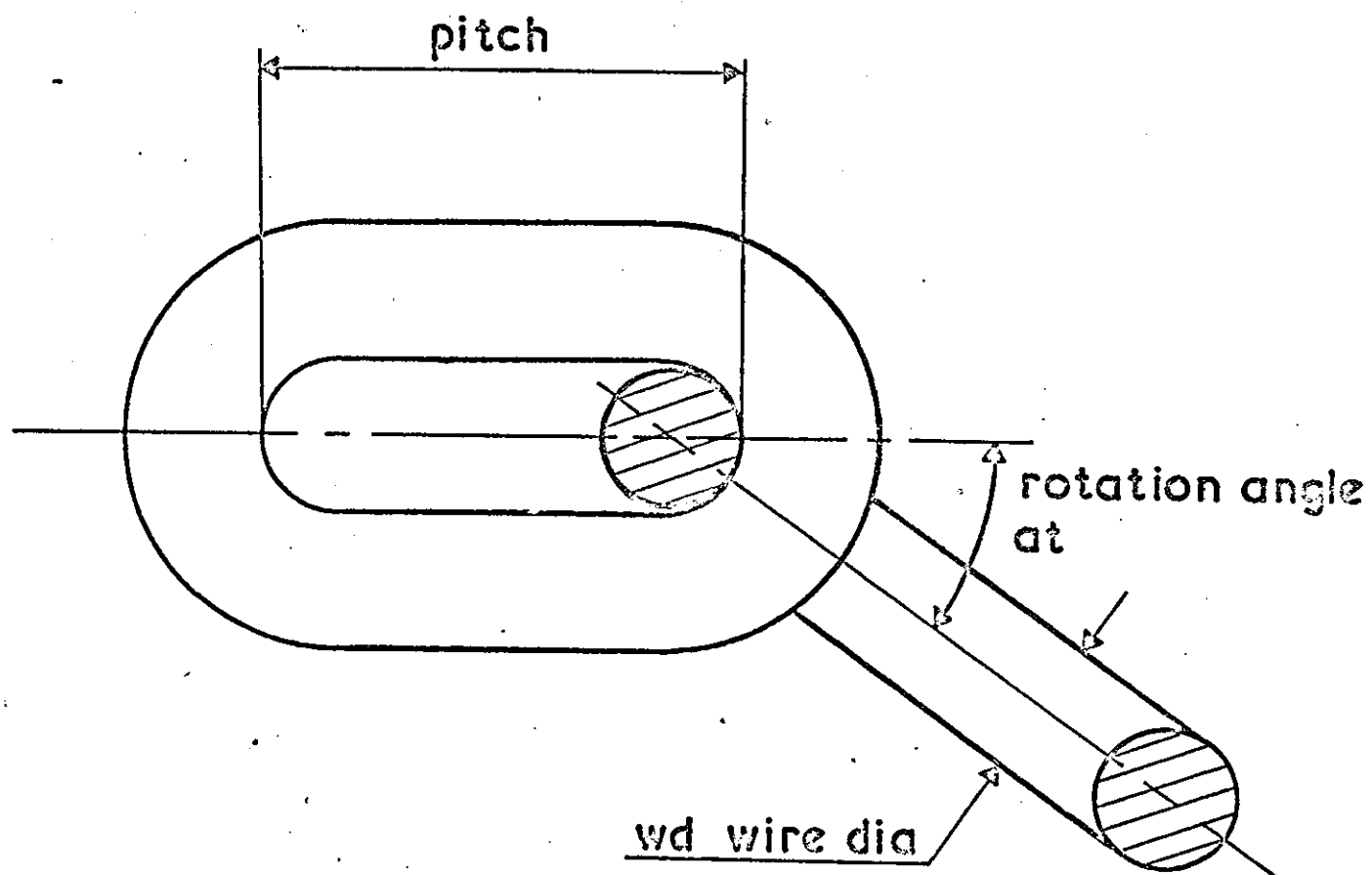


Figure 3.1 Tension loss on an idler sprocket

5 tooth sprocket
 18 mm round link chain
 Chain speed 5ft/min (.025 m/sec)



18 mm chain full scale

Fig.3-2 Typical Connection between two Links
of Haulage Chain

Tensioner pre-compression force p_c

Available compression

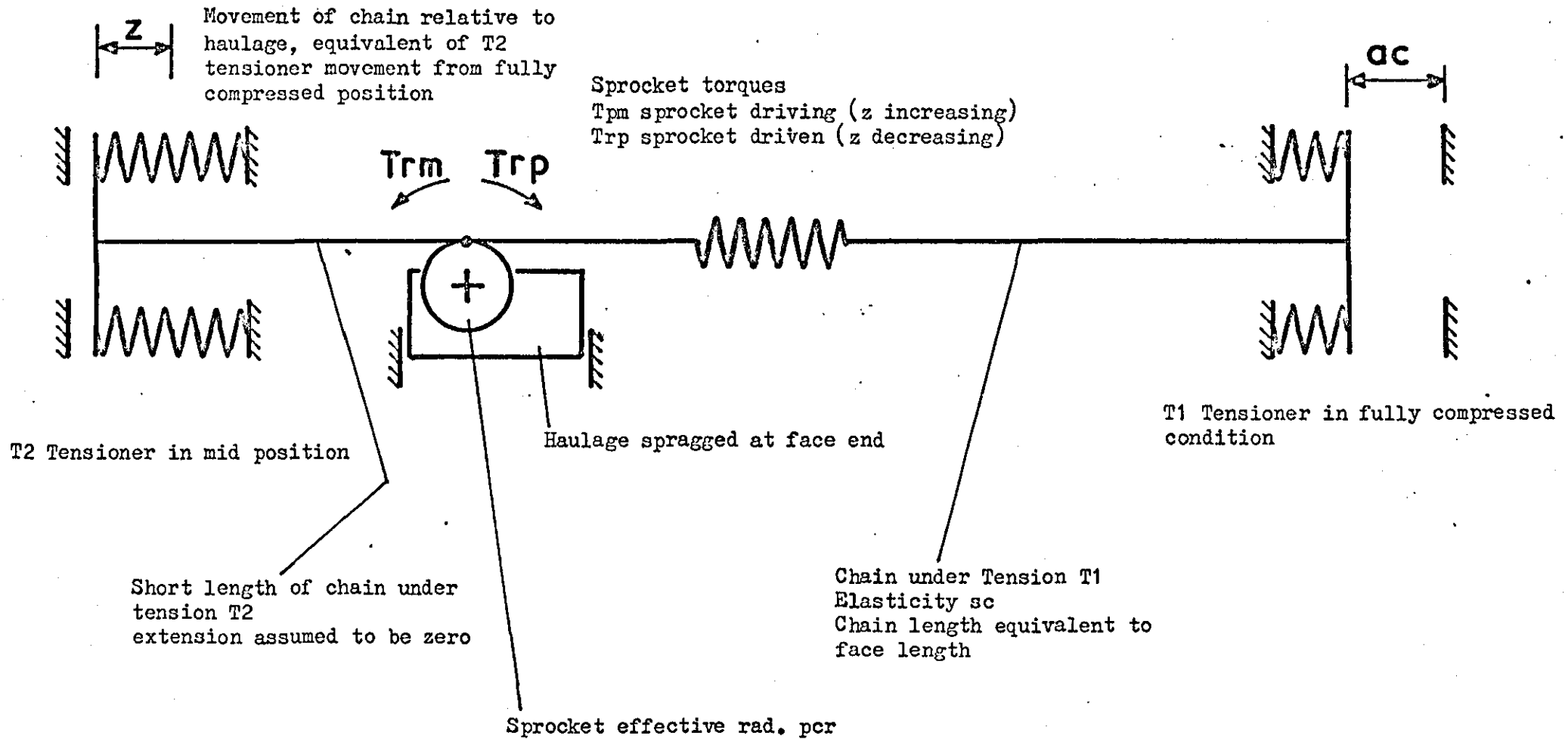


Fig. 3.3 Diagrammatic Representation of Face Chain System

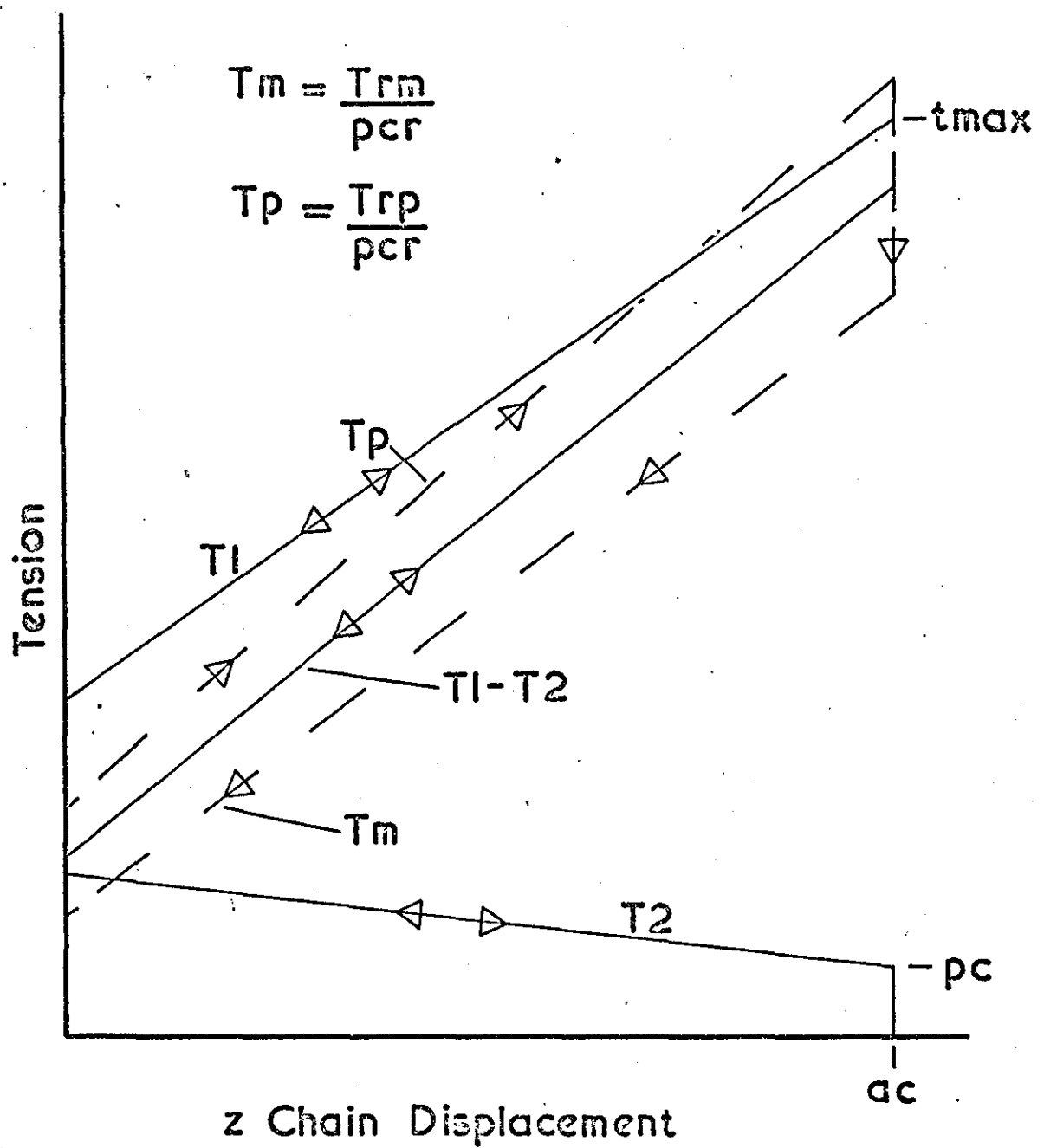
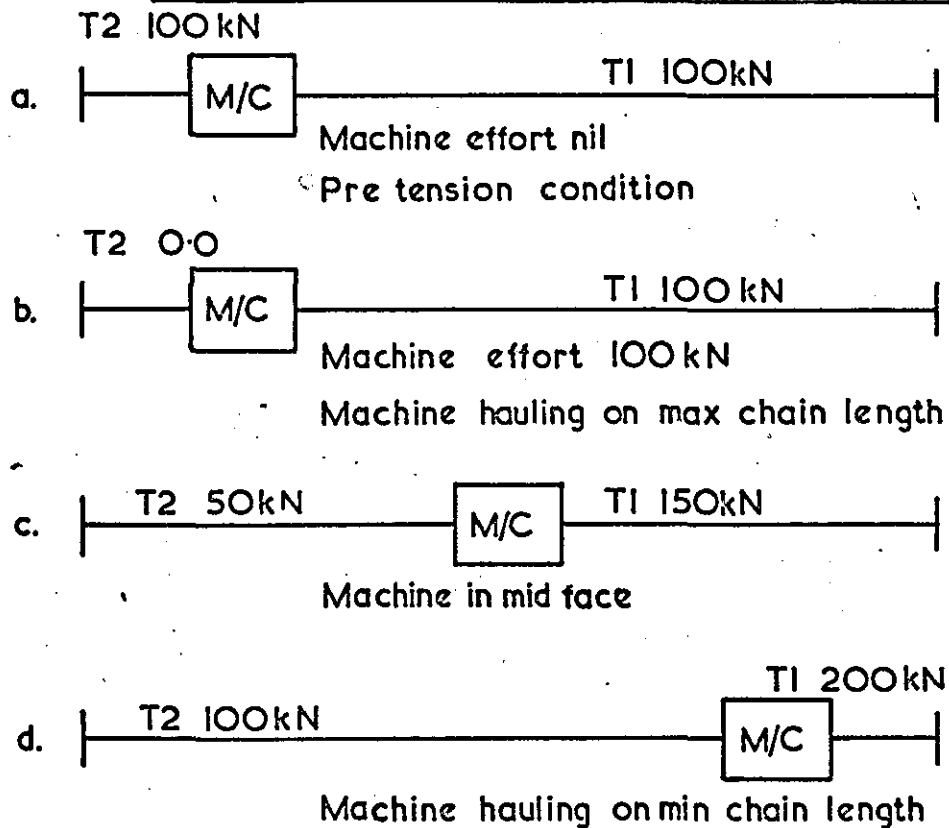


Fig.3:4 Typical Characteristics of a Face Chain System

Face Chain System with Solid Anchorage Points



Face Chain System with Spring Tensioners

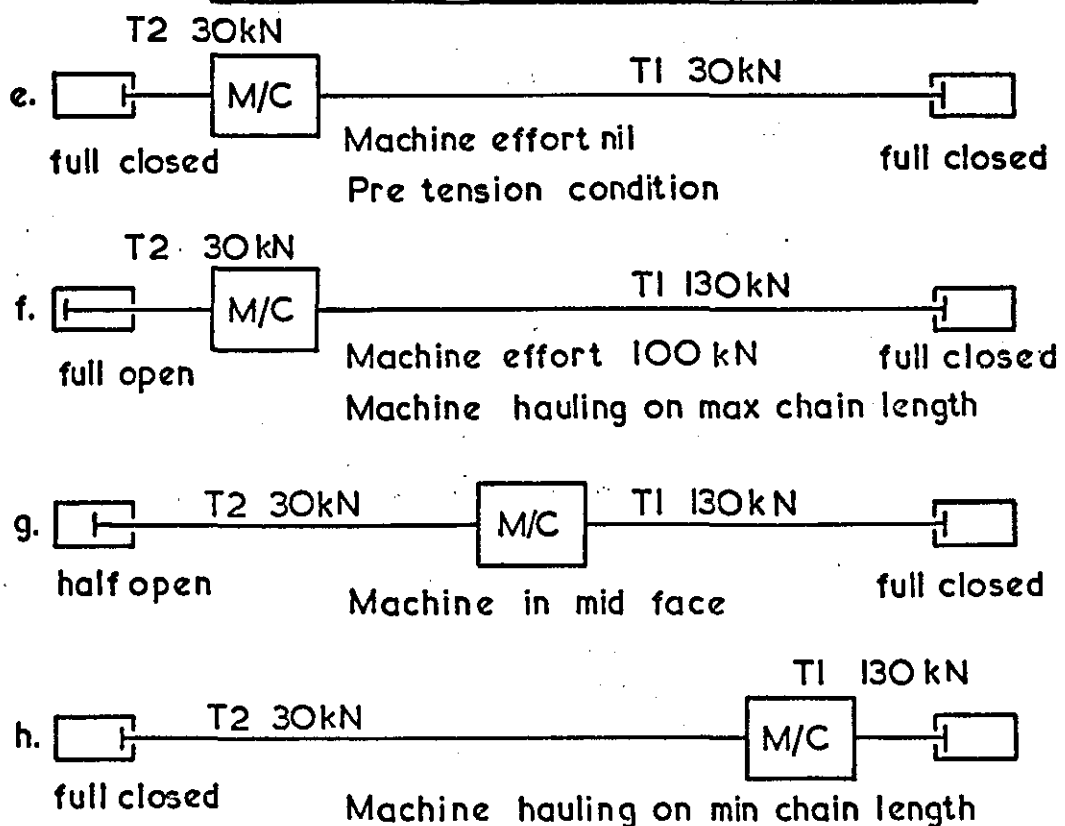


Fig. 3.5 Comparison between Face Chain Systems with Solid Anchorage and Chain Tensioners

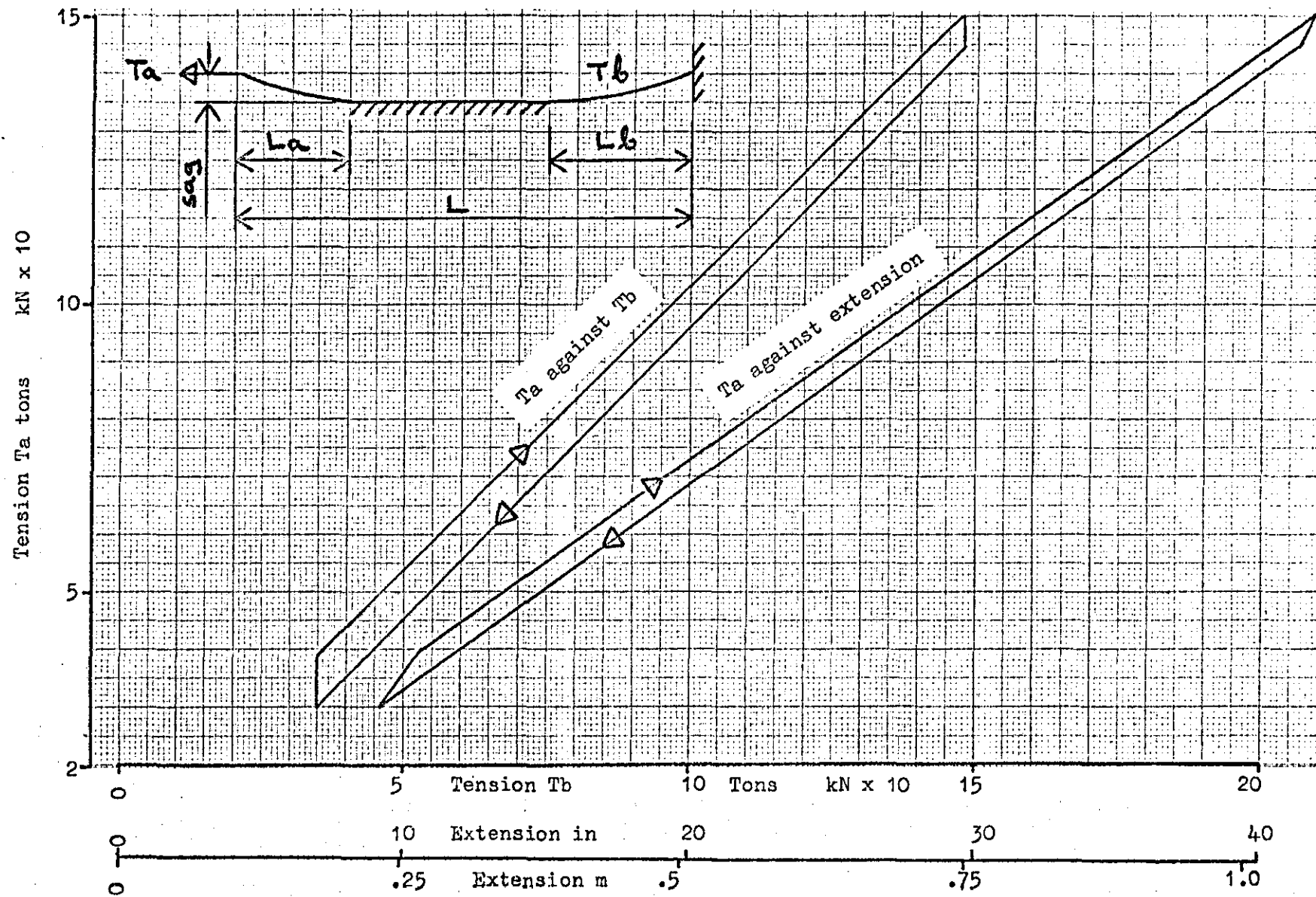


Fig. 3.6 Calculated chain drag characteristics for a typical face

4 EXPERIMENTAL EXAMINATION OF A POWER LOADER HAULAGE UNIT LOADED WITH A CHAIN SYSTEM

4.1 Introduction

To form a basis for the simulation of chain elasticity effects using hydrostatic power absorbers, it was necessary to obtain some experimental data from a haulage unit loaded with a chain system, such as would be used on a typical coal face. Due to the extreme difficulties involved in conducting underground experimental work, use was made of an existing mock face system at the Swadlincote Test Site of MRDE.

4.2 Description

The facility available at Swadlincote Test Site included a 200 m length of armoured face conveyor pans, 200 m of 18 mm round link chain, two Anderson Mavor spring type compensating devices and anchorage points for the chain and haulage unit. The haulage unit used was the same BJ-D B14 with 88 kW (120 hp) induction motor as used for the laboratory experiments. Photographs of the test facility are shown in Figs. 4.1, 4.2 and 4.3.

4.3 Instrumentation

As determination of the displacement-torque relationship was an important feature of this work a measurement was required of the haulage drive sprocket torque. To obtain this the first reduction shaft in the haulage gearbox was fitted with strain gauges (Fig. 4.4). The connecting terminal wires were taken inside the shaft up to a set of slip rings. Brush wires which contacted the slip rings were attached to the haulage cover. The strain gauged shaft was calibrated in the laboratory with the haulage unit loaded with a hydrostatic absorber through a British Hovercraft Ltd torque transducer. Signals from the torque transducer and the strain gauged shaft were compared on a Bryans X - Y plotter. The haulage unit was run in both the driving and driven modes at constant sprocket torque. Adjustments of gain were made to the signals from the

strain gauged shaft to show equal losses in both modes of operation. This gave an effective method of calibration and also an indication of the losses in the haulage gearbox between the strain gauged shaft and the drive sprocket.

Chain tensions were measured using a British Hovercraft Ltd 500 kN (50 ton) strain gauge tensometer fitted in the haulage chain either side of the haulage unit. A 10 turn rotary potentiometer, with a follower disc in contact with the drive sprocket, was used to give measurements of sprocket displacement. Haulage speed was determined using a magnetic pulse type tachometer, connected to the hydraulic motor, through a flexible coupling. This device operated with a fast response frequency to analog converter. Haulage pressure was measured using a strain gauge type pressure transducer fitted to a tapping in the high pressure side of the transmission unit.

Outputs from all the transducers were fed into a Bryans 2600 X - Y plotter via appropriate amplifier modules. A summing amplifier was available for use with the chain tensometers to give a measurement of the effective haulage force $T_1 - T_2$.

4.4 Test Procedure

As chain elasticity effects are greatest with the power loader hauling on the maximum length of chain, the haulage unit was positioned and fixed with 185 m of chain on the T_1 side and 15 m on the T_2 side.

The chain system was set up using the recommended procedures to give optimum performance of the compensators.

Tension was applied to T_2 sufficient to partially compress the springs and the compression locking device applied. Near maximum tension was then applied to T_1 , the chain extended and the slack chain pulled through the T_2 compensator and the chain attached. Removal of the compression lock allowed the slack chain that could not be pulled through to be tightened. An application of full tension up to the operation of the overload device

then showed whether sufficient chain had been pulled through the T2 compensator to eliminate slack chain at overload tension. Final corrections were made to achieve this condition.

A series of tests were carried out to obtain X - Y recordings of the basic system parameters against the sprocket displacement. For these recordings, the haulage unit was allowed to increase the tension T1 at $\frac{1}{4}$ speed up to the overload pressure, at which the by-pass valve operated and the chain relaxed rotating the haulage sprocket back to the equilibrium condition. These tests were made using the 1.02 mm (.040 in) by-pass valve to give a steady return speed. Checks were made for speed effects by repeating the tests with maximum forward speed and unrestricted by-pass valves, giving maximum return speed. Stall conditions were achieved by allowing the haulage to extend the chain at a minimum forward speed and prior to the operation of the overload valve, reversing the speed slightly until a minimum return speed was obtained.

Using by-pass valve spools with varying sizes of restricting annuli, a series of tests was carried out to observe the relationship between rate of release of energy from the chain and by-pass valve size. Here again, the haulage was driven up to the overload pressure at $\frac{1}{4}$ speed and allowed to reverse back to equilibrium conditions. Recordings were taken on the X - Y plotter of haulage speed against displacement, the second Y channel was used on time base to estimate the time taken for energy release.

Stabilisation of the fluid temperature was not easily achieved but attempts were made to obtain a sump temperature of 40°C to 60°C prior to the recordings by periods of continuous running.

4.5 Results

Figs. 4.5 to 4.8 show the X - Y recordings of T1 and T2, T1 - T2, sprocket torque and haulage pressure against sprocket angular displacement. For these recordings a forward speed of $\frac{1}{4}$ maximum was used and a return

speed controlled by a 1.02 mm (.040 in) by-pass valve.

A typical recording of haulage speed against sprocket angular displacement is shown in Fig. 4.9. The results for various sizes of by-pass valve spool are shown in Table 4.1.

4.6 Observations

4.6.1) Tension Characteristics

The recordings of T1 and T2 against sprocket displacement Fig. 4.5 clearly show the chain drag and hysteresis losses on T1 as described in Section 3.6. The non-linearity of this relationship can also be seen as described in reference 1. At a point of constant displacement the characteristic for tension increasing is separated from the decreasing tension characteristic by approximately 5 kN (.5 tons).

The losses associated with T2, directly due to the compensating device, are higher than the chain drag and hysteresis seen on the T1 recording. This was partly due to the compensating device not being mounted in the ideal position. The anchorage point available was high, allowing a sideways reaction on the guide rods which added to the frictional losses. Such losses however could be similar to those met in underground operations since the compensating device, mounted in a low position, is subject to being covered with coal and binding on the floor and other objects.

The combined effect of the T1 and T2 losses is seen in the recording of T1 - T2 against sprocket displacement characteristic Fig. 4.6. Here the haulage driving characteristic is separated from the haulage driven characteristic by approximately 10 kN (1 ton).

The tension-displacement characteristics were not appreciably altered by changes in the rates of increase or decrease.

On the T2 tension characteristic a reduction to zero at maximum displacement will be seen together with an associated modification to the T1 - T2 characteristic. This is due to the initial set up conditions of

the chain system. A small amount of slack chain can be accommodated by most haulage units and by setting the compensators to leave slack chain, the pre-tension of the chain (the tension at equilibrium) is reduced. After the T2 compensator has reached its maximum expanded condition the slack chain hangs in a catenary, this can provide sufficient back tension to eliminate bunching on the sprocket. If bunching does occur the amount of slack chain is reduced and the tension T2 increases sufficiently to free the chain. More slack chain can be accommodated in this way by haulage units with vertical sprockets.

4.6.2) Sprocket Torque Characteristics

The sprocket torque characteristic Fig. 4.7 clearly shows fluctuations due to the mesh pattern of the chain sprocket drive. Cyclic torque variations occur, of approximately $\pm 3\%$ at a frequency corresponding to the number of teeth on the sprocket (twice the chain pitch). Included in these cyclic operations, will be changes in the frictional losses, as links start and stop sliding on the drive and idler sprockets and various combinations of interlink rotation take place. The major contribution however, is thought to be due to changes in the effective radius of contact between chain and sprocket as the sprocket rotates.

The additional higher frequency noise on the signal, is due to the meshing of the small drive gear on the bottom of the shaft to which the strain gauges were attached, together with some cyclic variations in torque originating at the haulage hydrostatic motor.

A calculation of the factors k_1t and μ as described in Section 3.2 from the strain gauge torque characteristics gives values of approximately .07 and .5 respectively. Values for these calculations are taken at the point of change in direction of rotation, here T2 is near zero and can be neglected. At intermediate points, the characteristic is affected by chain drag and compensator friction, in addition to the interlink friction loss factor k_1t , as can be seen from the T1 - T2 against displacement characteristic Fig. 4.6.

4.6.3) Haulage Pressure Characteristic

The pressure-displacement characteristic Fig. 4.8 gives an indication of the levels of the combined frictional losses in the system. At the point of direction of rotation change, a pressure reduction of 8.96 MPa to 5.5 MPa (1300 lb/in^2 to 800 lb/in^2) can be seen. The factors producing the pressure drop include the efficiency of the hydrostatic motor and the speed reducing gearbox, and the frictional losses in the sprocket chain drive system.

4.6.4) Strain Energy Release Speed Characteristic

The results of recordings made using 4 by-pass valve spools with differing restricting annular passages are shown in Table 4.1.

Due to the unrepeatability of the results and difficulties involved in accurately controlling and recording the many experimental variables only a representative set of results were taken.

Throughout the tests the maximum pressure in the high pressure side of the hydrostatic transmissions, immediately after the change of direction of sprocket rotation, was not recorded at a higher value than 5.86 MPa (850 lb/in^2). Taking this value and corresponding flow rates for the by-pass valve spools, obtained from Fig. 5.12, hydrostatic motor speeds were calculated which would give this value of flow. These values are also shown on Fig. 4.10. It is significant that for the 1.02 mm and 1.27 mm (.040 in and .050 in) valve spools, speeds higher than the maximum calculated were recorded, indeed to achieve such high speeds haulage pressures in excess of 9.6 MPa (1400 lb/in^2) would be required, higher than the overload tripping pressure in the forward direction. From these calculated points, the motor would appear to be able to pass more flow over the by-pass valve than the by-pass valve pressure-flow characteristics indicate. This is thought to show the prime reason for discrepancy between individual results.

When the by-pass valve operates, pressure transients are produced in the transmission circuit. Any sub-atmospheric pressure transients

would lead to high flow rates being demanded through the circuit check valves. These valves are known to cavitate at low flow rates and are therefore unlikely to be able to deal with pressure transient conditions without cavitation. Such phenomena could lead to the higher than predicted strain energy release speeds.

There are also several additional causes of inconsistencies. No means were available to accurately control the haulage fluid temperature, although an attempt was made to perform the tests at 40°C - 60°C. Even an accurate control of sump temperature would not have ensured the necessary control of the circuit temperature. The pressure overload valve did not operate at a constant pressure. Due to the low connection capacitance, considerable pressure ripple existed in the transmission circuit. Although the haulage unit contained a damping coil to suppress these pressure fluctuations prior to the overload valve, inconsistencies were noted in the operating pressure. This effect was accentuated when high forward speeds were used, the overload valve response times allowing the haulage pressure to continue increasing until the by-pass valve spool operated. Any operation of the circuit relief valves set at 9.3 MPa (1350 lb/in²) (overload valve set to 8.62 MPa (1250 lb/in²)) could aggravate the inlet valve cavitation effect described above.

Test No	Valve size		Sprocket Rotation revs	Time secs	Speed revs/min
	in	mm			
X6	.035	.89	.46	34	470
X7	.035	.89	.48	37	390
X1	.040	1.02	.45	20	600
X5	.040	1.02	.44	24	550
X8	.040	1.02	.52	18	770
X9	.040	1.02	.54	18	880
X2	.050	1.27	.54	10	1130
X3	.050	1.27	.53	8.6	1450
X4	.050	1.27	.52	9	1500
X10	.050	1.27	.46	11	770
X11	.050	1.27	.55	10	1230
X12	.248	6.3	.59	4.5	2050
X13	.248	6.3	.58	4.4	2030
X14	.248	6.3	.56	4.4	1950
X15	.248	6.3	.58	4.4	2050

- Note - Time is time for the sprocket to return to to the equilibrium condition from the point of change of direction of sprocket rotation.
- Sprocket rotation is measured between the point of change of direction of rotation and equilibrium.
 - Speed is maximum speed during release of strain energy from chain systems.
 - Valve size is the reduction in diameter at the annular restriction.

Table 4.1 Results taken from X - Y recordings of strain energy release speed characteristics, haulage loaded with chain system

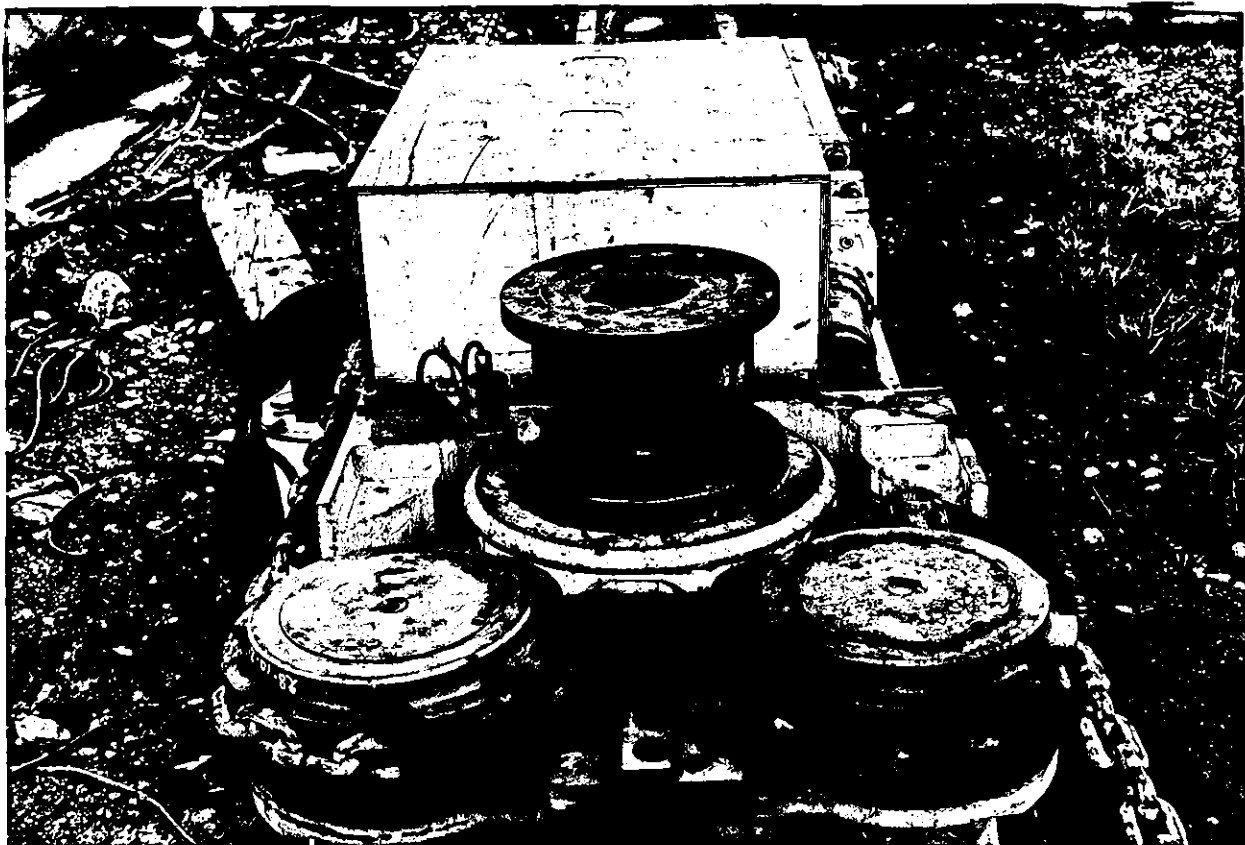


Fig. 4.1 Chain and Sprocket Details of the BJ-D Haulage
Unit used in the Surface Trials

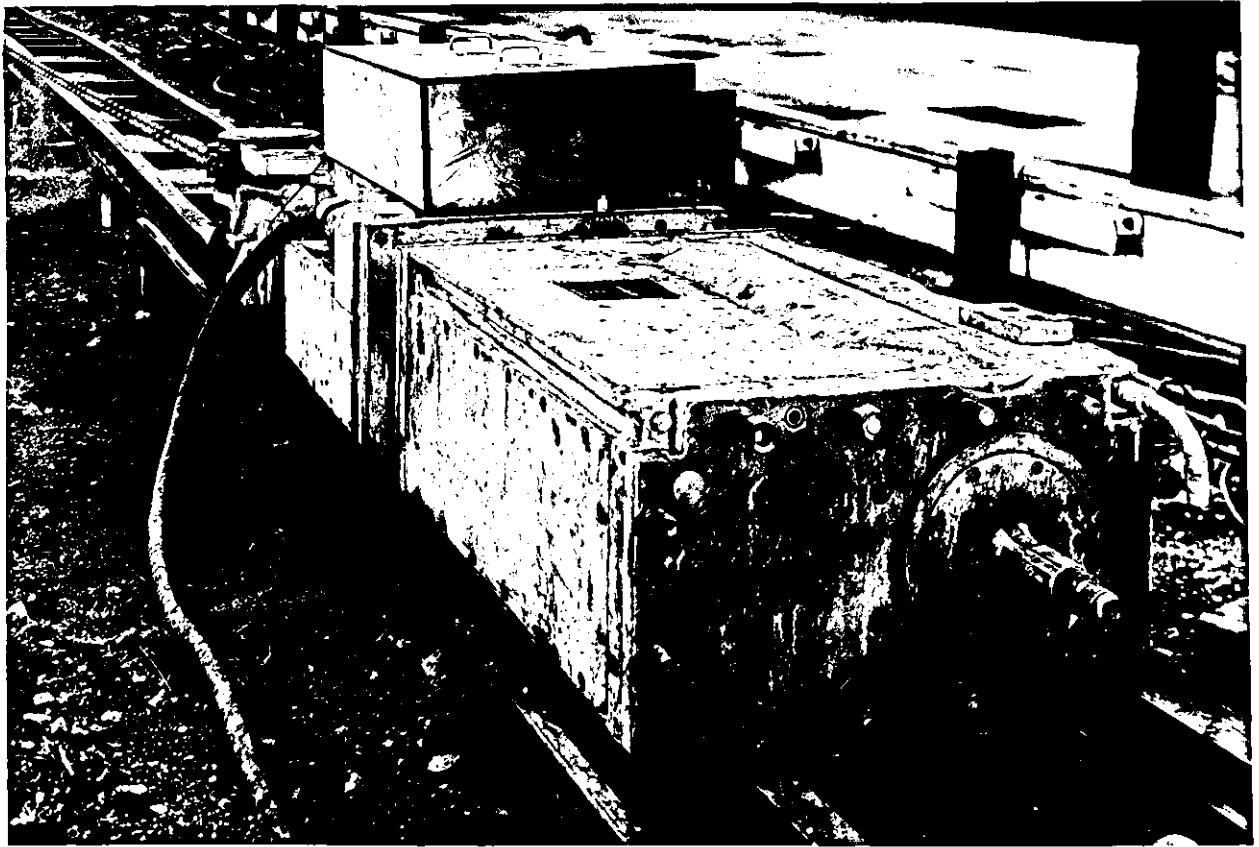


Fig. 4.2 BJ-D Haulage Unit undergoing Surface Trials



Fig. 4.3 Details of Chain Tensioner and Tensometer used in Surface Trials



Fig. 4.4 Strain Gauged Shaft and Slip Rings used for
Torque measurement within the Haulage Gearbox

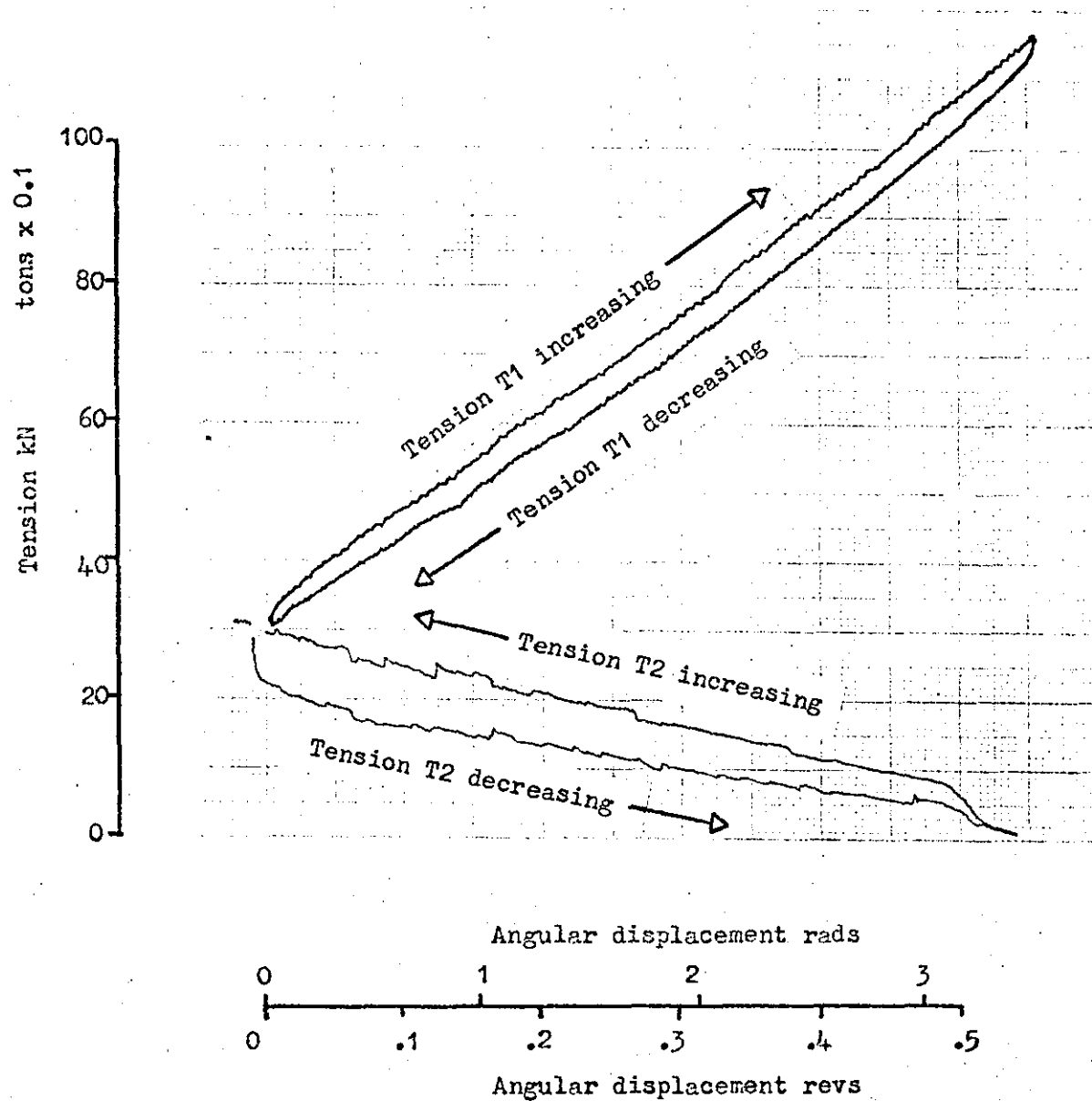


Figure 4.5 X - Y Recording of tension T1 & T2 against sprocket angular displacement

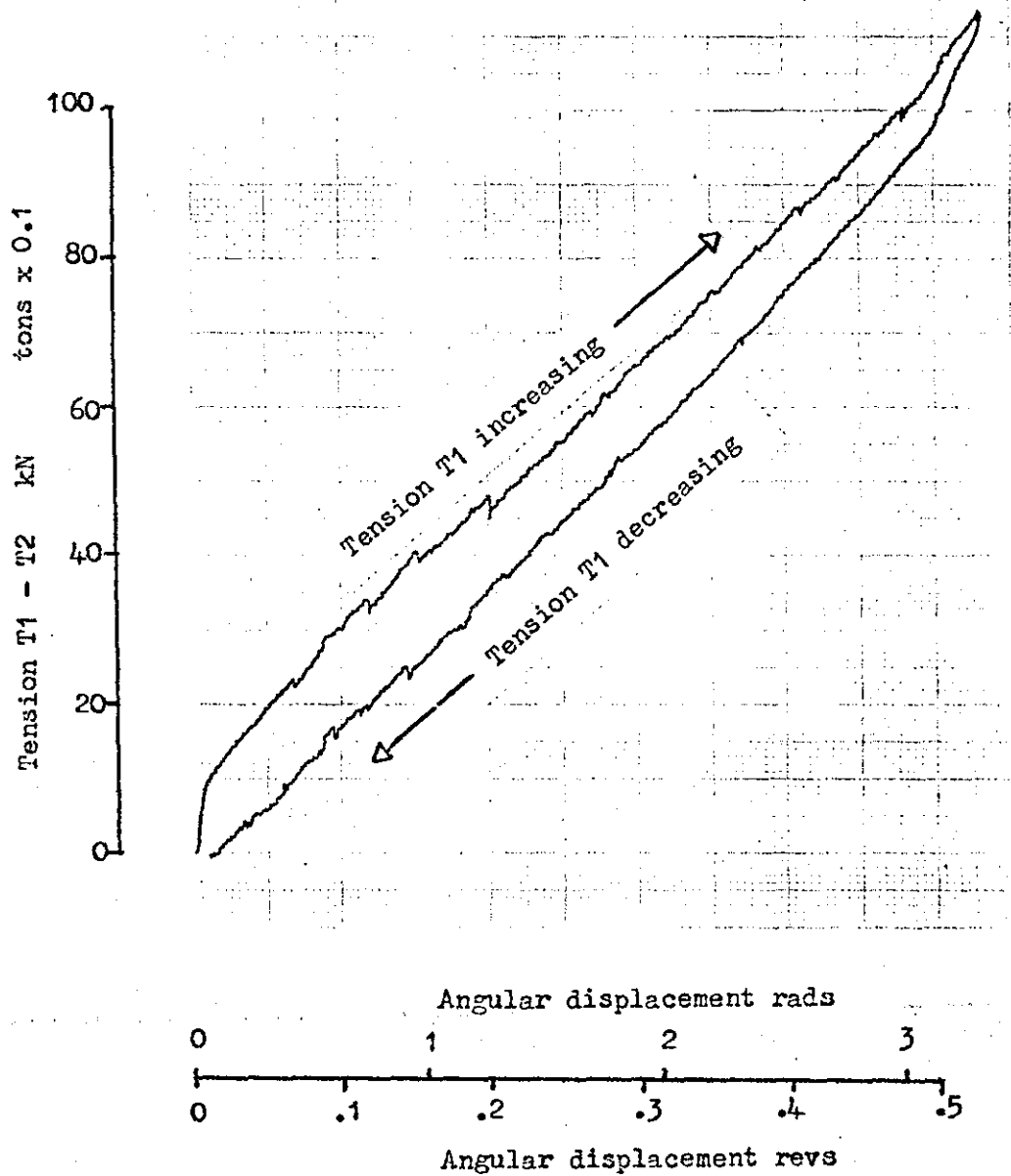


Figure 4.6 X - Y Recording of tension $T_1 - T_2$ against sprocket angular displacement

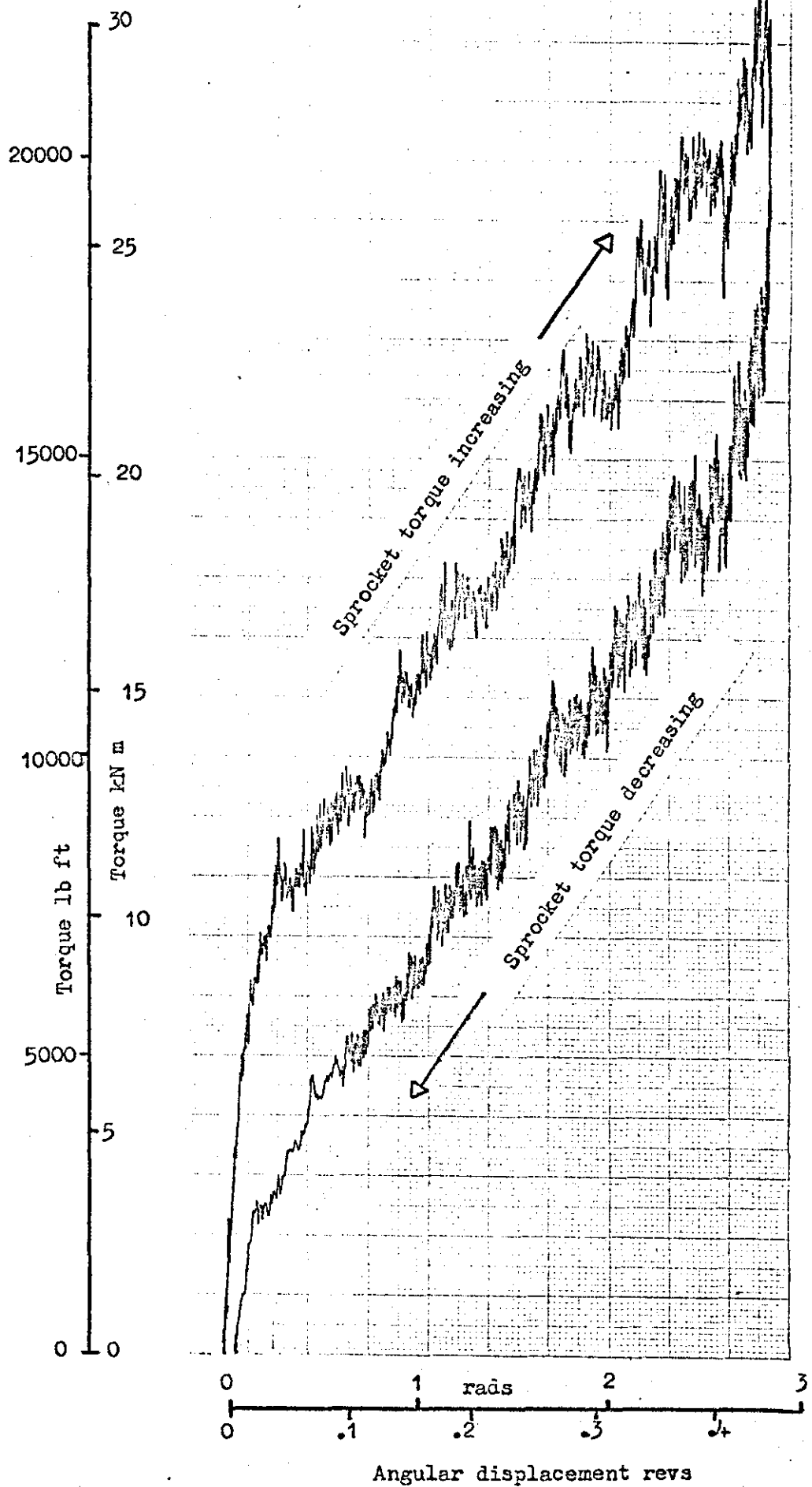


Figure 4.7 X - Y Recording of sprocket torque against sprocket displacement
haulage loaded with chain

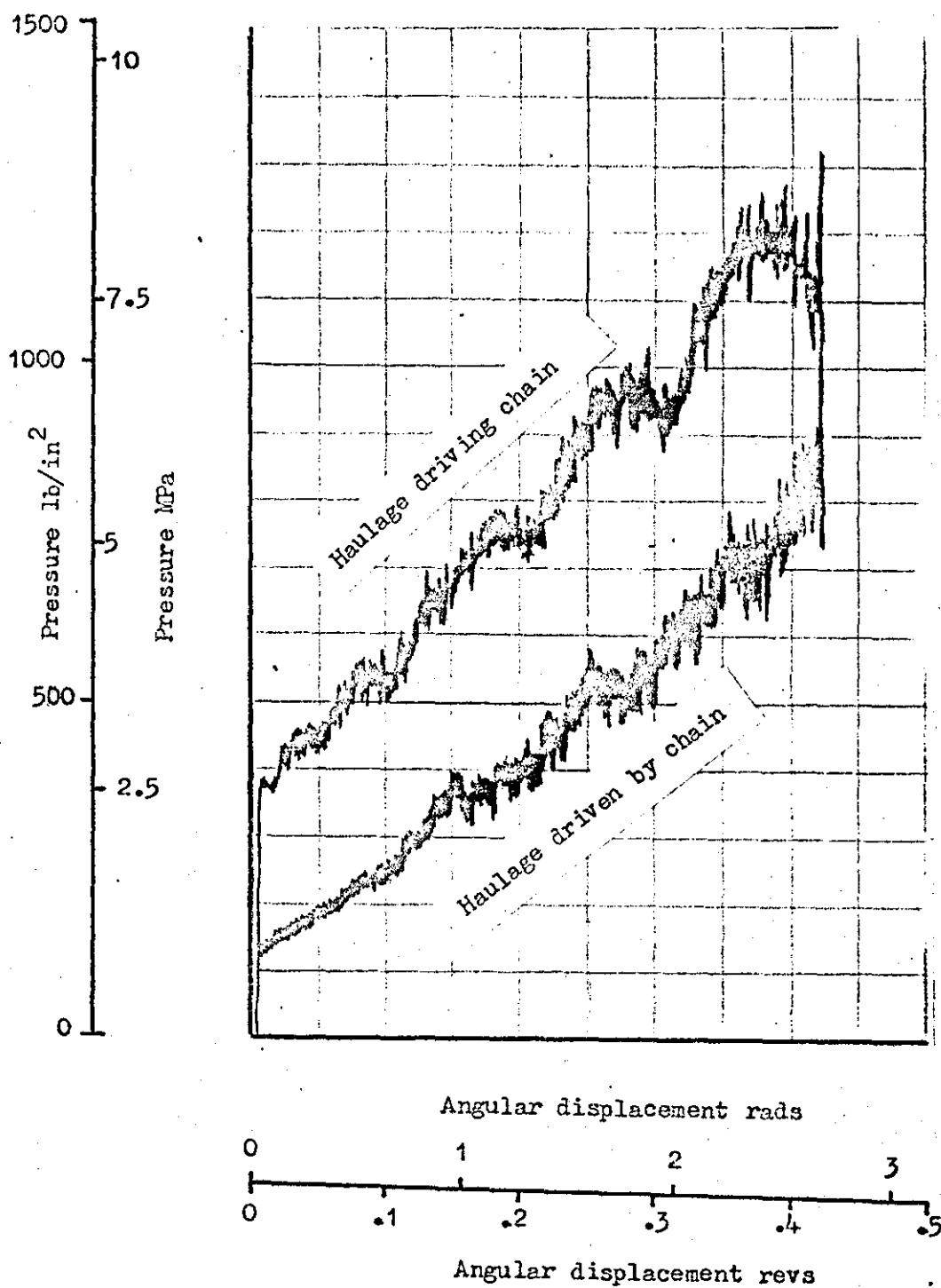


Figure 4.8 X - Y Recording of haulage pressure against sprocket
angular displacement haulage loaded with chain

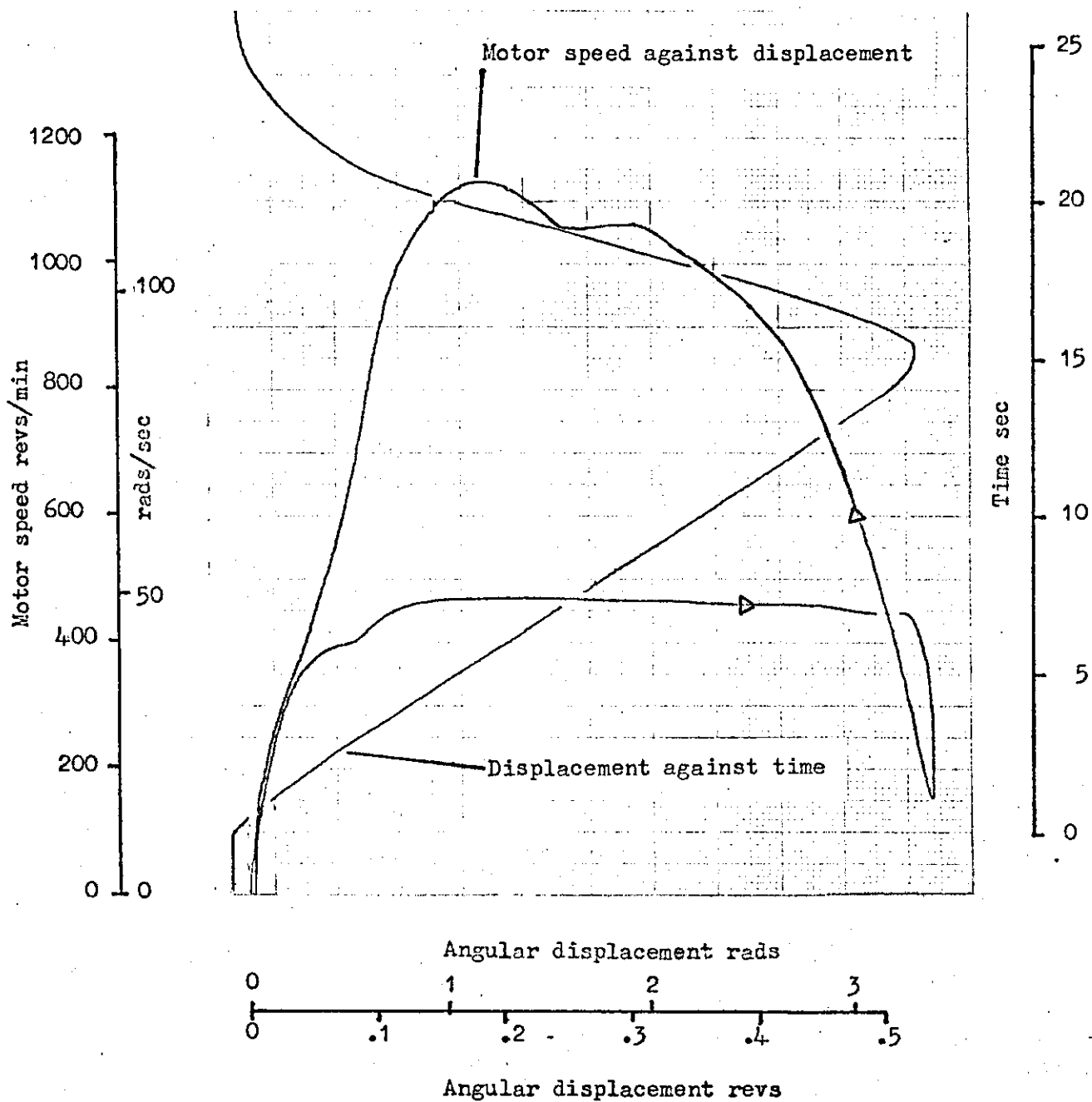


Figure 4.9 X-Y Recording of haulage motor speed and time against sprocket angular displacement, haulage loaded with chain

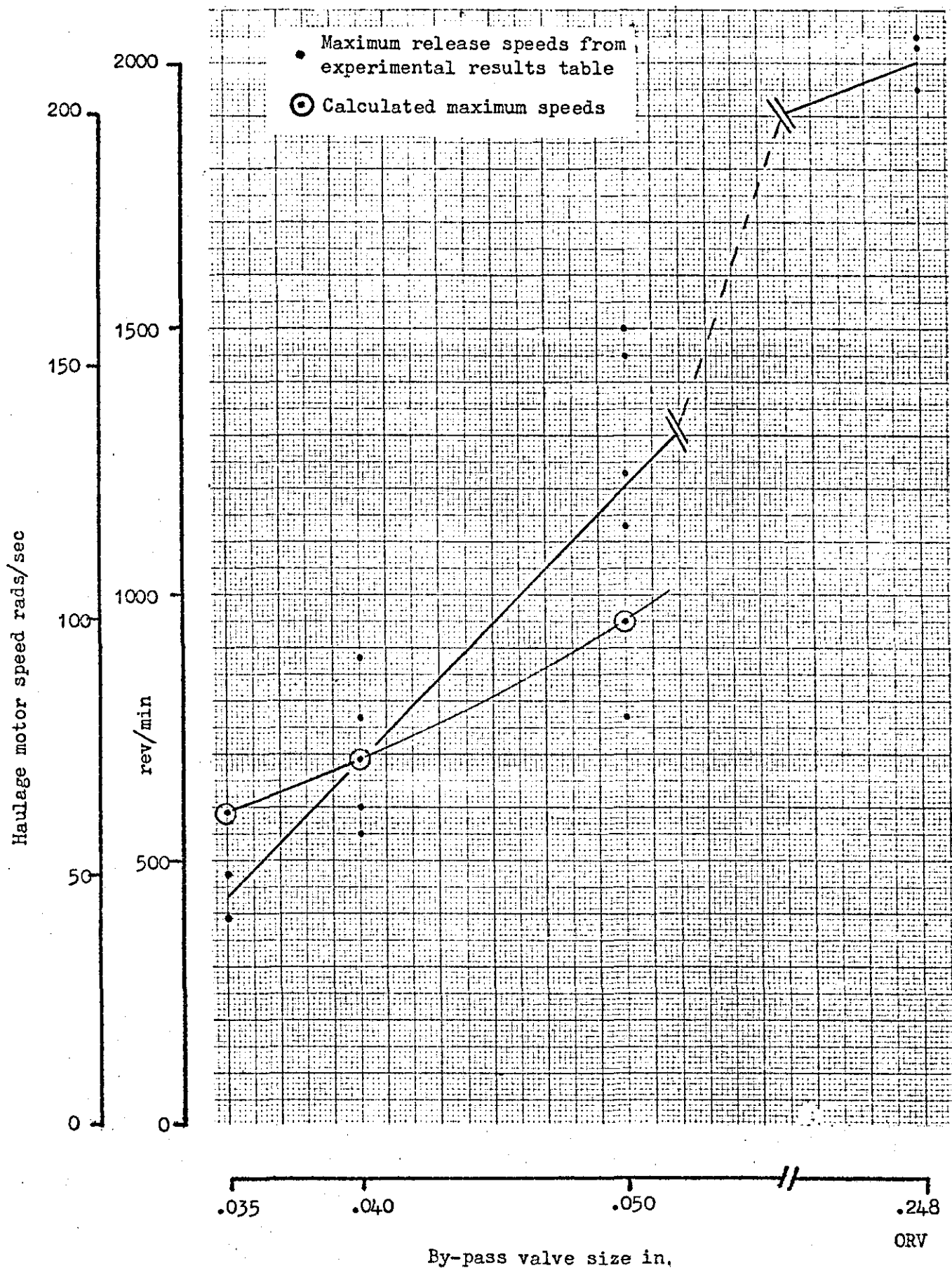


Figure 4.10 Maximum speeds of energy release haulage loaded with chain system

5 DETERMINATION OF HAULAGE UNIT AND ABSORBER CHARACTERISTICS

5.1 Introduction

In order to construct the dynamic model of the haulage unit and simulation system; inputs to the model were required of the basic haulage and absorber characteristics. These were experimentally determined where possible and obtained from alternative sources where the required data was beyond the scope of the experimental equipment.

For the dynamic model pressure-torque characteristics were required in both the driving and driven modes of operation. This information was not readily available from manufacturers since, in the case of the absorbers, hydrostatic motors are not generally operated as pumps and power loader haulage units are seldom used to absorb power.

5.2 Description

A BJ-D B14 haulage unit, as described in Section 2.5, was used throughout the course of the tests. The haulage unit was driven by its associated 110 kW (150 hp) water cooled induction motor. A drive from the output sprocket was taken through a torque transducer mounted between a pair of gear type flexible couplings to the input shaft of the power absorber. (Figs. 5.01 and 5.02).

Three types of hydrostatic power absorbers were available with capacities suitable for use with this haulage unit; a Chamberlain Industries Ltd Staffa B2700 with a 2/1 speed increasing epicyclic gearbox; a similar unit B270 H was identical to the B270D except for having hydrostatically balanced slipper pads instead of the plain bearing dynamically balanced type used in the B270D. A 4/1 speed increasing gearbox was also available for use with these units. The Hagglunds motor, having a rotating body, was mounted in a specially manufactured bearings assembly. This motor had sufficient capacity not to require a speed increasing gearbox. Diagrams of the Hagglunds 6185 and the Staffa B270H are shown in Figs. 5.03 and 5.04.

Common circuits were used for all the absorbers as shown in Fig. 5.05. To simplify the circuit pipework, manifold blocks were manufactured to enable the direction control valves to be bolted to the absorber ports.

Pressure sources for the absorber circuit were taken from a laboratory ring main system feed from a 90 kW (120 hp) power pack. This system enables rigs of this kind to be built without individual tanks, coolers, filters, boost pumps etc. Four connections were required to the ring main system feed and return pressure, high pressure feed (used to drive the absorbers as motors) and circuit drains.

The absorber circuit relief valve was a Denison two stage type with the pilot controlled by a Denison Electroilic valve. This enabled the absorber circuit pressure to be controlled remotely from the control panel. A non-return valve around the absorber provided protection from inadvertent reversal of the haulage unit, without the appropriate reversal of the two stage solenoid operated Denison direction control valve. The large accumulator on the return line, together with the low pressure relief valve to the feed line, prevented undue rises in the return line pressure with high absorber speeds, as occurred during simulation of chain strain energy release. Provision was made in the high pressure side of the circuit for a bank of accumulators, to enable energy to be stored corresponding to the energy in the chain.

5.3 Instrumentation

Strain gauge type pressure transducers were used in the haulage transmission circuit and the high pressure side of the absorber circuit. Sprocket torque measurements were made by means of the British Hovercraft strain gauge torque transducer. The strain gauged shaft in the haulage gear train and the slip rings as described in Section 4.3 were also available. Also common to the surface trials was the 10 turn displacement transducer and the pulse type motor speed transducer. These transducers are shown in Fig. 5.6.

Outputs from these transducers were available through amplifier modules to either the Bryans X-Y plotter or a 12 channel ultra violet recorder. For sprocket displacement measurements on the U/V recorder, a 360° rotary potentiometer was used, in place of the 10 turn potentiometer used in conjunction with the X-Y recorder.

5.4 Test Procedure

5.4.1) Absorber Torque-Pressure Characteristics

With the accumulator bank switched into the absorber circuit, the haulage was run in the forward direction starting from an unloaded condition with the absorber circuit valve set to its maximum value. This operation gradually charges the accumulator bank increasing the absorber circuit pressure, the absorber torque and the haulage circuit pressure. When a haulage circuit pressure of 10.3 MPa (1500 lb/in^2) was reached, the haulage speed was reversed, allowing the absorber to drive the haulage unit as the accumulators discharged. With the outputs from the absorber pressure and the torque transducer feed to the X-Y channels of the recorder respectively, a recording can be made of the pressure-torque characteristic in both the driven and driving modes of operation. This procedure was repeated at various speeds for the three absorbers available. During these tests the absorber circuit temperature was held constant at 50°C . The haulage overload device was disconnected from the circuit during these tests. The recordings are shown in Figs. 5.07 to 5.09.

5.4.2) Absorber Leakage Characteristics

Due to the difficulties of introducing positive displacement flow meters into the absorber circuit to determine its leakage characteristics, an alternative procedure was employed. The absorber circuit relief valve was set to its maximum value, and the haulage unit was used to drive the absorber at a series of very low speeds, the absorber pressure being noted at each speed. Under such conditions the total flow displaced by the absorber is lost in leakage and the pressure rises to correspond.

This method of leakage determination is similar to the blocked port tests described in reference 6. The leakage rate measured in this way, includes external and internal leakage from the absorber and also any losses from the absorber circuit. This procedure was carried out for the Hagglunds 6185 motor and the Staffa B270H. The results are shown in Fig. 5.10 after the haulage speeds had been converted to displaced volume flow rates at the absorber.

5.4.3) Haulage Leakage Characteristics

To give an indication of the haulage leakage characteristics, the haulage unit was run at full speed and changes in motor speed were noted as the haulage pressure was increased by increasing the absorber circuit pressure. These results are shown in Fig. 5.11. The leakage figures include both external and internal losses from the pump and motor together with any circuit losses. For the purpose of the dynamic model the total losses were equally split into internal and external losses.

5.4.4) System Inertia

The inertia of the absorbers was obtained from the manufacturers literature.

For the purpose of the dynamic model the inertia of the haulage unit was taken as the inertia of the hydrostatic motor. During the release of strain energy from the chain, the motor, gear train and sprocket are accelerated but owing to the high reduction ratio (215/1) only the motor inertia is significant when referred to the sprocket. The motor inertia was found using a trifilar suspension system at Loughborough University.

5.4.5) Pump Stroke Change Rate

The pump stroke change rate was obtained from recordings taken by running the haulage at full speed and increasing the pressure to operate the overload valve. Recordings were taken from the pump stroke position transducer on the U/V recorder.

5.4.6) Determination of the By-Pass Valve Pressure-Flow Characteristics

To control the rate of release of strain energy from the face chain system, the BJ-D B14 haulage unit has a by-pass valve spool with a restricting annular passage. The by-pass valve is brought into circuit across the hydraulic motor under conditions of overload or manual machine stops, the energy in the chain rotating the motor and forcing fluid through the valve. As this restricting by-pass valve spool is only in its development phase, several valves were available so that their effects on the rate of release of strain energy could be observed.

Due to the complex nature of the flow paths in the by-pass valve and the empirical nature of the theoretical analysis of such problems, it was decided to obtain the pressure-flow characteristics experimentally.

5.4.6.1) Experimental Method

To experimentally determine the pressure-flow characteristics of the by-pass valves, a valve block was made which held a by-pass spool and had identical ports to those in the haulage unit.

The input port was connected to a $4.54 \text{ dm}^3/\text{sec}$ (60 gal/min), 13.8 MPa (2000 lb/in^2) power pack and the output port returned through a positive displacement flow meter to the power pack tank. Pressure gauges on the input and output ports were used to assess the pressure drop across the valve. The flow through the valve was varied in increments by adjusting the supply pressure, readings of pressure and flow being taken at each increment.

The tests were repeated for several by-pass valves with varying dimension of restricting annulus. The results are shown in Table 5.1 and Fig. 5.12.

5.5 Observations

5.5.1) Absorber Torque-Pressure Characteristics

The overall mechanical efficiency of the Staffa B270D with 2/1 gearbox, the Staffa B270H with 2/1 gearbox and the Hagglunds 6185 hydrostatic

units are clearly shown on Figs. 5.07 to 5.09. As the frictional losses involved act against the direction of movement, the torque-pressure characteristics for the driving and driven modes of operation are equispaced about a theoretical no loss line.

The B270H and the Hagglunds 6185 characteristics were found to be independent of speed within the range $\frac{1}{2}$ - 6 rev/min (1 - 12 rev/min for the B270H due to the gearbox) within the limits of the experimental technique. The Hagglunds 6185 had the higher efficiency of approximately 97% against a combined efficiency for the Staffa B270H and gearbox of approximately 90%. In both cases the efficiency for the driving and driven modes of operation were similar.

A large degree of speed dependence is shown on the Staffa B270H characteristic Fig. 5.07 in the lower speed range. Efficiencies of 70% at stall speeds of around 1 rev/min are evident in both modes of operation, whereas at speeds above 2 rev/min the unit has an efficiency comparable to the Staffa B270D. This unpredictability of the torque-pressure characteristic for the Staffa B270D was thought to make this unit unacceptable for use as a chain tension simulation device and no further tests were carried out with this unit.

5.5.2) Absorber Leakage Losses

The absorber leakage characteristics are shown in Fig. 5.10. To judge the effects of absorber leakage on the use of hydrostatic absorbers for chain elasticity simulation, account must be taken of their differing capacities. A Staffa B270H with a 2/1 speed increasing gearbox has an effective displacement of 8.64 dm³ per revolution of the drive sprocket, whereas the Hagglunds 6185 has a displacement of 16.38 dm³ per revolution of the drive sprocket. This allows the Hagglunds 6185 to be operated at approximately half the pressures needed by the Staffa B270H for similar haulage sprocket torques. After adjusting by this factor and referring back to sprocket speed, it can be seen that for equivalent sprocket torques

the Hagglands 6185 has approximately twice the leakage effects of the Staffa B270H.

5.5.3) System Inertia

A measurement of the haulage transmission inertia using a trifilar suspension was found to be 4700 kg/m^2 when referred to the haulage sprocket. Absorber inertia values are 41.2 kg/m^2 for the Hagglands 6185 and 4.0 kg/m^2 for the Staffa B270H and gearbox, referred to the haulage sprocket (manufacturers information).

When a haulage sprocket is loaded by a face chain system inertia effects are very small, it is therefore important in dynamic work on haulage units that the inertia of the loading system is kept to a minimum. By the elimination of large speed increasing gearboxes between haulage unit and absorber, as is possible using hydrostatic absorbers, the inertia of the loading system can be kept to within approximately 1% of the haulage inertia.

Pressure		Valve Size							
		in	mm	in	mm	in	mm	in	mm
		.030	.76	.035	.89	.040	1.02	.050	1.27
Flow rates									
lb/in ²	MPa	gal/min	dm ³ /sec	gal/min	dm ³ /sec	gal/min	dm ³ /sec	gal/min	dm ³ /sec
200	1.38	4.0	.30	5.0	.38	6.0	.45	9.0	.68
400	2.76	7.0	.53	9.0	.68	10.0	.76	15.0	1.14
600	4.13	9.6	.73	11.5	.87	13.0	.98	19.0	1.44
800	5.51	11.8	.89	14.0	1.06	16.0	1.21	23.0	1.74
1000	6.89	13.0	.98	16.0	1.21	18.0	1.36	25.0	1.89
1200	8.27	14.5	1.10	17.5	1.33	20.5	1.55	28.0	2.12
1400	9.65	16.0	1.21	19.5	1.48	23.0	1.74	30.5	2.31
1600	11.02	17.0	1.29	21.0	1.59	25.0	1.89	34.0	2.58
1800	12.40	18.2	1.36	23.0	1.74	27.0	2.05	35.5	2.69

Original valve size .248 (6.30 mm)							
Inlet Pressure		Outlet Pressure		Pressure diff		Flow rate	
lb/in ²	MPa	lb/in ²	MPa	lb/in ²	MPa	gal/min	dm ³ /sec
160	1.10	80	.55	80	.55	23.5	1.78
190	1.31	100	.69	90	.62	27.0	2.05
240	1.65	120	.83	120	.82	32.5	2.46
300	2.07	150	1.03	150	1.04	38.0	2.88
400	2.76	200	1.38	200	1.38	45.5	3.45
460	3.17	230	1.58	230	1.59	49.0	3.71

Table 5.1 Bypass valve pressure flow characteristics

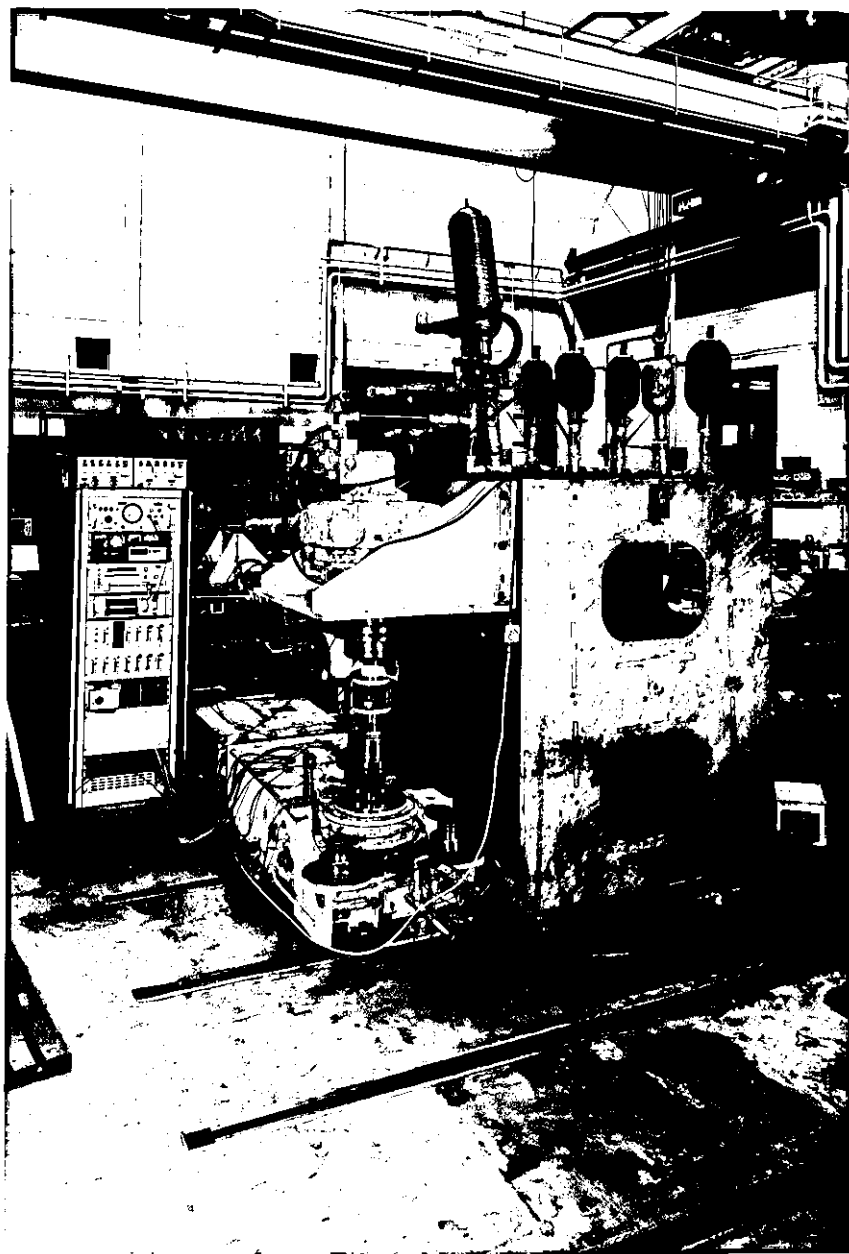


Fig. 5.01 BJ-D B14 Haulage Unit Loaded with Staffa B270H
Hydrostatic Motor and Accumulator Bank

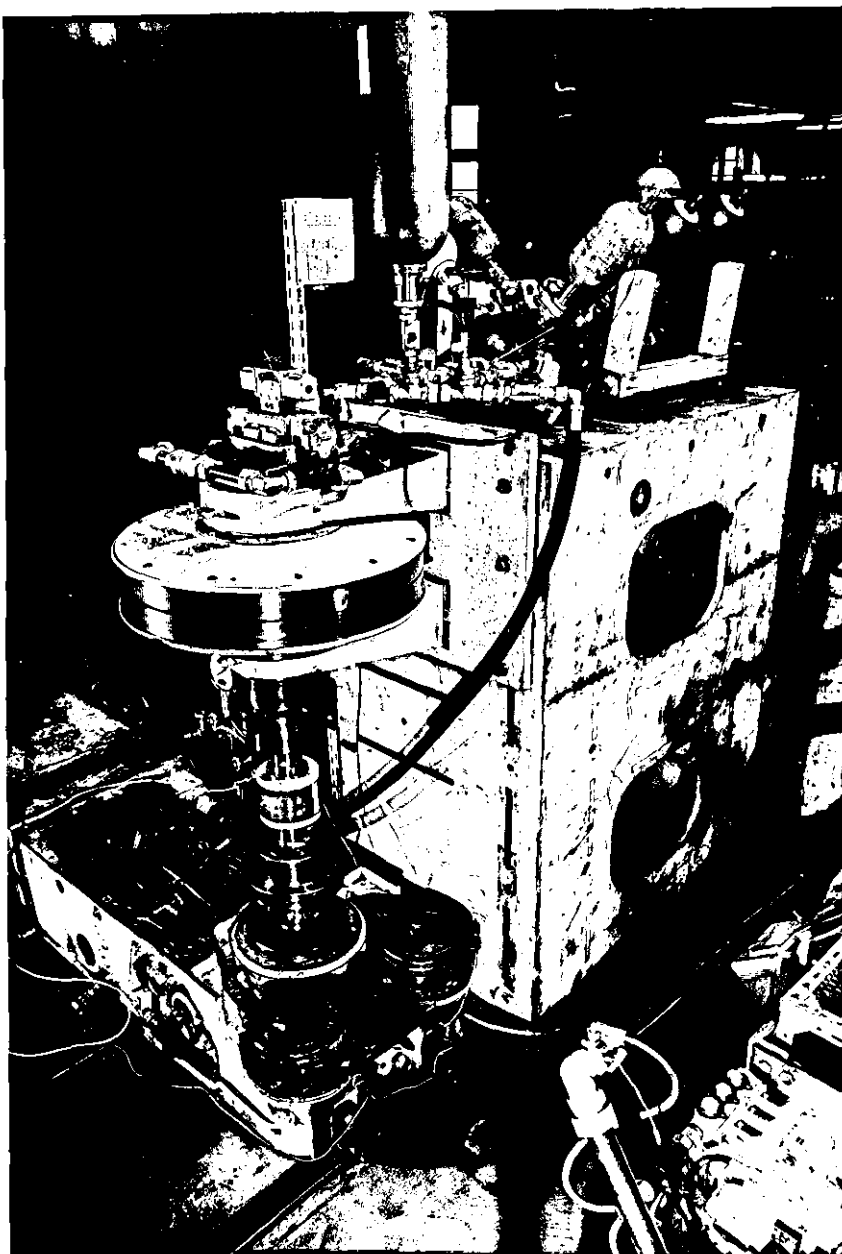
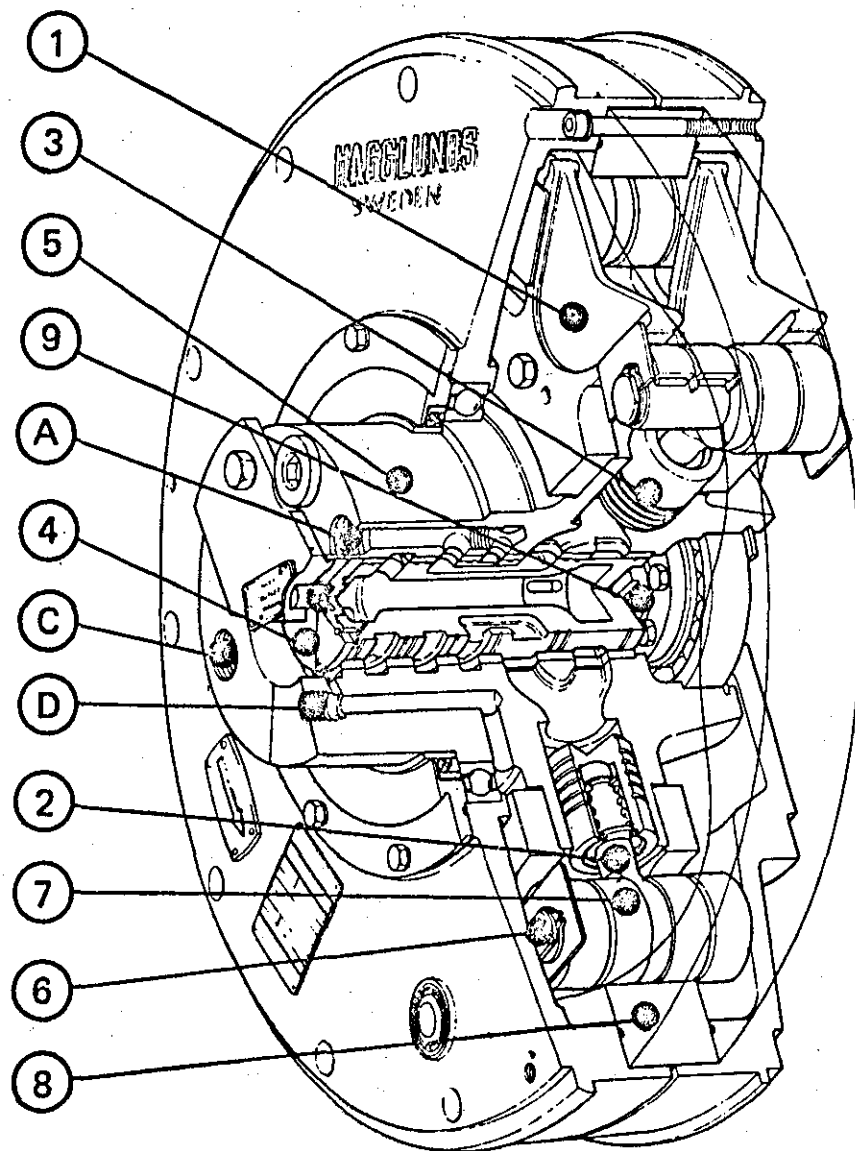


Fig. 5.02 BJ-D B14 Haulage Unit Loaded with Hagglands 6185
Hydrostatic Motor and Accumulator Bank



- 1. Guide-plate
- 2. Piston rod
- 3. Piston
- 4. Distributor
- 5. Cylinder block
- 6. Roller shaft
- 7. Cam rollers
- 8. Cam ring
- 9. Oldham coupling
- A=Port »A«
- C=Port »C«
- D=Drain port »D«

Fig. 503 Hagglunds 6185 Hydrostatic Motor

- A Motor Case
- C Valve Housing
- E Piston
- F Connecting Rod
- G Crankshaft
- I Valve Spool
- K Oldham's Coupling
- N Restrictor
- V Taper Roller Bearing

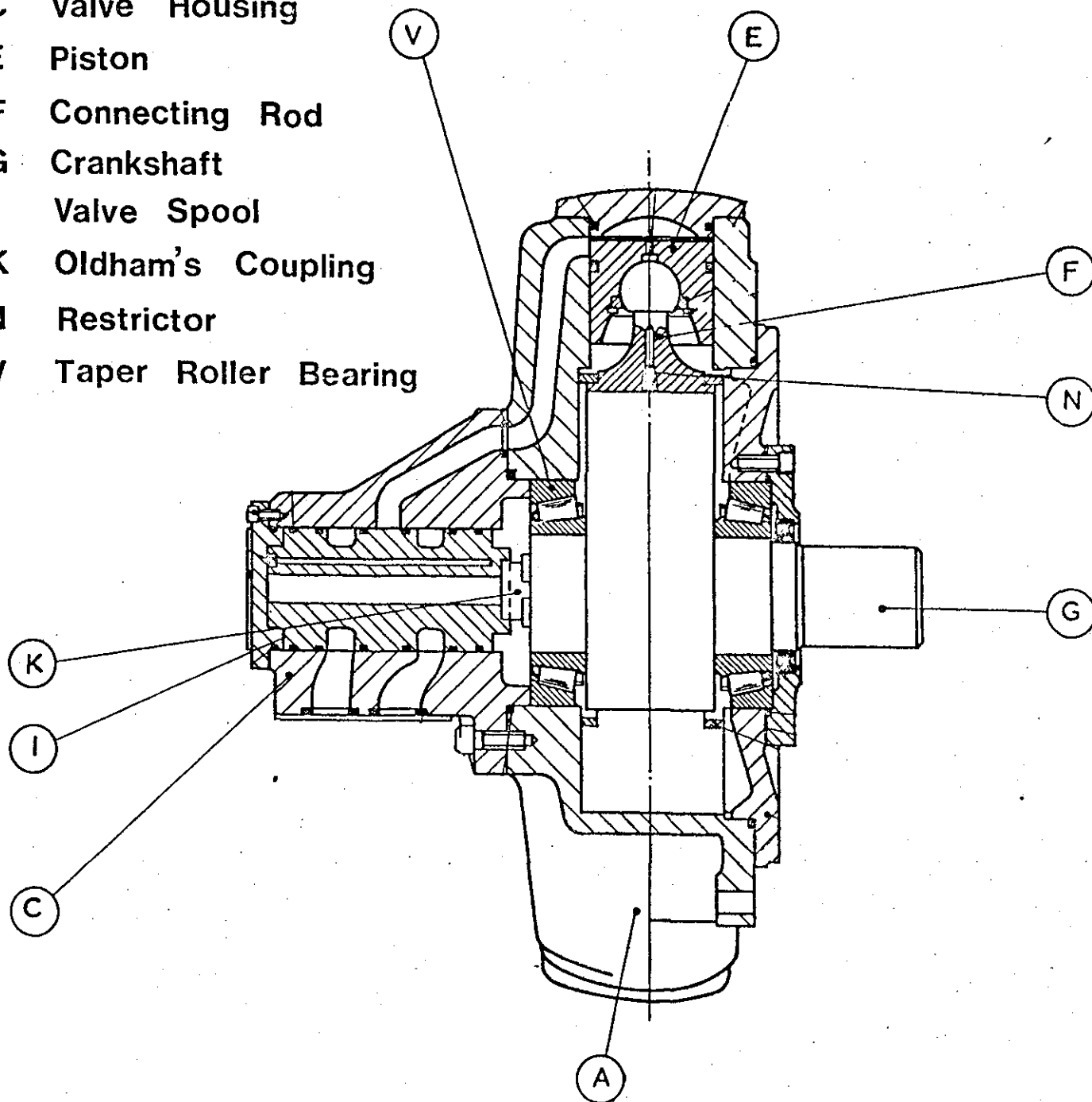
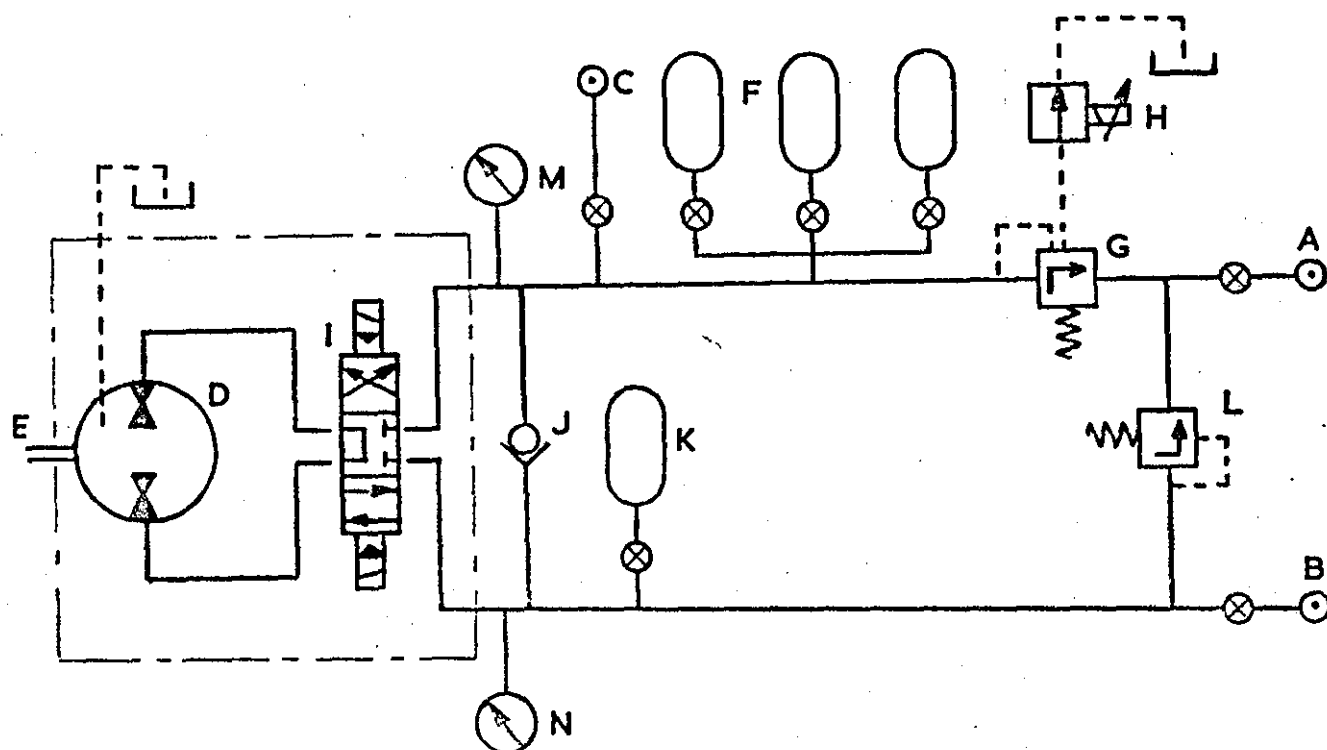


Fig.5-O4 Staffa B 270H Hydrostatic Motor



- A - Return line to power pack 110 lb/in² (0.76 MPa) nominal
- B - Feed line from power pack 100 lb/in² (0.69 MPa) nominal
- C - High pressure feed from power pack max 2000 lb/in² (14 MPa)
- D - High torque low speed motor acting as power absorber
- E - Drive from Haulage Unit
- F - Accumulator bank
- G - Pilot controlled relief valve
- H - 'Electroillic' pilot relief valve
- I - Direction control valve, manifold mounted
- J - Circuit protection check valve
- K - Pressure regulation accumulator
- L - Overpressure relief valve
- M - Pressure gauge & transducer
- N - Pressure gauge

Fig 5.05 Hydrostatic absorber circuit diagram used for chain elasticity simulation

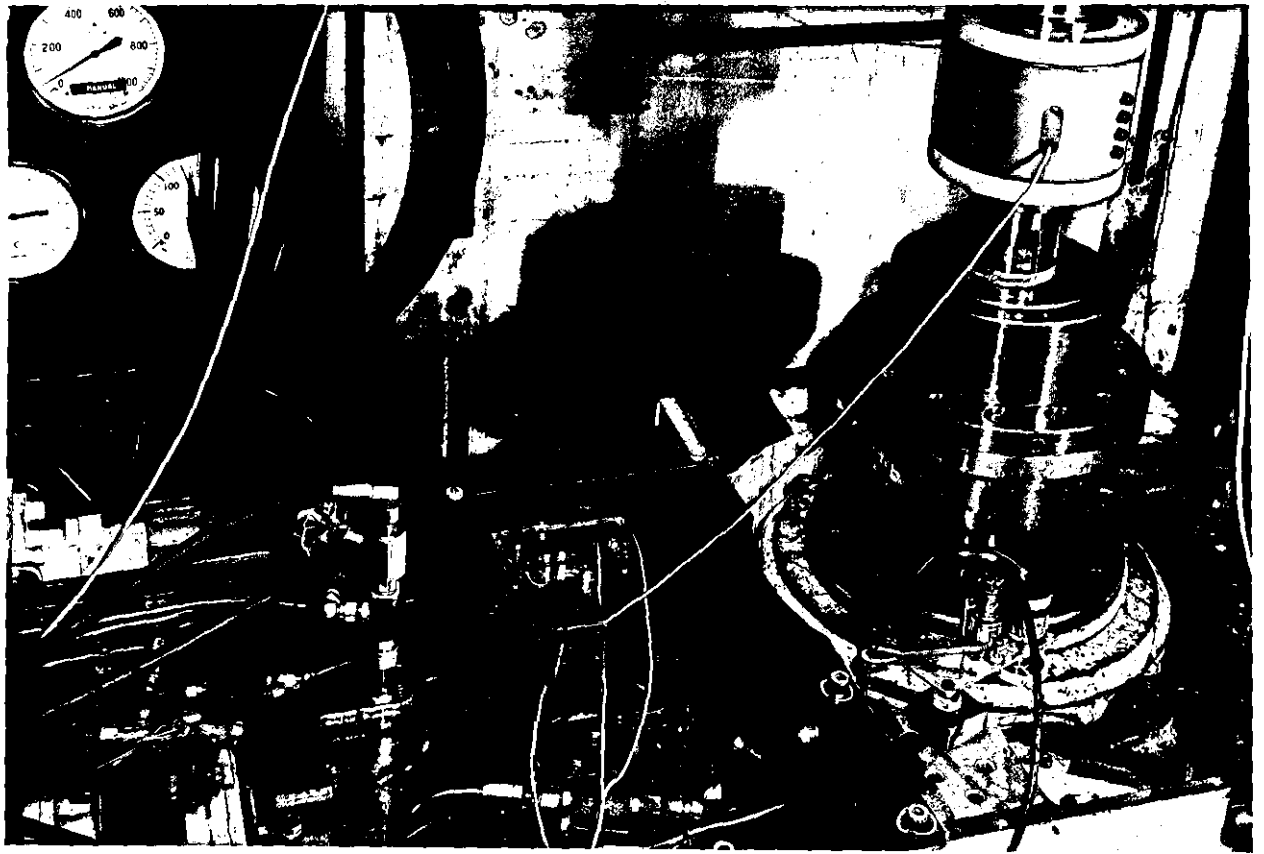


Fig. 5.06 Haulage Unit showing Speed, Angular Displacement,
Output Torque and Gearbox Torque Measuring Devices

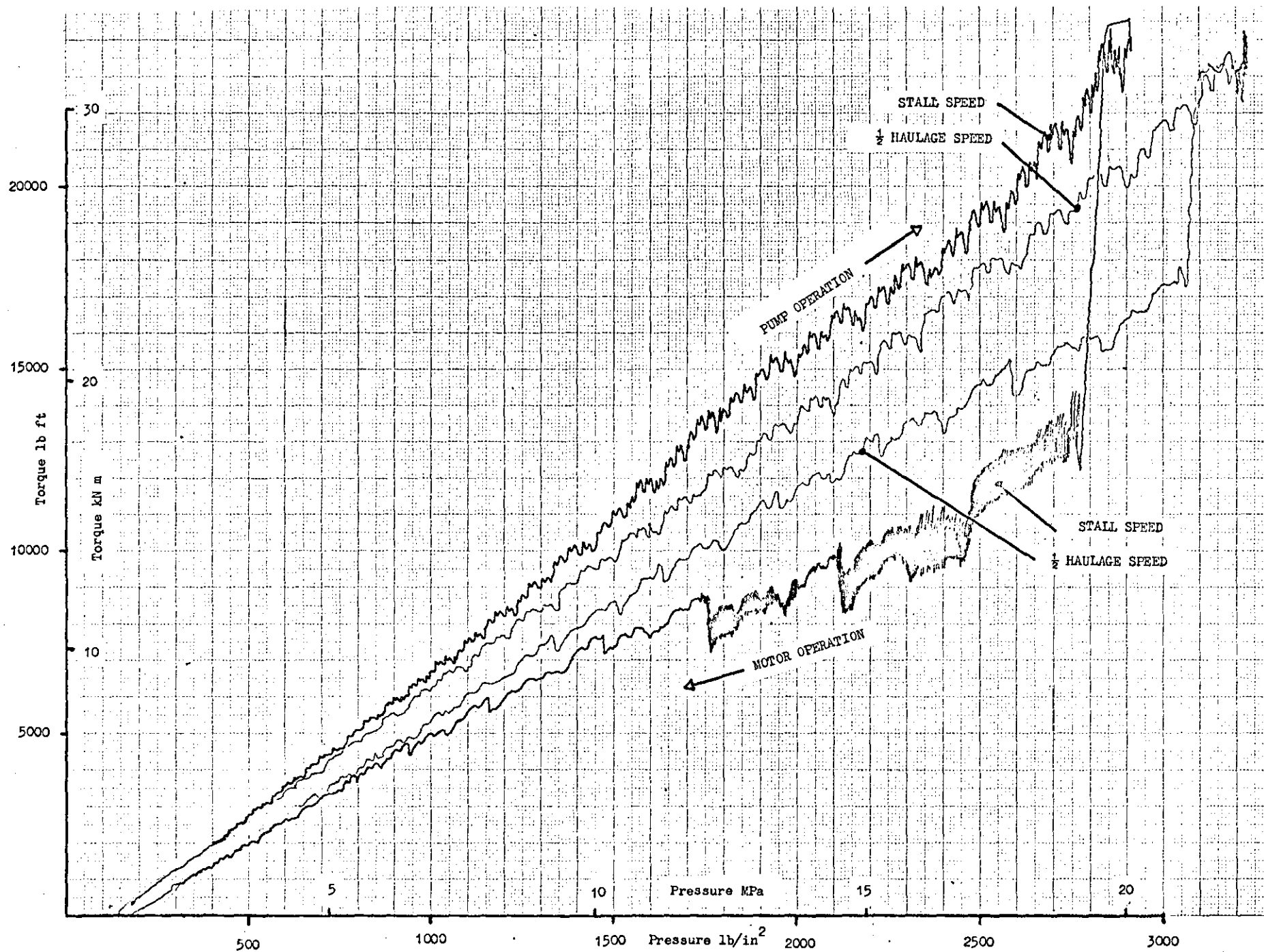


FIG.5-07.TORQUE - PRESSURE CHARACTERISTICS OF STAFFA B 270 D

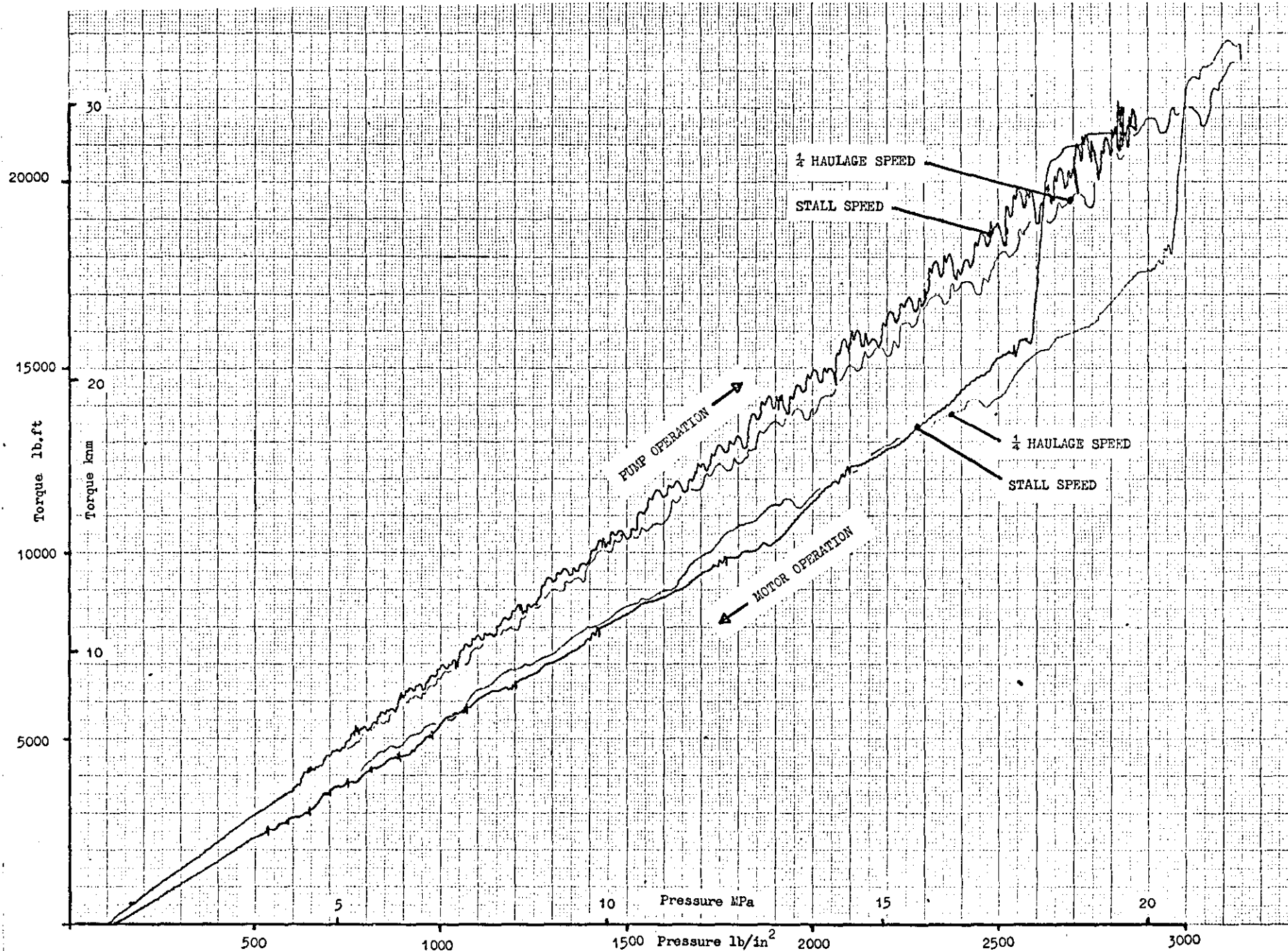


FIG.508 TORQUE - PRESSURE CHARACTERISTICS OF STAFFA B270H

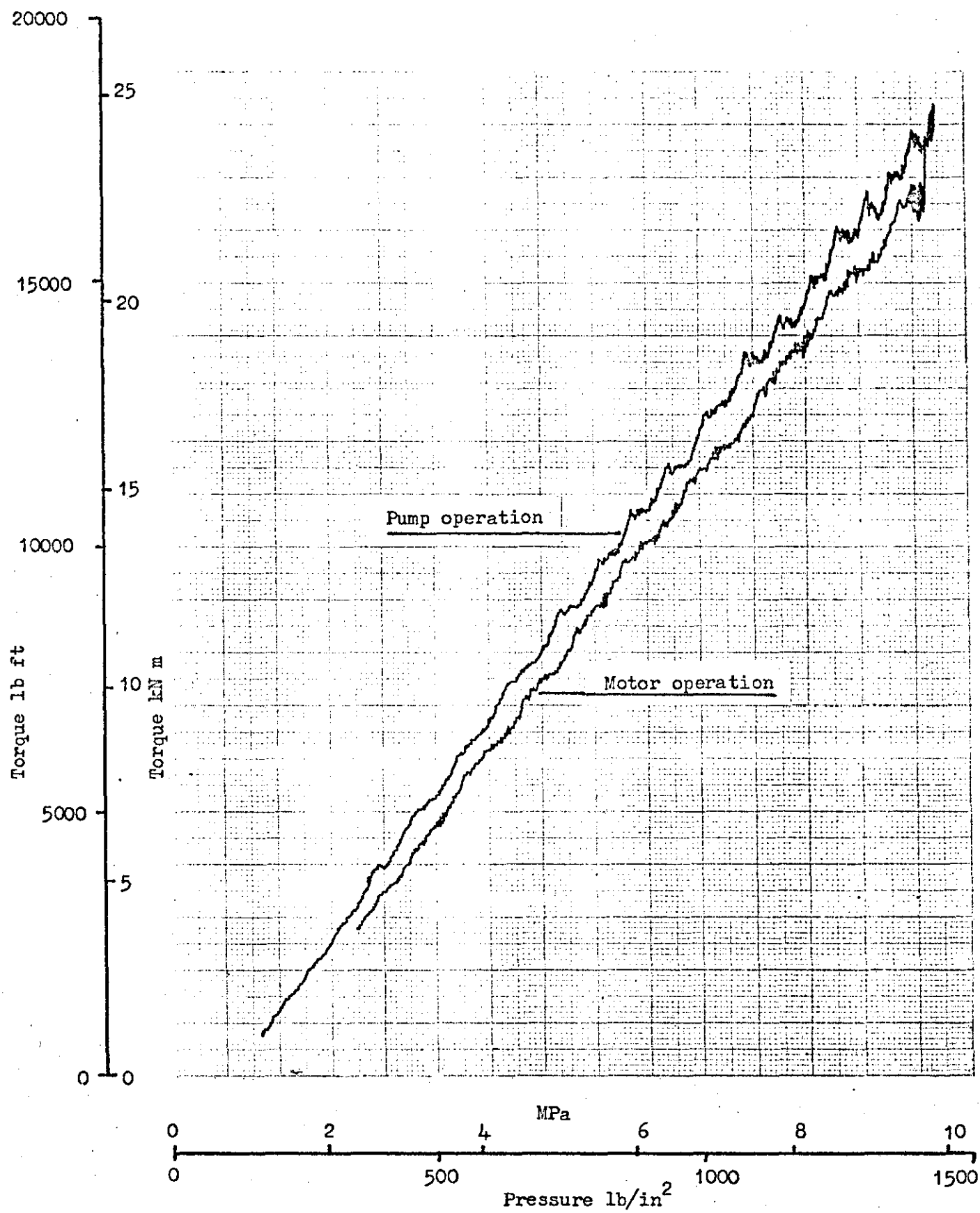


Fig. 5.09 X-Y Recording of pressure torque characteristic of Hagglund 6185 motor operating as both pump and motor

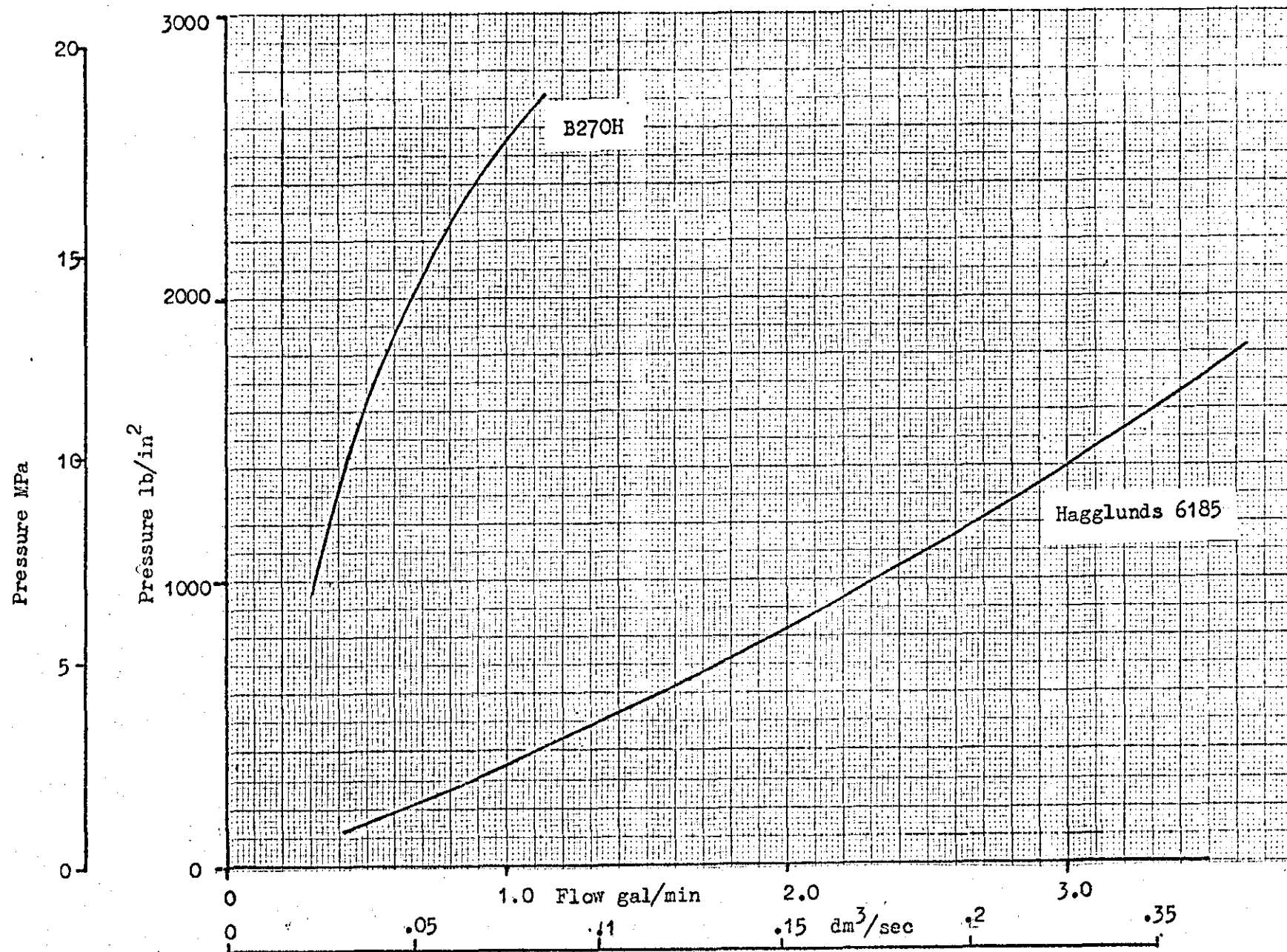


Fig. 5.10 Leakage characteristics of power absorbers

Fluid type Shell Tellus 27 temp 50°C
Return pressure 100 lb/in² (.75 MPa)

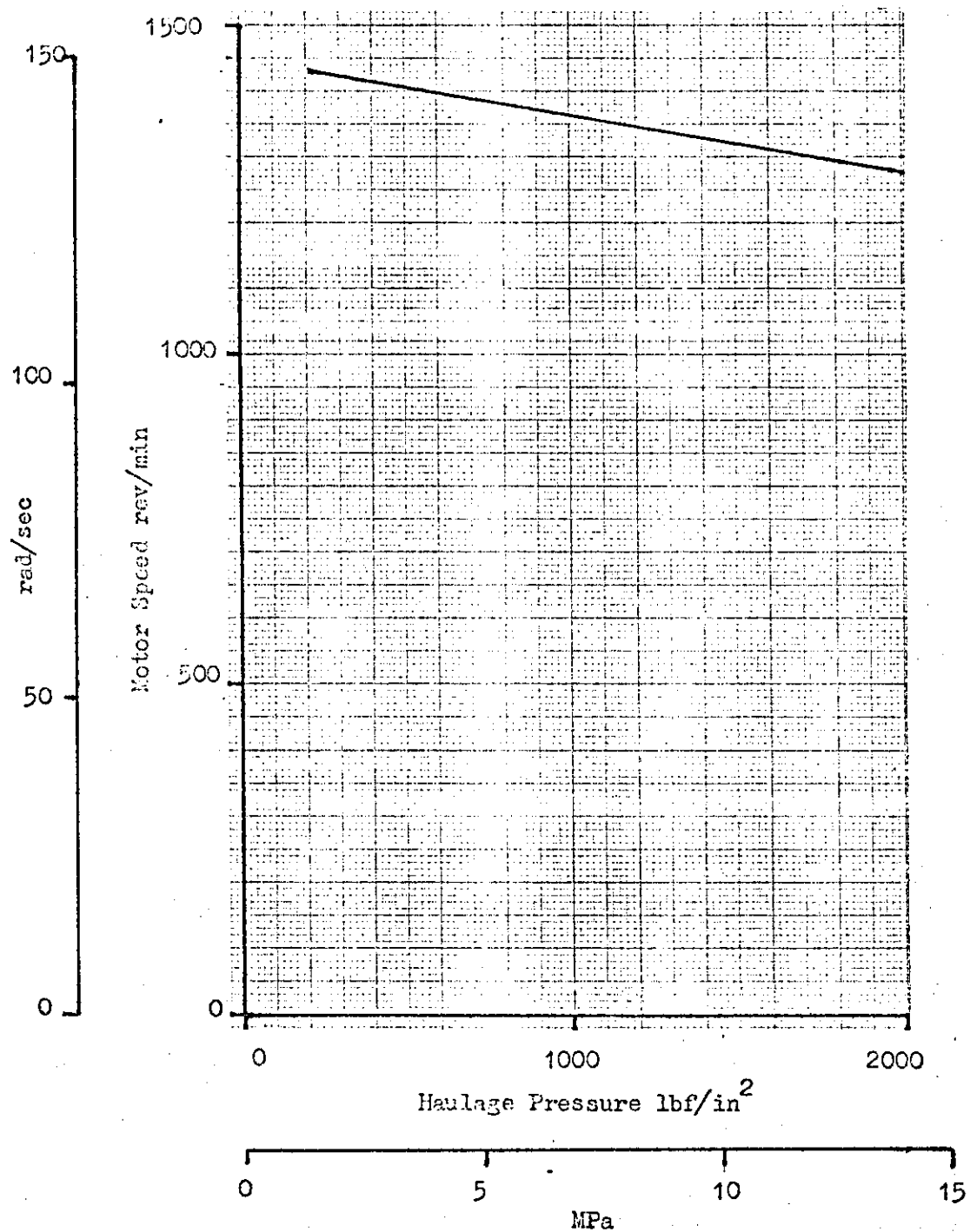


Fig. 5.11 HAULAGE PRESSURE SPEED CHARACTERISTICS

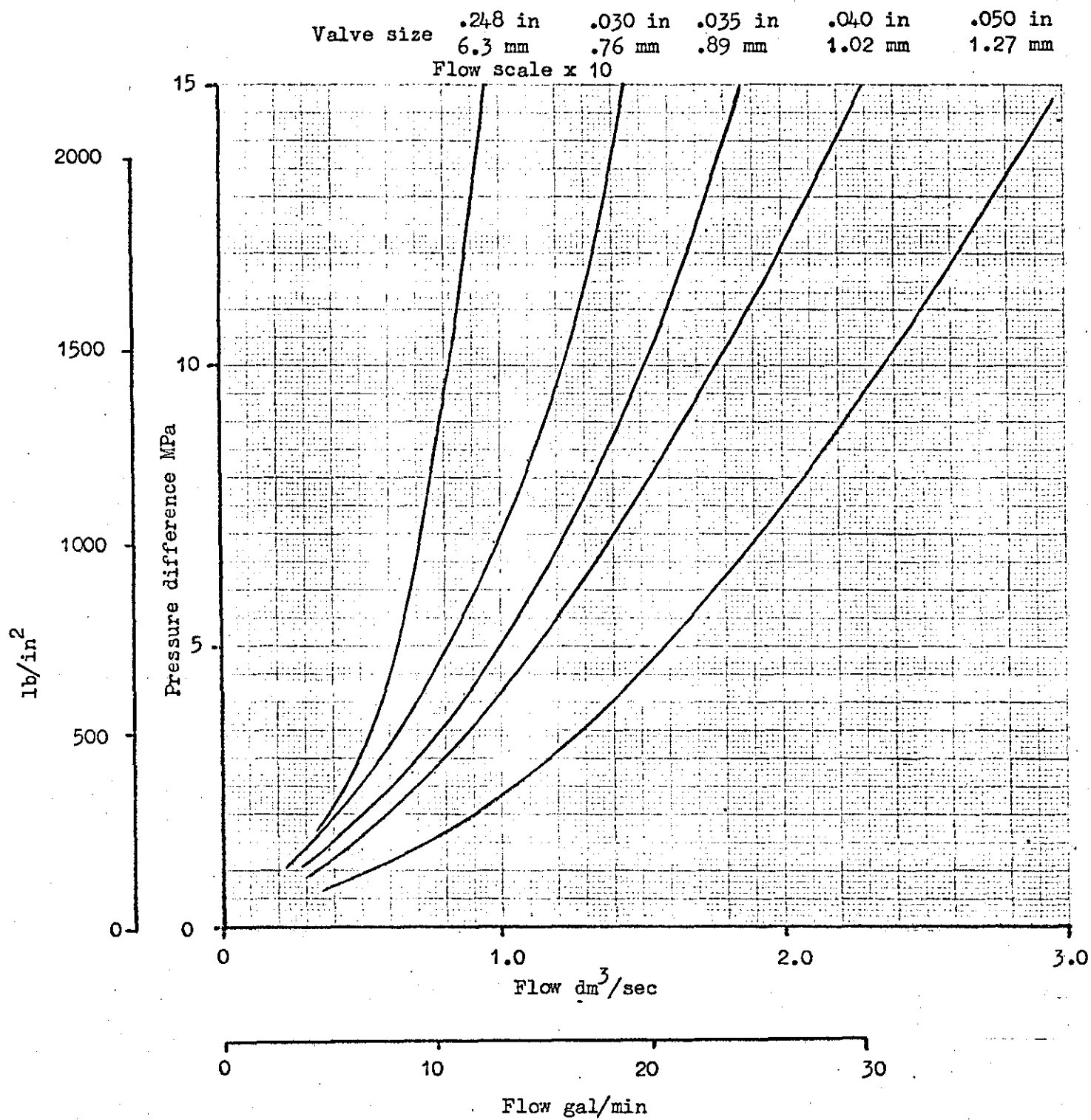


Figure 5.12 By-pass valve pressure flow characteristics

6 THE SELECTION OF ACCUMULATOR BANK CHARGING PRESSURES TO GIVE APPROXIMATIONS TO LINEAR PRESSURE - VOLUME RELATIONSHIPS

6.1 Pressure-Volume Characteristics of a Single Accumulator

Accumulator pressure-volume relationships are generally assumed to approximate to the gas law $P.V^n = \text{constant}$. This characteristic is clearly a curve of the form as shown in Fig. 6.1. For a given accumulator volume, determined by its physical size, the only variable which can be used to alter the characteristic is the pre-charge pressure, the gas pressure with maximum gas volume. The selection of accumulators for normal applications of shock suppression and energy storage is often carried out on a rule of thumb basis for several reasons; requirements can seldom be adequately specified; only fixed increments of accumulator volume are available; the polytropic indices of expansion and compression are not easily determined and exact mathematical solutions are difficult to achieve. The use of accumulators for simulation of chain elasticity requires that the accumulators fully discharge, this further complicates selection and pre-charge pressure calculations. When an accumulator is allowed to fully discharge from some load or supply pressure, the amount of fluid displaced is dependent on the maximum gas volume of the accumulator and the gas volume at the start of discharge. This volume is dependent on the accumulator pre-charge pressure and the conditions under which the accumulator has been charged. These factors complicate calculations of accumulator characteristics, particularly if the pressure-volume characteristic is to be approximated to linear with the accumulator fully discharging, as is the case with chain elasticity simulation.

To show the type of calculations involved suppose that it is required to find the charge pressure P_c , that will allow an accumulator to discharge a volume of fluid V_d , from a pressure P_s , to a final pressure P_f with the accumulator fully discharging. Where $V_d = V_a - V_s$ is related

to $P_d = P_s - P_f$ by $\frac{P_d}{V_d} = \text{slope (a constant)}$ & $n_1 = \text{charge index}$

& $n_2 = \text{discharge index}$

$$\frac{P_s - P_f}{V_a - V_s} = \text{slope} \quad \text{eqn. 6.01}$$

$$P_c.V_a^{n_1} = P_s.V_s^{n_1} \quad \text{eqn. 6.02}$$

$$P_f.V_a^{n_2} = P_s.V_s^{n_2} \quad \text{eqn. 6.03}$$

Inspection of eqn. 6.01, 6.02 and 6.03 shows that the solution for P_c , P_s & V_s involves the solution of simultaneous polynomial equations.

The problem is simplified however if the charge and discharge indices are assumed to be equal

Then $P_c = P_f$ & $n_1 = n_2$

eqn. 6.01 now becomes $\frac{P_s - P_c}{V_a - V_s} = \text{slope} \quad \text{eqn. 6.04}$

Solutions are now only required for P_s and V_s from eqn. 6.04 and 6.02 but again a polynomial is required to be solved.

6.2 Pressure-Volume Characteristics of Accumulator Banks

The use of hydrostatic power absorbers for chain elasticity simulation requires a nominally linear pressure-volume relationship with fluid discharge, due to the proportional nature of the chain stiffness. If accumulators are to be used to achieve this simulation some modification of the basic accumulator characteristic is required. Banks of accumulators with a range of charge pressures can be used to approximate to the linear characteristic, but the determination of the number of accumulators required, their size and charge pressures, are difficult to determine. Exact mathematical solutions to the problem involve the solution of sets of polynomial equations with many unknowns. Since these equations would require some numerical technique for solution, a more direct incremental computational technique is described for setting pre-charge pressures. As this itself has limitations and needs access to a computer an alternative empirical method is also shown. Both these methods of linear approximation are used in the terminal section of the CSMP model to assess their accuracy when used to simulate the chain elasticity.

These procedures for accumulator pre-charge pressure selections are only made possible by the assumption that the accumulators charge and discharge with the same polytropic index ie $n_1 = n_2 = n$. Any method involving charging and discharging with differing indices would be very much more complex. The assumptions however would be true if no heat was transferred during the charge-discharge operation and indeed with relatively rapid volume changes this is a fair assumption. However, the incremental method described has a facility to accept a bank of accumulators with previously determined pre-charge pressures, and compute the pressure-volume relationship, if charged at one value of the polytropic index and discharged at another, thus giving an indication of the errors involved in the assumption.

6.3 Empirical Method for Determining the Charge Pressures of Accumulator Banks for Linear Pressure-Volume Approximation

Consider a bank of four accumulators Fig. 6.1. Let $VV(1)$ to $VV(4)$ be the total gas volumes of the accumulator bank at pressures corresponding to the charge pressures $Pa(1)$ to $Pa(4)$.

$$\text{Then } VV(1) = Va(1) + Va(2) + Va(3) + Va(4) \quad \text{eqn. 6.05}$$

$$VV(2) = Va(1) \left(\frac{Pa(1)}{Pa(2)} \right)^{\frac{1}{n}} + Va(2) + Va(3) + Va(4) \quad \text{eqn. 6.06}$$

$$VV(3) = Va(1) \left(\frac{Pa(1)}{Pa(3)} \right)^{\frac{1}{n}} + Va(2) \left(\frac{Pa(2)}{Pa(3)} \right)^{\frac{1}{n}} + Va(3) + Va(4) \quad \text{eqn. 6.07}$$

$$VV(4) = Va(1) \left(\frac{Pa(1)}{Pa(4)} \right)^{\frac{1}{n}} + Va(2) \left(\frac{Pa(2)}{Pa(4)} \right)^{\frac{1}{n}} + Va(3) \left(\frac{Pa(3)}{Pa(4)} \right)^{\frac{1}{n}} + Va(4) \quad \text{eqn. 6.08}$$

For simplification let the accumulator volumes be equal and let the increments of charge pressure be equal

$$\text{Then } VV(1) = 4 \quad \text{eqn. 6.09}$$

$$VV(2) = \left(\frac{1}{2} \right)^{\frac{1}{n}} + 3 \quad \text{eqn. 6.10}$$

$$VV(3) = \left(\frac{1}{3} \right)^{\frac{1}{n}} + \left(\frac{2}{3} \right)^{\frac{1}{n}} + 2 \quad \text{eqn. 6.11}$$

$$VV(4) = \left(\frac{1}{4}\right)^{\frac{1}{n}} + \left(\frac{2}{4}\right)^{\frac{1}{n}} + 1 \quad \text{eqn. 6.12}$$

Now if $n = 1$ and $V_a = 1$, $VV(1) = 4$, $VV(2) = 3.5$, $VV(3) = 3$ and $VV(4) = 2.5$.

As the pressures associated with these points have equal increments the points lie on a linear pressure-volume relationship. Also for the point one pressure increment above $P_a(4)$ the linear relationship still holds.

$$\text{ie } VV(5) = \left(\frac{1}{5}\right)^{\frac{1}{n}} + \left(\frac{2}{5}\right)^{\frac{1}{n}} + \left(\frac{3}{5}\right)^{\frac{1}{n}} + \left(\frac{4}{5}\right)^{\frac{1}{n}} \quad \text{eqn. 6.13}$$

$$VV(5) = 2 \text{ for } n = 1 \text{ and } V_a = 1$$

A numerical example shows the linearity to hold within reasonable limits when realistic values of n are used ie $n = 1.2$ to $n = 1.5$ (see Table 6.1).

This relationship however still has only two variables to alter the slope of the pressure-volume relationship, accumulator volume and the charge pressure of the first accumulator.

In practice accumulators are limited on the minimum charge pressure to approximately 20% of the maximum working pressure. This however is compatible with the required characteristic, since due to sprocket friction the torque-displacement characteristic of the sprocket drive system does not usually reduce to zero.

A further factor is required, to alter the slope of the pressure-volume characteristic, by adjusting the increment between each accumulator charge pressure, whilst the lowest pressure $P_a(1)$ remains constant. This pressure must be of pre-determined value to correspond with the equivalent point on the torque-displacement characteristic.

Let this increment factor be y_i so that the first charge pressure remains $P_a(1)$, the second becomes $P_a(2).y_i$, the third $P_a(3).y_i$ etc. Note $P_a(2) = 2. P_a(1).y_i$ etc.

The total gas volumes now become

$$VV(1) = 4 \quad \text{eqn. 6.14}$$

$$VV(2) = \left(\frac{1}{2 \cdot y_i}\right)^{\frac{1}{n}} + 3 \quad \text{eqn. 6.15}$$

$$VV(3) = \left(\frac{1}{3 \cdot y_i}\right)^{\frac{1}{n}} + \left(\frac{2}{3}\right)^{\frac{1}{n}} + 2 \quad \text{eqn. 6.16}$$

$$VV(4) = \left(\frac{1}{4 \cdot y_i}\right)^{\frac{1}{n}} + \left(\frac{2}{4}\right)^{\frac{1}{n}} + \left(\frac{3}{4}\right)^{\frac{1}{n}} + 1 \quad \text{eqn. 6.17}$$

$$VV(5) = \left(\frac{1}{5 \cdot y_i}\right)^{\frac{1}{n}} + \left(\frac{2}{5}\right)^{\frac{1}{n}} + \left(\frac{3}{5}\right)^{\frac{1}{n}} + \left(\frac{4}{5}\right)^{\frac{1}{n}} \quad \text{eqn. 6.18}$$

Again the numerical example shows this to yield reasonably linear results in the range $y_i = 1$ to $y_i = 3$, $n = 1.2$ to $n = 1.5$ (see Table 6.1).

In this example the slopes of the characteristic are taken such that S_5 is the slope between points $Pa(5)$, $VV(5)$ and $Pa(1)$, $VV(1)$

$$\text{ie } s_5 = \frac{Pa(1) \cdot y_i \cdot 5 - Pa(5)}{Va(VV(1) - VV(5))} \quad \text{eqn. 6.19}$$

$$s_5 = \frac{Pa(1)}{Va} \frac{(5 \cdot y_i - 1)}{VV(1) - VV(5)} \quad \text{eqn. 6.20}$$

Similarly s_4 is the slope between $Pa(4)$, $VV(4)$, and $Pa(1)$, $VV(1)$

s_3 is the slope between $Pa(3)$, $VV(3)$, and $Pa(1)$, $VV(1)$

s_2 is the slope between $Pa(2)$, $VV(2)$, and $Pa(1)$, $VV(1)$

s_t is the slope between $Pa(5)$, $VV(5)$, and $Pa(2)$, $VV(2)$

Note that to convert the slope obtained with unity values of $Pa(1)$ and Va a multiplication is required by $\frac{Pa(1)}{Va}$.

A minimum value of the slope achievable from any bank of accumulators is set by the tangent of the PV^n relationship at a pressure corresponding to the pre-charge pressure on the first accumulator.

$$VV = Va \left(\frac{Pa}{P}\right)^{\frac{1}{n}} \quad \text{eqn. 6.21}$$

$$P = Pa \left(\frac{V}{Va}\right)^{-n} \quad \text{eqn. 6.22}$$

$$\frac{dP}{dV} = n \cdot Pa \cdot Va^{(-1-n)} V_a^n \quad \text{eqn. 6.23}$$

$$\frac{dP}{dV} = - \frac{n \cdot P_a}{V_a}$$

eqn. 6.24

To compare this with unity values in use above

$$\frac{dP}{dV} = - n \text{ at } P_a = 1 \text{ and } V_a = 1$$

This would give minimum unity slopes with $n = 1.4$ of slope = 1.4 corresponding to y_i increment values of about 0.7, but numerical examples show that y_i can be taken to 0.5 (at which $P_a(2) = P_a(1)$) without undue affect to the upper portion of the linear approximation. Below $y_i = 0.7$ the point $VV(2)$ lies above the linear relationship, but higher values of VV correspond well.

This now gives three variables which can be manipulated to give the desired linear pressure-volume characteristic.

6.3.1) $P_a(1)$ - the lowest charge pressure in the accumulator bank

This usually corresponds to a fixed value on the required characteristic so little variation is possible. Care must be taken not to operate lower than the minimum stated by the manufacturers. But accumulators are available which will operate at zero initial pressure if required.

6.3.2) V_a - accumulator initial gas volume

Accumulators are only available in fixed step sizes and this setting procedure requires them to be of the same volume. They can however be used in combination, ie a 1.0 dm^3 and 0.5 dm^3 accumulator can be considered to be one accumulator of 1.5 dm^3 volume and charged to the same value.

6.3.3) y_i - accumulator bank pressure increment factor

The value of y_i is adjustable to give the required slope after the initial volume and the lowest charge pressure have been determined. Low values of y_i will mean that more accumulators are required to cover a given pressure range but the characteristic will be nearer to linear. High values of y_i will need less accumulators to cover this range but the relationship will be less linear. The points at the charge pressure will lie on the line but the loops between these points will be more pronounced.

The data from the numerical example has been plotted on Fig. 6.2

and an example given on its interpolation and use. The slope s_4 was taken as an average point for the production of this diagram.

Also an empirical relationship for y_i has been determined where

$$usl = \text{unity slope} = \text{slope required multiplied by } \frac{V_a}{Pa(1)}$$

$$y_i = .36 - .2.n + (.56 - .13.n).usl \quad \text{eqn. 6.25}$$

or assuming $n = 1.4$

$$y_i = .08 + .37. \frac{V_a}{Pa(1)} \cdot \text{slope} \quad \text{eqn. 6.26}$$

$$\text{Thus giving } Pa(1) = Pa(1) - \text{specified value} \quad \text{eqn. 6.27}$$

$$Pa(2) = Pa(1).y_i.2 \quad \text{eqn. 6.28}$$

$$Pa(3) = Pa(1).y_i.3 \text{ etc.} \quad \text{eqn. 6.29}$$

Note - y_i is non-dimensional so any consistent units can be used.

6.4 Computational Methods for Determining the Charge Pressures of Accumulator Banks for Pre-Determined Pressure-Volume Approximations

The empirical method previously described has the disadvantage of working only for linear pressure-volume relationships and requiring the use of equal size accumulators. As an alternative an incremental computational technique is described for use in the Terminal Section of the CSMP module of the simulation system, Terminal Section 1.

6.4.1) Terminal Section 1 Accumulator Pre-charge Pressure Setting using Pressure Incrementing Technique

The CSMP dynamic model for the simulation system is arranged such that the pressure-volume relationship required from the power absorber to accurately reproduce the tension-displacement relationship of the chain under dynamic conditions is calculated and stored in array form. The Terminal Section takes input of the volumes and number of accumulators in the bank and the polytropic index under which the accumulators will charge. Initially all the accumulators are set with their pre-charge pressure to a maximum value with the exception of the first accumulator, the pre-charge pressure of which is set equal to the lowest pressure in pressure-

volume characteristic arrays BPA and BVOL. The programme then increments pressure by a value KR, and at each increment checks if the total gas volume of all the accumulators VV is greater than that needed to give the required characteristic VLINE. This is calculated by linearly interpolating the BPA and BVOL arrays at the incremented pressure KP. If VV is greater than VLINE, the second accumulator pre-charge pressure is set to the previous value of KP, otherwise the pressure is again increased and a further check made. The procedure continues until a maximum pressure is reached. Three arrays AP, AL and AV are also produced as the pressure is incremented which describe the accumulator bank pressure-volume characteristic and the simulation pressure-volume characteristic for re-use in the dynamic model. Printed outputs of the accumulator pre-charge pressure settings and all the array elements are produced as outputs. This technique is able to set more than one accumulator to the same pre-charge pressure if the pressure-volume characteristic so requires and can deal with accumulator banks containing accumulators of differing sizes.

6.4.2) Terminal Section 2

As a comparison with the accumulator pre-charge setting procedure used in Terminal Section 1, Terminal Section 2 approximates the BVOL and BPA arrays to linear and uses the empirical relationship to set the pre-charge pressures assuming a polytropic index POWC. An incremental procedure is then used to produce the arrays AP, AL and AV which are required by the second run of the dynamic model.

The incremental procedure is modified from that used in Terminal Section 1 to accommodate charging and discharging at different polytropic indices. Values VT are computed which are the individual accumulator gas volumes at the maximum operation pressure after charging from the set pre-charge pressures at the charging index POWC. Pressure is then incrementally reduced and the total gas volume calculated assuming the accumulators discharge at the polytropic index POWE. This procedure

gives an indication of the errors produced from the assumption that the accumulators charge and discharge with the same polytropic index. Also using this method, if POWC is made equal to POWE, a direct comparison can be made between the incremental accumulator pre-charge setting technique as used in Terminal Section 1 and the empirical method.

6.4.3) Terminal Section 3

Terminal Section 3 sets accumulator pre-charge pressures to fit a pressure-volume relationship from the absorber determined only from the static characteristics of the chain haulage absorber system, as an alternative to the dynamic derivation used with Terminal Sections 1 and 2. The empirical accumulator pre-charge setting procedure is used along with the pressure incrementing method described for Terminal Section 2.

Terminal Section 3 is used to examine the importance of the dynamic derivation of the required absorber pressure-volume relationship. The primary difference being that Terminal Section 3 does not take into consideration the absorber leakage. However an empirical factor FACT can be used to compensate the required volume RBV for absorber leakage losses.

n=1.20										
yi	v2	v3	v4	v5	s2	s3	s4	s5	st	
0.6	3.859	3.326	2.830	2.350	1.42	1.19	1.20	1.21	1.19	
1.0	3.561	3.114	2.663	2.211	2.28	2.26	2.24	2.24	2.22	
1.5	3.400	2.999	2.573	2.136	3.34	3.50	3.50	3.49	3.56	
2.0	3.315	2.938	2.525	2.096	4.38	4.71	4.75	4.73	4.92	
2.5	3.262	2.900	2.495	2.072	5.42	5.91	5.98	5.96	6.30	
n=1.25										
yi	v2	v3	v4	v5	s2	s3	s4	s5	st	
0.6	3.864	3.348	2.865	2.397	1.47	1.23	1.23	1.25	1.23	
1.0	3.574	3.138	2.699	2.257	2.35	2.32	2.31	2.30	2.28	
1.5	3.415	3.023	2.607	2.181	3.42	3.58	3.59	3.57	3.65	
2.0	3.330	2.961	2.558	2.140	4.48	4.81	4.86	4.84	5.04	
2.5	3.276	2.922	2.527	2.114	5.52	6.03	6.11	6.10	6.46	
n=1.30										
yi	v2	v3	v4	v5	s2	s3	s4	s5	st	
0.6	3.869	3.368	2.898	2.441	1.53	1.27	1.27	1.28	1.26	
1.0	3.587	3.162	2.732	2.301	2.42	2.39	2.37	2.35	2.33	
1.5	3.430	3.046	2.640	2.224	3.51	3.67	3.68	3.66	3.73	
2.0	3.344	2.984	2.590	2.182	4.57	4.92	4.97	4.95	5.16	
2.5	3.290	2.944	2.558	2.155	5.63	6.16	6.24	6.23	6.61	
n=1.35										
yi	v2	v3	v4	v5	s2	s3	s4	s5	st	
0.6	3.874	3.388	2.929	2.483	1.58	1.31	1.31	1.32	1.29	
1.0	3.598	3.184	2.765	2.343	2.49	2.45	2.43	2.41	2.39	
1.5	3.443	3.069	2.672	2.265	3.59	3.76	3.76	3.75	3.82	
2.0	3.358	3.006	2.621	2.222	4.67	5.03	5.08	5.06	5.28	
2.5	3.304	2.965	2.588	2.194	5.74	6.28	6.37	6.37	6.76	
n=1.40										
yi	v2	v3	v4	v5	s2	s3	s4	s5	st	
0.6	3.878	3.406	2.959	2.523	1.64	1.35	1.34	1.35	1.33	
1.0	3.610	3.205	2.795	2.383	2.56	2.51	2.49	2.47	2.45	
1.5	3.456	3.090	2.702	2.304	3.68	3.85	3.85	3.83	3.90	
2.0	3.371	3.027	2.650	2.260	4.77	5.14	5.19	5.17	5.40	
2.5	3.317	2.986	2.617	2.231	5.85	6.41	6.51	6.50	6.91	
n=1.45										
yi	v2	v3	v4	v5	s2	s3	s4	s5	st	
0.6	3.882	3.423	2.987	2.561	1.69	1.39	1.38	1.39	1.36	
1.0	3.620	3.225	2.824	2.422	2.63	2.58	2.55	2.53	2.50	
1.5	3.469	3.110	2.731	2.341	3.76	3.93	3.94	3.92	3.99	
2.0	3.384	3.047	2.678	2.296	4.87	5.24	5.30	5.28	5.51	
2.5	3.330	3.005	2.644	2.267	5.97	6.53	6.64	6.64	7.06	
n=1.50										
yi	v2	v3	v4	v5	s2	s3	s4	s5	st	
0.6	3.886	3.439	3.013	2.597	1.75	1.43	1.42	1.43	1.40	
1.0	3.630	3.244	2.852	2.458	2.70	2.64	2.61	2.59	2.56	
1.5	3.481	3.130	2.758	2.377	3.85	4.02	4.03	4.00	4.08	
2.0	3.397	3.066	2.705	2.331	4.97	5.35	5.41	5.39	5.63	
2.5	3.342	3.024	2.671	2.302	6.08	6.66	6.77	6.77	7.21	

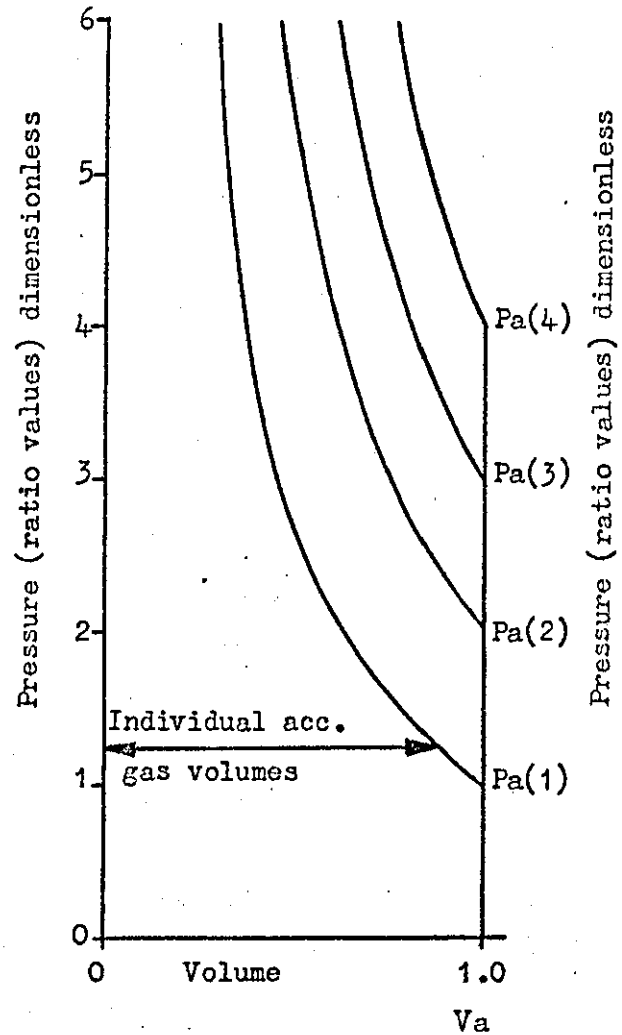
note V2 = VV(2), V3 = VV(3) etc

Table 6.1

Numerical example of expressions 6.14 to 6.18

Based on unity volume accumulators with a minimum unity pressure

INDIVIDUAL CHARACTERISTICS



COMBINED CHARACTERISTICS

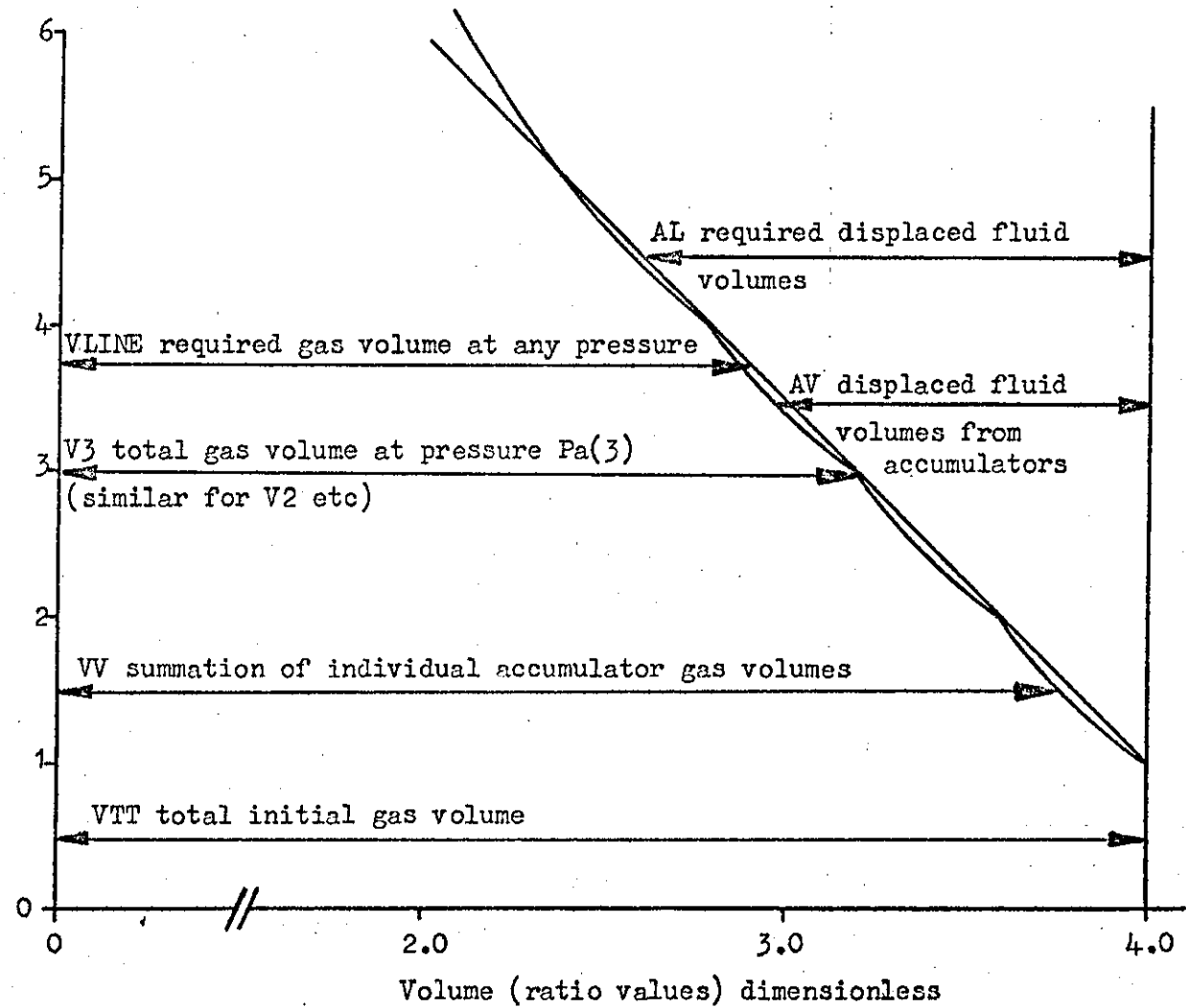
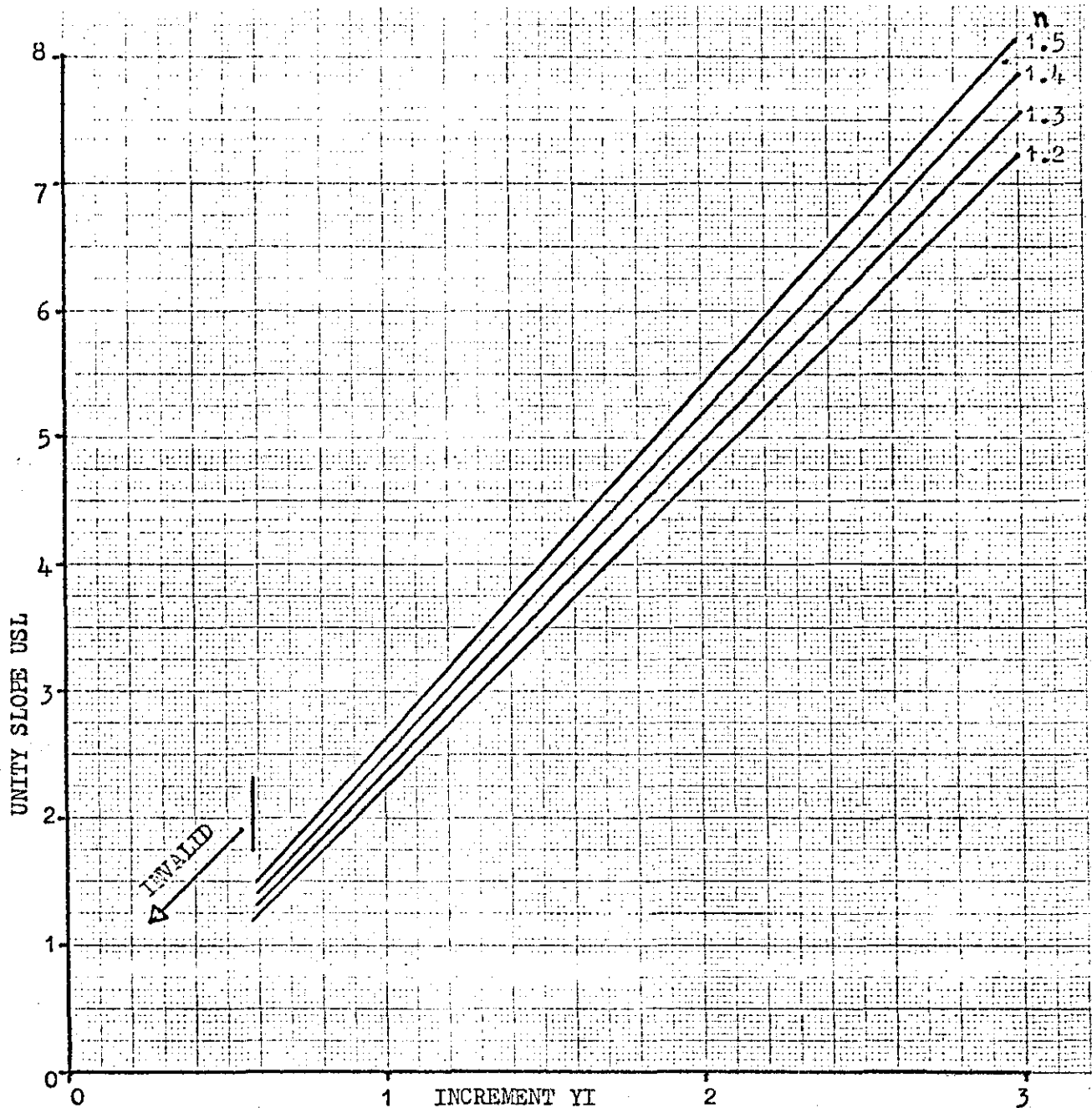


Fig 6.1 Diagrammatic representation of the addition of 4 accumulators charged to various pre-charge pressures to give an approximation to a linear pressure-volume discharge characteristics



How to use

Assume a bank of accumulators each of 60 in^3 ($.98 \text{ dm}^3$) capacity are required to give a linear pressure volume characteristic discharging 80 in^3 (1.31 dm^3) of fluid between 400 lb/in^2 (2.8 MPa) and 2000 lb/in^2 (13.8 MPa) with a polytropic index of $n = 1.4$

- Actual slope = $\frac{2000 - 400}{80} = 20 \text{ lb/in}^5$
- Unity slope = $20 \times \frac{60}{400} \left(\frac{\text{accumulator volume}}{\text{minimum pressure}} \right) = 3.0$ (dimensionless)
- From graph $n = 1.4$ at $USL = 3.0$ $YI = 1.18$ (dimensionless)
- Accumulator pre-charge pressures
 - $1) = 400 \text{ lb/in}^2$ (2.76 MPa)
 - $2) = 2 \times 400 \times 1.18 = 944 \text{ lb/in}^2$ (6.5 MPa)
 - $3) = 3 \times 400 \times 1.18 = 1416 \text{ lb/in}^2$ (9.8 MPa)
 - $4) = 4 \times 400 \times 1.18 = 1888 \text{ lb/in}^2$ (13.0 MPa)

Fig 6.2 Graph for determination of accumulator bank pre-charge pressures to achieve approximation to linear pressure - volume discharge characteristics

7 EXPERIMENTAL DETERMINATION OF HYDRO-PNEUMATIC ACCUMULATOR DISCHARGE CHARACTERISTICS

7.1 Introduction

Hydro-pneumatic accumulators are common components in hydraulic circuits where they are mainly used as either energy storage devices or for shock suppression. For these applications the capacitance requirements of the circuits can seldom be accurately specified and therefore accurate determination of accumulator performance is not required. Accumulator selection is made by a 'rule of thumb' procedure and by application of existing characteristics as stated in the manufacturers catalogues, whilst physical size also imposes limitations on choice. A section through a Greer-Mercier type hydro-pneumatic accumulator is shown in Fig. 7.1.

Several papers have been published on accumulator characteristics, most recently references 4 and 5. Initial use of data from reference 5 for setting accumulator pre-charge pressures for use in the chain tension simulation rig did not produce the expected results. Since the accumulators in use were not of the same capacity as those in reference 5, it was decided to conduct a series of tests to determine the characteristics of accumulators using an improvement of the method described in reference 5.

7.2 Experimental Method

To accurately determine accumulator charge-discharge characteristics, continuous measurements of fluid pressure and volume are required as the accumulator is charging and discharging. Pressure can easily be measured using strain gauge type pressure transducers, but volume is more difficult to determine if a continuous relationship with time is required.

Experiments described in reference 5 had assumed constant flow rates over a measured time, a total volume being obtained for a complete discharge by measurement into a container. To achieve a better representation of volume with time or pressure, a ram and displacement transducer were used for volume measurement.

A hydraulic circuit as shown in Fig. 7.2 was devised to determine the accumulator characteristics. Pressure from an external source could be switched to either pressurise or exhaust the greater area of a hydraulic ram. A connection from the smaller ram area was taken to the accumulator through a variable restrictor, for control of the flow rate into or out of the accumulator. Two additional stop valves assisted in calibration and de-aeration of the circuit.

Instrumentation consisted of a strain gauge type pressure transducer for accumulator fluid pressure measurement and a 10 turn rotary potentiometer for measurement of ram displacement. The rotary potentiometer had a 5 cm diameter wheel edged with foam plastic sealing strip to eliminate slip between the potentiometer and the rod, and was spring loaded into position in contact with the ram rod.

Measurements were taken on a Bryans X-Y plotter with the pressure reading onto the Y1 axis and ram displacement on the X axis. The second Y axis Y2 was used on time base to give a measurement of time and hence flow rates.

Volume calibration was made by measuring the ram displacement with a rule, the ram area being known, and adjusting the X axis gain control to give the required scale factors. This was checked by venting a given volume through valve A and measuring into a cylinder.

7.3 Experimental Procedure

Tests were carried out using C15 4.54 dm^3 (1 gal) and B23 1.14 dm^3 (1 qt) Greer-Mercier accumulators with pre-charge pressures of 5.2 MPa (750 lb/in^2). Pressure-volume recordings were taken for a range of restrictor valve settings by charging the accumulators to 17.2 MPa (2500 lb/in^2) followed by discharging back to zero pressure. Two sets of results were taken, by discharging immediately after the maximum pressure had been attained and by charging, holding at maximum pressure to allow gas temperature to reduce and then discharging.

An initial analysis of the results did not correspond to what had been expected, so checks were made of calibrations and the accumulator initial gas volumes.

7.3.1) Determination of Initial Gas Volume

This exercise was made using several methods for both accumulators.

7.3.1.1) With the accumulator disconnected from the rig the bag was pressurised with water which was subsequently measured into a cylinder. This gave volumes of 3.77 dm^3 for the 4.54 dm^3 (1 gal) accumulator and 1.14 dm^3 for the 1.14 dm^3 (1 qt) accumulator, agreeing with the gas volumes as quoted by the manufacturers.

7.3.1.2) The accumulators were held with the exhaust port uppermost with zero pressure in the bag. Water was introduced into the accumulator until overflowing. The bag was pressurised to displace the water, the water in the port removed and as the pressure in the bag was released, water which had been trapped in the accumulator was measured. These tests suggested that $.35 \text{ dm}^3$ (21.6 in^3) and $.15 \text{ dm}^3$ (9.0 in^3) of fluid could be trapped in the 4.54 dm^3 (1 gal) and 1.14 dm^3 (1 qt) accumulators.

7.3.1.3) With the accumulator on the rig, the gas valve was removed and the accumulator pressurised to .3 MPa (50 lb/in^2) using the ram system (this is not a recommended practice and was only employed for the initial volume tests). The variable restrictor was then completely closed and valve A opened, the bag pressurised and the displaced fluid measured into a cylinder. This gave initial volumes of 3.44 dm^3 (210 in^3) and $.98 \text{ dm}^3$ (60 in^3) for the 4.54 dm^3 (1 gal) and 1.14 dm^3 (1 qt) accumulators.

These tests clearly indicate that the initial gas volume is not the maximum volume of the accumulator vessel, but is affected by how much fluid can be trapped in the accumulator after the anti-extrusion valve has closed. Initial gas volumes of 3.44 dm^3 (210 in^3) and $.98 \text{ dm}^3$ (60 in^3) are used in subsequent calculations of accumulator characteristics for the 4.54 dm^3 (1 gal) and 1.14 dm^3 (1 qt) accumulators.

7.4 Experimental Results

A typical recording from the X-Y plotter is shown in Fig. 7.3. These recordings were analysed by transferring the pressure-volume characteristics to log-log scales Fig. 7.4, so that an assessment could be made of the polytropic index n in the PV^n gas law relationship, for both charging and discharging conditions. An estimate of the average charge and discharge flow rates was made from the time-volume trace on the X-Y recordings. (This was not linear due to the pressure-flow characteristic of the restrictor valve so only average flow rates were calculated).

Tabulations of the results are shown in Tables 7.1 and 7.2.

7.5 Observations

An examination of the tabulated data Tables 7.1 and 7.2 suggests the following values of the polytropic index n when assuming the PV^n relationship for accumulator charge and discharge.

7.5.1) For 4.54 dm^3 (1 gal) accumulators with 3.44 dm^3 (210 in^3) initial gas volume, charging and discharging at flow rates between $.076 \text{ dm}^3/\text{sec}$ to $.76 \text{ dm}^3/\text{sec}$ (1 gal/min to 10 gal/min) ie 3 to 15 sec charging and discharging time. The value of n lies between 1.4 to 1.5 during charging and 1.45 to 1.55 during discharging.

7.5.2) For 1.14 dm^3 (1 qt) accumulators with $.98 \text{ dm}^3$ (60 in^3) initial gas volumes, charging and discharging at flow rates between $.076 \text{ dm}^3/\text{sec}$ to $.76 \text{ dm}^3/\text{sec}$ (1 gal/min to 10 gal/min) ie 1 to 5 sec charging and discharging time. The value of n lies between 1.45 to 1.55 during charging and 1.5 to 1.6 during discharging.

7.5.3) Although an examination of slow discharge rates was not the objective of these tests it would appear that flow rates of less than $.04 \text{ dm}^3/\text{sec}$ (.5 gal/min) were required to reduce the value of n to 1.25.

The importance of the initial gas volume can be seen by taking results which give an index of 1.45 with the measured initial gas volume of $.98 \text{ dm}^3$ (60 in^3) and assuming the manufacturers quoted initial gas volume

of 1.14 dm^3 (70 in^3). This gives a calculated index of 1.83. It can be seen therefore that the initial gas volume is a critical factor in accumulator discharge characteristic prediction.

When accumulators, of the sizes tested, are charged and immediately discharged the final pressure can be expected to be only about .34 MPa (50 lb/in^2) lower than the charge pressure for flow rates around $.076 \text{ dm}^3/\text{sec}$ (1 gal/min). For rapid charge and discharge the resulting pressure is negligibly lower than the initial charge pressure, only a minimal heat loss can take place through the bay walls during the brief period of elevated gas temperature.

If the gas temperature is allowed to cool after charging, the following discharge results in a gas cooling which reduces the final pressure. Holding at a load pressure for 100 sec followed by a discharge produced a gas pressure of approximately 1.7 MPa (250 lb/in^2) lower than the charge pressure. A hold at pressure for 100 sec was not sufficient to reduce the gas temperature to ambient, the reduction obtained after this period was approximately equivalent to the temperature produced after a charge rate corresponding to $n = 1.06$.

The changes of gas temperature in accumulators are larger than might at first be anticipated. For example, in the case of an accumulator being charged at an index of 1.45 from an ambient temperature of 20°C and a pre-charge pressure of 5.1 MPa (750 lb/in^2), to a final pressure of 20.4 MPa (3000 lb/in^2), the final gas temperature would be 177°C . If the gas were allowed to cool back to ambient with the pressure maintained and then discharged at $n = 1.5$ the final gas pressure would be 2.6 MPa (375 lb/in^2) and the temperature -126°C .

The apparatus and experimental method proved to be successful for accumulator characteristic determination. There were however several areas of improvement.

7.5.4) Slight fluid compression effects could be seen on the X-Y

recordings. Replacement of the flexible pipes with short steel connections would reduce the capacitance effects of pipe elasticity and fluid bulk modulus.

7.5.5) The restrictor valve used for flow control gave a non-linear characteristic and unequal two way operation. Flow control valves were not used due to their unknown dynamic performance, but their inclusion in any further investigation would be appropriate.

7.5.6) The return to tank was excessively long and of small bore flexible hose, this restricted the maximum discharge rates.

7.5.7) The ram displacement technique for volume measurement gave excellent results but the conversion from linear to log-log scales was time consuming and of doubtful accuracy. The Bryans X-Y recorder can however be equipped with logarithmic amplifiers, which if used on both axes, would enable direct analysis of recordings to be made.

Although far from comprehensive, these results clearly show the importance of an accurate value for the initial gas volume when dealing with accumulator characteristics. To show how such a substantial volume of fluid can be trapped inside an accumulator, to effectively reduce the initial gas volume by $8\frac{1}{2}\%$ for the 4.54 dm^3 (1 gal) accumulator and 14% for the 1.14 dm^3 (1 qt) accumulator, a working model of the 1.14 dm^3 (1 qt) accumulator was constructed from perspex Fig. 7.5. Fig. 7.6 shows the accumulator with a fluid pressure larger than the pre-charge pressure, the bag compressed and the anti-extrusion valve in its maximum extended position. In Fig. 7.7 the fluid pressure has been released and the valve is seen fully closed with an annulus of fluid remaining between the accumulator wall and the gas bag.

7.6 Conclusions

The results suggest that an appropriate value for the polytropic index using 4.54 dm^3 (1 gal) and 1.14 dm^3 (1 qt) accumulators when discharging at flow rates above $.076 \text{ dm}^3/\text{sec}$ (1 gal/min) would be $n = 1.45$. This value

agrees with reference 5 which suggests that a 'rule of thumb' would be to use $n = 1.4$ for fast operation up to 13.8 MPa (2000 lb/in²) and $n = 1.5$ at 20.7 MPa (3000 lb/in²) for discharge with isothermal compression. This work was carried out without considering the trapped volume, but since the accumulators used were a minimum volume of 9.1 dm³ (2 gal) nominal capacity, the effect would not be as great as with smaller accumulators.

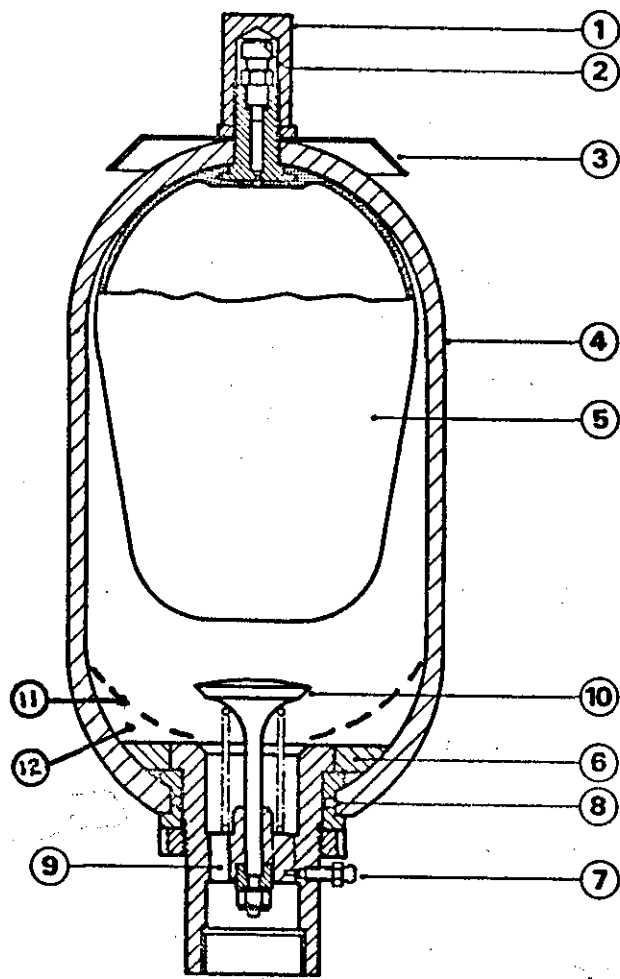
The results here show that charging also takes place under polytropic conditions $n = 1.45$ for flow rates above .076 dm³ (1 gal/min). Isothermal charging should only be considered if the temperature is allowed to stabilise at load pressure or if the charging time is in excess of 2 minutes.

Test No.			G1		G2		G5		G6		G3		G4	
Points during accumulator charge			Gas Volumes											
	lb/in ²	MPa	in ³	dm ³	in ³	dm ³	in ³	dm ³	in ³	dm ³	in ³	dm ³	in ³	dm ³
	2500	17.2	93	1.52	-	-	-	-	96	1.57	90	1.47	-	-
	2000	13.8	109	1.79	112	1.83	105	1.72	112	1.83	106	1.74	92	1.51
	1500	10.3	133	2.18	136	2.23	130	2.13	135	2.21	130	2.13	120	1.97
	1000	6.9	174	2.85	176	2.88	173	2.83	176	2.88	170	2.78	169	2.77
	800	5.5	201	3.29	202	3.31	201	3.29	203	3.33	197	3.23	198	3.24
Points during accumulator discharge	2500	17.2	93	1.52	-	-	-	-	95	1.56	70	1.15	-	-
	2000	13.8	106	1.74	112	1.83	101	1.65	108	1.77	80	1.31	92	1.51
	1500	10.3	126	2.06	134	2.19	121	1.98	129	2.11	96	1.57	111	1.82
	1000	6.9	163	2.67	176	2.88	157	2.57	168	2.75	127	2.08	149	2.44
	800	5.5	190	3.11	202	3.31	184	3.01	195	3.19	151	2.47	177	2.90
			lb/in ²	MPa	lb/in ²	MPa	lb/in ²	MPa	lb/in ²	MPa	lb/in ²	MPa	lb/in ²	MPa
Charge pressure			760	5.24	760	5.24	760	5.24	770	5.31	740	5.1	750	5.17
Pressure after discharge			700	4.82	760	5.24	660	4.55	720	4.96	550	3.8	660	4.55
			gal/min	dm ³ /sec	gal/min	dm ³ /sec	gal/min	dm ³ /sec	gal/min	dm ³ /sec	gal/min	dm ³ /sec	gal/min	dm ³ /sec
Charge flow rate			2.0	.15	9.0	.68	.9	.068	3.4	.26	2.2	.17	.2	.015
Discharge flow rate			2.0	.15	7.7	.58	1.7	.13	3.8	.29	2.0	.15	.7	.053
			sec		sec		sec		sec		sec		sec	
Time to start of discharge			14		2.9		33		8.3		180		150	
Time for discharge			13		3.1		14		7.4		16		38	
Charge index			1.45		1.5		1.4		1.5		1.5		1.2	
Discharge index			1.55		1.5		1.5		1.5		1.37		1.3	

Table 7.1 Results taken from X-Y recordings of accumulator charge-discharge characteristics
Nominal accumulator size 1 gal
Actual initial gas volume 210 in³ (3.44 dm³)
Nominal pre-charge pressure 750 lb/in² (5.0 MPa)

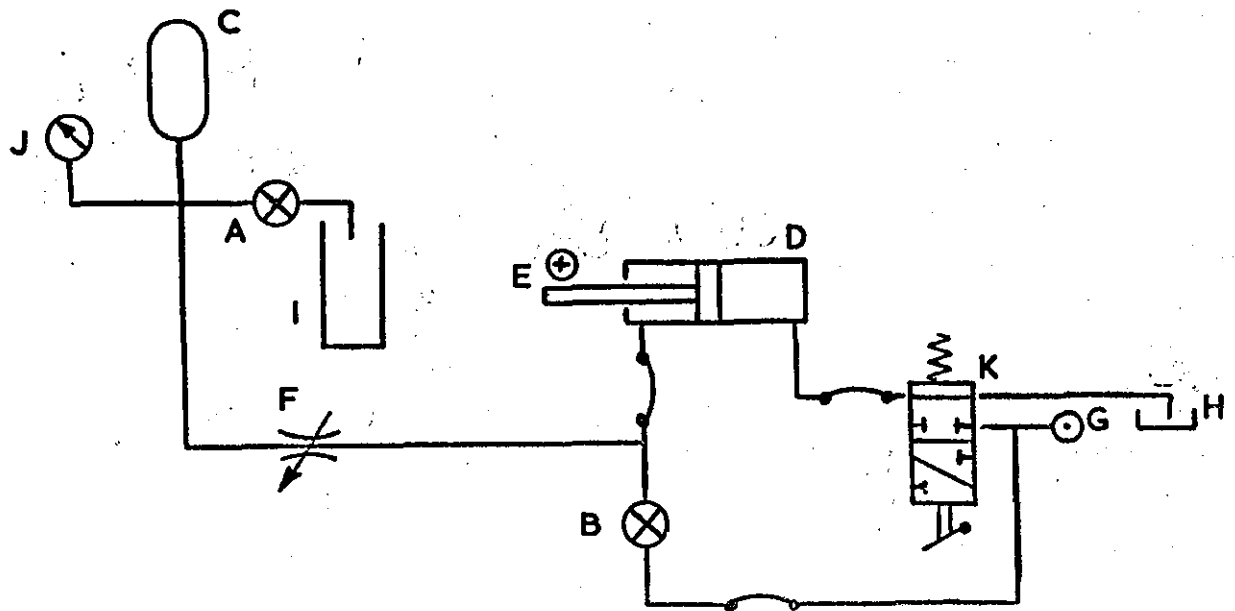
Test No.			A1		A2		A3		A4		A5		A6		A7		A8		A10		A11		
			Gas Volumes																				
			lb/in ²	MPa	in ³	dm ³	in ³	dm ³	in ³	dm ³	in ³	dm ³	in ³	dm ³	in ³	dm ³	in ³	dm ³	in ³	dm ³	in ³	dm ³	
Points during accumulator discharge		3000	20.6	-	-	-	-	-	-	24.5	.40	-	-	24		23.5	.39	-		-	-	-	-
		2500	17.2	27	.44	-	-	-	-	28	.46	26	.43	27	.44	27	.44	25	.41	22	.36	23	.38
		2000	13.8	31	.51	30	.49	29	.48	32	.52	30.5	.50	31.5	.52	31	.51	29.5	.48	27.5	.45	28.5	.47
		1500	10.3	37	.61	37	.64	36.5	.60	38	.62	37	.61	38	.62	38	.62	36.5	.60	35	.57	36	.59
		1000	6.9	48.5	.79	47.5	.78	48	.79	50	.82	49	.80	49	.80	49.5	.81	48	.79	47.5	.78	48	.79
		800	5.5	56	.92	55	.90	56	.92	57	.93	57	.93	57	.93	57	.93	55	.90	55	.90	56	.92
Points during accumulator discharge		3000	20.6	-	-	-	-	-	-	24.5	.40	-	-	18	.29	16.5	.27	-	-	-	-	-	-
		2500	17.2	27	.44	-	-	-	-	28	.46	26	.43	20	.33	19	.31	19	.31	19	.31	19	.31
		2000	13.8	31	.51	30	.49	29	.48	32	.52	29	.48	23	.38	22	.36	22	.36	22	.36	22	.36
		1500	10.3	37	.61	37	.61	35.5	.58	38	.62	35	.57	28	.46	26.5	.43	26.5	.43	26.5	.43	27	.44
		1000	6.9	48.5	.79	47.5	.78	46	.75	50	.82	45	.74	36	.59	34.5	.57	35	.57	35	.57	37	.61
		800	5.5	56	.92	55	.90	53	.87	57	.93	52.5	.86	42	.59	40	.66	41	.67	41	.67	45	.74
			lb/in ²	MPa	lb/in ²	MPa	lb/in ²	MPa	lb/in ²	MPa	lb/in ²	MPa	lb/in ²	MPa	lb/in ²	MPa	lb/in ²	MPa	lb/in ²	MPa	lb/in ²	MPa	
Charge Pressure			720	4.96	720	4.96	720	4.96	740	5.10	740	5.10	740	5.10	740	5.10	730	5.03	730	5.03	730	5.03	
Pressure after discharge			720	4.96	700	4.83	660	4.55	740	5.10	620	4.27	480	3.31	430	2.96	480	3.31	480	3.31	600	4.14	
			gal/min	dm ³ /sec	gal/min	dm ³ /sec	gal/min	dm ³ /sec	gal/min	dm ³ /sec	gal/min	dm ³ /sec	gal/min	dm ³ /sec	gal/min	dm ³ /sec	gal/min	dm ³ /sec	gal/min	dm ³ /sec	gal/min	dm ³ /sec	
Charge flow rate			4.5	.34	3.0	.23	.8	.06	9.5	.72	2.0	.15	7.7	.58	9.0	.68	1.8	.14	.3	.02	.5	.04	
Discharge flow rate			7.2	.55	2.0	.15	5.5	.27	9.5	.72	2.0	.15	7.7	.58	9.0	.68	1.8	.14	2.2	.17	.5	.04	
			sec		sec		sec		sec		sec		sec		sec		sec		sec		sec		
Time to start of discharge			1.0		2.0		4.5		1.3		2.5		80		75		100		103		100		
Time for discharge			1.3		2.6		3.0		.75		4.0		1.0		.8		5.0		4		15		
Charge index			1.54		1.55		1.45		1.56		1.45		1.5		1.5		1.45		1.25		1.27		
Discharge index			1.54		1.55		1.5		1.56		1.6		1.5		1.5		1.45		1.4		1.25		

Table 7.2 Results taken from X - Y recordings of accumulator charge - discharge characteristics.
Nominal accumulator size 1 QT.
Actual initial gas volume 60 in³ (.93 dm³).
Nominal pre-charge pressure 750 lb/in² (5.0 MPa).



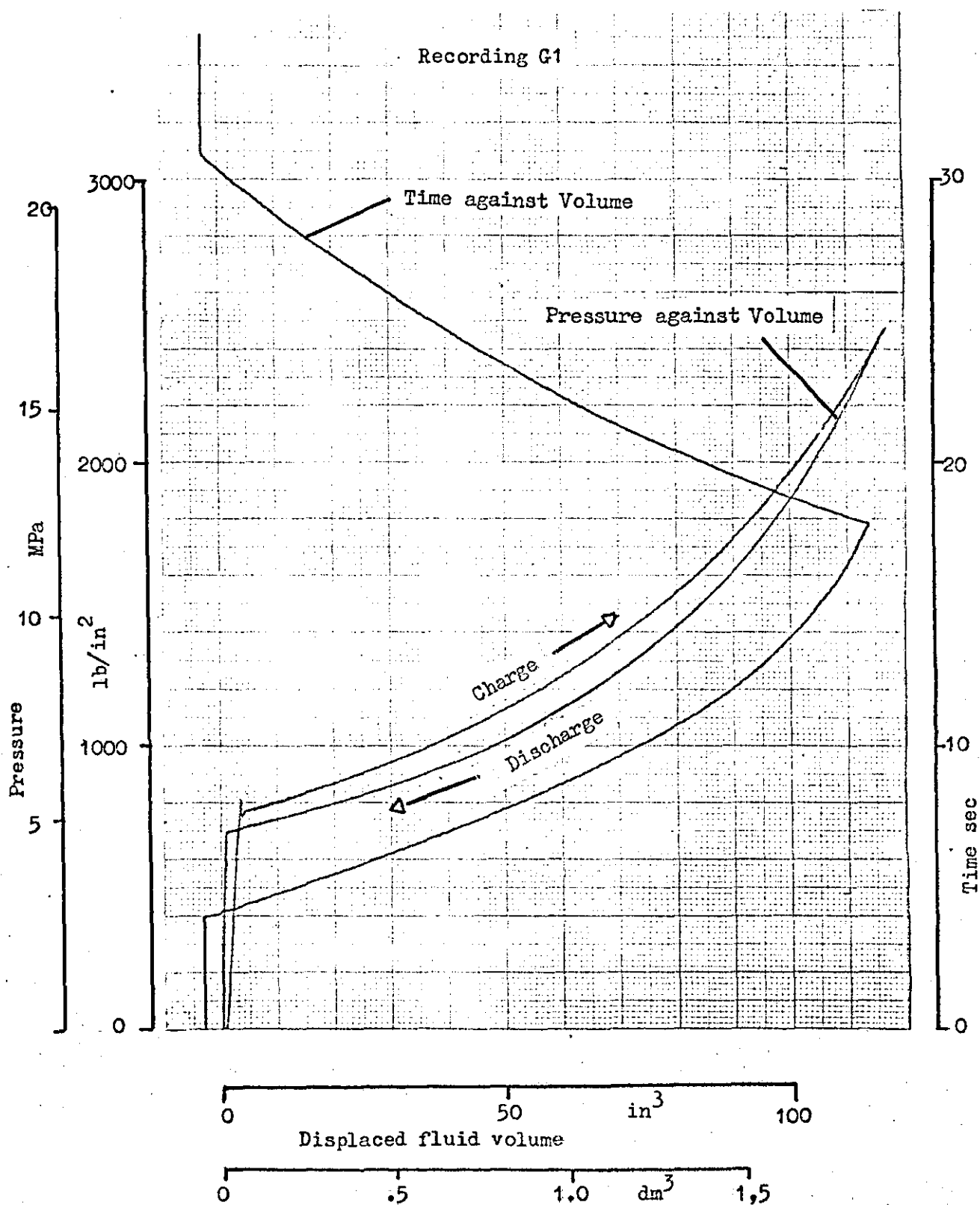
- 1) Protective cap
- 2) Sealing cap
- 3) Nameplate
- 4) Shell
- 5) Separator bag
- 6) Anti-Extrusion ring
- 7) Bleed valve
- 8) 'O' ring seal
- 9) Fluid port
- 10) Poppet valve
- 11) Separator bag position with pre-charge pressure greater than fluid pressure
- 12) Trapped fluid volume

Figure 7.1 Section through Greer-Mercier hydro-pneumatic accumulator showing trapped fluid volume



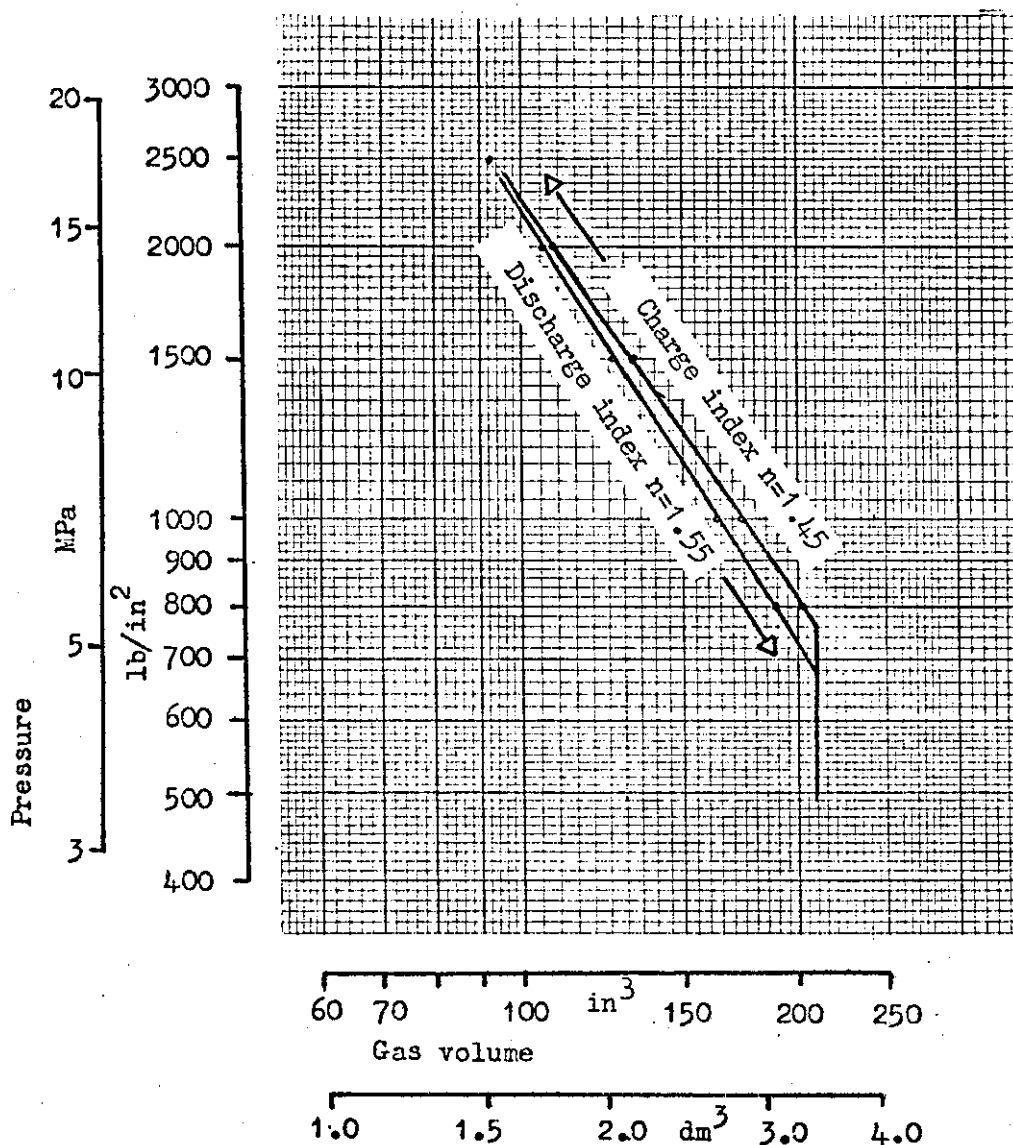
- A - Calibration and bleed valve normally shut
- B - Calibration valve normally shut
- C - Accumulator under test
- D - Double acting ram
 Rod dia = 2.25 in (50.63 mm)
 Bore dia = 3.5 in (88.9 mm)
 Stroke = 27 in (680 mm)
- E - Displacement transducer
- F - Throttle valve
- G - Pressure supply
- H - Return to tank
- I - Measuring cylinder
- J - Pressure transducer
- K - Direction valve

Fig. 7.2 Circuit diagram of accumulator charge - discharge characteristics rig



Nominal accumulator size 1 gal
 Actual initial gas volume 3.44 dm³ (210 in³)
 Nominal pre-charge pressure 5.0 MPa (750 lb/in²)

Fig. 7.3 X-Y Recording of accumulator pressure volume characteristics



Points taken from X-Y recording G1 Figure

Fig. 7.4 Accumulator charge - discharge characteristics plotted on log-log scales

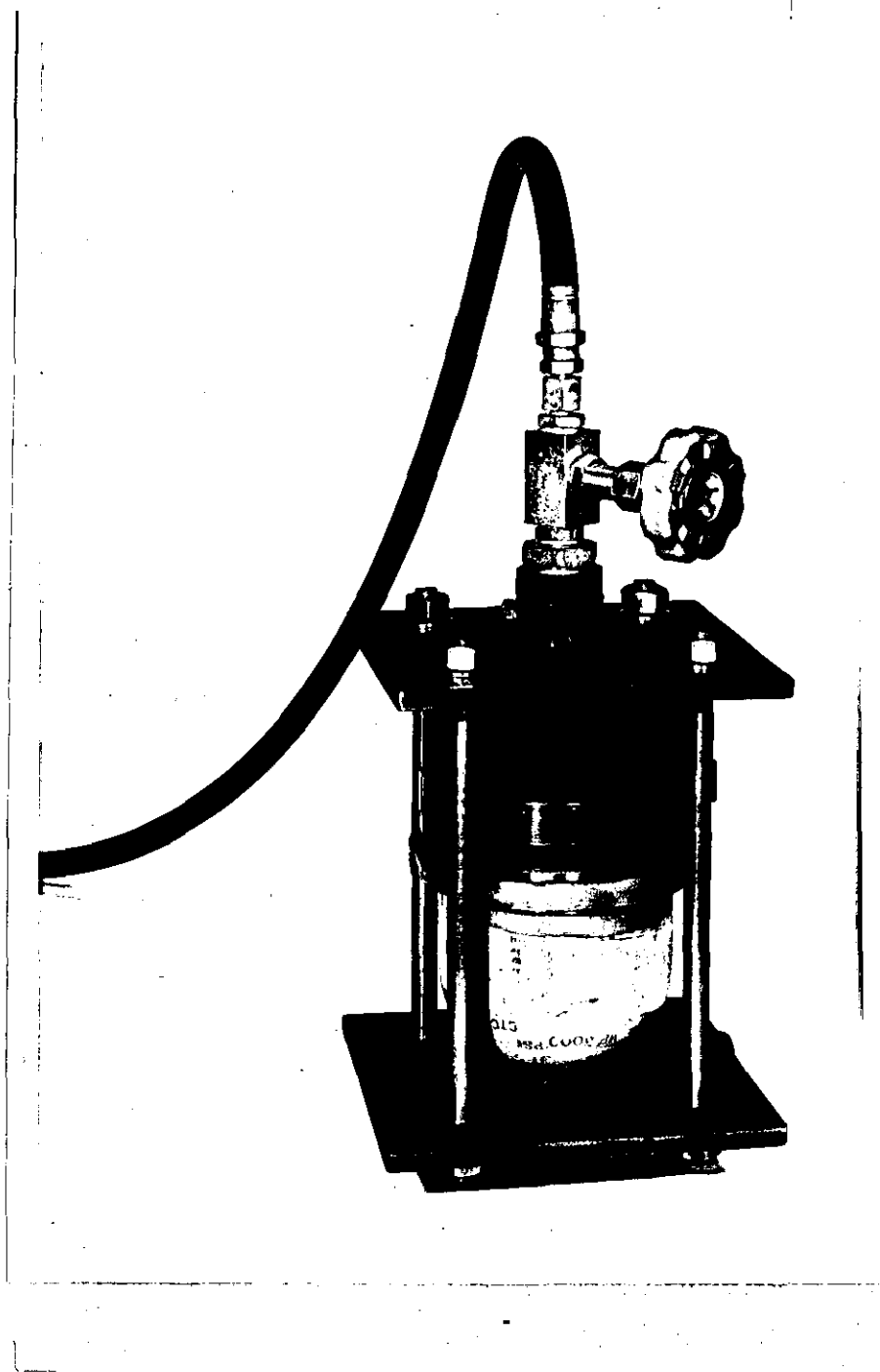


Fig. 7.5 Perspex Model of Greer-Mercier Accumulator



Fig. 7.6 Perspex Model Accumulator with Poppet Valve Open



Fig. 7.7 Perspex Model Accumulator with Poppet Valve Closed showing Trapped Fluid Volume

8 EXPERIMENTAL EXAMINATION OF ACCUMULATOR AND CURVE FOLLOWER CHAIN ELASTICITY SIMULATION TECHNIQUES

8.1 Introduction

To simulate chain elasticity effects using hydrostatic power absorbers, it is necessary to either store or provide energy for the absorber sufficient to give the equivalent torque-displacement relationship to that given by the chain when the haulage drive is interrupted. Two systems were developed to achieve this requirement, the use of banks of hydro-pneumatic accumulators in the absorber circuit and the use of an additional power supply to the absorber, controlled by a function generator attachment (curve follower) on the Bryans X - Y plotter.

8.2 Description

The rig equipment was as previously described for the absorber characteristics determination.

Two banks of accumulators were available for use in the absorber circuit, a bank of eight B23 1.14 dm^3 (1 qt) and six C15 4.54 dm^3 (1 gal) with one D13 9.08 dm^3 (2 gal). All were standard Greer-Mercier accumulators.

The Bryans curve follower attachment for the X - Y plotter enables an output voltage to be obtained, proportional to the amplitude of a pre-drawn line. The curve follower module replaces the Y1 axis amplifier and connects to a light sensitive head fitted into the Y1 pen holder. Any desired function can thus be generated between an input to the X axis, or the X axis time base signal, and the output voltage from the curve follower. The Y2 channel can simultaneously monitor the effects of this control signal.

For use in chain tension simulation, the signal from the sprocket displacement potentiometer is fed to the X axis and the control signal from the curve follower is fed through an amplifier to the 'Electroilic'

valve controlling the absorber circuit relief valve. In this way, with the correct function drawn for the curve follower, the absorber pressure can be related to the haulage sprocket displacement. An additional high pressure supply to the circuit allows the absorber to provide energy into the haulage unit under stop or overload conditions.

8.3 Test Procedure

8.3.1) Simulation using the Accumulator Banks

Development work on the accumulator bank simulation method was carried out using the Staffa B270H absorber. This work indicated that a more precise knowledge of the discharge characteristics of accumulators was needed, to enable the pre-charge pressure to be accurately determined, to produce linear pressure-volume characteristics. This instigated the experiments previously described on individual accumulator discharge characteristics.

Using the Hagglunds 6185 absorber, a series of tests was carried out using the bank of 4.54 dm^3 (1 gal) accumulators set to pre-charge pressures determined by the TERMINAL section of the CSMP model of the system.

Recordings were taken of the haulage sprocket torque (from the strain gauge shaft in the gearbox) against the sprocket displacement and the absorber pressure against sprocket displacement Figs. 8.1 to 8.3. To obtain these results the haulage was run in the forward direction at $\frac{1}{4}$ speed with the absorber circuit relief valve set to maximum. This charged the accumulators, increased the absorber circuit pressure which in turn increased the haulage pressure. When the haulage circuit overload pressure was reached the by-pass valve operated and the accumulators discharged, driving the haulage in the reverse direction. The torque-displacement recordings were carried out at two overload valve settings TRIP and PCOMP. The value PCOMP compensates for the difference between the frictional losses of the chain system and the absorber.

Recordings of the energy release speeds using various by-pass spools were taken using the same procedure as for the torque-displacement characteristics. These were also carried out for both the values TRIP and PCOMP. Readings were taken from the recordings and are shown in Table 8.1.

A recording of the haulage pressure was taken against time to show the transients existing in the circuit at the time of by-pass operation
Fig. 8.4.

8.3.2) Simulation using Curve Follower Technique

The curve follower technique of chain elasticity simulation involves the generation of a function, to relate the absorber circuit pressure, controlled by a voltage input to the 'Electroilic' valve, to the sprocket angular displacement. The pressure-displacement characteristic was obtained from the CSMP model, but the non-linear voltage characteristic of the 'Electroilic' valve eliminates its direct use as the function for the curve follower.

To simplify the development of the correct function for the curve follower the following technique was adopted. The chart on the X - Y plotter was divided into upper and lower sections. On the upper section the pressure (Y axis)-displacement (X axis) relationship required from the absorber was plotted using data from the CSMP model. With a pen replacing the light sensitive head of the curve follower in the Y1 pen holder, and the absorber pressure signal fed into the Y2 pen, the control signal being fed to the 'Electroilic' valve from the curve follower unit was reduced from a maximum value in increments giving a corresponding movement of the Y1 pen. At each increment, using the X zero position control on the plotter, the Y2 pen was made to coincide with the pre-drawn pressure-displacement relationship, a point was then made with the Y2 pen on the lower section of the chart. In this manner, a function for the light sensitive head to follow was made which would reproduce the required pressure-volume characteristic on the absorber, and display this relationship on the Y1 channel for comparison with the pre-drawn line.

To eliminate the need to adjust the overload pressure from TRIP to PCOMP, the upper part of the curve, above a pressure equivalent to PCOMP, was made at the maximum gradient acceptable to the curve follower. In this way as the haulage begins to reverse after tripping, due to an overload condition, a rapid reduction in absorber pressure is made down to the haulage pressure PCOMP. After this initial pressure drop has been obtained, the curve follower continues down the line to give the desired pressure-sprocket displacement relationship.

The curve generated using this procedure, and the corresponding pressure-displacement recording made using this curve to control the absorber pressure are shown in Fig. 8.5. A recording of torque, from the strain gauge shaft, against displacement taken using this technique is shown in Fig. 8.6.

8.4 Observation

8.4.1) Simulation using Accumulator Banks

By taking recordings of sprocket torque (from the strain gauged shaft) against displacement, a direct comparison can be made between the results obtained from the laboratory simulation Fig. 8.1 and 8.2, and the chain loaded tests at Swadlincote Test Site. The accuracy of the simulation is dependent on the accurate reproduction of the torque-displacement relationship of the chain sprocket drive. Using hydrostatic absorbers, it is clearly not possible to simulate chain elasticity for both the driving and driven modes of operation. The driving mode of operation is not however important since the rig is primarily intended for investigations into phenomena associated with the release of energy from the chain. Accumulator pre-charge pressures are selected to achieve the correct torque-displacement relationship only during the driven mode of operation.

Several factors combined to make this system inadequate for simulation of both modes of operation. The leakage from the absorber allows a net positive rotation of the haulage sprocket. This can be seen

in Figs. 8.1 to 8.3, after a cycle of load increase and subsequent release, leakage allows the sprocket displacement to move forward approximately 15%. The chain sprocket drive system has frictional losses composed of elements both constant and proportional to sprocket torque, whereas the absorber frictional losses are of a predominantly proportional nature. This effect makes the driving and driven torque-displacement characteristics approximately parallel for the chain drive system and divergent for the absorber system. There is also variation in the accumulator pressure-volume relationship between charging and discharging.

The most critical aspect of the simulation is the accuracy of the torque-displacement characteristic at the change in direction of rotation and up to the point of maximum speed in the reverse direction. Investigations into the speed of release of strain energy by haulage units, with associated control and circuit phenomenon, are the primary needs for the simulation system. This makes the accuracy of the torque-displacement characteristic after maximum reverse speed and the accurate reproduction of the total displacement of secondary importance.

Because of the difference in losses between the chain drive and the absorber it is necessary to adjust the overload pressure of the haulage unit to compensate. In the tests this was achieved by changing the overload pressure from TRIP to PCOMP. This adjustment allows the absorber to give the same torque at the change of direction of rotation as that produced by the chain sprocket drive. The effect of this adjustment on the accuracy of simulation can be seen in Figs. 8.1 and 8.2 (recordings of the torque-displacement characteristics using values of TRIP and PCOMP compared with the characteristics from the chain loaded tests).

The importance of overload pressure adjustment for adequate simulation can also be seen on the results from the tests on the energy release speeds using different valves Table 8.1. Although these results show more consistency than those obtained with chain loading, the factors

affecting these results mentioned in Section 4.6.4 still apply. These factors, concerned mainly with the transient behaviour of the haulage circuit, invalidate any attempt to assess the accuracy of the simulation system on comparisons of energy release speeds. A more accurate assessment of the effects of adjustment to the overload tripping pressure is made using the CSMP model.

The main advantage gained by the use of accumulator banks with hydrostatic absorbers for chain elasticity simulation is their reliability and ease of use. Once the correct volumes and pre-charge pressures have been determined, the system can be left unattended for long periods during either performance or life tests. No additional power supply is needed as the required energy is stored in the accumulators. This system is particularly suitable for endurance tests on haulage units operating under simulated underground working conditions. Here the haulage can be run at continuous speeds with the accumulators able to produce the elasticity effects from any speed or load condition.

The torque-displacement characteristic produced from the absorber and accumulator bank is affected by the absorber leakage. The nominally correct relationship can only be approached for one rate of energy release. Any modifications to the haulage unit, affecting the rate of release of energy, will require a modification to the pre-charge pressures, if slight errors to the torque-displacement characteristic are not to result.

During the development work on this rig parameters were recorded on the U/V recorder. Although the U/V recorder has a far superior response and can take information from more channels than the X - Y plotter the recordings obtained are difficult to interpret and reproduce. The X - Y plotter results are thought to be more appropriate to this work and its response adequate to show the required parameters. The transient in the haulage pressure at by-pass operation is however beyond the response of the X - Y plotter Fig. 8.4. This recording shows the transient to exist but the amplitude is not accurately indicated.

8.4.2) Simulation using the Curve Follower Technique

A comparison between the required pressure-displacement relationship on the absorber and the relationship produced by the curve follower system can be seen in Fig. 8.5. The errors between the driving and driven characteristics are due mainly to the pressure-flow relationship of the main circuit relief valve. When the absorber is being driven the relief valve passes the flow from the high pressure connection plus the flow generated by the absorber. With the absorber driving, the relief valve passes the high pressure flow minus the flow being used to drive the absorber. This large difference in flow can be seen to make approximately .34 MPa (50 lb/in²) difference between the required and the actual pressure. Also due to the large flows passed by this valve the minimum absorber circuit pressure is relatively high 3.1 MPa (450 lb/in²) compared with the return pressure of .689 MPa (100 lb/in²), this pressure difference is sufficient to turn the haulage unit under haulage stop conditions. Other errors in the pressure-displacement relationship arise from hysteresis in the Electroilic valve, the method used to generate the follower line, the accuracy of the curve follower system and the dynamic response of the complete system.

The method described to compensate for the differing efficiencies of the absorber and chain sprocket drives was not entirely satisfactory with this particular haulage unit. On the upper part of the curve, it is necessary to increase the pressure at the maximum rate acceptable to the curve follower, such that an initial drop is obtained as the haulage reverses after overload operation. Due to the heavy damping in the overload valve circuit the rapid increase in load is not immediately sensed. This results in the pressure increasing to a point where the main circuit relief valves operate. To eliminate this effect, a horizontal portion of the curve is required which gives a haulage pressure below the relief valve setting of sufficient duration to allow the overload

valve to operate. This is unacceptable as it clearly alters the pressure-displacement characteristic. This effect was eliminated in the experiments by the introduction of a positive stop on the displacement transducer and a slipping drive between the transducer and the drive wheel in contact with the sprocket. The drive is arranged to slip, against the positive stop, at a point coincident with the upper part of the curve above the overload pressure and below the main circuit relief valve settings. This allows the haulage to continue forward rotation at a pressure above overload for a period sufficient for the overload valve to operate. Upon reverse rotation, a rapid pressure drop is achieved for compensation, as the displacement transducer moves off its positive stop, after which the correct pressure-displacement relationship is followed.

The accuracy of the simulation is shown in Fig. 8.6 a recording of the torque-displacement characteristic with the results from the chain loaded tests superimposed. As with the accumulator technique, it can again be seen that simulation of both the driving and driven modes cannot be achieved.

Although the curve follower technique requires an additional power source and considerable instrumentation, it can produce a more consistent torque relationship than that produced by the accumulator bank. Any rate of release of energy can be accommodated within the limits of the power supply without effects from the absorber leakage. The curve follower technique has limitations when used for endurance tests, the slipping displacement transducer drive enables energy release effects to be produced in between periods of continuous running but it will only operate from one load, unlike the accumulator bank technique which is able to operate from any load during simulated cutting cycle tests.

The curve follower technique would have far greater accuracy if operated under closed loop control. Direct calibration for the curve

follower would be obtained, eliminating the non-linear 'Electroilic' valve characteristics and effects due to the pressure-flow characteristics of the absorber circuit relief valve would be minimised.

Test No	Valve size		Speed	Time	Tripping Pressure
	in	mm	rev/min	sec	
1	.248	6.3	1500	9.0	PCOMP
3	.248	6.3	1500	9.0	PCOMP
4	.248	6.3	1400	9.0	PCOMP
2	.248	6.3	2100	9.0	TRIP
5	.248	6.3	2100	9.0	TRIP
6	.030	.76	1100	16.0	TRIP
7	.030	.76	1100	16.5	TRIP
8	.030	.76	800	13.5	PCOMP
9	.030	.76	800	14.5	PCOMP
10	.050	1.27	1200	9.5	PCOMP
11	.050	1.27	1500	8.5	TRIP
12	.050	1.27	1600	9.5	TRIP
13	.040	1.02	1250	13.5	TRIP
16	.040	1.02	1330	12.5	TRIP
14	.040	1.02	900	13.0	PCOMP
15	.040	1.02	850	13.5	PCOMP

Table 8.1 Results taken from X - Y recordings of energy release speeds produced by absorber and accumulator bank

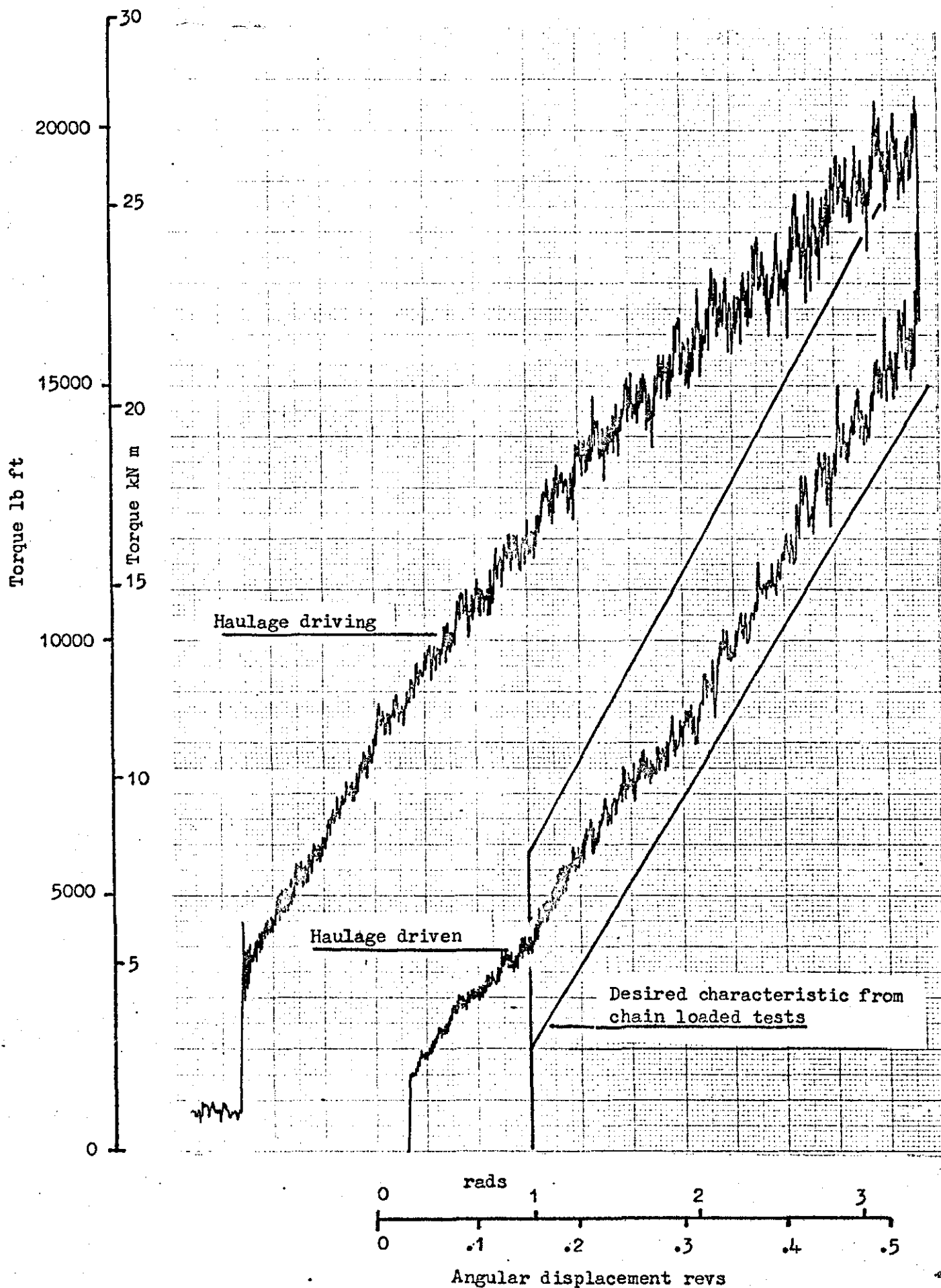


Fig. 8.1 X-Y Recording of sprocket torque against sprocket angular displacement, haulage loaded by hydrostatic power absorber and accumulator bank. Haulage overload valve set at TRIP

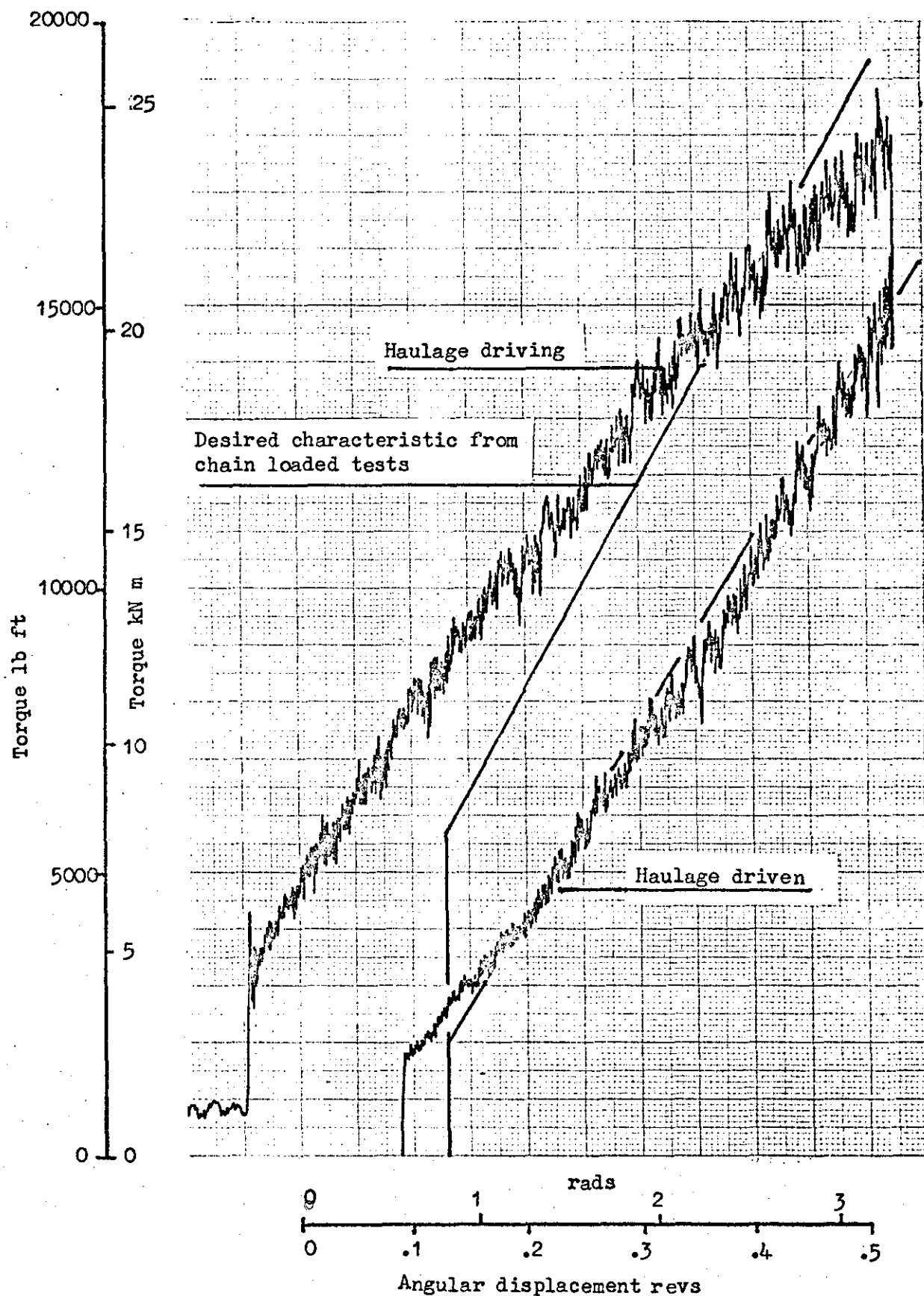


Fig. 8.2 X-Y Recording of sprocket torque against sprocket angular displacement, haulage loaded by hydrostatic power absorber and accumulator bank. Haulage overload valve set at PC/MP

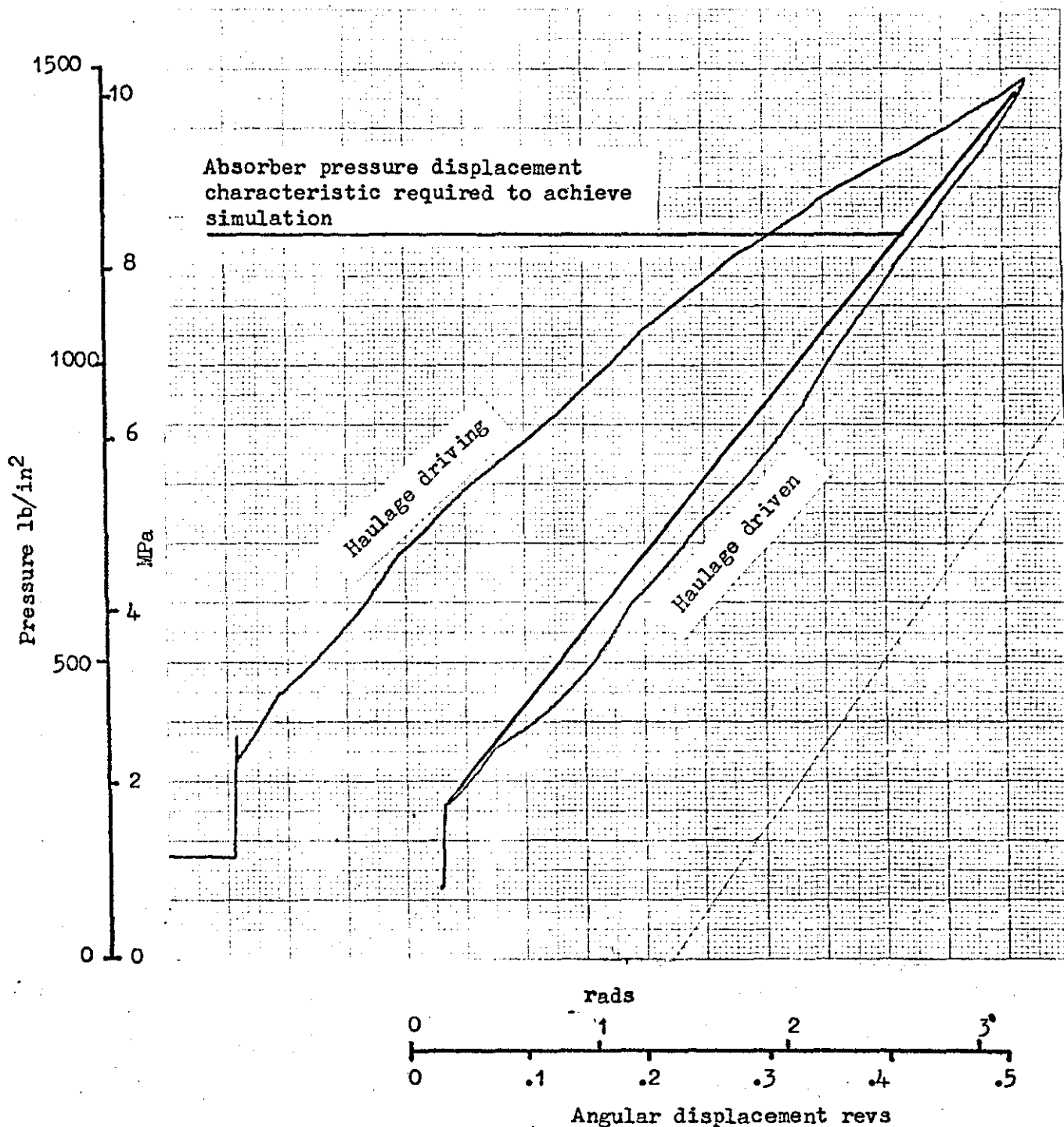


Fig. 8.3 X-Y Recording of absorber pressure against sprocket angular displacement, haulage loaded with hydrostatic absorber and accumulator bank together with the desired characteristic

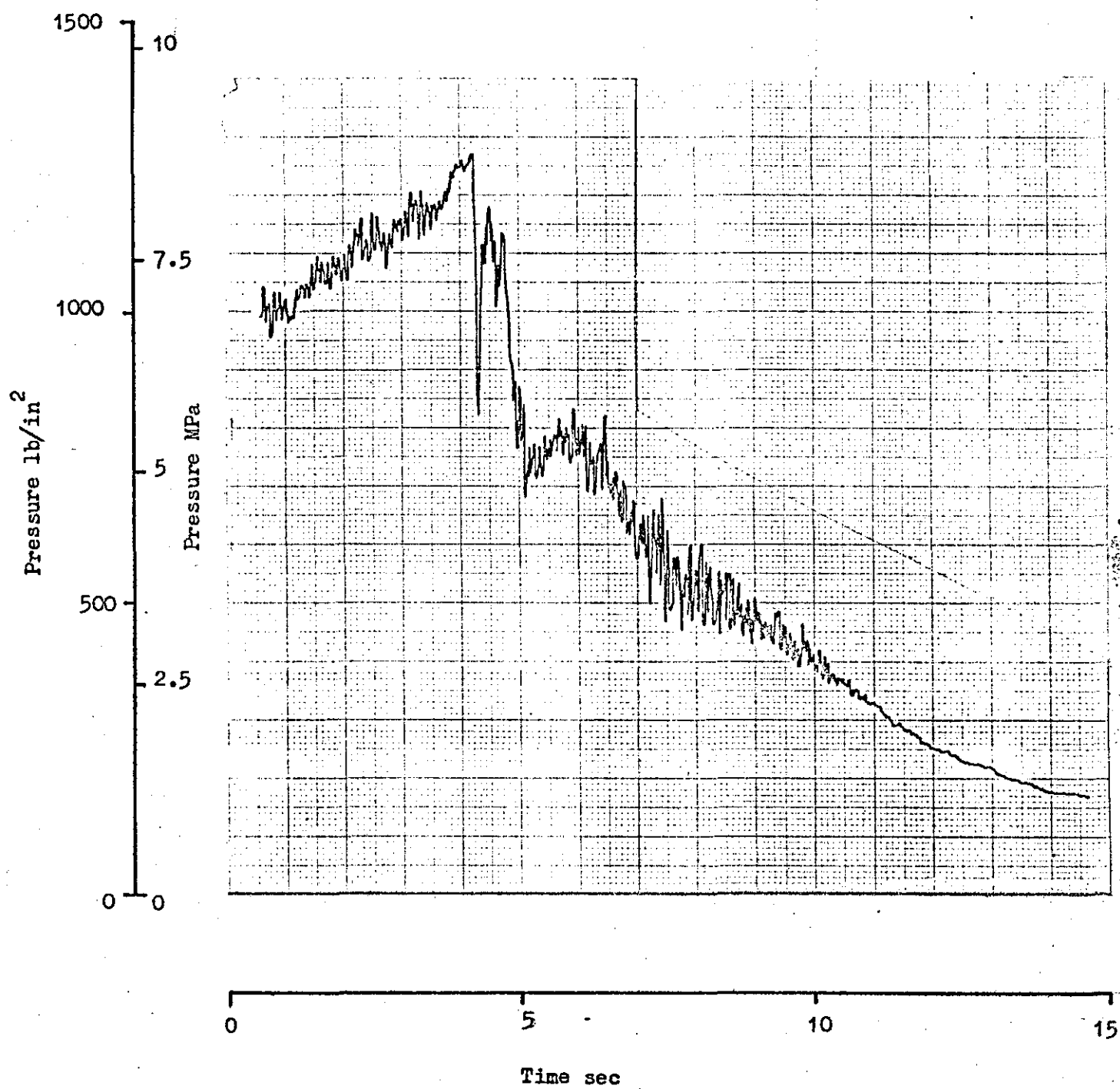


Fig. 8.4

X-Y Recording of haulage pressure against time for a typical energy release

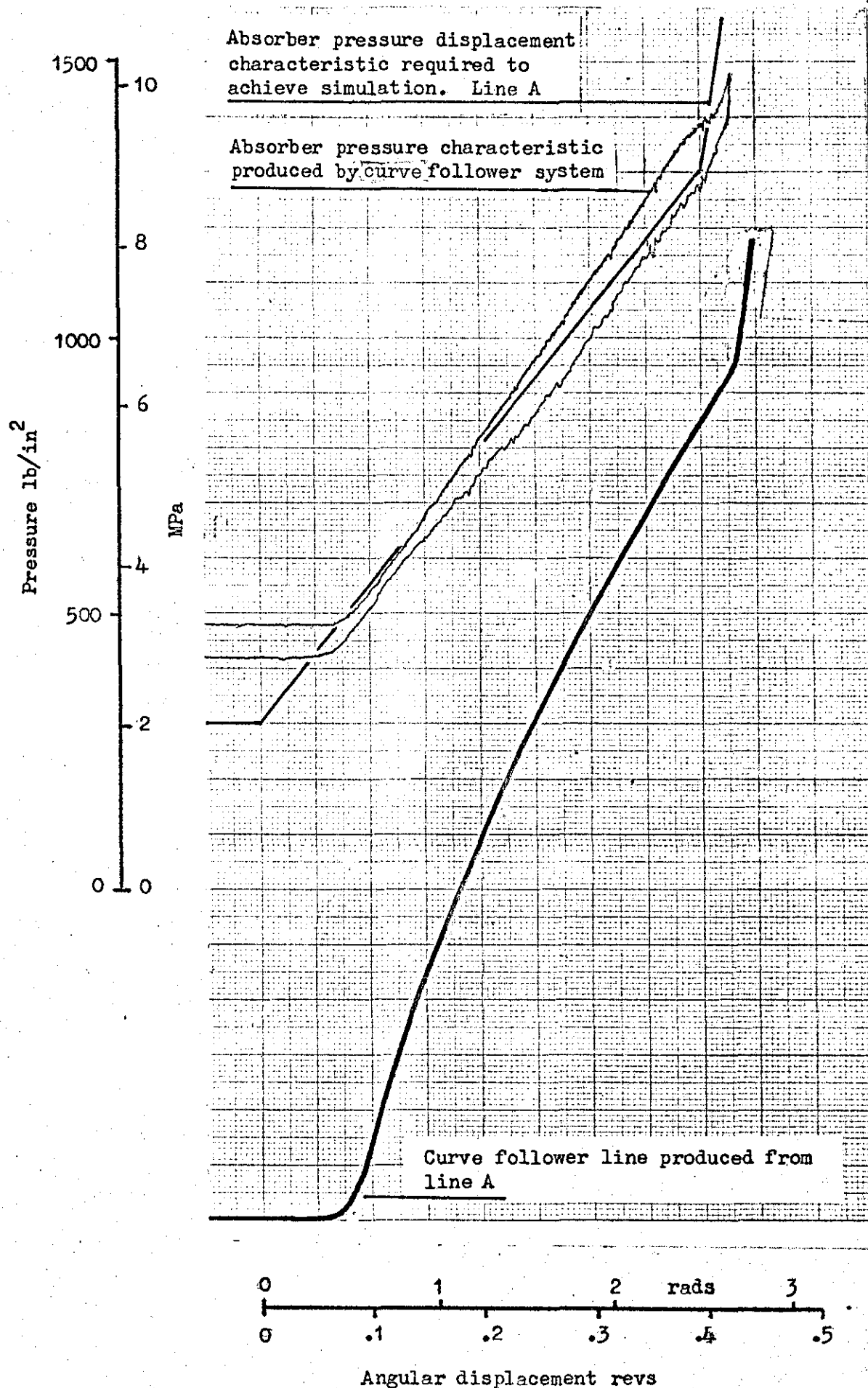


Fig. 8.5 X-Y recording of absorber pressure - sprocket angular displacement characteristic obtained using the curve follower technique shown together with the desired characteristics and the generated curve for the curve follower

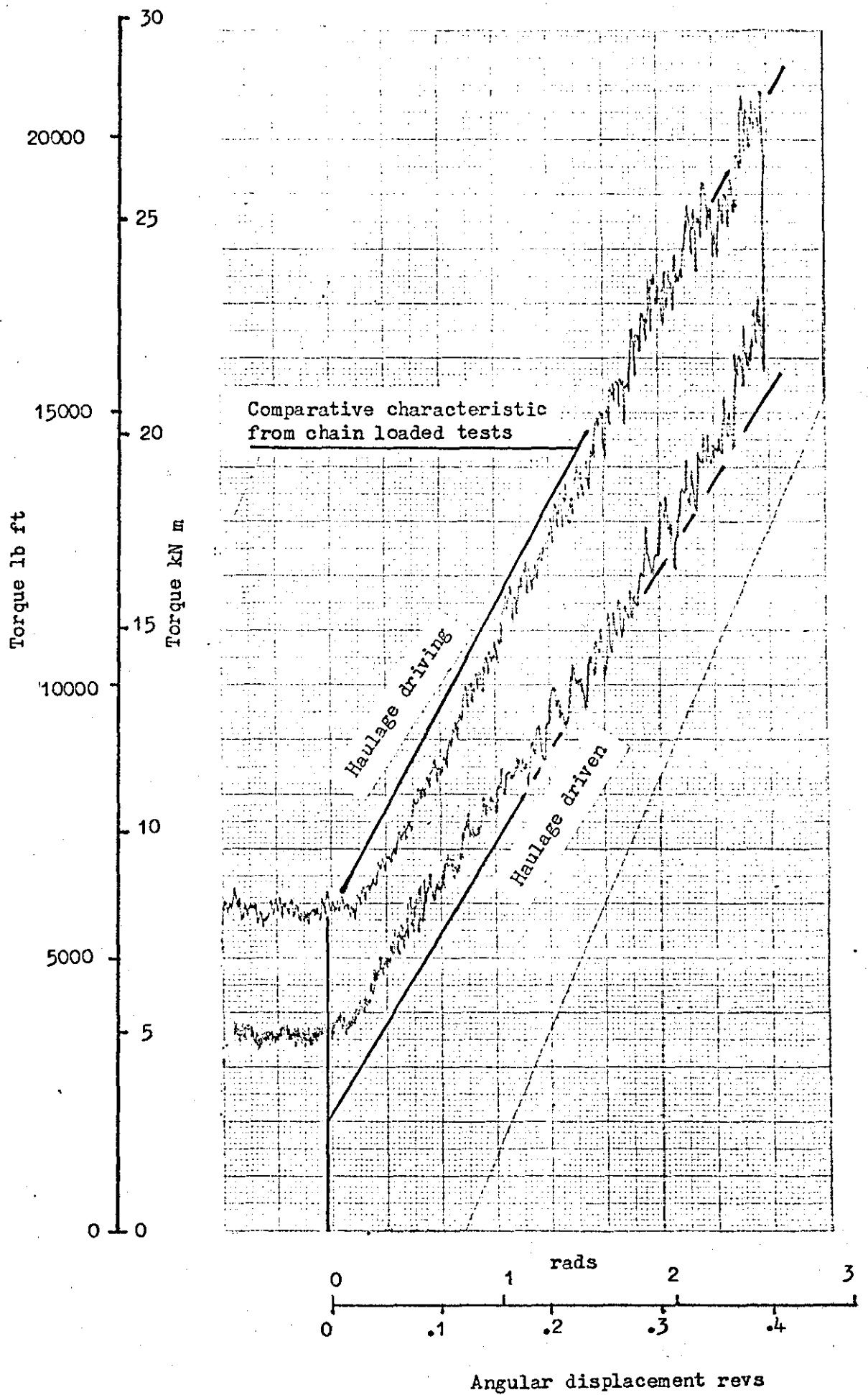


Fig. 8.6 X-Y Recording of sprocket torque against sprocket angular displacement haulage loaded with hydrostatic power absorber and curve follower device

9 THE SIMULATION LANGUAGE

The language used for the dynamic model is the S/360 continuous modelling programme CSMP (reference 9). It was developed by International Business Machines (IBM) to simulate problems from either a block diagram representation or a set of differential equations. CSMP contains many built in functions, sub-routines and procedures which are translated into a Fortran programme for compilation.

Compared with general purpose high level languages such as Fortran, CSMP language statements are simple to construct and relatively few are required to describe highly complex systems. However, the programme does accept standard Fortran statements, allowing the user to augment the analogue-type block statements of CSMP with the logical branching and conditional capabilities of Fortran. A knowledge of the latter is therefore helpful but not essential.

Together with standard logical and trigonometrical functions, available with Fortran, CSMP provides a comprehensive library of simulation functions including conventional analogue integrators and relays and many special purpose functions such as, pulse generators, limiter and arbitrary function generators. These functions can be combined using a macro facility, similarly logical and conditional Fortran statements can be combined using a procedural facility.

The core of a continuous system simulation programme is integration. CSMP provides the user with a choice of six integration routines varying in complexity from a fixed step, rectangular method to a Milne, fifth-order, predictor-corrector method which automatically adjusts the integration interval to meet user-specified error criteria. If none of the seven methods are suitable, the user may supply his own.

The language statements representing the dynamic system being modelled need not be presented to the programme in their correct computational sequence. The translation phase sorts the structure

statements so that the inputs to a statement are either known values or have been previously computed in the current iteration cycle. This relieves the user of the need to order the structure statements to ensure that no phase lag is introduced into the computation. The sorting option can be overridden if necessary.

Standard fixed format output is provided for printing and print-plotting variables at user selected increments of the independent variable. Data can be transferred to storage for subsequent use in graph plotting or for display purposes.

Also available are simple facilities for performing a sequence of runs of the same model structure with different parameters, integration interval etc. A terminal section allows a group of Fortran statements to be performed at the end of each run through the model. This facility can be used as either an output device or to modify the input data or model structure prior to a successive run.

10 A CSMP MODEL OF THE HAULAGE UNIT LOADED BY THE CHAIN SYSTEM AND THE HYDROSTATIC ABSORBER

10.1 Introduction

If hydrostatic power absorbers are to be used to simulate chain elasticity effects on haulage units, some method is required to determine the pressure-volume relationship for the absorber which gives a displacement-torque relationship, at the haulage sprocket, equivalent to that produced by the chain system. Static determination of this pressure-volume relationship cannot take into account factors which vary with the dynamics of the system.

A mathematical model allows the effects of statically and dynamically determined pressure-volume relationship, to be observed together with the effects of the use of accumulators to achieve chain elasticity simulation.

10.2 Representation of the Haulage Unit

The haulage unit is basically a hydrostatic transmission system with a variable displacement pump and fixed displacement motor. The dynamic analysis of such systems usually employ the coefficient model technique to describe the characteristics of the pump and motor, references 7 and 11. Since the coefficients for the units in this haulage were not readily available, use was made of the CSMP FUNCTION statement. Here graphical characteristics obtained experimentally are entered into the programme in X-Y pairs, interpolation being carried out by either linear or Lagrange quadratic interpolation.

The dynamic statements of the model are obtained from the block diagram Fig. 10.1 and 10.2, equations being written to represent each block. A listing of the CSMP programme is shown in Appendix I.

As in reference 7 the circuit pressures are obtained by integrating the flow into the transmission lines and multiplying by a stiffness factor, dependent on the fluid bulk modulus and the line volume. A clearer

indication of this summation of flows into each line can be seen in Fig. 10.3.

Frictional losses act against the direction of motion and therefore have opposite sign to the sprocket angular velocity THD. As graphical characteristics are used in this model, as opposed to coefficients, the CSMP input switch statement INSW is used to change from a driven to driving characteristics, dependent on the sign of sprocket angular velocity.

To determine haulage torque from haulage pressure, with the sprocket driving ie the sprocket velocity is positive, a value is obtained from the pressure-torque characteristic FUNCTION PTHM. If the sprocket is driven ie the sprocket velocity is negative, a value from FUNCTION PTHP is used. As these characteristics are for a pressure difference $P1 - P2$ against sprocket torque, to obtain the correct sign for the torque, an absolute value of the pressure difference APDF is used to obtain torque from the characteristics, the result being multiplied by the sign of the pressure difference SPDF.

$$\text{ie } TM = INSW (THD, AFGEN (PTHP, APDF), AFGEN (PTHM, APDF)) * SPDF.$$

Similar techniques are used for the absorber pressure-torque characteristic and the sprocket torque-displacement characteristic.

The flow from the pump FPUMP and the flow across the by-pass valve FBP are time variant. The operation of the pressure overload device initiates the reduction of the pump swash and brings the by-pass valve into circuit. To effect this requirement, the CSMP PROCEDURE function is used to set the logical operator LSWICH from 0 - 1 when the circuit pressure P1 reaches the overload value TRIP.

With the value LSWICH at 0 FPUMP is set to its initial value and FBP to zero, with LSWICH at 1 a pump flow is calculated dependent on the elapsed time from the initiation of LSWICH, TBP1 and the FUNCTION SWASH which describes the pump swash reduction in relation to time. A value

of FBP is computed from the by-pass valve pressure-flow characteristic FUNCTION BYPS and the value APDF.

The integrations to determine TH, THD, P1 and P2 are obtained using the CSMP integration statement INTGRL eg $TH = INTGRL (STT, THD)$ where STT is the value of TH at time zero.

10.3 Representation of the Absorber Unit

The absorber unit is treated as a hydrostatic unit working with constant feed pressure, the pressure-torque characteristic being used in the model is dependent only on the pressure on the high pressure side of the device. The fluid volumes are obtained by integrating the flow rates in the absorber circuit after the pressure dependent leakage has been obtained from the FUNCTION ALEAK and subtracted from the flow calculated from the absorber displacement and the input angular velocity.

10.4 Model Organisation

The CSMP system is organised in 3 sections; INITIAL, DYNAMIC and TERMINAL. The initial section of the model, performed only at time zero, is used to calculate the initial values of the integrations and constants used in the dynamic section and to input data. The DYNAMIC section contains the statements to describe the dynamic behaviour of the system and the TERMINAL section is used for any final calculation required after the dynamic run. By adjustment of the timer conditions and use of END and CONTINUE cards the model can be organised to either re-run with differing parameters or continue with varying factors such as integration method of integration interval.

The model is arranged to simulate the condition where the power loader is at the end of a face and stalled into cut. This condition produces no movement of the machine and allows maximum tensions to be applied to the chain and produces the maximum strain energy in the chain.

As concern is with the release of strain energy, the model is initialised with a sprocket angular displacement of STT and a sprocket

angular velocity corresponding to the maximum value of the FUNCTION SWASH. Other integration initial values are computed to comply with these values.

The DYNAMIC section allows the sprocket displacement to increase, thus increasing chain tension and sprocket torque, until the pressure reaches the value TRIP after which the strain energy of the chain is dissipated over the by-pass valve. Use of the FINISH statement stops the simulation at an appropriate value of sprocket displacement.

The model is arranged to perform two sequential runs. With the switch $KAB = 0$, outputs are obtained of the major parameters assuming the haulage to be loaded with the face chain system. A TERMINAL section used with $KAB = 0$, calculates the optimum pre-charge pressures for a bank of accumulators to simulate the chain loading system and defines the discharge pressure-volume characteristic in array form. A second run is then made with $KAB = 1$, assuming the haulage unit to be loaded by the absorber and the accumulator bank, so that a comparison can be made with the chain loaded system.

As only a few statements vary between the two runs, the CSMP input switch statement is used to alter the programme dependent on the switch KAB.

eg $TH2D = INSW (FKAB, (TM - TCH)/HJ, (TM - TCH)/(HJ + AJ))$

where $FKAB = KAB - 0.5$

For the second run with the absorber loading the haulage unit, an alteration is made to the value of TRIP, the pressure at which the overload device operates. Since the chain system has a different efficiency to that of the absorber, it is necessary to re-set this value to achieve an adequate simulation. The value TRIP is set to PCOMP, this being the haulage overload pressure required to give the same sprocket torque at commencement of the reverse sprocket rotation with the absorber as obtained with the chain system. This compensated tripping pressure is calculated in the terminal section of the model, after the first run,

from the chain tension-displacement, haulage pressure-torque and absorber pressure-torque characteristics. Interpolation of these characteristics is made from these FUNCTIONS using the CSMP AFGEN statement, the complete statement being

```
PCOMP = AFGEN (TPHM, AFGEN (PTAP, AFGEN (TPAM, AFGEN (DTIN, ...  
AFGEN (TDDG, AFGEN (PTHM, TRIP))))))
```

Three TERMINAL sections have been used with the model to compare various techniques for selection of accumulator pre-charge pressures. In two of these, TERMINAL sections 1 and 3, the first run, $KAB = 0$, computes the pressure-volume relationship required from the absorber to reproduce the same dynamic performance as obtained by the chain load. This relationship is contained in arrays EVOL and BPA, values being taken during the dynamic run by use of a NOSORT statement at the end of the DYNAMIC section of the model. The NOSORT label ensures that the statements are not sorted by the sorting algorithm and allows conditional Fortran statements to be used. TERMINAL section 2 uses a statically calculated absorber pressure-volume relationship for accumulator pre-charge determination as a comparison with the dynamically determined relationships.

A variation of the model containing only the first run $KAB = 0$ can be used to show the effects of various sized by-pass valves. The FUNCTION BYPS is changed at the end of each run by the use of the OVERLAY statement, a run being completed for each function used.

10.5 Model Outputs

Outputs from the dynamic section of the model are obtained using the CSMP PREPLOT statement. This gives a print plot output from the line printer of a specified variable and listings of 3 others together with the appropriate TIME value. Use of the CSMP PREPAR statement transfers specified variables to a tape for subsequent interpolation by a graph plotting programme.

Outputs from the `TERMINAL` section, such as accumulator pre-charge pressures and pressure-volume characteristics are obtained with Fortran `WRITE` and `FORMAT` statements.

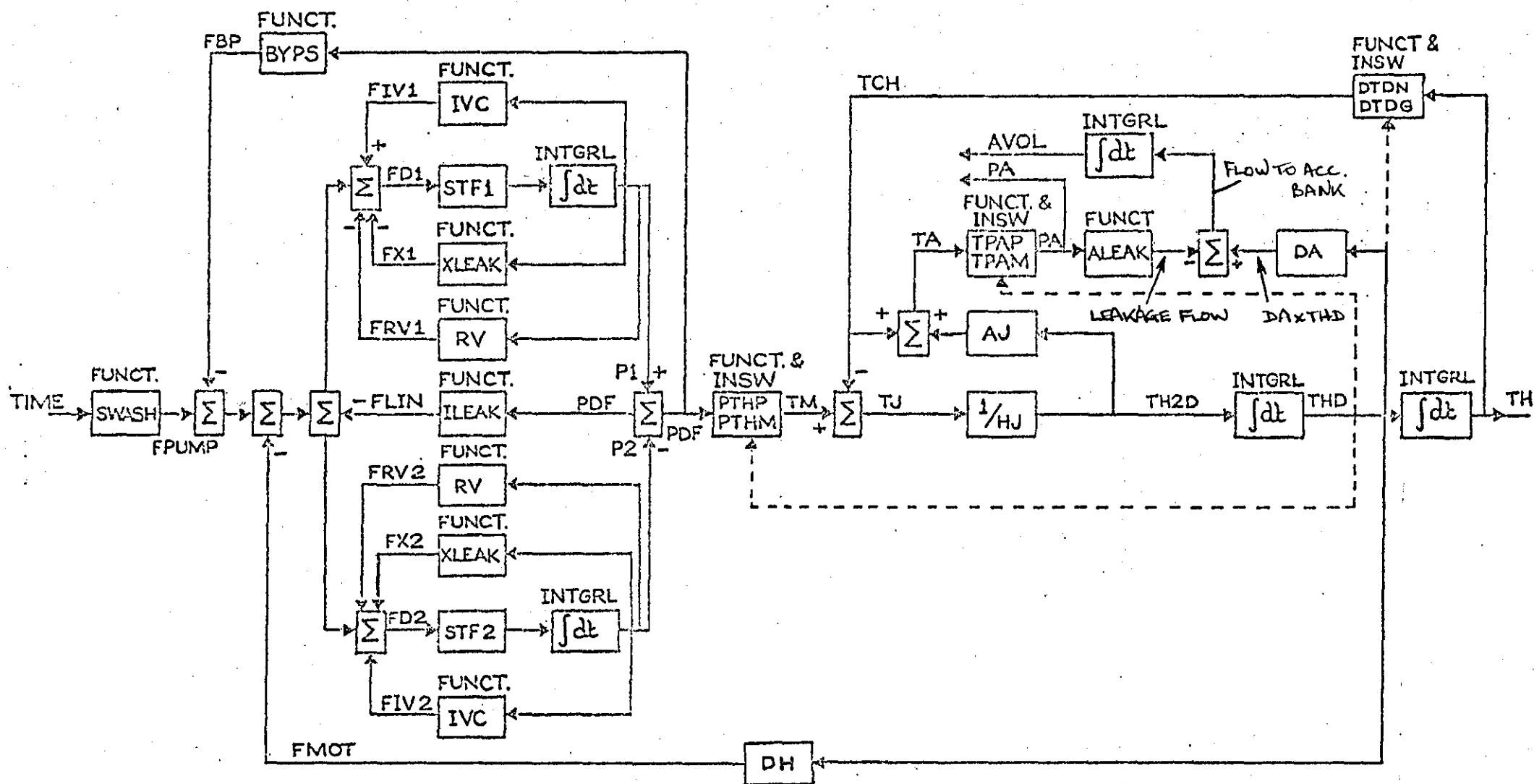


Fig. 10.1 Block Diagram for CSMP Model, Haulage Loaded by Chain System

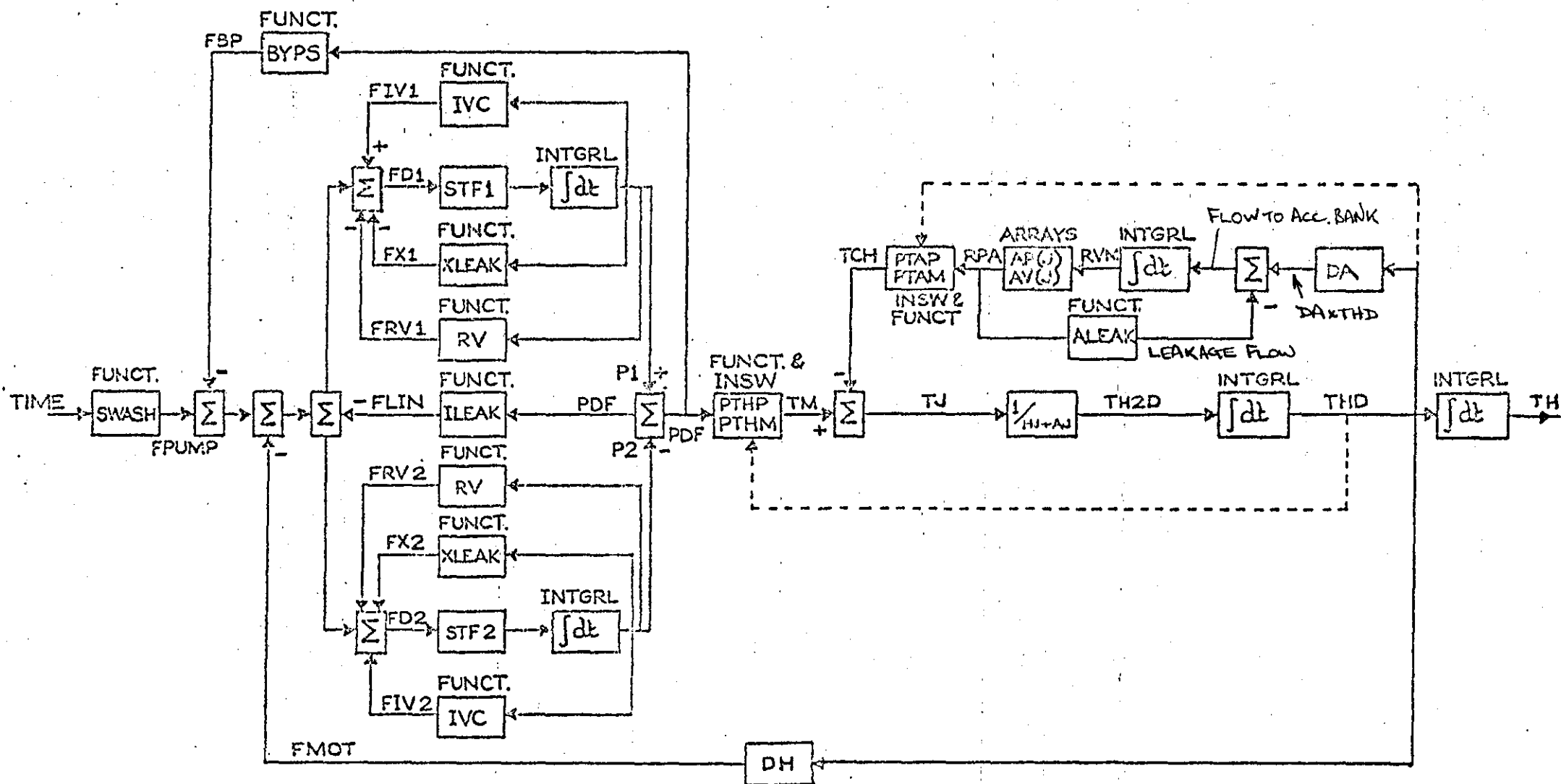
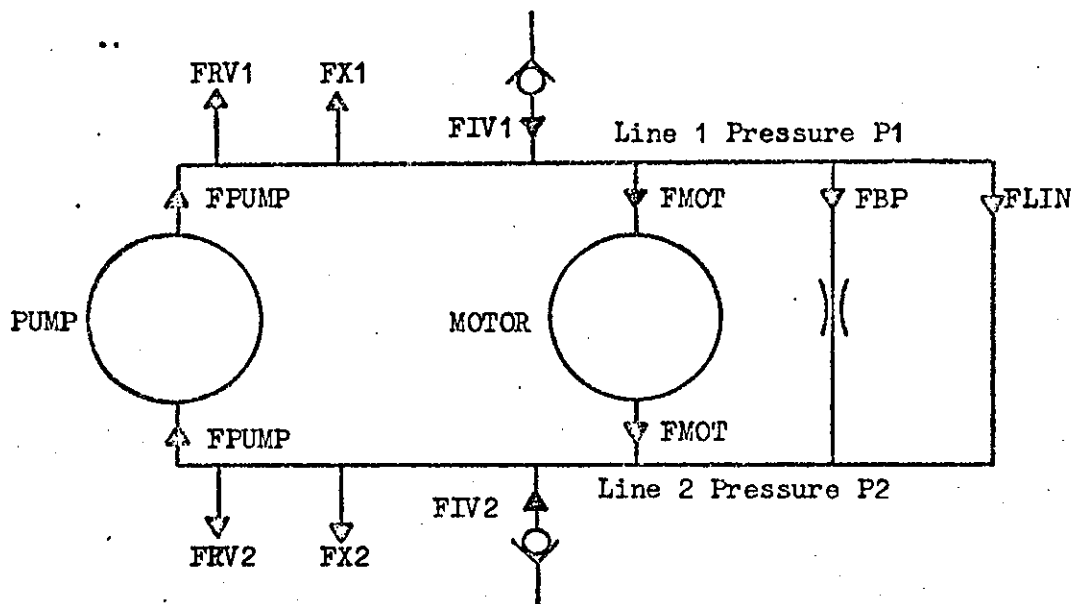


Fig. 10.2 Block Diagram for CSMP Model, Haulage Loaded by Absorber and Accumulator Bank



Note - The direction of FBP & FLIN is dependent on the sign of $(P_1 - P_2)$

Flow into line 1 =

$$FD1 = FPUMP - FBP - FLIN - FX1 - FRV1 - FMOT + FIV1$$

Flow into line 2 =

$$FD2 = -FPUMP + FBP + FLIN - FX2 - FRV2 + FMOT + FIV2$$

$$P1 = \text{INTGRL}(\text{STY}, FD1 \times \text{STF1})$$

$$\& \quad P2 = \text{INTGRL}(\text{SP2}, FD2 \times \text{STF2})$$

where STF1 & STF2 are stiffness factors for lines 1 & 2 respectively.

Figure 10.3 Simplified haulage circuit diagram describing transmission flow line equations.

11 APPLICATION OF THE DYNAMIC MODEL TO THE HAULAGE UNIT AND ABSORBER LOADING SYSTEM

11.1 Introduction

The primary application of the model is to assess the viability of the use of accumulator banks with hydrostatic drives for chain elasticity simulation. The structure of the model, fully described in Section 10, allows the effects produced on the haulage unit by the chain system, to be compared with those produced by the absorber loading system using various accumulator pre-charge pressure setting procedures. Comparisons can also be made to show the effects of the differing losses of the chain system and the absorber. By performing multiple runs with slight alteration to the model structure, comparisons of the energy release speeds with various by-pass valve sizes can be made.

The outputs from the model are shown in graph plotted form. A typical run from the model involving two runs through the Dynamic Section produces three graphs. On the first run through the Dynamic Section, simulating the release of energy produced by the chain system, data is produced for the first graph which shows the variation of several system variables against time. The second run through the Dynamic Section simulates the release of energy with the haulage unit loaded by the absorber. For this a second graph similar to the first is produced for comparison. Also during the second run, data is collected for a third graph showing the absorber pressure against the volume of fluid required by the absorber. Two traces are produced on this graph, the first shows the pressure-volume relationship required by the absorber to give a true simulation, calculated during the first run through the Dynamic Section, and a second showing the pressure-volume relationship produced by the accumulators as calculated in the Terminal Section of the model.

Comparisons of release characteristics from differing runs through the Dynamic Section must be made from the time of by-pass operation since the time for operation can vary, depending on accumulator bank characteristics. Any comparison of release displacements must also be made from points coincident on the two curves at by-pass operation. The outputs have been extrapolated to zero sprocket torque conditions, eliminating the restrictions of the FINISH statement, to enable comparisons of release times and displacements to be made.

11.2 Comparisons of Accumulator Pre-charge Pressure Setting Procedures

11.2.1) The Pressure Increment Method of Accumulator Pre-charge Pressure Setting

The model was run with Terminal Section (1) described in Section 6.4.1. This procedure takes the pressure-volume requirements of the absorber loading system, obtained during the first run through the Dynamic Section when the haulage is assumed to be loaded by the chain system, and using the pressure increment technique, sets the pre-charge pressures of a bank of accumulators to give a similar characteristic.

The output from the model with chain loading is shown in Fig. 11.01, sprocket displacement, angular velocity and torque are shown together with haulage circuit pressure against time. Fig. 11.02 shows the same variables from the second run through the model, where the haulage unit is assumed to be loaded with the absorber and accumulator bank. For comparison, the angular velocity from Fig. 11.02 is also shown traced on to Fig. 11.01. To assess the performance of the accumulator pre-charge setting technique Fig. 11.03 shows the desired pressure-volume characteristic together with the characteristic of the accumulator bank.

To achieve the simulation using the absorber and accumulator bank, Terminal Section (1) set accumulator pressures at 2.25, 2.25, 4.55, 4.85, 6.90 and 7.35 MPa. Although the procedure required that two accumulators were set at the lowest pressure, producing a considerable loop in the low pressure part of the characteristic, the high pressure portion had a good fit and reproduced the maximum release speed very accurately.

A comparison between the release displacements produced, shows the accumulator bank to give less displacement than the chain. This, however, is mainly due to the method used to set the initial accumulator pressure. In Terminal Section (1) the first accumulator pressure is set to the lowest pressure in the array BPA, a value corresponding to the absorber pressure at the end of the chain loaded run determined by the FINISH statement. If the initial pressure had been set to correspond to zero angular displacement as in Terminal Section (2) the release displacements would have been more accurate.

The distribution of accumulator pre-charge pressures obtained in this example is characteristic of this pre-charge pressure setting technique. During the development of this technique similar distributions were obtained with several differing combinations of accumulator volume and required pressure-volume characteristics. Variations of the pressure increment KR can give quite different pre-charge pressure distributions for the same required characteristic without noticeable alteration to the overall characteristic. The technique seldom sets accumulator pressures with equal pre-charge pressure increment. When successive accumulators are set with pre-charge pressures near together this has the effect of forming larger loops in the accumulator bank characteristic taking it away from the desired characteristic. These loops are minimised if the accumulator pre-charge pressures are at equal increments, and are less obvious at higher pressures when more of the accumulators in the bank are operative. If, however, the desired pressure-volume characteristic was non-linear, the ideal accumulator pre-charge pressures would move away from the equal increment values required to reproduce the near linear characteristics obtained with chain elasticity simulation. Although not shown in this example the pressure increment technique does not need accumulators of equal volume.

11.2.2) Empirical Method of Accumulator Pre-charge Pressure Setting

Similar outputs to those described in Section 11.2.1 are shown in Fig. 11.04 and 11.05 for the model run with Terminal Section (2), described in Section 6.4.2.

Fig. 11.04 shows the absorber and accumulator bank to give a very accurate reproduction of the release speed characteristic. To meet the desired pressure-volume characteristic, Terminal Section (2) set accumulator pre-charge pressures at 1.93, 2.49, 3.73, 4.98, 6.23 and 7.47 MPa. With this method accumulators are set at equal pre-charge pressure increment, apart from between the first two, this minimises the loops away from the desired characteristic. In this example the degree of simulation could have been improved, as will be seen from Fig. 11.05, by the introduction of a further accumulator into the bank. A comparison between the chain load and absorber load Fig. 11.04 shows Terminal Section (2) to give a very accurate reproduction of release displacement. This is due to the correct setting of the initial accumulator pre-charge pressure. Increase in the initial pre-charge pressure away from the ideal, as in Terminal Section (1), reduces the release displacement in comparison with the true value obtained with the chain system. In practice, however, there is often a need to keep the minimum pre-charge pressure to 20% of the maximum absorber system pressure for satisfactory operation of the accumulators.

It is interesting to note that though there are wide differences between the pre-charge pressures required to produce the simulation as calculated by Terminal Sections 1 and 2, very similar results are obtained.

11.2.3) Empirical Method of Accumulator Pre-charge Pressure Setting

without the use of Dynamically Determined Pressure-Volume Characteristics

For this run Terminal Section (3) was used to set the accumulator bank pre-charge pressures, this procedure does not take into account the absorber leakage, as described in Section 6.4.3. A comparison between

the outputs from the chain loaded system and the absorber loaded system is shown in Fig. 11.06. Here the technique is seen to give a reasonable maximum release speed reproduction but as the leakage is not considered, the error increases with displacement, due to the accumulator not being able to supply sufficient fluid volume. A comparison of the release displacements between the chain and absorber loaded system shows the leakage to account for about 15% of the total displacement. The ability of the empirical method of accumulator pre-charge determination to reproduce linear pressure-volume characteristics with high accuracy is also clearly shown in Fig. 11.07.

11.3 Effects of Accumulators Charging and Discharging at Differing Polytopic Indices

Both the pressure increment method of accumulator pre-charge determination and the empirical method, assume that the accumulators charge and discharge at the same polytropic index. The pressures are in fact determined to give the desired characteristics when charging, calculations involving discharging accumulators being of far greater complexity.

To show the errors likely within a practical situation of charging at $n = 1.3$ and discharging at $n = 1.45$, the model was run with Terminal Section 2 arranged to predict the pre-charge pressure assuming the accumulators charged at $n = 1.3$. To complete the second dynamic run with the absorber loading, characteristics of the accumulator bank were used assuming discharge at $n = 1.45$.

Output from the second dynamic run, absorber loading, is shown in Fig. 11.08 together with a comparison of the release speed from the first dynamic run, chain loading. Again it is seen that the maximum release speed is well reproduced with errors of around -10% during the centre section. The accumulator pressures are higher than actually required for discharge at $n = 1.45$, giving an accumulator bank pressure-volume characteristic below that required, as seen on Fig. 11.09. This gives a reduced release speed and a lower release displacement. Fig. 11.09 also shows the expected accumulator discharge volume to be reduced by about 5%.

The value of $n = 1.3$ and $n = 1.45$ are within what would be expected for accumulators charging and discharging in this time period, If, however, a charge period was followed by a period at constant pressure, prior to discharge, values of charge index would approach isothermal conditions. This emphasises that when using these techniques for pre-charge pressure selection, to obtain the most accurate results the rig should be operated by immediately discharging the accumulator bank after charging.

11.4 The Effects of Tripping Pressure Adjustment for Frictional Loss Compensation between Chain System and Absorber

As described in Section 3.2 the frictional losses in the chain system are of a differing nature and value to those in hydrostatic absorbers. This necessitates that an adjustment is required to the tripping pressure when the haulage is loaded by the absorber, to give an equivalent torque at the commencement of energy release as would be expected from the correct tripping pressure with the chain system.

The previously described outputs from the model have been made with this compensation in operation. To show its effects Fig. 11.10 shows an output from the model without this compensation. Here the haulage is loaded by the absorber without compensation with comparisons from the chain loaded output. This shows that without compensation the absorber is unable to reproduce the correct maximum release speed. Due to the absorber having lower frictional losses than the chain system, the absorber gives higher release speeds. Other system variables, such as haulage pressure and sprocket torque are also considerably higher than required. Release displacement is increased by approximately 10%.

In the previous examples the normal tripping pressure was set at 8.62 MPa (1250 lb/in²) and the calculated compensated tripping pressure 7.82 MPa (1130 lb/in²). This reduction in tripping pressure is due to the absorber having less frictional losses than the chain system.

However, the absorber being used here has a particularly high efficiency,

compared with alternative absorbers or an alternative sprocket configuration, the variation in tripping pressures could well be reduced or the compensated tripping pressure could be higher than the original set value.

11.5 A Comparison between the Release Speeds for By-pass Valves with Varying Restriction

In order to compare the energy release speeds for various by-pass valves, an alteration was made to the structure of the model. This allowed multiple runs through the Dynamic Section of the model, each run being with the chain loading system only.

The output Fig. 11.11 shows the energy release speeds for the original by-pass valve spool and three spools with increasing flow restriction. As would be expected the increasing restriction reduces the maximum release speeds and increases the time for energy release. The original by-pass valve spool gives little restriction and allows the maximum release speed to reach twice the maximum forward speed. With this valve, it can be seen that the haulage still has rotational speed with zero displacement. In a practical situation, not shown by the model or the experimental work with the absorber, this energy would cause a rapid increase in the tension, T_2 , causing the chain to snatch dangerously and lurching of the machine. This effect can also be seen with the higher restriction valves but is small in comparison and not likely to have dangerous consequences. A complete elimination of this effect is unlikely, due to the nature of the sprocket torque-displacement characteristics since torque exists at zero displacement, as can be seen from the experimental results, Fig. 4.7.

11.6 Some General Observations on the Model and its Operation

As described in Section 10.4, the model is initialised with a forward speed and an angular displacement to give a haulage pressure of about 75% of the tripping value. A typical output Fig. 11.01 shows angular displacement increasing, so increasing sprocket torque and haulage pressure. During this period haulage speed slightly decreases due to

increasing haulage leakage with increasing pressure. When the pressure reaches the tripping value, the by-pass valve operates and the pump begins to reduce swash. This introduces a large transient into the haulage pressure line with an associated transient in the return line, not shown on the plotted output. At this point the angular velocity begins to reduce. When this passes through zero the sprocket torque drops due to the chain frictional losses acting in the opposite direction to sprocket velocity and the angular displacement begins to reduce. The angular velocity continues to increase in a negative direction until the pump swash reaches zero. This point represents the maximum release speed and the flow conditions existing in the circuit produce a small increase in haulage pressure. From here the release speed is determined by the pressure-flow characteristics of the by-pass valve. The model is halted at an angular displacement just prior to zero $TH = .11$.

During the development of this programme the model was run with only one pressure line and the pressure in this line was allowed to go negative at the transient condition of by-pass operation. Here satisfactory operation was obtained with a value of DELT the integration interval of .005 seconds. When the second line was introduced, together with the function describing the inlet valve flow, considerable instabilities occurred needing a value of DELT = .001 sec. to produce a stable solution. As the investigations of circuit transients and inlet valve problems was not the object of this work, the programme was modified to increase the system volume by a factor PAR if the pressure went below zero. This enabled the programme to operate at a value of DELT = .001 with PAR = 20.

The need for a reduced value of DELT, with the introduction of the second line, lies in the function describing the inlet valve flow. This gives large flows for small values of inlet pressure. Consequently smaller values of DELT are required to give numerical stability. A

further problem with the inlet valve function, as initially written, was that it failed to satisfy the transient flow conditions existing when the by-pass valve was switched into circuit without the need for large negative pressures. At this point flows are demanded through the valve which are larger than the valves are capable of passing, indicating that the fluid must cavitate. As this is outside the scope of this work, the function was modified to enable large flows to pass through the valve into the circuit without the pressure falling below vacuum conditions. This allows the model to operate, but in practice the condition represents cavitation at the inlet valve.

At the conception of this model it was decided to input the system characteristics in graphical form and use the CSMP FUNCTION statements to assess the data. Although this at first seems to simplify the problem, as coefficients do not have to be determined, several pitfalls can arise. Instances in the development of the programme occurred where the functions had to be specified outside the expected range of operation. Although such values might not be needed as outputs, the numerical techniques involved in the CSMP system can call on such values to produce convergence. Care must be taken in the choice of either linear (AFGEN) or Lagrange (NLFGN) interpolation. If the function represents continuous information and AFGEN is used, small changes in slope can appear as transients in the system. If, however, the desired function contains an abrupt discontinuity, NLFGN cannot represent it without distortion. In the model the inlet valve characteristic, defined by IVC, contains both these situations and it was necessary to combine both AFGEN and NLFGN by the statement

FIV2 = IWSW (P2 1.8 E5) NLFGN (IVC, P2), AFGEN (IVC, P2))

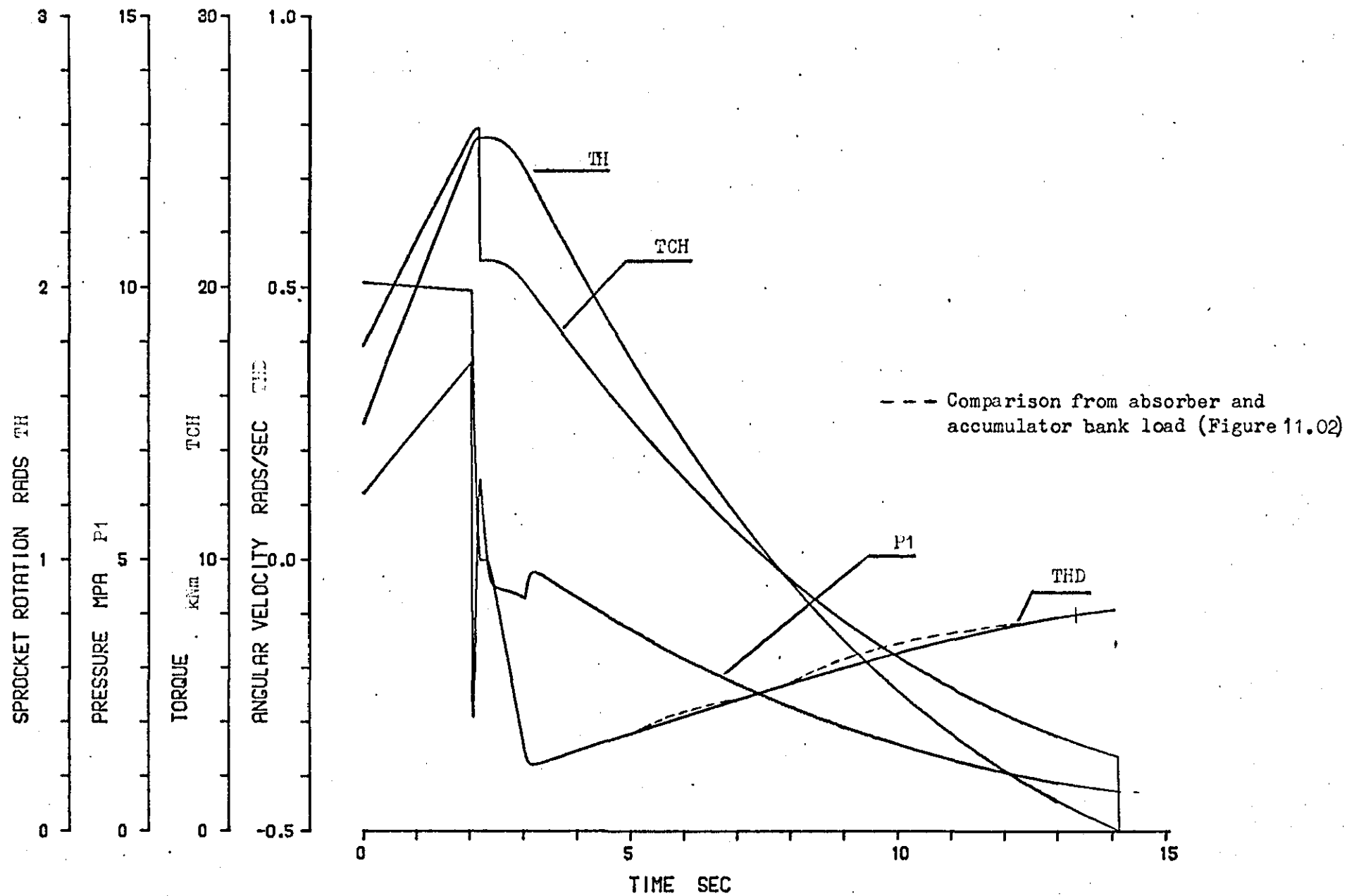


Fig. 11.01 Dynamic model output, haulage loaded with chain system.

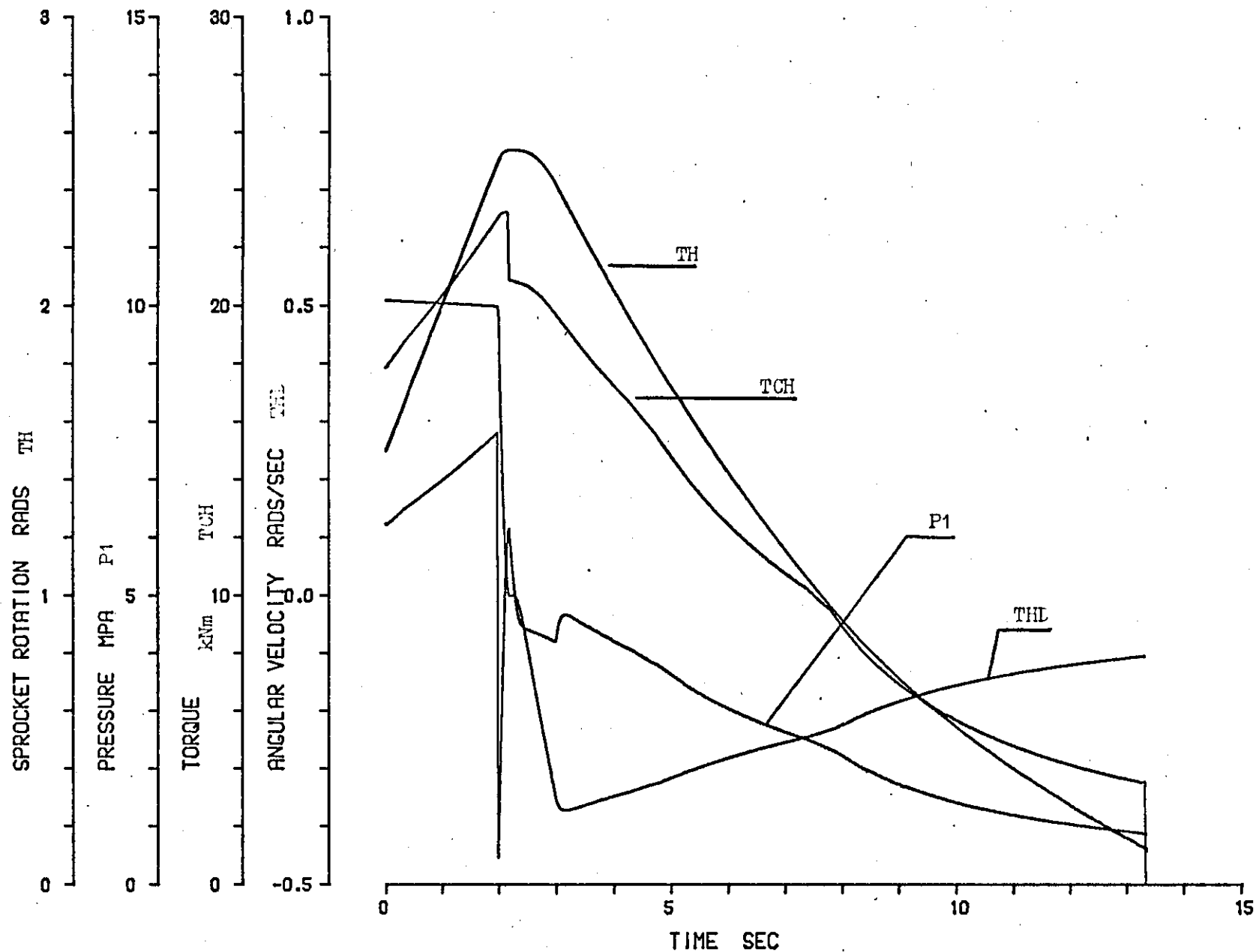


Fig. 11.02 Dynamic model output. haulage loaded with absorber and accumulator bank, pre-charge pressures set using Terminal Section 1.

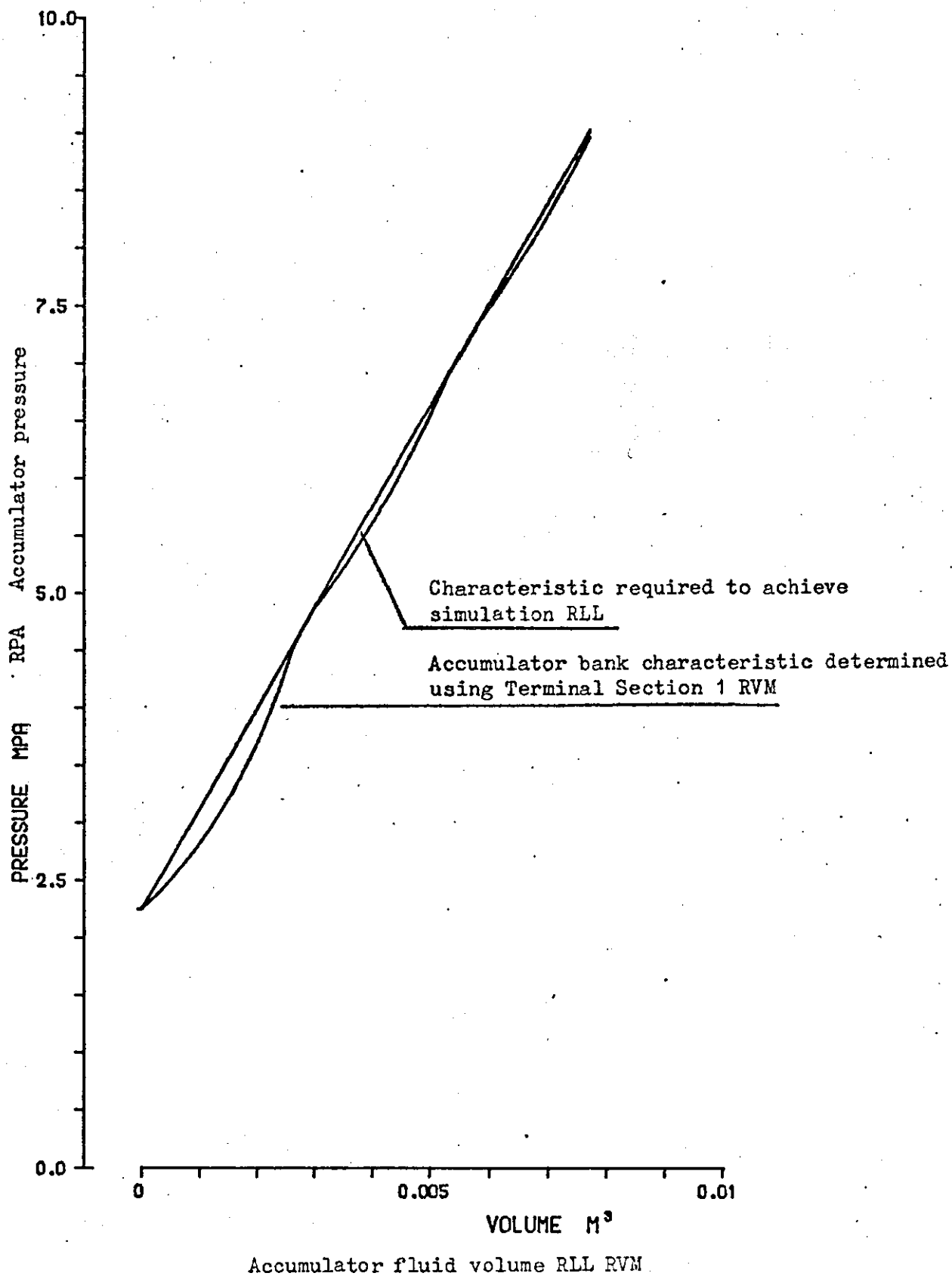


Fig. 11.03 Accumulator bank pressure-volume characteristic, pre-charge pressures set using Terminal Section 1.

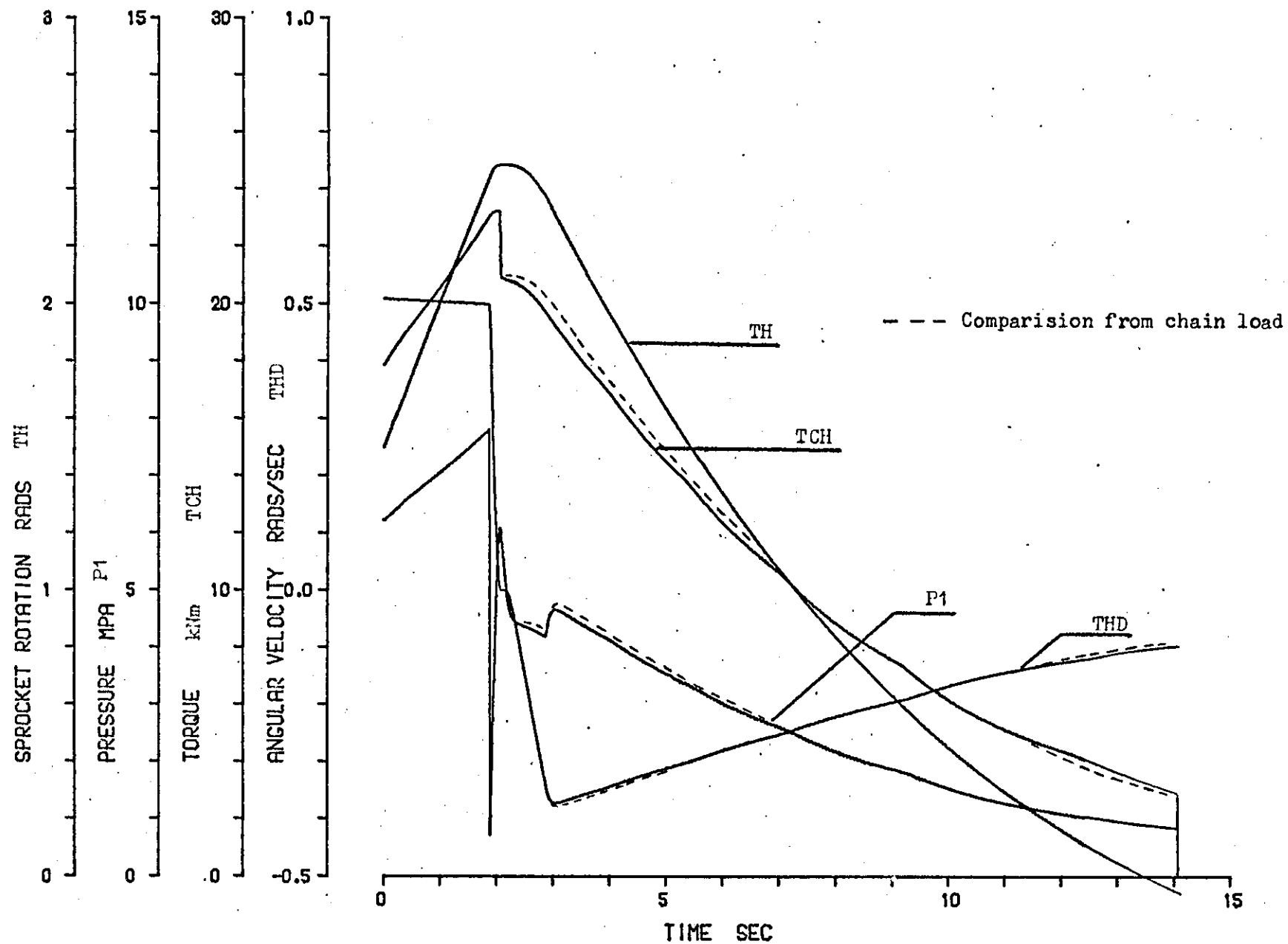


Fig. 11.04 Output from dynamic model, haulage loaded with absorber and accumulator bank pre-charge pressures set using Terminal Section 2.

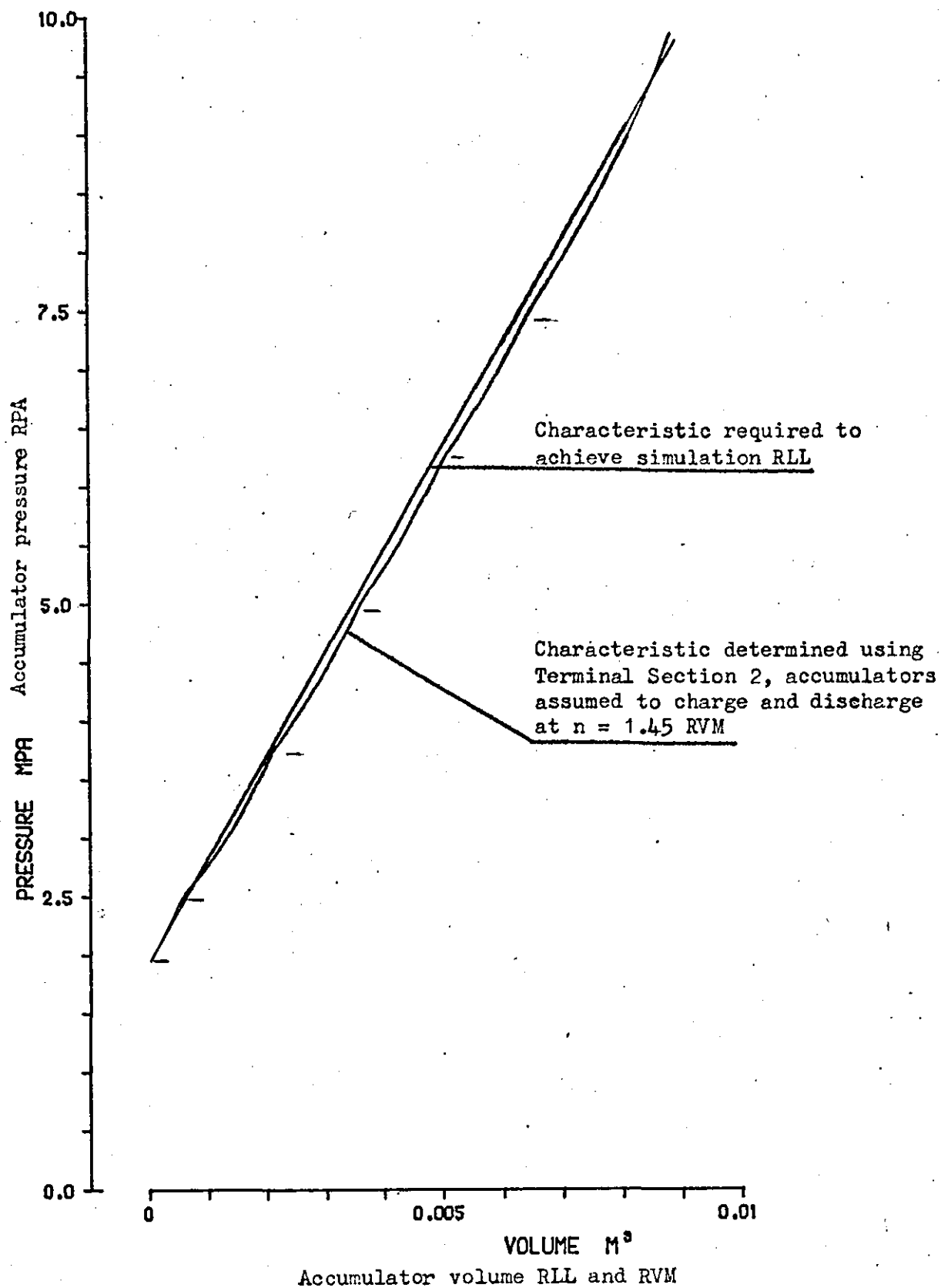


Fig. 11.05 Accumulator bank pressure-volume characteristics, pre-charge pressures determined using Terminal Section 2.

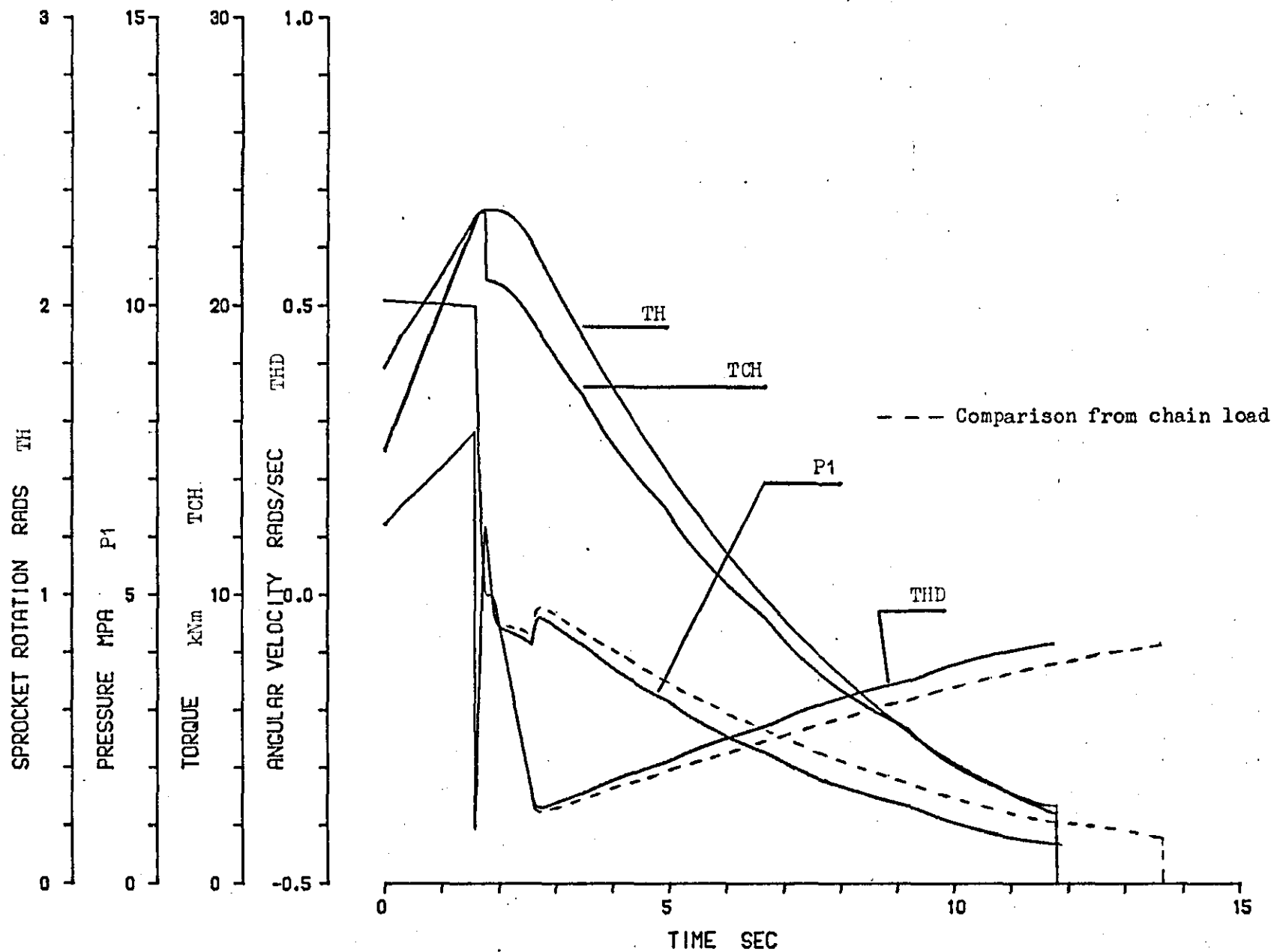


Fig. 11.06 Dynamic model output, haulage loaded with absorber and accumulator bank, pressure-volume characteristic calculated from Terminal Section 3, i.e. no leakage taken into account.

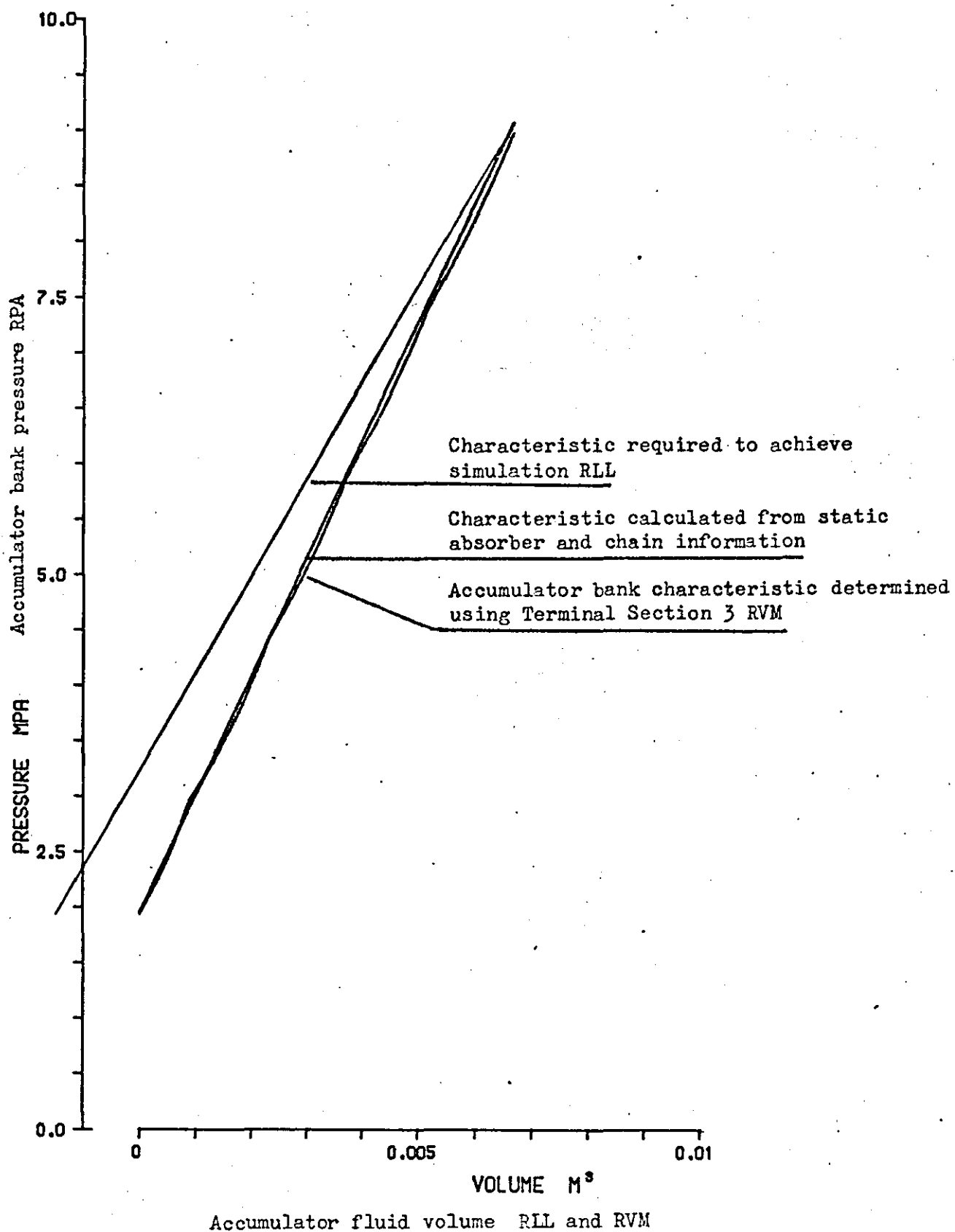


Fig. 11.07 Accumulator pressure-volume characteristic determined neglecting absorber leakage.

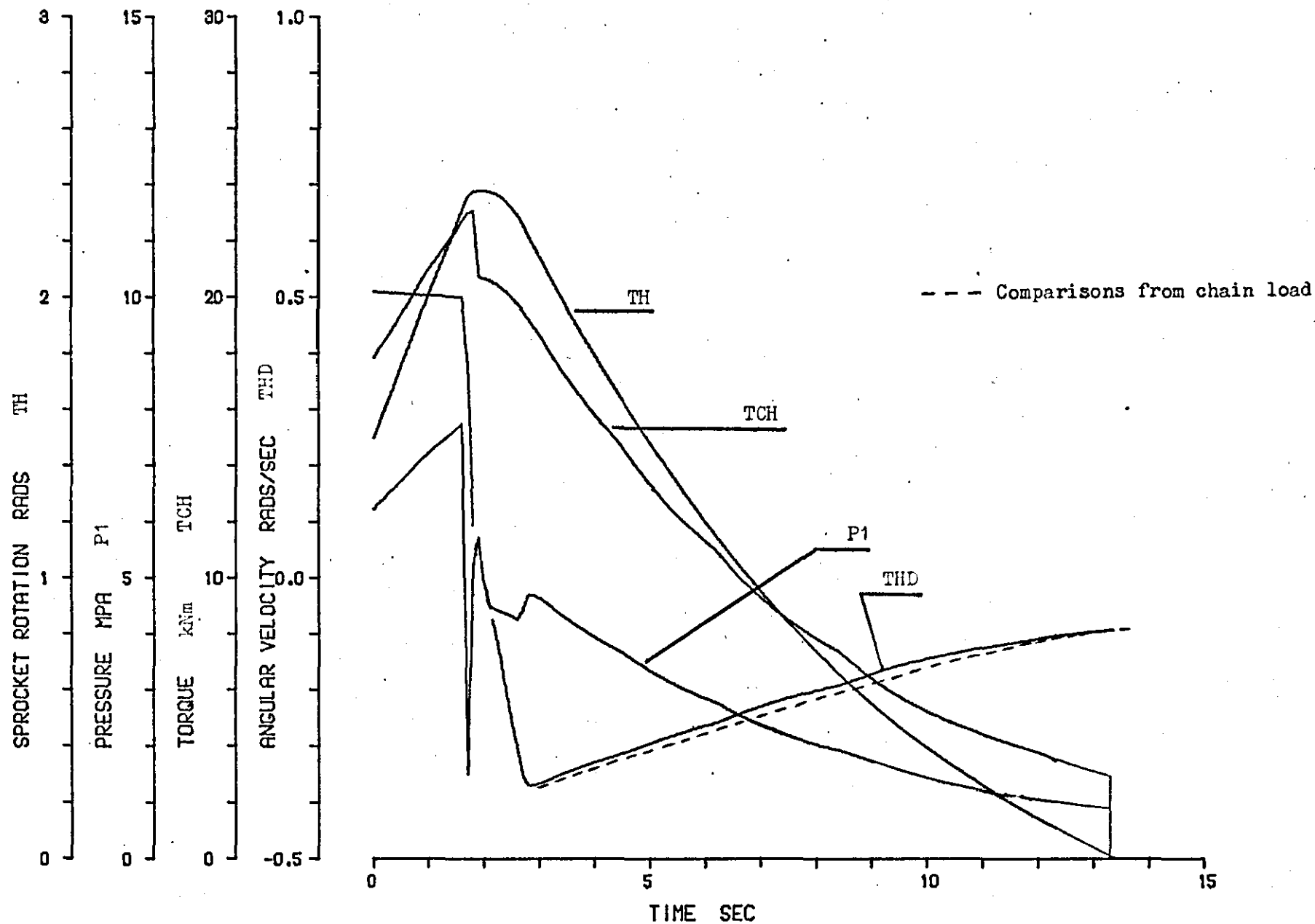
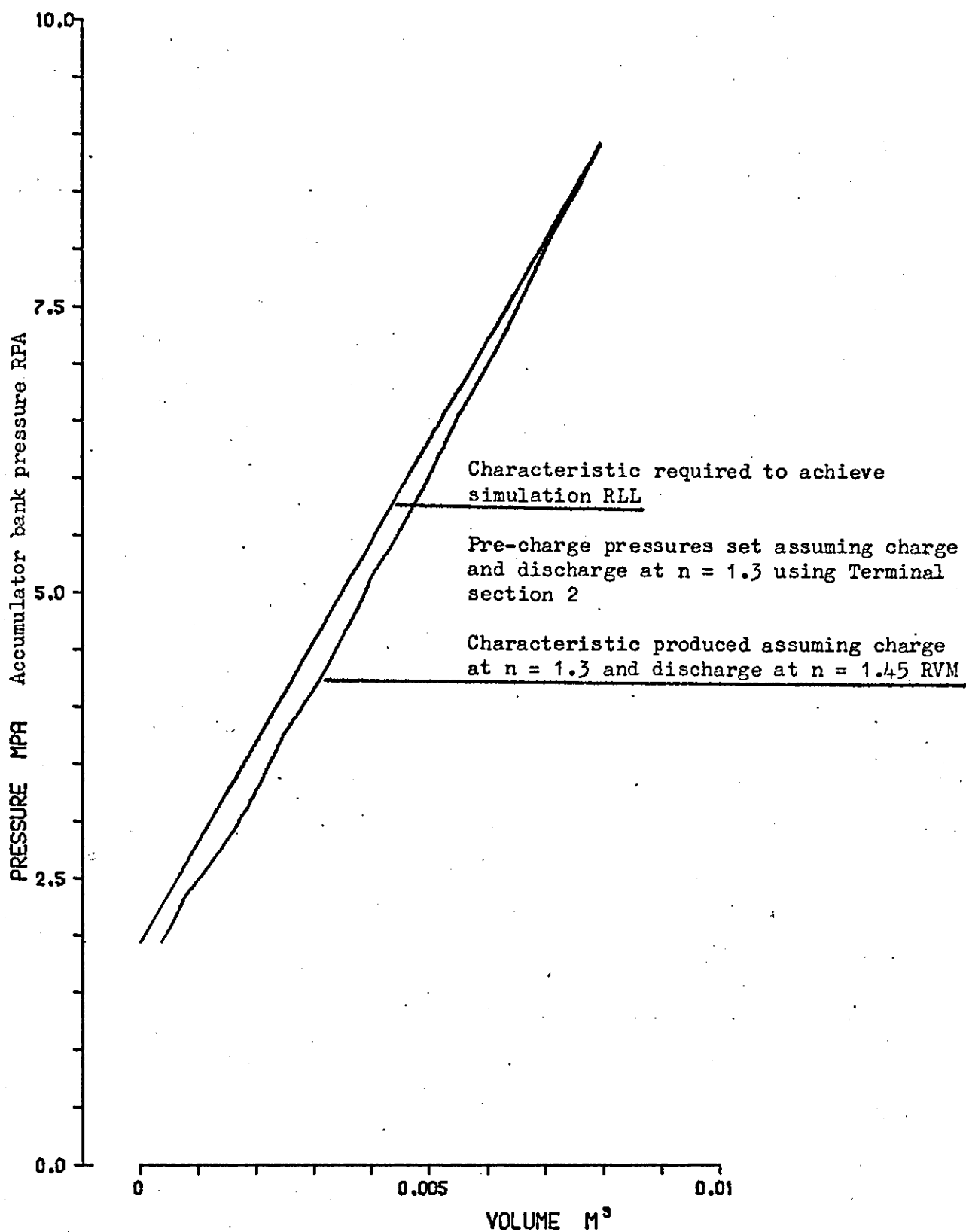


Fig. 11.08 Dynamic model output haulage loaded with absorber and accumulator bank, accumulator pre-charge pressures set assuming charge and discharge at $n = 1.3$, discharge pressure-volume characteristics determined by assuming charge at $n = 1.3$ and discharge at $n = 1.45$.



Accumulator volume RLL and RVM

Fig. 11.09 Accumulator bank pressure-volume characteristic showing errors produced by assuming that charge and discharge take place at the same polytropic index.

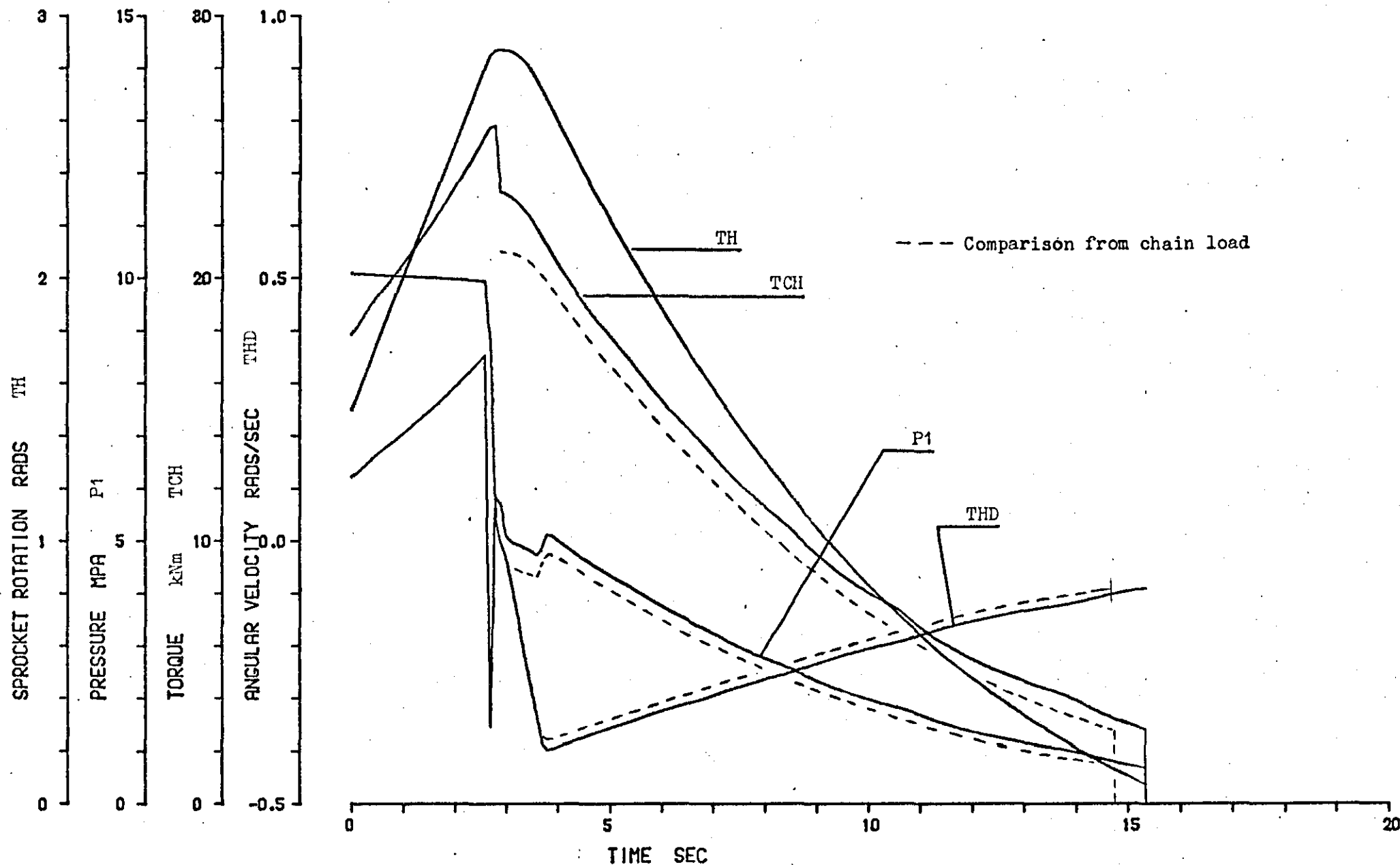


Fig. 11.10 Dynamic model output showing a simulation with absorber and accumulator bank without compensation of the tripping pressure for the difference between the efficiency of the chain and absorber load.

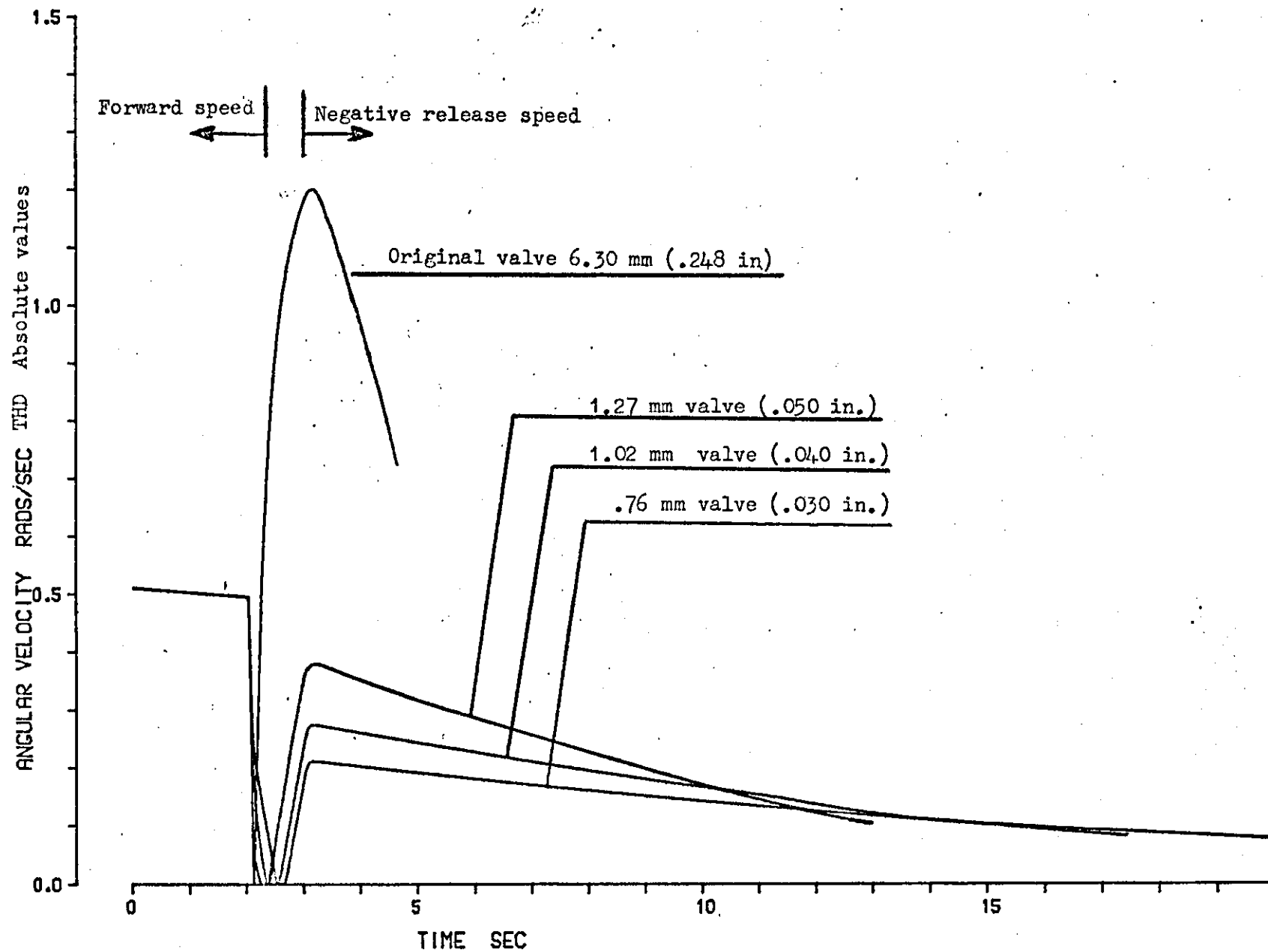


Fig. 11.11 Dynamic model output showing comparison of rates of release of energy from the haulage chain system for various by-pass valves.

12 A CONVERSATIONAL PROGRAMME FOR SETTING THE PRE-CHARGE PRESSURES OF A BANK OF ACCUMULATORS TO ENABLE A HYDROSTATIC POWER ABSORBER TO SIMULATE CHAIN ELASTICITY EFFECTS ON POWER LOADER HAULAGE UNITS

This programme shown in Appendix II uses the IBM conversational language CPS (Conversational Programming System), which accesses a computer through a remote Teletype terminal.

The programme inputs data defining the face chain system, ie chain type and compensator details; haulage details, ie sprocket geometry; maximum torque level; and absorber characteristics. Where possible comment statements are used to give indications of the values of the input data associated with the main system components. In this way relevant information can be stored in the programme with its input controlled by the programme operator.

The programme utilises the methods described in Section 3 to calculate the torque-displacement relationships produced by the chain on the haulage sprocket. Sprocket losses are calculated as described in Section 3.2 with the interlink friction coefficient taken as 0.5. The absorber loss characteristics are described by a mechanical efficiency and an absorber leakage factor. This leakage factor is derived from the experimental work and is the ratio between the volume of fluid supplied to the absorber and its displaced volume under conditions typical to release of strain energy in power loader haulage units. This factor can only be typical, since in practice it would vary with the rate of release of strain energy.

The empirical method of setting accumulator pre-charge pressures, as described in Section 6.3 is used with a value of polytropic index taken at 1.45.

When operating the programme, initial concern should be with obtaining a satisfactory chain system, if necessary several attempts should be made to achieve a chain pre-tension of around 50 kN (5 tons).

The programme gives several choices of compensator units and also a facility for the introduction of slack chain, if the available compression from any compensator is not sufficient to give a reasonable value of pre-tension.

An indication of the amount of adjustment required to compensate for the differing frictional losses between the chain drive system and the absorber is given by (pchpr), the percentage haulage pressure reduction. Any haulage boost pressure is not included in this reduction, ie pchpr operates only on the difference between the tripping pressure and boost pressure. Under conditions where the absorber losses are greater than the chain system losses, it is possible that pchpr could be above 100%, needing an increase in haulage tripping pressure for compensation.

After the chain system details have been finalised the programme gives a choice of accumulator size. All the accumulators in the bank are required to be of equal volume. To achieve a satisfactory simulation a minimum of four accumulators will be required. If the programme indicates either too few or too many accumulators are required to cover the pressure range of the absorber, alternative accumulator volumes can be tried. If a satisfactory simulation cannot be achieved with the accumulators available, either they can be used in combinations and treated as single accumulators with the same pre-charge pressures, or the type of absorber can be changed. Some adjustment can also be achieved by alteration of $P_a(1)$ the lowest pre-charge pressure. Although this will move the displacement achieved with the simulation (accrot) away from the required displacement (rot), it might be preferable to changing the accumulators or absorber available for use. Adjustment of $P_a(1)$ might also be required, if this is below that recommended by the manufacturers taking into account the maximum absorber pressures.

The programme outputs the recommended pre-charge pressures for the accumulator bank, together with a list of input data and other parameters calculated during the execution.

13 A DYNAMIC MODEL OF A MECHANICAL HAULAGE UNIT

13.1 Description

A CSMP model of a simple mechanical haulage unit is shown in Appendix III. The model includes the effects of haulage inertia, viscous damping and the braking torque used to reduce the energy release speeds of mechanical haulage units.

The haulage sprocket torque T_M is calculated from the sprocket-torque relationship, defined by the CSMP FUNCTION statements $DTIN$ and $DTDG$, dependent on the direction of the sprocket rotation THD , ie whether the haulage unit is driving or is being driven by the chain system. An INSW statement ensures that the frictional braking torque R_T acts against the direction of rotation. A viscous damping force VTR acts in the opposite direction to sprocket rotation. This force is estimated by assuming the unit to take 500 N m (370 lb ft) torque at the sprocket, to drive the haulage unit in reverse direction at a speed equal to the max forward speed. Two CSMP INTGRL statements define in turn the angular velocity and displacement from the angular acceleration, which is obtained from the system torque balance divided by inertia.

The initial conditions for the programme assume the haulage to be stalled in cut and to have the drive interrupted at the sprocket torque $TTRIP$ whilst driving at a forward speed $FS*FRAC$. A CSMP FINISH statement stops the run if either the release speed or the angular displacement approaches zero. Outputs of the main system variables are obtained using the CSMP PRINT statement and the data required for a plotting programme is obtained with the PREPARE statement. Multiple runs can be obtained by use of either successive END cards or the multiple PARAMETER statement.

Outputs from the model are shown in Figs. 13.1 and 13.2. The effects of variation of BT , braking torque, on the energy release speeds is shown in Fig. 13.1 together with and without viscous damping. Fig. 13.2 shows the effects of variation of haulage inertia on release speeds.

13.2 Observations on the Outputs of the Mechanical Haulage Model

Existing mechanical haulage units have only one device, the parking brake, with which the rate of release of energy from the chain system can be controlled. Although in practice, the setting of this brake would be determined by other factors, such as the incline of the face (the parking brake has to be set high enough to stop the machine sliding down the face under its own weight) and the maximum level of tension difference allowable across the haulage unit under equilibrium conditions with the machine stalled into cut.

The effect of variation of parking brake settings on energy release speeds with constant haulage inertia is shown in Fig. 13.1. The levels of parking brake torque are seen to be high in comparison with the maximum driving torque. A parking brake torque of 10 000 N m (7 380 lb ft) with a tripping torque of 26 500 N m (19 500 lb ft) gives a maximum release speed 2.7 times the maximum forward speed. With such a parking brake setting, a residual force of approximately 30% of the maximum value could be left across the haulage unit if it was stalled in cut. An important observation from these results is that it is possible to still have haulage rotation, hence kinetic energy, with zero displacement. In a practical situation, not shown in the model, this energy would cause a rapid increase in the tension T_2 causing the chain to snatch dangerously and lurching of the machine.

The estimated level of viscous damping is assumed to exist in the haulage unit without special provision. Damping is shown in Fig. 13.1. to have considerable effect on the maximum release speeds indicating that some specially designed viscous damping device would be useful for control of energy release speeds.

The use of haulage inertia as a means of controlling energy release speeds can be seen from Fig. 13.2. Here a typical haulage inertia is considered to be 4700 kg m^2 . Large increase in inertia can be obtained,

however, with little additional mass due to the large reduction ratios of haulage gearboxes.

Although this model is not meant to show a particular haulage unit with accurate parameter values, it does show the effects of parameter variation and indicate what is required to improve the energy release characteristics of mechanical haulage units. Considerably more sophistication could be introduced into the model, with little effort, such as the reaction times of the parking brake and any non-linear experimentally derived frictional and damping effects.

Haulage inertia constant
at 4700 kg m^2

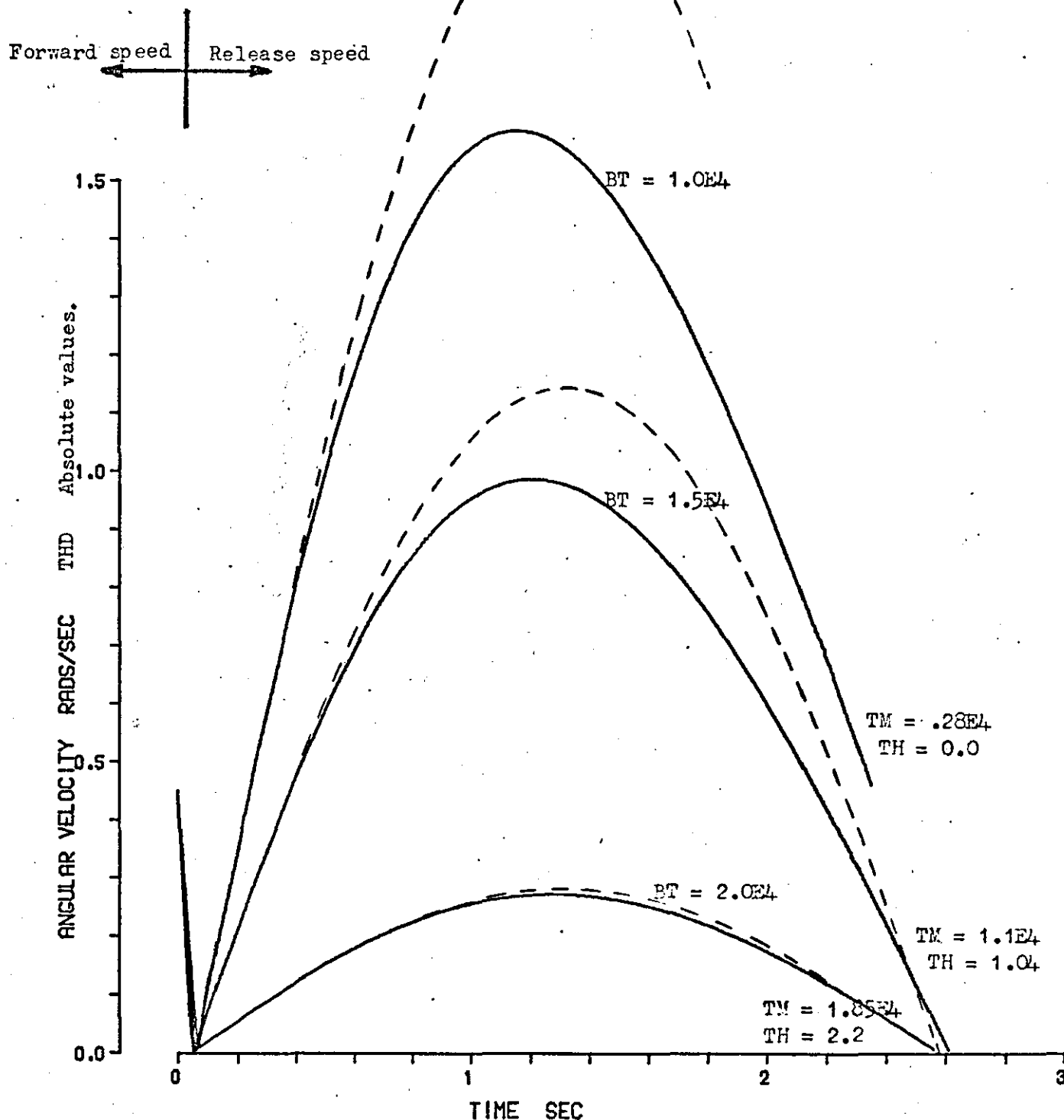


Fig.13.1 Output from dynamic model of mechanical haulage, showing variation in release speed with haulage braking torque, with and without velocity damping.

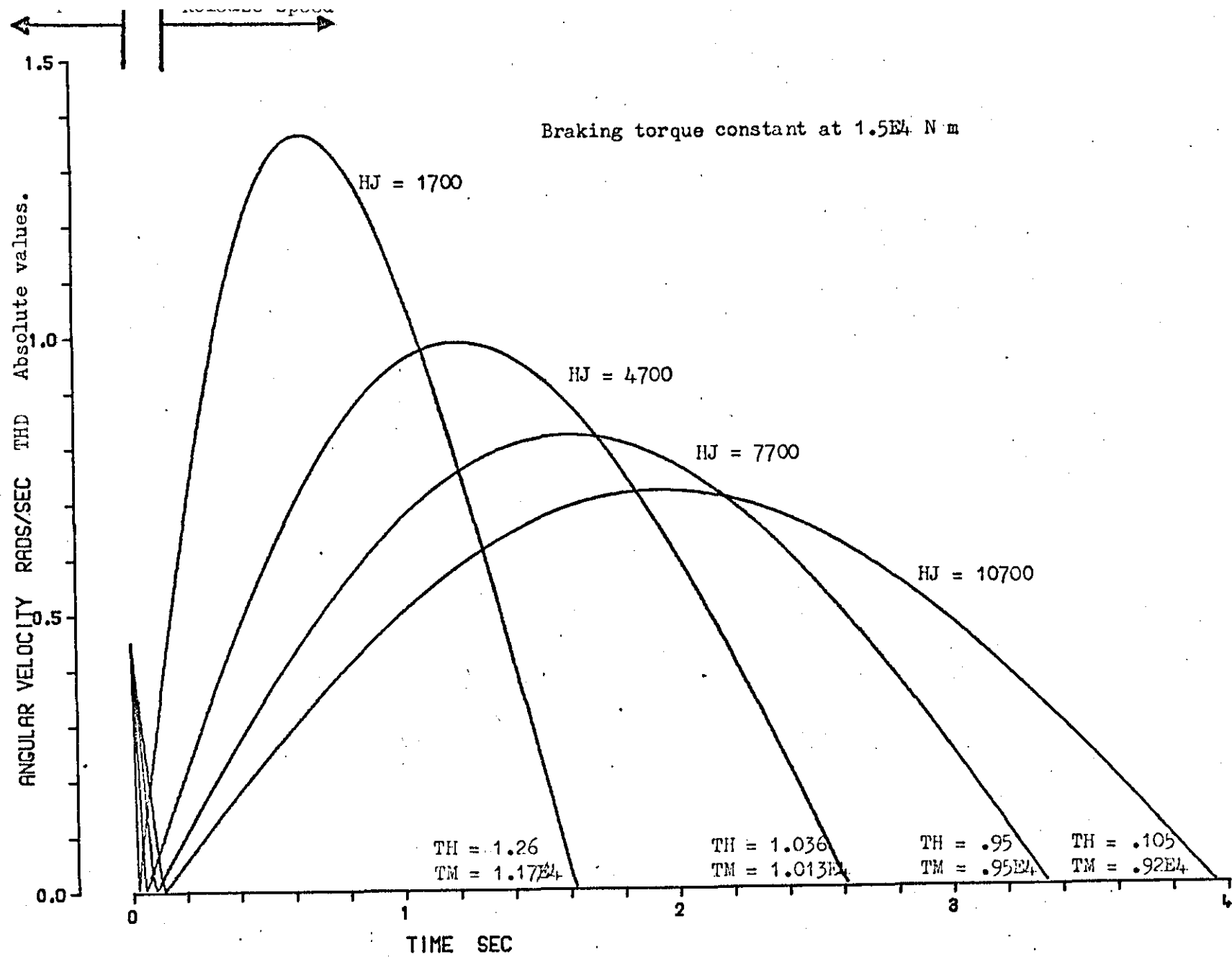


Fig. 13.2 Output from dynamic model of mechanical haulage unit showing variation in energy release speeds with haulage inertia.

14 CONCLUSIONS

14.1 Chain System

The sprocket torque-chain extension relationship, for a given haulage unit, is made variable by the conditions and associated machinery existing on the coal face where the unit is to be used. In particular, the total extension and the pre-tension produced by the haulage unit, on a face installation, can vary with the type of chain tensioners used and the set up conditions.

Sprocket losses need to be included in the prediction of sprocket torque-displacement relationships. Accurate values however, are not available and are subject to sprocket and chain wear conditions and the presence or lack of materials acting as lubricants on the contacting surfaces.

The tests in which the haulage was loaded with the chain system, showed the most dangerous aspect of excessive release speeds to occur when the extended chain has moved through the haulage unit. Here the sprocket drive still has rotation. The energy contained is dissipated by a sudden increase in the tension T_2 , producing a reverse force on the haulage unit. This causes whipping of the slack side chain and lurching of the machine out of cut. Although neither the absorber tests or the CSMP model reproduce this effect, their results do show the haulage unit to have speed at zero displacement after energy release. This effect is particularly dangerous where chain systems have been set up to include slack chain in the T_2 side under maximum extension conditions, a common procedure for both compensated and solid anchorage installations.

14.2 Absorber Type

Both the Hagglunds 6185 and the Staffa B270H hydrostatic motors are suitable for chain elasticity simulation. The Staffa B270H has lower leakage effects and an efficiency nearer that of the chain system than the Hagglunds 6185. When the Staffa B270H is used in conjunction with a 4/1 speed increasing gearbox it has a similar capacity to the Hagglunds 6185.

14.3 Accumulator Performance

Accumulators charge and discharge under polytropic conditions when operated at rates corresponding to those found in chain elasticity simulation. Their characteristics can be defined by $PV^n = C$ with values of n between 1.3 and 1.45. A knowledge of the correct initial gas volume is essential to the accurate prediction of their pressure-volume characteristics.

14.4 Accumulator Bank Pre-charge Pressure Setting Procedures

The empirical method of accumulator pre-charge pressure setting gives good results and is very easy to use, requiring only a simple algebraic expression. If the pressure-volume characteristics is non-linear the empirical method is unsuitable and the pressure increment technique should be used. This does however, involve computer calculations and can give less accurate results than the empirical method when used for linear characteristics.

Although both these procedures assume accumulators to charge and discharge at the same polytropic index, the CSMP model shows that this assumption not to introduce unreasonable errors with the differing values of the index likely to be found in chain elasticity simulation.

14.5 The CSMP Model

CSMP provides a facility whereby engineers can quickly construct models of dynamic systems from block diagrams without an extensive knowledge of computer languages or numerical techniques. Non-linearities and time variant problems, common in hydraulic systems, are easily included into models by use of an extensive library of sub-programmes. Outputs from a model in either tabular, print-plotted or X - Y graph plotted form can be obtained by use of single word CSMP statements.

The model described in this work shows the flexibility in operation of CSMP that can be introduced by use of the Terminal Section and the re-run facility. Here the Terminal Section is used to process data, produced by the first run, through the Dynamic Section of the model and

create new data, which is used in a second run through the Dynamic Section in which the structure of the model is also altered. Essentially two models are run in series the first producing data for the second. CSMP however, has one inherent disadvantage when applied to hydraulic systems, fluid in a given volume is usually determined by integration of the product of a flow rate and a fluid stiffness factor. Since the volumes are usually small and the stiffness factors high, being dependent on bulk modulus, this technique necessitates the use of extremely small time intervals, if the numerical integration methods employed for solutions are to remain stable. High computer run times result if models of hydraulic systems simulation, involving this method of pressure determination, are used for purposes other than investigations of transient behaviour.

The numerical simulation approach to the problem of chain elasticity effects proved to have benefits beyond the mere production of theoretical results. Construction of a model demands a detailed examination of the system to enable mathematical expressions and hence CSMP statements to be written. This discipline yields a greater understanding of the system even before the programme has been put into operation. Data can be retrieved from models which would be difficult to obtain experimentally, due either to problems of instrumentation or complex modes of operation.

No direct comparisons can be drawn between the model and the experimental work due to irregularities in the operation of the haulage unit. This, however, shows the true use of the model, comparisons are not possible unless operating conditions can be kept constant as is the case with the model.

Although not constructed for this purpose the model shows a failure of the hydrostatic transmission inlet valves to deal with pressure transients without cavitation. A more detailed description of the circuit would yield further information in this interesting field.

14.6 Curve Follower and Accumulator Simulation Techniques

The curve follower technique can be used to give chain elasticity simulation, but an additional power input is required into the absorber system and complex instrumentation is needed for control. The accumulator system is easy to use and once the pre-charge pressures have been set requires no further attention. It is capable of operating from any load condition and is ideal for use in life testing procedures simulating working conditions.

For precise representation of a given system the curve follower technique can automatically compensate for the differing efficiencies of the chain and absorber, whereas for the accumulator technique, adjustment is required to the haulage tripping pressure. The effects of differing efficiencies however, are not excessive and correct selection of the absorber type can reduce the compensation required.

The conversational programme, developed for accumulator pre-charge pressure setting, provides a rapid method of both determining an appropriate chain system for a given haulage unit and selecting a compatible absorber and accumulator bank. Most of the data relevant to the problem is stored in the programme for selection by the operator to give optimum performance.

14.7 Mechanical Haulage Unit

The CSMP model of a mechanical haulage unit suggests that some form of rotational viscous damper, in addition to a frictional parking brake, would significantly improve the control of release of energy from the chain. In a practical situation this would imply incorporating a fluid damping device in the sprocket drive.

14.8 Further use of Hydrostatic Power Absorbers for Chain Elasticity Simulation

Testing facilities for power loader haulage units are used by three organisations, MRDE, NCB Central Workshops and power loader manufacturers. Some installations utilise dynamometers unable to reproduce chain

elasticity effects. Where hydrostatic power absorbers are in use and chain elasticity simulation is required, it is unlikely that users outside MRDE will have sufficient facilities to accurately measure the degree of simulation being achieved. In most cases it will be sufficient if the loading device possesses an amount of stiffness which can be expressed in terms of sprocket rotation. If this is the case, an accumulator pre-charge setting procedure should be adopted whereby the available accumulators are set with equal pressure increment between the maximum absorber pressure and the boost pressure. The maximum and minimum pre-charge pressures should be one pressure increment above and below the boost pressure and the maximum absorber pressure, eg if four accumulators are available, the maximum absorber pressure is 14.5 MPa (2100 lb/in²) and the boost pressure .69 MPa (100 lb/in²) pre-charge pressures should be set at 2.75 MPa (400 lb/in²) increments giving 3.44 MPa (500 lb/in²), 6.2 MPa (900 lb/in²), 8.96 MPa (1300 lb/in²) and 11.7 MPa (1700 lb/in²). A trial and error method should then be adopted, adjusting the number of accumulators until the amount of reverse rotation is correct. This will involve re-adjustment of the pre-charge pressures. If the accumulators are of equal volume and there are at least four accumulators in the bank a reasonably linear chain elasticity simulation will be produced. The characteristic will be similar to that achieved with the empirical method which also uses fixed increments between pre-charge pressures. This procedure although cumbersome requires no calculations, is easily understood by workshop personnel and is suitable for such work as functional checks on re-conditioned haulage units.

Where a more accurate simulation is required to assess release speeds for compliance with regulations recourse should be made to the accumulator pre-charge setting technique as described in the conversational computer programme.

15 RECOMMENDATIONS

At the present time, no guide has been given by the NCB on the maximum allowable level of energy release speeds from power loader haulage units. As a results of this work it is suggested that a reasonable specification would be to limit the maximum release speed to the maximum forward speed of the haulage unit. As no definite release displacement can be stated for any haulage type and since conditions can arise where chain is pulled through the haulage unit by factors other than elasticity, it is also suggested that the unit be capable of continuous reverse operation with the sprocket driven at a torque corresponding to the maximum forward value for periods of say one minute, without the reverse speed increasing beyond the maximum forward speed.

Further experimental and theoretical work should be carried out on mechanical haulage units, to determine their ability to deal with the release of energy from the cahin system in a safe manner. Particular attention should be paid to restricting both the maximum release speed and the speed at the point where all the extended chain has moved through the sprocket system.

APPENDIX I

A CSMP Model of a Power Loader Haulage
Unit with Chain and Absorber Loading

CONTINUOUS SYSTEM MODELING PROGRAM

PROBLEM INPUT STATEMENTS

TITLE B.J.D. B14 RUNBACK SIMULATION USING HAGGLUNDS 6185 MOTOR
INITIAL

METHOD RKSF

CONSTANT HJ=4700.,AJ=41.2,HRATIO=215.,DM=1.641E-5,DA=2.59E-3

CONSTANT RM=6.49E8,VP=1.63E-4

INCON KHC=0,KH=0,LS=0,LP=0,VTT=0.0

PARAMETER PAR=20.0,AFAC=1.0

PARAMETER KAB=0,TBP=0,TBP1=0,LSWICH=0,STT=1.5,KSTOP=0

PARAMETER FMAX=2.576E-3,TRIP=8.62E6,SPD=0.01

FUNCTION RV=0.0,0.0,8.83E6,0.0,8.96E6,3.78E-4,9.65E6,3.03E-3

FUNCTION SWASH=0.0,0.75,1.0,0.0,30.0,0.0

FUNCTION XLEAK=0.0,0.0,1.38E7,1.51E-4

FUNCTION ILEAK=0.0,0.0,1.38E7,1.51E-4

FUNCTION DTDG=0.,6.4E3,4.4,4.E4

FUNCTION TODG=6.4E3,0.,4.E4,4.4

FUNCTION DTDN=0.,2.7E3,5.2,4.E4

FUNCTION TODN=2.7E3,0.,4.E4,5.2

FUNCTION TPHM=-4.E4,-1.E7,0.,.7E6,4.E4,1.31E7

FUNCTION PTHM=-1.E7,-4.E4,.7E6,0.,1.31E7,4.E4

FUNCTION TPHP=-4.E4,-1.E7,0.,0.,4.E4,9.7E6

FUNCTION PTHP=-1.E7,-4.E4,0.,0.,9.7E6,4.E4

FUNCTION VIC=0.0,0.0,1.13E01,-1.03E9

FUNCTION IVC=-1.E9,1.21E-3,-1.E7,1.19E-3,-1.E6,1.17E-3,-1.5E5,
1.15E-3,-1.4E5,1.145E-3,-1.3E5,1.12E-3,-1.1E5,1.04E-3,-.9E5,
.9E-3,-.8E5,.82E-3,0.0,0.0,1.E9,0.0

FUNCTION BYPS= .0 .0 .3E6, .20E-3, .5E6, .30E-3,
.7E6, .40E-3, .1E7, .52E-3,1.5E6, .72E-3,
.2E7, .90E-3,2.5E6,1.06E-3, .3E7,1.20E-3,
.4E7,1.44E-3, .5E7,1.66E-3, .6E7,1.86E-3,
.7E7,2.04E-3, .8E7,2.20E-3, .9E7,2.34E-3,
1.0E7,2.48E-3,1.1E7,2.60E-3,1.2E7,2.72E-3,
1.3E7,2.82E-3,2.0E7,3.56E-3

FUNCTION TPAM=-4.0E4,-1.5E7,0.0,8.95E5,33400.,13.8E6

FUNCTION TPAP=-4.0E4,-1.6E7,0.0,5.51E5,36500.,13.8E6

FUNCTION PTAM=-1.5E7,-4.E4,8.95E5,0.,13.8E6,33400.

FUNCTION PTAP=-1.6E7,-4.E4,5.51E5,0.,13.8E6,36500.

FUNCTION ALEAK=0.0,0.0,2.41E6,75.8E-6,5.37E6,1.51E-4,9.86E6,2.27E-4,
1.35E7,3.03E-4

*

STORAGE AV(300),AP(300),AL(300)

TABLE AV(1-300)=300*0.0,AP(1-300)=300*0.0,AL(1-300)=300*0.0

FIXED IN,KPA,IV,IZ,KR,KPX,KPMAX,KP,LS,LSM,LP,LSWICH

FIXED K,J,KH,KHMAX,KHC,KAB,IA,KPMIN

STORAGE BVOL(500),BPA(500),KPA(11),VA(11),VT(11)

TABLE BVOL(1-500)=500*0.0,BPA(1-500)=500*0.0,KPA(1-11)=11*0.0,
VA(1-11)=11*3.4413E-3,VT(1-11)=11*0.0

PARAMETER IN=6,POWC=1.45,POWE=1.45,KR=100000,KPMAX=15000000

PCOMP=AFGEN(TPHM,AFGEN(PTAP,AFGEN(TPAM,AFGEN(DDTN,AFGEN(TDDG,
AFGEN(PTHM,TRIP))))))

STF=RM/VP

VFAC=29.0/38.0

DH=HRATIO*DM

SPOS=AFGEN(SWASH,0.0)

STX=AFGEN(DDTG,STT)

STA=AFGEN(TPAP,STX)

STY=AFGEN(TPHM,STX)

STZ=AFGEN(XLEAK,STY)*2.0

SP2=AFGEN(VIC,STZ)

STH=(SPOS*FMAX-STZ)/DH

Initial Section performed
only at TIME = 0.0

Initial Section inputs data
and evaluates constants for
use in Dynamic Section

DYNAMIC

*

FKAB=KAB-0.5

*

PROCEDURE F1,TBP1,FPUMP,FBP=FT(P1,LSWICH,PCOMP,APDF,SPDF)

*

* PROCEDURE FOR PRESSURE SWITCHED VARIABLES

*

IF (KAB.EQ.1) TRIP=PCOMP
IF (TIME.LT.0.1) LSWICH=0
IF (P1.GE.TRIP) LSWICH=1
IF (LSWICH.GT.0) GO TO 32
FBP=0.0
TBP=TIME
FPUMP=FMAX*SPOS
GO TO 33

32 FBP=NLFGEN(BYPS,APDF)*SPDF*VFAC

LSWICH=1

TBP1=TIME-TBP

FPUMP=FMAX*AFGEN(SWASH,TBP1)

33 CONTINUE

ENDPRO

*

PROCEDURE RPA,RPL=ACH(RVM,LSM)

*

* LINEAR INTERPOLATION OF ACCUMULATOR CHARACTERISTIC ARRAYS AP,AL,AV

*

IF (FKAB.GT.0.0) GO TO 75

RPL=0.0

RPA=0.0

GO TO 26

75 DO 2 J=1,LSM

IF (AV(J)-RVM) 3,4,5

5 IF (J.EQ.1) GO TO 4

RPA=AP(J-1)+(RVM-AV(J-1))*(AP(J)-AP(J-1))/(AV(J)-AV(J-1))

GO TO 6

4 RPA=AP(J)

GO TO 6

3 CONTINUE

2 CONTINUE

6 CONTINUE

DO 22 J=1,LSM

IF (AL(J)-RVM) 23,24,25

25 IF (J.EQ.1) GO TO 24

RPL=AP(J-1)+(RVM-AL(J-1))*(AP(J)-AP(J-1))/(AL(J)-AL(J-1))

GO TO 26

24 RPL=AP(J)

GO TO 26

23 CONTINUE

22 CONTINUE

26 CONTINUE

ENDPRO

*

* HAULAGE TRANSMISSION FLOW EQUATIONS

*

FD1=FPUMP-FBP-FLIN-FX1-FRV1+FIV1-THD*DH

FD2=-FPUMP+FBP+FLIN-FX2-FRV2+THD*DH+FIV2

FRV1=AFGEN(RV,P1)

FRV2=AFGEN(RV,P2)

FX1=AFGEN(XLEAK,P1)

FX2=AFGEN(XLEAK,P2)

FIV2=INSW(P2+.8E5,NLFGEN(IVC,P2),AFGEN(IVC,P2))

FIV1=INSW(P1+.8E5,NLFGEN(IVC,P1),AFGEN(IVC,P1))

FLIN=AFGEN(ILEAK,APDF)*SPDF

DYNAMIC section performed at each time increment DELT until FINISH statement is satisfied

PROCEDURE functions enable Fortran logical statements to be used in DYNAMIC section

CMP statements put in correct sequence by sorting algorithm



*
* HAULAGE TRANSMISSION PRESSURE EQUATIONS
*

```
PDF=P1-P2
APDF=ABS(PDF)
SPDF=SIGN(1.0,PDF)
P1=INTGRL(STY,FD1*STF1)
P2=INTGRL(SP2,FD2*STF2)
STF1=INSW(P1,STF/PAR,STF)
STF2=INSW(P2,STF/PAR,STF)
```

*
* SPROCKET MOTION EQUATIONS
*

```
TM=INSW(THD,AFGEN(PTHP,APDF),AFGEN(PTHM,APDF))*SPDF
TH2D=INSW(FKAB,(TM-TCH)/HJ,(TM-TCH)/(HJ+AJ))
THD=INTGRL(STH,TH2D)
TH=INTGRL(STT,THD)
```

*
* CHAIN LOAD

```
TCH=INSW(FKAB,INSW(THD,AFGEN(DTDM,TH),AFGEN(DTDG,TH)),INSW(THD ..
,AFGEN(PTAM,RPA),AFGEN(PTAP,RPA)))
```

*
* ABSORBER LOAD FROM ACCUMULATOR CHARACTERISTICS
*

```
TA=INSW(FKAB,TCH+AJ*TH2D,0.0)
PA=INSW(FKAB,INSW(THD,AFGEN(TPAM,TA),AFGEN(TPAP,TA)),0.0)
AVOL=INSW(FKAB,INTGRL(0.0,THD*DA-AFGEN(ALEAK,PA)),0.0)
RVM=INSW(FKAB,0.0,INTGRL(STB,DA*THD-AFGEN(ALEAK,RPA)))
RLL=INSW(FKAB,0.0,RPL)
```

*
NOSORT

*
* NOSORT SECTION TO SET BVOL AND BPA ARRAYS TO DESCRIBE THE REQUIRED
* PRESSURE-VOLUME CHARACTERISTIC
*

```
121 CONTINUE
IF(KAB.EQ.1)GO TO 40
IF(TBP1.LT.2.5)GO TO 40
IF(LSWICH.EQ.0.AND.TBP1.LT.2.0.AND.KEEP.EQ.0)GO TO 40
KH=KH+1
IF(KH.EQ.100)GO TO 41
GO TO 40
41 KHC=KHC+1
KH=0
BVOL(KHC)=AVOL
BPA(KHC)=PA
KHMAX=KHC
40 CONTINUE
```

*Nosort section ensures that
the csmf statements below
are not sorted.*

*
TERMINAL

*
* TERMINAL SECTION (2)
* DETERMINATION OF THE REQUIRED PRESSURE-VOLUME CHARACTERISTIC BY
* LINEARISING DATA IN BVOL AND BPA ARRAYS
* ACCUMULATORS SET USING IMPERICAL METHOD.
*

```
IF(KAB.NE.0)GO TO 15
```

*
* INVERSION EXTENSION AND INITIALISATION OF BVOL AND BPA ARRAYS
*

```
RVMAX=BVOL(KHMAX)
DO 42 J=1,KHMAX
K=KHMAX-J+1
DYV=BVOL(J)
```

*TERMINAL section performed only
at the end of a DYNAMIC run*

```

DXV=BVOL(K)
DYP=BPA(J)
DXP=BPA(K)
BVOL(J)=DXV
BVOL(K)=DYP
BPA(J)=DXP
BPA(K)=DYP
K=1
IF(J+J.EQ.KHMAX.OR.J+J+K.EQ.KHMAX)GO TO 46
42 CONTINUE
46 CONTINUE
    DO 57 J=1,KHMAX
57 BVOL(J)=BVOL(J)-BVMAX
    BVOL(KHMAX+1)=(2000.*6894-BPA(1))*(BVOL(KHMAX)-BVOL(1))/
    (BPA(KHMAX)-BPA(1))
    BPA(KHMAX+1)=2000.*6894
    KHMAX=KHMAX+1
    WRITE(3,311)
311 FORMAT('//20X,'ELEMENTS OF ARRAY BVOL'/)
    WRITE(3,303)(BVOL(J),J=1,KHMAX)
    WRITE(3,310)
310 FORMAT('//20X,'ELEMENTS OF ARRAY BPA '/)
    WRITE(3,303)(BPA(J),J=1,KHMAX)
*
* DETERMINATION OF THE REQUIRED PRESSURE VOLUME CHARACTERISTICS FROM
* THE CHAIN AND ABSORBER CHARACTERISTICS
*
    KPA(1)=AFGEN(TPAM,AFGEN(DTON,0.0))
    KPA1=KPA(1)
    AB=KPA1
    PATR=AFGEN(TPAP,AFGEN(PTHM,PCOMP))
    RBV=AFGEN(TDDG,AFGEN(PTHM,TRIP))*DA*AFAC
*
* ACCUMULATOR PRE-CHARGE PRESSURE SETTING USING IMPERICAL METHOD
*
* USE OF THIS STATEMENT FOR USL CONVERTS TERMINAL SECTION 2 TO TERMINAL
* SECTION 3
* ACCUMULATORS SET USING IMPERICAL METHOD. REQUIRED PRESSURE VOLUME
* CHARACTERISTIC FOUND FROM STATIC CHAIN AND ABSORBER CHARACTERISTICS
*
    USL=(PATR-KPA(1))*VA(1)/RBV/KPA(1)
*
    USL=(BPA(KHMAX-10)-BPA(1))/(BVOL(KHMAX-10)-BVOL(1))*VA(1)/KPA(1)
    YI=.36-.2*POWC+(.549-.125*POWC)*USL
    EPOW=1.0/POWE
    CPOW=1.0/POWC
    DO 54 J=2,IN
    KPA(J)=J*YI*AB
54 CONTINUE
*
* ADDITION OF INDIVIDUAL ACCUMULATORS TO FIND COMBINED CHARACTERISTIC
*
    VTT=IN*VA(1)
    AD=KPMAX
    VTA=0.0
    AE=PATR+1.0E-9
    DO 20 J=1,IN
    AA=KPA(J)
    VT(J)=VA(J)*(AA/AE)**CPOW
    VTA=VTA+VA(J)
20 CONTINUE
    K=0
    KPMIN=AB

```

```

DO 29 KP=KPMIN,KPMAX,KR
AC=KP
VV=0.0
DO 28 J=1,IN
VJ=VT(J)*(AE/AC)**EPOW
IF(VJ.GE.VA(J))VJ=VA(J)
VV=VV+VJ
28 CONTINUE

```

```

*
* SETTING OF ACCUMULATOR CHARACTERISTIC DESCRIBING ARRAYS AV,AP,AL
* FOR USE IN SECOND RUN
*

```

```

LS=LS+1
AV(LS)=VTT-VV
AP(LS)=KP
AL(LS)=(KP-KPA(1)+1.E-9)/USL/KPA(1)*VA(1)
LSM=LS
29 CONTINUE

```

```

*
* DETERMINATION OF INITIAL VOLUME FOR SECOND RUN
*

```

```

DO 7 J=1,LSM
IF(AP(J)-STA)8,9,10
10 IF(J.EQ.1)GO TO 9
STB=AV(J-1)+(STA-AP(J-1))*(AV(J)-AV(J-1))/(AP(J)-AP(J-1))
GO TO 11
9 STB=AV(J)
GO TO 11
8 CONTINUE
7 CONTINUE
11 CONTINUE
STB=STB+1.0E-9

```

```

*
WRITE(3,317)
317 FORMAT(/20X,'ACCUMULATOR VOLUME ARRAY '/')
WRITE(3,303)(VA(J),J=1,IN)
WRITE(3,315)
315 FORMAT(/20X,'ACCUMULATOR CHARGE PRESSURES ARRAY KPA')
WRITE(3,305)(KPA(J),J=1,IN)
WRITE(3,314)
314 FORMAT(/20X,'ELEMENTS OF ARRAY AP '/')
WRITE(3,303)(AP(J),J=1,LSM)
WRITE(3,312)
312 FORMAT(/20X,'ELEMENTS OF ARRAY AV '/')
WRITE(3,303)(AV(J),J=1,LSM)
WRITE(3,313)
313 FORMAT(/20X,'ELEMENTS OF ARRAY AL '/')
WRITE(3,303)(AL(J),J=1,LSM)
WRITE(3,316)PCOMP
316 FORMAT(/2X,'COMPENSATED HAULAGE TRIPPING PRESSURE PCOMP=',1F11.1)
WRITE(3,318)YI
318 FORMAT(/2X,'ACCUMULATOR INCREMENT FACTOR YI=',1F11.4)
15 CONTINUE
306 FORMAT(1I10,1E11.3)
303 FORMAT(10E11.3)
305 FORMAT(10I10)

```

*Outputs from
TERMINAL section*

*Programme control and
output statements*

```

*
* OUTPUT ROUTINE
*
TIMER FINTIM=15.0,DELT=0.001,OUTDEL=0.3,PRDEL=0.3
FINISH TH=.11
PRIPLOT THD(TH,TH2D,FBP),PI(TM,TCH,FPUMP),PA(AVOL,TA)
LABEL HAULAGE LOADED WITH CHAIN
END

```

```

RESET
LABEL  HAULAGE LOADED WITH  HYDROSTATIC ABSORBER AND ACCUMULATOR BAN
FINISH TH=.11,RVM=0.0
TIMER FINTIM=15.0,DELT=0.001,OUTDEL=0.3,PRODEL=0.3
PRTPLOT THD(TH,TH2D,FBP),P1(TM,TCH,FPUMP),RPA(RVM,RLL)
PARAMETER KAB=1,TRP=0,TRP1=0,LSWICH=0,KSTOP=0
END
STOP

```

OUTPUT	VARIABLE	SEQUENCE							
PCOMP	STF	VFAC	STX	STA	STY	STZ	SP2	DH	SPOS
STH	STF1	FIV1	FRV1	FX1	PDF	SPDF	APDF	FLIN	F8P
FPUMP	TBP1	FI	FD1	ZZ0010	P1	STF2	FIV2	FRV2	FX2
FD2	ZZ0012	P2	FK4B	RVM	RPL	RPA	TCH	TM	TH2D
THD	TH	TA	PA	ZZ0017	ZZ0015	ZZ0019	ZZ0018	AVOL	RLL
ZZ0020	KH	KHC	KH	KHMAX	ZZ0021	BVMAX	K	DYV	DXV
DYP	DXP	K	KHMAX	KPA1	AB	PATR	RBV	USL	YI
EPOW	CPOW	VTT	AD	VTA	AE	AA	VTA	K	KPMIN
AC	VV	VJ	VJ	VV	LS	LSM	STB	STB	STB

PARAMETERS NOT INPUT OR OUTPUTS NOT AVAILABLE TO SORT SECTION***SET TO ZERO**

LSM STB J KP

OUTPUTS	INPUTS	PARAMS	INTEGS	+	MEM	BLKS	FORTTRAN	DATA	CDS
94(500)	191(1400)	56(400)	6+	0=	6(300)	196(600)		53	

ENDJOB

TERMINAL

*
* TERMINAL SECTION (1)
* ACCUMULATORS SET USING PRESSURE INCREMENT METHOD. REQUIRED PRESSURE
* VOLUME CHARACTERISTIC FOUND FROM RUN 1
*

IF(KAB.NE.0)GO TO 122

*
* INVERSION EXTENSION AND INITIALISATION OF BVOL AND RPA ARRAYS
*

RVMAX=BVOL(KHMAX)

DO 42 J=1,KHMAX

K=KHMAX-J+1

DYV=BVOL(J)

DXV=BVOL(K)

DYP=BPA(J)

DXP=BPA(K)

RVOL(J)=DXV

RVOL(K)=DYV

RPA(J)=DXP

RPA(K)=DYP

K=1

IF(J+J.EQ.KHMAX.OR.J+J+K.EQ.KHMAX)GO TO 46

42 CONTINUE

46 CONTINUE

DO 57 J=1,KHMAX

57 RVOL(J)=RVOL(J)-RVMAX

RVOL(KHMAX+1)=(2000.*6894-RPA(1))*(RVOL(KHMAX)-RVOL(1))/
(RPA(KHMAX)-RPA(1))

RPA(KHMAX+1)=2000.*6894

KHMAX=KHMAX+1

WRITE(3,311)

311 FORMAT(/20X,'ELEMENTS OF ARRAY BVOL'/)

WRITE(3,303)(RVOL(J),J=1,KHMAX)

WRITE(3,310)

310 FORMAT(/20X,'ELEMENTS OF ARRAY BPA '/)

WRITE(3,303)(RPA(J),J=1,KHMAX)

*
* ACCUMULATOR PRE-CHARGE SETTING PROCEDURE
*

PARAMETER IN=9,POWC=1.45,KR=50000

CPOW=1.0/POWC

DO 43 J=1,IN

VTT=VTT+VA(J)

43 KPA(J)=RPA(KHMAX)

VA(IN+1)=0.0

VTF=VTT

KPA(1)=RPA(1)

KPX=KPA(1)

KPMAX=RPA(KHMAX)

*
* ACCUMULATOR PRE-CHARGE SETTING LOOP
*

DO 44 IZ=1,IN

VTF=VTF-VA(IZ)

*

*This TERMINAL section is
used in the place of TERMINAL
sections 2 or 3.*

```

* PRESSURE INCREMENT LOOP
*
  DO 45 KP=KPX,KPMAX,KR
  AC=KP
  VV=0.0
*
* LINEAR INTERPOLATION OF BVOL AND BPA ARRAYS TO FIND REQUIRED VOLUME AT
* PRESSURE KP
*
  DO 49 J=1,KHMAX
  IF (BPA(J)-AC) 50,51,52
52 VLINE=VTT-BVOL(J-1)-(AC-BPA(J-1))*(BVOL(J)-BVOL(J-1))/
  (BPA(J)-BPA(J-1))
  GO TO 48
51 VLINE=VTT-BVOL(J)
  GO TO 48
50 CONTINUE
49 CONTINUE
48 CONTINUE
*
* VOLUME ADDITION LOOP
*
  DO 53 K=1,IZ
  AA=KPA(K)
  VV=VV+VA(K)*(AA/KP)**CPOW
53 CONTINUE
  VV=VV+VTF
*
* ACCUMULATOR PRE-CHARGE SETTING CRITERIA
*
  IF (VV.GT.VLINE) GO TO 60
*
* SETTING OF ACCUMULATOR CHARACTERISTIC DESCRIBING ARRAYS AV,AP,AL
* FOR USE IN SECOND RUN
*
  IF (LP.EQ.KP) GO TO 59
  LS=LS+1
  AL(LS)=VTT-VLINE
  AV(LS)=VTT-VV
  AP(LS)=KP
  LSM=LS
59 LP=KP
45 CONTINUE
60 IA=IZ+1
  KPA(IA)=KP-KR
44 KPX=KPA(IA)

```

1
*
*
*

DETERMINATION OF INITIAL VOLUME FOR SECOND RUN

```
DO 7 J=1,LSM
  IF(AP(J)-STA)8,9,10
10 STB=AV(J-1)+(STA-AP(J-1))*(AV(J)-AV(J-1))/(AP(J)-AP(J-1))
  GO TO 11
  9 STB=AV(J)
  GO TO 11
  8 CONTINUE
  7 CONTINUE
11 CONTINUE
  STB=STB+1.0E-9
303 FORMAT(10E11.3)
305 FORMAT(10I10)
  WRITE(3,317)
317 FORMAT('//20X,'ACCUMULATOR VOLUME ARRAY  '/')
  WRITE(3,303)(VA(J),J=1,IN)
  WRITE(3,315)
315 FORMAT('//20X,'ACCUMULATOR CHARGE PRESSURES ARRAY KPA'/)
  WRITE(3,305)(KPA(J),J=1,IN)
  WRITE(3,312)
312 FORMAT('//20X,'ELEMENTS OF ARRAY AV  '/')
  WRITE(3,303)(AV(J),J=1,LSM)
  WRITE(3,313)
313 FORMAT('//20X,'ELEMENTS OF ARRAY AL  '/')
  WRITE(3,303)(AL(J),J=1,LSM)
  WRITE(3,314)
314 FORMAT('//20X,'ELEMENTS OF ARRAY AP  '/')
  WRITE(3,303)(AP(J),J=1,LSM)
122 CONTINUE
```


	MINIMUM -3.7853E-01		THD	VERSUS TIME	MAXIMUM 5.0897E-01				
TIME	THD	I			I	TH	TH2D	FBP	
0.0	5.0892E-01	-----+				1.5000E 00	8.5331E-03	0.0	
3.0000E-01	5.0673E-01	-----+				1.6522E 00	1.6563E-02	0.0	
6.0000E-01	5.0451E-01	-----+				1.8038E 00	1.7873E-02	0.0	
9.0000E-01	5.0230E-01	-----+				1.9546E 00	1.9219E-02	0.0	
1.2000E 00	5.0009E-01	-----+				2.1049E 00	2.0558E-02	0.0	
1.5000E 00	4.9790E-01	-----+				2.2544E 00	2.1855E-02	0.0	
1.8000E 00	4.9572E-01	-----+				2.4033E 00	2.3181E-02	0.0	
2.1000E 00	2.2349E-01	-----+				2.5434E 00	-3.7644E 00	9.5959E-04	
2.4000E 00	-1.9544E-02	-----+				2.5511E 00	-3.6224E-01	1.2147E-03	
2.7000E 00	-1.7316E-01	-----+				2.5224E 00	-4.9684E-01	1.1809E-03	
3.0000E 00	-3.3113E-01	---+				2.4469E 00	-4.8342E-01	1.1612E-03	
3.3000E 00	-3.7692E-01	+				2.3359E 00	6.5596E-02	1.2333E-03	
3.6000E 00	-3.6699E-01	+				2.2241E 00	7.1302E-02	1.2023E-03	
3.9000E 00	-3.5678E-01	--				2.1154E 00	6.9905E-02	1.1703E-03	
4.2000E 00	-3.4664E-01	--				2.0098E 00	6.8431E-02	1.1387E-03	
4.5000E 00	-3.3674E-01	---+				1.9072E 00	6.5333E-02	1.1071E-03	
4.8000E 00	-3.2735E-01	---+				1.8074E 00	6.2546E-02	1.0774E-03	
5.1000E 00	-3.1805E-01	---+				1.7105E 00	6.2458E-02	1.0485E-03	
5.4000E 00	-3.0871E-01	---+				1.6164E 00	6.2308E-02	1.0193E-03	
5.7000E 00	-2.9912E-01	---+				1.5251E 00	1.2127E-01	1.0025E-03	
6.0000E 00	-2.8978E-01	---+				1.4366E 00	1.2074E-01	9.7336E-04	
6.3000E 00	-2.8047E-01	---+				1.3510E 00	1.2070E-01	9.4434E-04	
6.6000E 00	-2.7124E-01	---+				1.2681E 00	1.2011E-01	9.1530E-04	
6.9000E 00	-2.6207E-01	---+				1.1880E 00	1.2238E-01	8.8756E-04	
7.2000E 00	-2.5293E-01	---+				1.1106E 00	1.2573E-01	8.5998E-04	
7.5000E 00	-2.4380E-01	---+				1.0360E 00	1.2940E-01	8.3250E-04	
7.8000E 00	-2.3473E-01	---+				9.6418E-01	1.3334E-01	8.0525E-04	
8.1000E 00	-2.2573E-01	---+				8.9511E-01	1.3759E-01	7.7833E-04	
8.4000E 00	-2.1685E-01	---+				8.2873E-01	1.4210E-01	7.5182E-04	
8.7000E 00	-2.0808E-01	---+				7.6499E-01	1.4665E-01	7.2573E-04	
9.0000E 00	-1.9949E-01	---+				7.0386E-01	9.3080E-02	6.8299E-04	
9.3000E 00	-1.9105E-01	---+				6.4528E-01	1.0115E-01	6.5859E-04	
9.6000E 00	-1.8276E-01	---+				5.8922E-01	1.0711E-01	6.3421E-04	
9.9000E 00	-1.7471E-01	---+				5.3561E-01	1.1064E-01	6.0973E-04	
1.0200E 01	-1.6683E-01	---+				4.8438E-01	1.1276E-01	5.8548E-04	
1.0500E 01	-1.5911E-01	---+				4.3550E-01	1.1335E-01	5.6145E-04	
1.0800E 01	-1.5176E-01	---+				3.8888E-01	1.1463E-01	5.3783E-04	
1.1100E 01	-1.4464E-01	---+				3.4442E-01	1.1335E-01	5.1377E-04	
1.1400E 01	-1.3780E-01	---+				3.0206E-01	1.1267E-01	4.9104E-04	
1.1700E 01	-1.3113E-01	---+				2.6173E-01	1.1260E-01	4.6960E-04	
1.2000E 01	-1.2467E-01	---+				2.2337E-01	1.1245E-01	4.4918E-04	
1.2300E 01	-1.1867E-01	---+				1.8688E-01	1.1438E-01	4.3048E-04	
1.2600E 01	-1.1289E-01	---+				1.5215E-01	1.1710E-01	4.1298E-04	
1.2900E 01	-1.0729E-01	---+				1.1913E-01	1.1974E-01	3.9644E-04	
1.2986E 01	-1.0572E-01	---+				1.0997E-01	1.1968E-01	3.9224E-04	

listing of PRINTPLOT output
from DYNAMIC section of a
typical run

HAULAGE LOADED WITH CHAIN

PAGE 1

	MINIMUM		P1	VERSUS TIME	MAXIMUM				
	8.8103E 05				8.6190E 06				
TIME	P1	I			I	TM	TCH	FPUMP	
0.0	6.2349E 06	06	-----+			1.7895E 04	1.7855E 04	1.9320E-03	
3.0000E-01	6.5647E 06	06	-----+			1.9095E 04	1.9017E 04	1.9320E-03	
6.0000E-01	6.9224E 06	06	-----+			2.0258E 04	2.0174E 04	1.9320E-03	
9.0000E-01	7.2786E 06	06	-----+			2.1417E 04	2.1326E 04	1.9320E-03	
1.2000E 00	7.6332E 06	06	-----+			2.2570E 04	2.2473E 04	1.9320E-03	
1.5000E 00	7.9862E 06	06	-----+			2.3718E 04	2.3616E 04	1.9320E-03	
1.8000E 00	8.3377E 06	06	-----+			2.4861E 04	2.4753E 04	1.9320E-03	
2.1000E 00	3.1409E 06	06	-----+			8.1292E 03	2.5822E 04	1.8190E-03	
2.4000E 00	4.6303E 06	06	-----+			1.9297E 04	2.0999E 04	1.2394E-03	
2.7000E 00	4.4288E 06	06	-----+			1.8461E 04	2.0796E 04	6.5978E-04	
3.0000E 00	4.3132E 06	06	-----+			1.7980E 04	2.0252E 04	8.0180E-05	
3.3000E 00	4.7421E 06	06	-----+			1.9764E 04	1.9455E 04	0.0	
3.6000E 00	4.5558E 06	06	-----+			1.8989E 04	1.8654E 04	0.0	
3.9000E 00	4.3668E 06	06	-----+			1.8203E 04	1.7874E 04	0.0	
4.2000E 00	4.1830E 06	06	-----+			1.7438E 04	1.7116E 04	0.0	
4.5000E 00	4.0034E 06	06	-----+			1.6687E 04	1.6380E 04	0.0	
4.8000E 00	3.8285E 06	06	-----+			1.5959E 04	1.5665E 04	0.0	
5.1000E 00	3.6608E 06	06	-----+			1.5263E 04	1.4970E 04	0.0	
5.4000E 00	3.4979E 06	06	-----+			1.4587E 04	1.4294E 04	0.0	
5.7000E 00	3.3232E 06	06	-----+			1.4210E 04	1.3640E 04	0.0	
6.0000E 00	3.1731E 06	06	-----+			1.3573E 04	1.3005E 04	0.0	
6.3000E 00	3.0280E 06	06	-----+			1.2958E 04	1.2391E 04	0.0	
6.6000E 00	2.8881E 06	06	-----+			1.2361E 04	1.1796E 04	0.0	
6.9000E 00	2.7507E 06	06	-----+			1.1797E 04	1.1222E 04	0.0	
7.2000E 00	2.6174E 06	06	-----+			1.1258E 04	1.0667E 04	0.0	
7.5000E 00	2.4883E 06	06	-----+			1.0740E 04	1.0131E 04	0.0	
7.8000E 00	2.3635E 06	06	-----+			1.0243E 04	9.6161E 03	0.0	
8.1000E 00	2.2431E 06	06	-----+			9.7673E 03	9.1207E 03	0.0	
8.4000E 00	2.1268E 06	06	-----+			9.3124E 03	8.6445E 03	0.0	
8.7000E 00	2.0148E 06	06	-----+			8.8766E 03	8.1873E 03	0.0	
9.0000E 00	1.9027E 06	06	-----+			8.1863E 03	7.7488E 03	0.0	
9.3000E 00	1.8131E 06	06	-----+			7.8040E 03	7.3287E 03	0.0	
9.6000E 00	1.7209E 06	06	-----+			7.4299E 03	6.9265E 03	0.0	
9.9000E 00	1.6278E 06	06	-----+			7.0620E 03	6.5419E 03	0.0	
1.0200E 01	1.5362E 06	06	-----+			6.7045E 03	6.1745E 03	0.0	
1.0500E 01	1.4474E 06	06	-----+			6.3566E 03	5.8239E 03	0.0	
1.0800E 01	1.3658E 06	06	-----+			6.0282E 03	5.4895E 03	0.0	
1.1100E 01	1.2894E 06	06	-----+			5.7033E 03	5.1706E 03	0.0	
1.1400E 01	1.2173E 06	06	-----+			5.3962E 03	4.8667E 03	0.0	
1.1700E 01	1.1471E 06	06	-----+			5.1066E 03	4.5774E 03	0.0	
1.2000E 01	1.0781E 06	06	-----+			4.8307E 03	4.3022E 03	0.0	
1.2300E 01	1.0178E 06	06	-----+			4.5781E 03	4.0405E 03	0.0	
1.2600E 01	9.5813E 05	05	-----+			4.3417E 03	3.7914E 03	0.0	
1.2900E 01	8.9903E 05	05	-----+			4.1173E 03	3.5545E 03	0.0	
1.2986E 01	8.8103E 05	05	-----+			4.0513E 03	3.4888E 03	0.0	

HAULAGE LOADED WITH CHAIN

PAGE 1

TIME	PA	MINIMUM		PA	VERSUS TIME	MAXIMUM		I	AVOL	TA
		2.2449E 06	I			9.9259E 06	I			
0.0	7.0320E 06		-----+						0.0	1.7855E 04
3.0000E-01	7.4541E 06		-----+						3.3978E-04	1.9018E 04
6.0000E-01	7.8742E 06		-----+						6.7567E-04	2.0175E 04
9.0000E-01	8.2924E 06		-----+						1.0077E-03	2.1327E 04
1.2000E 00	8.7088E 06		-----+						1.3359E-03	2.2474E 04
1.5000E 00	9.1234E 06		-----+						1.6603E-03	2.3616E 04
1.8000E 00	9.5361E 06		-----+						1.9809E-03	2.4753E 04
2.1000E 00	9.8677E 06		-----+						2.2765E-03	2.5667E 04
2.4000E 00	9.0028E 06		-----+						2.2312E-03	2.0984E 04
2.7000E 00	8.9222E 06		-----+						2.0944E-03	2.0776E 04
3.0000E 00	8.7121E 06		-----+						1.8355E-03	2.0232E 04
3.3000E 00	8.4131E 06		-----+						1.4867E-03	1.9458E 04
3.6000E 00	8.1035E 06		-----+						1.1376E-03	1.8657E 04
3.9000E 00	7.8023E 06		-----+						7.9797E-04	1.7877E 04
4.2000E 00	7.5095E 06		-----+						4.6775E-04	1.7119E 04
4.5000E 00	7.2250E 06		-----+						1.4679E-04	1.6383E 04
4.8000E 00	6.9485E 06		-----+						-1.6520E-04	1.5667E 04
5.1000E 00	6.6799E 06		-----+						-4.6854E-04	1.4972E 04
5.4000E 00	6.4190E 06		-----+						-7.6328E-04	1.4297E 04
5.7000E 00	6.1669E 06		-----+						-1.0493E-03	1.3645E 04
6.0000E 00	5.9218E 06		-----+						-1.3267E-03	1.3010E 04
6.3000E 00	5.6844E 06		-----+						-1.5957E-03	1.2396E 04
6.6000E 00	5.4547E 06		-----+						-1.8563E-03	1.1801E 04
6.9000E 00	5.2327E 06		-----+						-2.1085E-03	1.1227E 04
7.2000E 00	5.0183E 06		-----+						-2.3519E-03	1.0672E 04
7.5000E 00	4.8116E 06		-----+						-2.5867E-03	1.0137E 04
7.8000E 00	4.6125E 06		-----+						-2.8128E-03	9.6216E 03
8.1000E 00	4.4212E 06		-----+						-3.0304E-03	9.1263E 03
8.4000E 00	4.2373E 06		-----+						-3.2396E-03	8.6504E 03
8.7000E 00	4.0607E 06		-----+						-3.4406E-03	8.1934E 03
9.0000E 00	3.8904E 06		-----+						-3.6335E-03	7.7527E 03
9.3000E 00	3.7282E 06		-----+						-3.8186E-03	7.3328E 03
9.6000E 00	3.5729E 06		-----+						-3.9956E-03	6.9309E 03
9.9000E 00	3.4244E 06		-----+						-4.1649E-03	6.5465E 03
1.0200E 01	3.2825E 06		-----+						-4.3270E-03	6.1791E 03
1.0500E 01	3.1470E 06		-----+						-4.4819E-03	5.8285E 03
1.0800E 01	3.0178E 06		-----+						-4.6299E-03	5.4942E 03
1.1100E 01	2.8946E 06		-----+						-4.7713E-03	5.1752E 03
1.1400E 01	2.7772E 06		-----+						-4.9064E-03	4.8713E 03
1.1700E 01	2.6654E 06		---+						-5.0354E-03	4.5820E 03
1.2000E 01	2.5591E 06		---+						-5.1585E-03	4.3069E 03
1.2300E 01	2.4580E 06		--+						-5.2758E-03	4.0452E 03
1.2600E 01	2.3618E 06		+						-5.3879E-03	3.7962E 03
1.2900E 01	2.2703E 06		+						-5.4947E-03	3.5595E 03
1.2986E 01	2.2449E 06		+						-5.5243E-03	3.4938E 03

TIME	MINIMUM -3.7249E-01		THD I	VERSUS TIME	MAXIMUM 5.0898E-01	TH	TH2D	FBP
	THD	I						
0.0	5.0892E-01	-----+				1.5000E 00	8.4622E-03	0.0
3.0000E-01	5.0727E-01	-----+				1.6523E 00	1.7542E-02	0.0
6.0000E-01	5.0574E-01	-----+				1.8041E 00	1.9672E-02	0.0
9.0000E-01	5.0429E-01	-----+				1.9555E 00	2.0260E-02	0.0
1.2000E 00	5.0277E-01	-----+				2.1064E 00	2.0850E-02	0.0
1.5000E 00	5.0116E-01	-----+				2.2568E 00	2.1532E-02	0.0
1.8000E 00	4.9947E-01	-----+				2.4068E 00	2.2226E-02	0.0
2.1000E 00	-5.5238E-04	-----+				2.4851E 00	7.3538E-01	1.4069E-03
2.4000E 00	-9.0850E-02	-----+				2.4765E 00	-4.8617E-01	1.1770E-03
2.7000E 00	-2.4849E-01	-----+				2.4254E 00	-4.8604E-01	1.1562E-03
3.0000E 00	-3.7122E-01	+				2.3288E 00	-1.7096E-02	1.2152E-03
3.3000E 00	-3.6603E-01	+				2.2176E 00	7.0090E-02	1.1993E-03
3.6000E 00	-3.5621E-01	+				2.1091E 00	6.7308E-02	1.1686E-03
3.9000E 00	-3.4703E-01	--+				2.0035E 00	6.4981E-02	1.1398E-03
4.2000E 00	-3.3693E-01	---+				1.9008E 00	6.7929E-02	1.1076E-03
4.5000E 00	-3.2699E-01	---+				1.8011E 00	6.2947E-02	1.0763E-03
4.8000E 00	-3.1781E-01	---+				1.7043E 00	6.0774E-02	1.0478E-03
5.1000E 00	-3.0915E-01	---+				1.6101E 00	5.8994E-02	1.0207E-03
5.4000E 00	-3.0070E-01	----+				1.5185E 00	1.1911E-01	1.0074E-03
5.7000E 00	-2.9058E-01	----+				1.4297E 00	1.2302E-01	9.7587E-04
6.0000E 00	-2.8072E-01	-----+				1.3439E 00	1.2062E-01	9.4513E-04
6.3000E 00	-2.7154E-01	-----+				1.2610E 00	1.1801E-01	9.1635E-04
6.6000E 00	-2.6308E-01	-----+				1.1807E 00	1.1620E-01	8.9061E-04
6.9000E 00	-2.5512E-01	-----+				1.1028E 00	1.1934E-01	8.6661E-04
7.2000E 00	-2.4665E-01	-----+				1.0274E 00	1.3028E-01	8.4107E-04
7.5000E 00	-2.3645E-01	-----+				9.5488E-01	1.3480E-01	8.1043E-04
7.8000E 00	-2.2689E-01	-----+				8.8540E-01	1.3693E-01	7.8180E-04
8.1000E 00	-2.1810E-01	-----+				8.1867E-01	1.3916E-01	7.5556E-04
8.4000E 00	-2.0998E-01	-----+				7.5448E-01	1.4155E-01	7.3140E-04
8.7000E 00	-2.0252E-01	-----+				6.9262E-01	9.2186E-02	6.9380E-04
9.0000E 00	-1.9557E-01	-----+				6.3293E-01	1.2723E-01	6.8265E-04
9.3000E 00	-1.8857E-01	-----+				5.7526E-01	1.4029E-01	6.6225E-04
9.6000E 00	-1.7894E-01	-----+				5.2013E-01	1.1304E-01	6.2273E-04
9.9000E 00	-1.6991E-01	-----+				4.6783E-01	1.1379E-01	5.9494E-04
1.0200E 01	-1.6169E-01	-----+				4.1811E-01	1.1287E-01	5.6954E-04
1.0500E 01	-1.5433E-01	-----+				3.7073E-01	1.1208E-01	5.4627E-04
1.0800E 01	-1.4772E-01	-----+				3.2345E-01	1.1066E-01	5.2405E-04
1.1100E 01	-1.4169E-01	-----+				2.8205E-01	1.0874E-01	5.0379E-04
1.1400E 01	-1.3611E-01	-----+				2.4040E-01	1.0732E-01	4.8554E-04
1.1700E 01	-1.3096E-01	-----+				2.0035E-01	1.0646E-01	4.6906E-04
1.2000E 01	-1.2617E-01	-----+				1.6179E-01	1.0587E-01	4.5400E-04
1.2300E 01	-1.2170E-01	-----+				1.2461E-01	1.0877E-01	4.3984E-04
1.2422E 01	-1.1960E-01	-----+				1.0989E-01	1.1132E-01	4.3333E-04

	MINIMUM	P1	VERSUS TIME	MAXIMUM			
	4.6551E 05			7.8195E 06			
TIME	P1	I		I	TM	TCH	FPUMP
0.0	6.2349E 06	-----+			1.7895E 04	1.7854E 04	1.9320E-03
3.0000E-01	6.4810E 06	-----+			1.8822E 04	1.8739E 04	1.9320E-03
6.0000E-01	6.7291E 06	-----+			1.9629E 04	1.9536E 04	1.9320E-03
9.0000E-01	6.9615E 06	-----+			2.0385E 04	2.0289E 04	1.9320E-03
1.2000E 00	7.2062E 06	-----+			2.1181E 04	2.1082E 04	1.9320E-03
1.5000E 00	7.4641E 06	-----+			2.2020E 04	2.1918E 04	1.9320E-03
1.8000E 00	7.7360E 06	-----+			2.2904E 04	2.2799E 04	1.9320E-03
2.1000E 00	5.8590E 06	-----+			2.4385E 04	2.0898E 04	1.5253E-03
2.4000E 00	4.4056E 06	-----+			1.8364E 04	2.0669E 04	9.4571E-04
2.7000E 00	4.2840E 06	-----+			1.7858E 04	2.0163E 04	3.6611E-04
3.0000E 00	4.6326E 06	-----+			1.9310E 04	1.9391E 04	0.0
3.3000E 00	4.5378E 06	-----+			1.8914E 04	1.8582E 04	0.0
3.6000E 00	4.3564E 06	-----+			1.8159E 04	1.7840E 04	0.0
3.9000E 00	4.1891E 06	-----+			1.7464E 04	1.7156E 04	0.0
4.2000E 00	4.0061E 06	-----+			1.6699E 04	1.6377E 04	0.0
4.5000E 00	3.8218E 06	-----+			1.5931E 04	1.5633E 04	0.0
4.8000E 00	3.6565E 06	-----+			1.5245E 04	1.4957E 04	0.0
5.1000E 00	3.5055E 06	-----+			1.4619E 04	1.4339E 04	0.0
5.4000E 00	3.3489E 06	-----+			1.4318E 04	1.3754E 04	0.0
5.7000E 00	3.1859E 06	-----+			1.3627E 04	1.3043E 04	0.0
6.0000E 00	3.0318E 06	-----+			1.2974E 04	1.2402E 04	0.0
6.3000E 00	2.8932E 06	-----+			1.2382E 04	1.1823E 04	0.0
6.6000E 00	2.7655E 06	-----+			1.1858E 04	1.1297E 04	0.0
6.9000E 00	2.6488E 06	-----+			1.1385E 04	1.0819E 04	0.0
7.2000E 00	2.5282E 06	-----+			1.0899E 04	1.0281E 04	0.0
7.5000E 00	2.3871E 06	-----+			1.0336E 04	9.6968E 03	0.0
7.8000E 00	2.2585E 06	-----+			9.8278E 03	9.1785E 03	0.0
8.1000E 00	2.1430E 06	-----+			9.3758E 03	8.7160E 03	0.0
8.4000E 00	2.0388E 06	-----+			8.9704E 03	8.2993E 03	0.0
8.7000E 00	1.9518E 06	-----+			8.3583E 03	7.9213E 03	0.0
9.0000E 00	1.8770E 06	-----+			8.1808E 03	7.5776E 03	0.0
9.3000E 00	1.7935E 06	-----+			7.8609E 03	7.1957E 03	0.0
9.6000E 00	1.6774E 06	-----+			7.2565E 03	6.7205E 03	0.0
9.9000E 00	1.5722E 06	-----+			6.8431E 03	6.3036E 03	0.0
1.0200E 01	1.4768E 06	-----+			6.4730E 03	5.9379E 03	0.0
1.0500E 01	1.3940E 06	-----+			6.1423E 03	5.6109E 03	0.0
1.0800E 01	1.3218E 06	-----+			5.8421E 03	5.3174E 03	0.0
1.1100E 01	1.2580E 06	-----+			5.5684E 03	5.0528E 03	0.0
1.1400E 01	1.1995E 06	-----+			5.3219E 03	4.8131E 03	0.0
1.1700E 01	1.1452E 06	-----+			5.0993E 03	4.5945E 03	0.0
1.2000E 01	1.0942E 06	-----+			4.8958E 03	4.3939E 03	0.0
1.2300E 01	1.0484E 06	-----+			4.7045E 03	4.1888E 03	0.0
1.2422E 01	1.0272E 06	-----+			4.6166E 03	4.0888E 03	0.0

	MINIMUM		RPA	VERSUS TIME		MAXIMUM		
	2.4748E 06					8.9836E 06		
TIME	RPA	I				I	RVM	RLL
0.0	7.0319E 06	06	-----	-----	-----		6.0025E-03	7.2053E 06
3.0000E-01	7.3531E 06	06	-----	-----	-----		6.3422E-03	7.5034E 06
6.0000E-01	7.6423E 06	06	-----	-----	-----		6.6790E-03	7.7990E 06
9.0000E-01	7.9156E 06	06	-----	-----	-----		7.0133E-03	8.0923E 06
1.2000E 00	8.2035E 06	06	-----	-----	-----		7.3451E-03	8.3835E 06
1.5000E 00	8.5068E 06	06	-----	-----	-----		7.6741E-03	8.6722E 06
1.8000E 00	8.8257E 06	06	-----	-----	-----		8.0003E-03	8.9584E 06
2.1000E 00	8.9697E 06	06	-----	-----	-----		8.1396E-03	9.0806E 06
2.4000E 00	8.8811E 06	06	-----	-----	-----		8.0537E-03	9.0053E 06
2.7000E 00	8.6854E 06	06	-----	-----	-----		7.8586E-03	8.8341E 06
3.0000E 00	8.3872E 06	06	-----	-----	-----		7.5467E-03	8.5604E 06
3.3000E 00	8.0745E 06	06	-----	-----	-----		7.1989E-03	8.2552E 06
3.6000E 00	7.7880E 06	06	-----	-----	-----		6.8595E-03	7.9574E 06
3.9000E 00	7.5235E 06	06	-----	-----	-----		6.5290E-03	7.6674E 06
4.2000E 00	7.2225E 06	06	-----	-----	-----		6.2072E-03	7.3850E 06
4.5000E 00	6.9351E 06	06	-----	-----	-----		5.8949E-03	7.1109E 06
4.8000E 00	6.6741E 06	06	-----	-----	-----		5.5914E-03	6.8446E 06
5.1000E 00	6.4353E 06	06	-----	-----	-----		5.2960E-03	6.5854E 06
5.4000E 00	6.2091E 06	06	-----	-----	-----		5.0085E-03	6.3332E 06
5.7000E 00	5.9346E 06	06	-----	-----	-----		4.7294E-03	6.0882E 06
6.0000E 00	5.6870E 06	06	-----	-----	-----		4.4595E-03	5.8514E 06
6.3000E 00	5.4631E 06	06	-----	-----	-----		4.1982E-03	5.6221E 06
6.6000E 00	5.2600E 06	06	-----	-----	-----		3.9449E-03	5.3998E 06
6.9000E 00	5.0754E 06	06	-----	-----	-----		3.6998E-03	5.1847E 06
7.2000E 00	4.8675E 06	06	-----	-----	-----		3.4624E-03	4.9764E 06
7.5000E 00	4.6416E 06	06	-----	-----	-----		3.2341E-03	4.7761E 06
7.8000E 00	4.4414E 06	06	-----	-----	-----		3.0151E-03	4.5840E 06
8.1000E 00	4.2626E 06	06	-----	-----	-----		2.8048E-03	4.3994E 06
8.4000E 00	4.1016E 06	06	-----	-----	-----		2.6023E-03	4.2217E 06
8.7000E 00	3.9556E 06	06	-----	-----	-----		2.4070E-03	4.0503E 06
9.0000E 00	3.8228E 06	06	-----	-----	-----		2.2184E-03	3.8848E 06
9.3000E 00	3.6753E 06	06	-----	-----	-----		2.0360E-03	3.7248E 06
9.6000E 00	3.4916E 06	06	-----	-----	-----		1.8615E-03	3.5717E 06
9.9000E 00	3.3306E 06	06	-----	-----	-----		1.6957E-03	3.4262E 06
1.0200E 01	3.1892E 06	06	-----	-----	-----		1.5377E-03	3.2875E 06
1.0500E 01	3.0629E 06	06	-----	-----	-----		1.3868E-03	3.1551E 06
1.0800E 01	2.9495E 06	06	-----	-----	-----		1.2422E-03	3.0282E 06
1.1100E 01	2.8473E 06	06	-----	-----	-----		1.1033E-03	2.9064E 06
1.1400E 01	2.7547E 06	06	-----	-----	-----		9.6974E-04	2.7891E 06
1.1700E 01	2.6702E 06	06	-----	-----	-----		8.4097E-04	2.6762E 06
1.2000E 01	2.5927E 06	06	-----	-----	-----		7.1668E-04	2.5671E 06
1.2300E 01	2.5134E 06	06	-----	-----	-----		5.9652E-04	2.4617E 06
1.2422E 01	2.4748E 06	06	-----	-----	-----		5.4889E-04	2.4199E 06

ELEMENTS OF ARRAY BVOL

0.0	0.859E-05	0.173E-04	0.259E-04	0.346E-04	0.434E-04	0.521E-04	0.610E-04	0.698E-04	0.787E-04
0.877E-04	0.966E-04	0.106E-03	0.115E-03	0.124E-03	0.133E-03	0.142E-03	0.151E-03	0.160E-03	0.170E-03
0.179E-03	0.188E-03	0.198E-03	0.207E-03	0.217E-03	0.226E-03	0.236E-03	0.245E-03	0.255E-03	0.264E-03
0.274E-03	0.284E-03	0.293E-03	0.303E-03	0.313E-03	0.323E-03	0.333E-03	0.343E-03	0.353E-03	0.363E-03
0.373E-03	0.383E-03	0.393E-03	0.403E-03	0.413E-03	0.423E-03	0.434E-03	0.444E-03	0.454E-03	0.465E-03
0.475E-03	0.486E-03	0.496E-03	0.507E-03	0.518E-03	0.528E-03	0.539E-03	0.550E-03	0.560E-03	0.571E-03
0.582E-03	0.593E-03	0.604E-03	0.615E-03	0.626E-03	0.637E-03	0.648E-03	0.659E-03	0.671E-03	0.682E-03
0.693E-03	0.704E-03	0.716E-03	0.727E-03	0.739E-03	0.750E-03	0.762E-03	0.773E-03	0.785E-03	0.797E-03
0.808E-03	0.820E-03	0.832E-03	0.844E-03	0.856E-03	0.868E-03	0.880E-03	0.892E-03	0.904E-03	0.916E-03
0.928E-03	0.941E-03	0.953E-03	0.965E-03	0.978E-03	0.990E-03	0.100E-02	0.101E-02	0.103E-02	0.104E-02
0.105E-02	0.107E-02	0.108E-02	0.109E-02	0.110E-02	0.112E-02	0.113E-02	0.114E-02	0.116E-02	0.117E-02
0.118E-02	0.120E-02	0.121E-02	0.122E-02	0.124E-02	0.125E-02	0.126E-02	0.128E-02	0.129E-02	0.130E-02
0.132E-02	0.133E-02	0.134E-02	0.136E-02	0.137E-02	0.139E-02	0.140E-02	0.141E-02	0.143E-02	0.144E-02
0.146E-02	0.147E-02	0.148E-02	0.150E-02	0.151E-02	0.153E-02	0.154E-02	0.156E-02	0.157E-02	0.159E-02
0.160E-02	0.161E-02	0.163E-02	0.164E-02	0.166E-02	0.167E-02	0.169E-02	0.170E-02	0.172E-02	0.173E-02
0.175E-02	0.177E-02	0.178E-02	0.180E-02	0.181E-02	0.183E-02	0.184E-02	0.186E-02	0.187E-02	0.189E-02
0.191E-02	0.192E-02	0.194E-02	0.195E-02	0.197E-02	0.199E-02	0.200E-02	0.202E-02	0.203E-02	0.205E-02
0.207E-02	0.208E-02	0.210E-02	0.212E-02	0.213E-02	0.215E-02	0.217E-02	0.218E-02	0.220E-02	0.222E-02
0.223E-02	0.225E-02	0.227E-02	0.228E-02	0.230E-02	0.232E-02	0.234E-02	0.235E-02	0.237E-02	0.239E-02
0.241E-02	0.242E-02	0.244E-02	0.246E-02	0.248E-02	0.249E-02	0.251E-02	0.253E-02	0.255E-02	0.257E-02
0.258E-02	0.260E-02	0.262E-02	0.264E-02	0.266E-02	0.267E-02	0.269E-02	0.271E-02	0.273E-02	0.275E-02
0.277E-02	0.279E-02	0.280E-02	0.282E-02	0.284E-02	0.286E-02	0.288E-02	0.290E-02	0.292E-02	0.294E-02
0.296E-02	0.298E-02	0.300E-02	0.301E-02	0.303E-02	0.305E-02	0.307E-02	0.309E-02	0.311E-02	0.313E-02
0.315E-02	0.317E-02	0.319E-02	0.321E-02	0.323E-02	0.325E-02	0.327E-02	0.329E-02	0.331E-02	0.333E-02
0.335E-02	0.337E-02	0.340E-02	0.342E-02	0.344E-02	0.346E-02	0.348E-02	0.350E-02	0.352E-02	0.354E-02
0.356E-02	0.358E-02	0.360E-02	0.363E-02	0.365E-02	0.367E-02	0.369E-02	0.371E-02	0.373E-02	0.375E-02
0.378E-02	0.380E-02	0.382E-02	0.384E-02	0.386E-02	0.388E-02	0.391E-02	0.393E-02	0.395E-02	0.397E-02
0.400E-02	0.402E-02	0.404E-02	0.406E-02	0.409E-02	0.411E-02	0.413E-02	0.415E-02	0.418E-02	0.420E-02
0.422E-02	0.424E-02	0.427E-02	0.429E-02	0.431E-02	0.434E-02	0.436E-02	0.438E-02	0.441E-02	0.443E-02
0.445E-02	0.448E-02	0.450E-02	0.452E-02	0.455E-02	0.457E-02	0.459E-02	0.462E-02	0.464E-02	0.467E-02
0.469E-02	0.471E-02	0.474E-02	0.476E-02	0.479E-02	0.481E-02	0.484E-02	0.486E-02	0.488E-02	0.491E-02
0.493E-02	0.496E-02	0.498E-02	0.501E-02	0.503E-02	0.506E-02	0.508E-02	0.511E-02	0.513E-02	0.516E-02
0.518E-02	0.521E-02	0.523E-02	0.526E-02	0.528E-02	0.531E-02	0.534E-02	0.536E-02	0.539E-02	0.541E-02
0.544E-02	0.546E-02	0.549E-02	0.552E-02	0.554E-02	0.557E-02	0.559E-02	0.131E-01		

Listing of outputs
from the TERMINAL
section

ELEMENTS OF ARRAY BPA

0.225E 07	0.226E 07	0.227E 07	0.227E 07	0.228E 07	0.229E 07	0.230E 07	0.230E 07	0.231E 07	0.232E 07
0.233E 07	0.233E 07	0.234E 07	0.235E 07	0.236E 07	0.237E 07	0.237E 07	0.238E 07	0.239E 07	0.240E 07
0.241E 07	0.241E 07	0.242E 07	0.243E 07	0.244E 07	0.245E 07	0.245E 07	0.246E 07	0.247E 07	0.248E 07
0.249E 07	0.250E 07	0.250E 07	0.251E 07	0.252E 07	0.253E 07	0.254E 07	0.255E 07	0.256E 07	0.257E 07
0.258E 07	0.258E 07	0.259E 07	0.260E 07	0.261E 07	0.262E 07	0.263E 07	0.263E 07	0.264E 07	0.265E 07
0.266E 07	0.267E 07	0.268E 07	0.269E 07	0.270E 07	0.271E 07	0.272E 07	0.273E 07	0.273E 07	0.274E 07
0.275E 07	0.276E 07	0.277E 07	0.278E 07	0.279E 07	0.280E 07	0.281E 07	0.282E 07	0.283E 07	0.284E 07
0.285E 07	0.286E 07	0.287E 07	0.288E 07	0.289E 07	0.290E 07	0.291E 07	0.292E 07	0.293E 07	0.294E 07
0.295E 07	0.296E 07	0.297E 07	0.298E 07	0.299E 07	0.300E 07	0.301E 07	0.302E 07	0.303E 07	0.304E 07
0.305E 07	0.307E 07	0.308E 07	0.309E 07	0.310E 07	0.311E 07	0.312E 07	0.313E 07	0.314E 07	0.315E 07
0.316E 07	0.317E 07	0.319E 07	0.320E 07	0.321E 07	0.322E 07	0.323E 07	0.324E 07	0.325E 07	0.326E 07
0.328E 07	0.329E 07	0.330E 07	0.331E 07	0.332E 07	0.333E 07	0.335E 07	0.336E 07	0.337E 07	0.338E 07
0.339E 07	0.341E 07	0.342E 07	0.343E 07	0.344E 07	0.345E 07	0.347E 07	0.348E 07	0.349E 07	0.350E 07
0.352E 07	0.353E 07	0.354E 07	0.355E 07	0.357E 07	0.358E 07	0.359E 07	0.360E 07	0.362E 07	0.363E 07
0.364E 07	0.366E 07	0.367E 07	0.368E 07	0.370E 07	0.371E 07	0.372E 07	0.373E 07	0.375E 07	0.376E 07
0.377E 07	0.379E 07	0.380E 07	0.382E 07	0.383E 07	0.384E 07	0.386E 07	0.387E 07	0.388E 07	0.390E 07
0.391E 07	0.392E 07	0.394E 07	0.395E 07	0.397E 07	0.398E 07	0.399E 07	0.401E 07	0.402E 07	0.404E 07
0.405E 07	0.407E 07	0.408E 07	0.410E 07	0.411E 07	0.413E 07	0.414E 07	0.415E 07	0.417E 07	0.418E 07
0.420E 07	0.421E 07	0.423E 07	0.424E 07	0.426E 07	0.427E 07	0.429E 07	0.430E 07	0.432E 07	0.433E 07
0.435E 07	0.436E 07	0.438E 07	0.440E 07	0.441E 07	0.443E 07	0.444E 07	0.446E 07	0.447E 07	0.449E 07
0.451E 07	0.452E 07	0.454E 07	0.455E 07	0.457E 07	0.459E 07	0.460E 07	0.462E 07	0.464E 07	0.465E 07

0.467E 07	0.468E 07	0.470E 07	0.472E 07	0.473E 07	0.475E 07	0.477E 07	0.478E 07	0.480E 07	0.482E 07
0.484E 07	0.485E 07	0.487E 07	0.489E 07	0.490E 07	0.492E 07	0.494E 07	0.496E 07	0.497E 07	0.499E 07
0.501E 07	0.502E 07	0.504E 07	0.506E 07	0.508E 07	0.510E 07	0.511E 07	0.513E 07	0.515E 07	0.517E 07
0.518E 07	0.520E 07	0.522E 07	0.524E 07	0.526E 07	0.528E 07	0.529E 07	0.531E 07	0.533E 07	0.535E 07
0.537E 07	0.539E 07	0.541E 07	0.542E 07	0.544E 07	0.546E 07	0.548E 07	0.550E 07	0.552E 07	0.554E 07
0.556E 07	0.558E 07	0.560E 07	0.561E 07	0.563E 07	0.565E 07	0.567E 07	0.569E 07	0.571E 07	0.573E 07
0.575E 07	0.577E 07	0.579E 07	0.581E 07	0.583E 07	0.585E 07	0.587E 07	0.589E 07	0.591E 07	0.593E 07
0.595E 07	0.597E 07	0.599E 07	0.601E 07	0.603E 07	0.605E 07	0.607E 07	0.609E 07	0.611E 07	0.613E 07
0.615E 07	0.617E 07	0.620E 07	0.622E 07	0.624E 07	0.626E 07	0.628E 07	0.630E 07	0.632E 07	0.634E 07
0.636E 07	0.639E 07	0.640E 07	0.643E 07	0.645E 07	0.647E 07	0.649E 07	0.651E 07	0.653E 07	0.656E 07
0.658E 07	0.660E 07	0.662E 07	0.664E 07	0.667E 07	0.669E 07	0.671E 07	0.673E 07	0.675E 07	0.678E 07
0.680E 07	0.682E 07	0.684E 07	0.687E 07	0.689E 07	0.691E 07	0.693E 07	0.696E 07	0.698E 07	0.700E 07
0.702E 07	0.705E 07	0.707E 07	0.709E 07	0.712E 07	0.714E 07	0.716E 07	0.138E 08		

ACCUMULATOR VOLUME ARRAY

0.344E-02 0.344E-02 0.344E-02 0.344E-02 0.344E-02 0.344E-02

ACCUMULATOR CHARGE PRESSURES ARRAY KPA

1938211 2492349 3738524 4984698 6230873 7477050

ELEMENTS OF ARRAY AP

0.194E 07	0.204E 07	0.214E 07	0.224E 07	0.234E 07	0.244E 07	0.254E 07	0.264E 07	0.274E 07	0.284E 07
0.294E 07	0.304E 07	0.314E 07	0.324E 07	0.334E 07	0.344E 07	0.354E 07	0.364E 07	0.374E 07	0.384E 07
0.394E 07	0.404E 07	0.414E 07	0.424E 07	0.434E 07	0.444E 07	0.454E 07	0.464E 07	0.474E 07	0.484E 07
0.494E 07	0.504E 07	0.514E 07	0.524E 07	0.534E 07	0.544E 07	0.554E 07	0.564E 07	0.574E 07	0.584E 07
0.594E 07	0.604E 07	0.614E 07	0.624E 07	0.634E 07	0.644E 07	0.654E 07	0.664E 07	0.674E 07	0.684E 07
0.694E 07	0.704E 07	0.714E 07	0.724E 07	0.734E 07	0.744E 07	0.754E 07	0.764E 07	0.774E 07	0.784E 07
0.794E 07	0.804E 07	0.814E 07	0.824E 07	0.834E 07	0.844E 07	0.854E 07	0.864E 07	0.874E 07	0.884E 07
0.894E 07	0.904E 07	0.914E 07	0.924E 07	0.934E 07	0.944E 07	0.954E 07	0.964E 07	0.974E 07	0.984E 07
0.994E 07	0.100E 08	0.101E 08	0.102E 08	0.103E 08	0.104E 08	0.105E 08	0.106E 08	0.107E 08	0.108E 08
0.109E 08	0.110E 08	0.111E 08	0.112E 08	0.113E 08	0.114E 08	0.115E 08	0.116E 08	0.117E 08	0.118E 08
0.119E 08	0.120E 08	0.121E 08	0.122E 08	0.123E 08	0.124E 08	0.125E 08	0.126E 08	0.127E 08	0.128E 08
0.129E 08	0.130E 08	0.131E 08	0.132E 08	0.133E 08	0.134E 08	0.135E 08	0.136E 08	0.137E 08	0.138E 08
0.139E 08	0.140E 08	0.141E 08	0.142E 08	0.143E 08	0.144E 08	0.145E 08	0.146E 08	0.147E 08	0.148E 08
0.149E 08									

ELEMENTS OF ARRAY AV

0.373E-08	0.117E-03	0.225E-03	0.325E-03	0.418E-03	0.504E-03	0.627E-03	0.792E-03	0.946E-03	0.109E-02
0.123E-02	0.136E-02	0.148E-02	0.159E-02	0.170E-02	0.181E-02	0.191E-02	0.200E-02	0.209E-02	0.224E-02
0.238E-02	0.252E-02	0.265E-02	0.278E-02	0.290E-02	0.301E-02	0.312E-02	0.323E-02	0.333E-02	0.343E-02
0.353E-02	0.365E-02	0.379E-02	0.392E-02	0.404E-02	0.417E-02	0.429E-02	0.440E-02	0.452E-02	0.463E-02
0.473E-02	0.484E-02	0.494E-02	0.504E-02	0.517E-02	0.530E-02	0.543E-02	0.555E-02	0.567E-02	0.578E-02
0.590E-02	0.601E-02	0.612E-02	0.622E-02	0.633E-02	0.643E-02	0.655E-02	0.667E-02	0.680E-02	0.692E-02
0.704E-02	0.716E-02	0.727E-02	0.738E-02	0.749E-02	0.760E-02	0.771E-02	0.781E-02	0.791E-02	0.801E-02
0.811E-02	0.821E-02	0.830E-02	0.839E-02	0.848E-02	0.857E-02	0.866E-02	0.874E-02	0.883E-02	0.891E-02
0.899E-02	0.907E-02	0.915E-02	0.923E-02	0.931E-02	0.938E-02	0.946E-02	0.953E-02	0.960E-02	0.967E-02
0.974E-02	0.981E-02	0.987E-02	0.994E-02	0.100E-01	0.101E-01	0.101E-01	0.102E-01	0.103E-01	0.103E-01
0.104E-01	0.104E-01	0.105E-01	0.106E-01	0.106E-01	0.107E-01	0.107E-01	0.108E-01	0.108E-01	0.109E-01
0.109E-01	0.110E-01	0.110E-01	0.111E-01	0.111E-01	0.112E-01	0.112E-01	0.113E-01	0.113E-01	0.114E-01
0.114E-01	0.115E-01	0.115E-01	0.116E-01	0.116E-01	0.116E-01	0.117E-01	0.117E-01	0.118E-01	0.118E-01
0.118E-01									

ELEMENTS OF ARRAY AL

0.114E-17 0.114E-03 0.228E-03 0.342E-03 0.456E-03 0.570E-03 0.684E-03 0.798E-03 0.912E-03 0.103E-02

0.114E-02	0.125E-02	0.137E-02	0.148E-02	0.160E-02	0.171E-02	0.182E-02	0.194E-02	0.205E-02	0.217E-02
0.228E-02	0.239E-02	0.251E-02	0.262E-02	0.274E-02	0.285E-02	0.296E-02	0.308E-02	0.319E-02	0.330E-02
0.342E-02	0.353E-02	0.365E-02	0.376E-02	0.387E-02	0.399E-02	0.410E-02	0.422E-02	0.433E-02	0.444E-02
0.456E-02	0.467E-02	0.479E-02	0.490E-02	0.501E-02	0.513E-02	0.524E-02	0.536E-02	0.547E-02	0.558E-02
0.570E-02	0.581E-02	0.593E-02	0.604E-02	0.615E-02	0.627E-02	0.638E-02	0.650E-02	0.661E-02	0.672E-02
0.684E-02	0.695E-02	0.707E-02	0.718E-02	0.729E-02	0.741E-02	0.752E-02	0.764E-02	0.775E-02	0.786E-02
0.798E-02	0.809E-02	0.821E-02	0.832E-02	0.843E-02	0.855E-02	0.866E-02	0.878E-02	0.889E-02	0.900E-02
0.912E-02	0.923E-02	0.934E-02	0.946E-02	0.957E-02	0.969E-02	0.980E-02	0.991E-02	0.100E-01	0.101E-01
0.103E-01	0.104E-01	0.105E-01	0.106E-01	0.107E-01	0.108E-01	0.109E-01	0.111E-01	0.112E-01	0.113E-01
0.114E-01	0.115E-01	0.116E-01	0.117E-01	0.119E-01	0.120E-01	0.121E-01	0.122E-01	0.123E-01	0.124E-01
0.125E-01	0.126E-01	0.128E-01	0.129E-01	0.130E-01	0.131E-01	0.132E-01	0.133E-01	0.134E-01	0.136E-01
0.137E-01	0.138E-01	0.139E-01	0.140E-01	0.141E-01	0.142E-01	0.144E-01	0.145E-01	0.146E-01	0.147E-01
0.148E-01									

COMPENSATED HAULAGE TRIPPING PRESSURE PCOMP= 7819873.0

ACCUMULATOR INCREMENT FACTOR YI= 0.6430

APPENDIX II

A Conversational Programme for Setting the Pre-Charge
Pressures of a Bank of Accumulators to enable a
Hydrostatic Power Absorber to Simulate Chain
Elasticity Effects on Power Loader Haulage Units

```

10. PUT LIST('This programme calculates the pre-charge pressures of a bank of accumulators to');
11. PUT LIST('enable a hydrostatic power absorber to simulate chain elasticity effects on');
12. PUT LIST('power loader haulage units');
13. PUT LIST('This programme uses english units');
14. DECLARE pa(20);
15. high,ret,rt,lb=99;
16. pa=1;
17. pi=3.142;
18. PUT LIST('what are the sprocket details spt=drive sprocket teeth ldt=idler teeth');
19. GET LIST(spt,ldt);
20. mu=.5;
21. PUT LIST('what are the absorber characteristics ad=displacement cu.in/rev abeff=efficiency');
22. PUT LIST('aufac=leakage factor up=boost pressure lbs/sq.in');
23. PUT LIST('for Hasklunas 6185 motor ad=996 abeff=.975 abfac=1.15 bp=100');
24. PUT LIST('for Staffa B270H with 2/1 a/b ad=526 abeff=.9 abfac=1.08 bp=100');
25. PUT LIST('for Staffa B270H with 4/1 a/b ad=1056 abeff=.9 aufac=1.04 bp=100');
26. GET LIST(ad,abeff,aufac,bp);
27. PUT LIST('what is the maximum sprocket torque tmm lbs.ft');
28. GET LIST(tmm);
29. PUT LIST('chain tensioners available');
30. PUT LIST('chain size (wd)mm available compression (ac)in pre-compression (pc)lbs full compression (fc)lbs');
31. PUT LIST('wd ac pc fc');
32. PUT LIST('22 26 3000 9300 spring type');
33. PUT LIST('22 17 3000 9300');
34. PUT LIST('18 33.5 2400 5500');
35. PUT LIST('18 25 2400 5500');
36. PUT LIST('18 17 2400 5500');
37. PUT LIST('18 24 2400 12000 beechdale');
38. PUT LIST('18 33 7200 7201 MRUE also for 22mm chain');
39. PUT LIST('18 24 9800 9801 wolton also for 22mm chain');
40. hg: GET LIST(wd,ac,pc,fc);
41. IF wd=18 THEN pitch=64;
42. IF wd=18 THEN sc=.35;
43. IF wd=22 THEN pitch=86;
44. IF wd=22 THEN sc=.49;
45. IF wd=26 THEN pitch=92;
46. IF wd=26 THEN sc=.47;
47. at1=pi/spt*2*pi/ldt;
48. s=(fc-pc)/2240/ac;
49. k1t=mu*wd*at1/2/pitch;
50. k2t=1+k1t;
51. k3t=1-k1t;
52. pcr=spt*pitch/25.4/pi/12;
53. tmax=tmm/pcr/k2t/2240;
54. tml=tmax*k2t-pc*k3t/2240;
55. tpl=tmax*k3t-pc*k2t/2240;

```

Programme listing

```

56.      chs1=sc*k3t+s*k2t;
57.      tp2=tp1-ac*chs1;
58.      IF tp2<=0 THEN tp2=0;
59.      tau=tp1/aveff/abeff;
60.      pcnpr=tau*100/tmax;
61.      pcnpr=floor(pcnpr);
62.      PUT LIST('adjust haulage tripping pressure to',pcnpr,' % to compensate for efficiency difference');
63.      PUT LIST('remember this % does not include the effect of haulage boost pressure');
64.      pa(1)=bp+tp2*2240*24*pi*pcr/ad/aveff;
65.      IF tp2<=0 THEN pa(1)=bp;
66.      IF tp2<=0 THEN zmax=tp1/chs1; ELSE zmax=ac;
67.      rot=zmax/12/pcr/2/pi;
68.      prtn=tmax-zmax*sc;
69.      PUT IMAGE(prtn)(lm17);
70.      lm17:  IMAGE;
the value of pre tension in the chain system is ---- tons
71.      IF prtn<5 THEN GO TO skip;
72.      PUT LIST('the value of pre-tension is above 5tons put high=1 to try a tensiometer with more ');
73.      PUT LIST('available compression or increase the value of ac by up to');
74.      PUT LIST('5 chain pitches thus introducing the equivalent of slack chain');
75.      GET LIST(high);
76.      IF high=1 THEN GO TO ng;
77.      skip:  pamax=bp+tp1*2240*24*pi*pcr/au/aveff;
78.      pamax=floor(pamax);
79.      IF pamax>3000 THEN PUT LIST('absorber pressure above 3000 lbs/sq.in. ');
80.      IF pamax>3000 THEN PUT LIST('re-xeq to input alternative absorber');
81.      slope=12*2240*48*chs1*pcr*pcr*pi*pi/au/au/aveff/aufac;
82.      PUT LIST('what is the accumulator initial gas volume');
83.      PUT LIST('accumulators available load va=210cub.in. 1qt va=60cub.in. ');
84.      PUT LIST('note these can be used in combination ie.210+60=270 or 60+60=120');
85.      acc:  lg=9;
86.      GET LIST(va);
87.      palit:  IF rt=2 THEN GET LIST(pa(1));
88.      accrot=(zmax-((pa(1)-bp)*ad*aveff/2240/24/pi/pcr-tp2)/chs1)/12/pcr/2/pi;
89.      IF ret=1 THEN PUT IMAGE(pa(1),rot,accrot)(lm15);
90.      lm15:  IMAGE;
pa(1)      ----      rot      ----      accrot      ----
91.      us1=slope*va/pa(1);
92.      y1=.08+.369*us1;
93.      IF y1<.6 THEN PUT IMAGE(y1,va)(lm16);
94.      lm16:  IMAGE;
yi(accumulator increment factor)=--- this is below the linear range of the ---cub.in. accumulator
95.      IF y1<.6 THEN PUT LIST('try a larger accumulator put lg=1 to input a larger size');
96.      IF y1<.6 THEN GET LIST(lg);
97.      IF lg=1 THEN GO TO acc;
98.      PUT LIST('accumulator pre-charge pressures in lbs/sq.in. ');
99.      GO j=2 TO 10;

```

```

100.      pa(j)=pa(1)*yl*j;
101.      END ;
102.      DO j=1 TO 10;
103.      pa(j)=floor(pa(j));
104.      PUT LIST('pa(',j,')', '=', pa(j));
105.      IF pa(j+1)>=pamax THEN GO TO nd;
106.      END ;
107.      nd:      b=1;
108.      IF pa(j+1)>=pamax THEN PUT LIST(j,'accs. are required to reach max adsorber pressure',pamax,'lbs/sq.in. ');
109.      nu=floor(pamax/pa(1)/yl);
110.      IF nu>10 THEN PUT LIST(nu,'accs. would be required to reach max adsorber pressure ',pamax,'lbs/sq.in. ');
111.      IF ret=1 THEN GO TO dz;
112.      ret=1;
113.      PUT LIST('If more accumulators are required than are available or the number is lower than required');
114.      PUT LIST('to achieve a satisfactory simulation put rt=1 to try an alternative size acc. ');
115.      PUT LIST('If a satisfactory mach cannot be achieved by use of alternative accumulators adjust the value');
116.      PUT LIST('of pa(1) this will alter the max sprocket rotation away from the desired value , if adjustment');
117.      PUT LIST('is required put rt=2 chain rotation=rot accumulator rotation=accrot');
118.      PUT LIST('adjustment might also be required if pa(1) is less than 20% of pamax');
119.      dz:      GET LIST(rt);
120.      IF rt=1 THEN GO TO acc;
121.      IF rt=2 THEN GO TO pal;
122.      PUT LIST('the following is a list of programm inputs');
123.      PUT IMAGE(ac,pc,fc)(im20);
124.      im20:      IMAGE;
ac      = --      ln.      pc      = ----      lbs      fc      = ----      lbs.
125.      PUT IMAGE(spt,ldt,wd)(im21);
126.      im21:      IMAGE;
spt      = --      teeth      ldt      = --      teeth      wd      = --      mm.
127.      PUT IMAGE(tmm)(im22);
128.      im22:      IMAGE;
tmm      = -----      lb.ft.
129.      PUT IMAGE(abeff,au,aufac)(im23);
130.      im23:      IMAGE;
abeff      = .----      factor      au      = ----      cuo.in.      aufac      = .---      factor
131.      PUT IMAGE(va,bp)(im24);
132.      im24:      IMAGE;
va      = ---      cuo.in.      up      = ---      lbs/sq.in.
133.      PUT LIST('additional programm outputs');
134.      PUT IMAGE(tmax,pcnpr,pamax)(im25);
135.      im25:      IMAGE;
tmax      = ---.---      tons      pcnpr      = ----.---      %      pamax      = ----.---      lbs/sq.in
136.      PUT IMAGE(rot,accrot)(im26);
137.      im26:      IMAGE;
rot      = .----      revs.      accrot      = .----      revs.

```

xeg

This programme calculates the pre-charge pressures of a bank of accumulators to enable a hydrostatic power absorber to simulate chain elasticity effects on power loader haulage units

This programme uses english units

what are the sprocket details spt=drive sprocket teeth ldt=idler teeth

spt

10 8

what are the absorber characteristics au=displacement cuv.in/rev aueff=efficiency

abfac=leakage factor up=boost pressure lbs/sq.in

for nabalunds 6185 motor ad=996 aueff=.975 abfac=1.15 up=100

for Staffa B270n with 2/1 s/b ad=526 aueff=.9 abfac=1.08 up=100

for Staffa B270n with 4/1 s/b ad=1056 aueff=.9 abfac=1.04 up=100

au

1056 .9 1.04 100

what is the maximum sprocket torque tmm lbs.ft

tmm

20000

chain tensioners available

chain size (wd)mm available compression (ac)in pre-compression (pc)lbs full compression (fc)lbs

wd ac pc fc

22 26 3000 9300 spring type

22 17 3000 9300

18 33.5 2400 5500

18 25 2400 5500

18 17 2400 5500

18 24 2400 12000 beechdale

18 33 7200 7201 MRUE also for 22mm chain

18 24 9800 9801 Bolton also for 22mm chain

wd

18 17 2400 5500

adjust haulage tripping pressure to 102 % to compensate for efficiency difference

remember this % does not include the effect of haulage boost pressure

the value of pre tension in the chain system is 6.45 tons

the value of pre-tension is above 5tons put nign=1 to try a tensioner with more

available compression or increase the value of ac by up to

5 chain pitches thus introducing the equivalent of slack chain

nign

1

wd

18 25 2400 5500

adjust haulage tripping pressure to 102 % to compensate for efficiency difference

remember this % does not include the effect of haulage boost pressure

the value of pre tension in the chain system is 3.65 tons

what is the accumulator initial gas volume

accumulators available 12all va=210cub.in. 1qt va=60cub.in.

note these can be used in combination ie.210+60=270 or 60+60=120

va

60

Programme Execution
Input & Output

yi(accumulator increment factor)=.33 this is below the linear range of the 60cu.in. accumulator
try a larger accumulator put lb=1 to input a larger size

lg

1

vd

210

accumulator pre-charge pressures in lvs/sq.in.

pa(1) = 185

pa(2) = 352

pa(3) = 529

pa(4) = 705

pa(5) = 882

pa(6) = 1058

pa(7) = 1235

7 accs. are required to reach max absorber pressure 1321 lbs/sq.in

if more accumulators are required than are available or the number is lower than required
to achieve a satisfactory simulation put rt=1 to try an alternative size acc.

if a satisfactory mach cannot be achieved by use of alternative accumulators adjust the value
of pa(1) this will alter the max sprocket rotation away from the desired value , if adjustment
is required put rt=2 chain rotation=rot accumulator rotation=accrot
adjustment might also be required if pa(1) is less than 20% of pamax

rt

2

pa(1)

264

pa(1) = 264 rot =.496 accrot =.462

accumulator pre-charge pressures in lbs/sq.in.

pa(1) = 264

pa(2) = 365

pa(3) = 548

pa(4) = 730

pa(5) = 913

pa(6) = 1096

pa(7) = 1278

7 accs. are required to reach max absorber pressure 1321 lbs/sq.in

rt

99

the following is a list of program inputs

ac	= 25	in.	pc	= 2400	lbs	fc	= 5500	lbs.
----	------	-----	----	--------	-----	----	--------	------

spt	= 10	teeth	lut	= 8	teeth	wd	= 18	mm.
-----	------	-------	-----	-----	-------	----	------	-----

tmm	= 20000	lb.ft.	ad	= 1056	cub.in.	awfac	= 1.04	factor
-----	---------	--------	----	--------	---------	-------	--------	--------

abeff	= .900	factor	op	= 100	lvs/sq.in.			
-------	--------	--------	----	-------	------------	--	--	--

va = 210 cu.in.

additional program outputs

tmax	= 12.40	tons	pchpr	= 102.0	%	pamax	= 1321	lbs/sq.in
------	---------	------	-------	---------	---	-------	--------	-----------

rot	= .496	revs.	accrot	= .462	revs.			
-----	--------	-------	--------	--------	-------	--	--	--

APPENDIX III

A CSMP Model of a Mechanical Haulage Unit

****CONTINUOUS SYSTEM MODELING PROGRAM****

PROBLEM INPUT STATEMENTS

```

TITLE B.J.D. B14 MECHANICAL HAULAGE RUNBACK
INITIAL
PARAMETER FRAC=.75,TTRIP=2.65E4,BT=1.5E4 ,FS=.6
PARAMETER KSTOP=0.5
PARAMETER HJ=1700.0
FUNCTION DTDG=0.,6.4E3,4.4,4.E4
FUNCTION TODG=6.4E3,0.,4.E4,4.4
FUNCTION DTDN=0.,2.7E3,5.2,4.E4
      XTH=AFGEN(TODG,TTRIP)
      XTHD=FRAC*FS
DYNAMIC
      RT=INSW(THD,BT,-BT)
      TM=INSW(THD,AFGEN(DTDN,TH),AFGEN(DTDG,TH))
      TH=INTGRL(XTH,THD)
      THD=INTGRL(XTHD,TH2D)
      VTR=-500.*THD*THD/.36*SIGN(1.0,THD)
      TH2D=(RT+VTR-TM)/HJ
NOSORT
      IF (TIME.GE.0.5.AND.TH2D.GT.-0.01)KSTOP=1.0
PRINT THD,TH,TH2D,TM,RT,VTR
PREPARE THD
FINISH TH=.11,KSTOP=0.6
TIMER FINTIM=4.0 ,DELT=.005,OUTDEL=.01 ,PRDEL=.05
END
PARAMETER HJ=4700.0
PARAMETER KSTOP=0.5
END
PARAMETER KSTOP=0.5
PARAMETER HJ=7700.0
END
PARAMETER KSTOP=0.5
PARAMETER HJ=10700.0
END
STOP

```

*Use of END statements
for multiple runs.*

OUTPUT VARIABLE SEQUENCE

XTH	XTHD	TH	TM	VTR	RT	TH2D	THD	KSTOP
-----	------	----	----	-----	----	------	-----	-------

OUTPUTS	INPUTS	PARAMS	INTEGS	MEM	RLKS	FORTRAN	DATA	CDS
13(500)	39(1400)	13(400)	2+	0=	2(300)	10(600)	21	

ENDJOB

B.J.D. R14 MECHANICAL HAULAGE RUNBACK

RKS

INTEGRATION

TIME	THD	TH	TH2D	TM	RT	VTR
0.0	4.5000E-01	2.6321E 00	-2.4577E 01	2.6500E 04	-1.5000E 04	-2.8125E 02
5.0000E-02	-1.2330E-01	2.6343E 00	-3.8676E 00	2.1596E 04	1.5000E 04	2.1115E 01
1.0000E-01	-3.1422E-01	2.6233E 00	-3.7531E 00	2.1517E 04	1.5000E 04	1.3713E 02
1.5000E-01	-4.9706E-01	2.6030E 00	-3.5461E 00	2.1371E 04	1.5000E 04	3.4316E 02
2.0000E-01	-6.6753E-01	2.5738E 00	-3.2608E 00	2.1162E 04	1.5000E 04	6.1888E 02
2.5000E-01	-8.2214E-01	2.5365E 00	-2.9152E 00	2.0895E 04	1.5000E 04	9.3876E 02
3.0000E-01	-9.5836E-01	2.4919E 00	-2.5288E 00	2.0575E 04	1.5000E 04	1.2756E 03
3.5000E-01	-1.0747E 00	2.4410E 00	-2.1208E 00	2.0209E 04	1.5000E 04	1.6040E 03
4.0000E-01	-1.1704E 00	2.3848E 00	-1.7081E 00	1.9806E 04	1.5000E 04	1.9024E 03
4.5000E-01	-1.2456E 00	2.3243E 00	-1.3044E 00	1.9372E 04	1.5000E 04	2.1549E 03
5.0000E-01	-1.3011E 00	2.2605E 00	-9.1986E-01	1.8915E 04	1.5000E 04	2.3513E 03
5.5000E-01	-1.3380E 00	2.1945E 00	-5.6156E-01	1.8441E 04	1.5000E 04	2.4865E 03
6.0000E-01	-1.3578E 00	2.1270E 00	-2.3340E-01	1.7957E 04	1.5000E 04	2.5604E 03
6.5000E-01	-1.3619E 00	2.0590E 00	6.2914E-02	1.7469E 04	1.5000E 04	2.5760E 03
7.0000E-01	-1.3520E 00	1.9911E 00	3.2750E-01	1.6982E 04	1.5000E 04	2.5387E 03
7.5000E-01	-1.3296E 00	1.9240E 00	5.6162E-01	1.6501E 04	1.5000E 04	2.4555E 03
8.0000E-01	-1.2963E 00	1.8583E 00	7.6729E-01	1.6029E 04	1.5000E 04	2.3339E 03
8.5000E-01	-1.2533E 00	1.7945E 00	9.4693E-01	1.5572E 04	1.5000E 04	2.1817E 03
9.0000E-01	-1.2020E 00	1.7331E 00	1.1031E 00	1.5131E 04	1.5000E 04	2.0066E 03
9.5000E-01	-1.1434E 00	1.6744E 00	1.2383E 00	1.4711E 04	1.5000E 04	1.8157E 03
1.0000E 00	-1.0785E 00	1.6188E 00	1.3550E 00	1.4312E 04	1.5000E 04	1.6154E 03
1.0500E 00	-1.0081E 00	1.5666E 00	1.4553E 00	1.3938E 04	1.5000E 04	1.4116E 03
1.1000E 00	-9.3316E-01	1.5181E 00	1.5413E 00	1.3589E 04	1.5000E 04	1.2094E 03
1.1500E 00	-8.5422E-01	1.4734E 00	1.6146E 00	1.3269E 04	1.5000E 04	1.0135E 03
1.2000E 00	-7.7189E-01	1.4327E 00	1.6768E 00	1.2977E 04	1.5000E 04	8.2751E 02
1.2500E 00	-6.8670E-01	1.3962E 00	1.7292E 00	1.2715E 04	1.5000E 04	6.5493E 02
1.3000E 00	-5.9911E-01	1.3641E 00	1.7729E 00	1.2485E 04	1.5000E 04	4.9852E 02
1.3500E 00	-5.0954E-01	1.3363E 00	1.8088E 00	1.2286E 04	1.5000E 04	3.6059E 02
1.4000E 00	-4.1835E-01	1.3131E 00	1.8376E 00	1.2119E 04	1.5000E 04	2.4308E 02
1.4500E 00	-3.2589E-01	1.2945E 00	1.8599E 00	1.1986E 04	1.5000E 04	1.4750E 02
1.5000E 00	-2.3246E-01	1.2806E 00	1.8762E 00	1.1885E 04	1.5000E 04	7.5053E 01
1.5500E 00	-1.3836E-01	1.2713E 00	1.8868E 00	1.1819E 04	1.5000E 04	2.6589E 01
1.6000E 00	-4.3869E-02	1.2667E 00	1.8920E 00	1.1786E 04	1.5000E 04	2.6729E 00

One PRINT output only shown

PREPARE data plotted on
Fig. 13.2

SIMULATION HALTED KSTOP = 1.0000E 00

1.6200E 00 -6.0205E-03 1.2662E 00 1.8926E 00 1.1783E 04 1.5000E 04 5.0342E-02

APPENDIX IV

References

REFERENCES

1 R J BRADBURY

'26 mm, 22 mm and 18 mm Diameter Haulage Chain'

NCB Mining Research and Development Establishment

Test Report No PA/MT(72)34

2 A WRIGHT

'Notes for Guidance on Load Limitation in Power Loader Haulage Chain'

NCB Mining Department

Mechanical Engineering Information Paper MI/C(72)10

3 J Z GRZECOWIAK

'Strength and Wear of 18 mm Round-Link Chain on Machine Haulage Sprockets'

NCB Mining Research and Development Establishment

MRDE Report No 35

4 Dr L GOTTSCHALD

'Criteria for the Discharge of Hydropneumatic Accumulators'

First Europlan Fluid Power Conference

Paper No 27 10 - 12 September 1973

5 W L GREEN

'The Effects of Discharge Times on the Selection of Gas Charged Hydraulic Accumulators'

3rd International Fluid Power Symposium

Turin, Italy

Papers D1, 9 - 11 May 1973

6 J THOMA

'Hydrostatic Power Transmission'

Trade and Technical Press Ltd 1964

7 BLACKBURN, REETHOR AND SHEARER

'Fluid Power Control'

M.I.T. Press

8 J J BATES

'Application of Chains to Power Loader Haulages'

Colliery Guardian August 1968

9 'System/360 Continuous System Modelling Programme, Users Manual'

Programme No 360A-CX-16X

IBM Ltd

10 'Handbook of the Greer-Mercier Hydro-Pneumatic Accumulator'

Fawcett Engineering Ltd

11 H E MERRITT

'Hydraulic Control Systems'

John Wiley and Sons Inc. 1967

APPENDIX V

Instrumentation

INSTRUMENTATION

1 Sprocket Torque External

British Hovercraft Corporation Ltd

Torque Transducer Type FC 0 - 20.3 kN m (0 - 15,000 lb ft)

Strain gauged shaft with slip ring connections

Output 1.5 mV/V at full rated load

Used with British Hovercraft TM6 indicator

2 Gearbox Torque Internal

Strain gauge bridge bonded to first reduction wheel shaft in

BJ-D Ltd B14 Haulage Unit

Strain gauges Philips 600 Type PR 9832K/10FE

External connections via IDM Electronics Ltd slip ring assembly

3 Haulage Speed Measurement

Racal Electronics Ltd Tachometer Type No MA 38

Output 60 pulses per revolution

4 Pressure Measurement

Bell and Howell Ltd, Consolidated Electrodynamics Division

Pressure Transducer Type 4-326

Pressure range 0 - 24.13 MPa (0 - 3,500 lbf/in²)

Output 4 mV/V at full rated pressure

5 Displacement

Penney and Giles Ltd

Potentiometer Model No RP 25/15 100 ohm 10 turn

5 cm drive wheel with foam strip

6 Chain Tension

British Hovercraft Corporation Ltd

Strain Gauge Tensometer. Load range 0 - 500 kN (0 - 50 tons)

Output 1.5 mV/V at full load

7 X - Y Plotter

Bryans Southern Instruments Ltd

Model No 26000 (metric axis)

Max writing speed Y axis 125 cm/sec (two channel), X axis 66 cm/sec

Pre-amplifiers 26102/26116

Max sensitivity 0.05 mV/cm

Curve follower attachment Model No 26236

Max following speed 40 cm/sec

Accuracy 0.8 mm

8 Signal Conditioning Equipment

Brethby Modular Instrumentation System (MRDE Internal Report 71/72)

Active, Passive and Frequency to Analogue Modules feeding X - Y Recorder

